UNIVERSITÀ DEGLI STUDI DI SALERNO
FACOLTÀ DI INGEGNERIA

CORSO DI LAUREA SPECIALISTICA IN INGEGNERIA CIVILE

Tesi di Laurea
in
Tecnica delle Costruzioni

DESIGN–ORIENTED ANALYSIS METHODS FOR MASONRY STRUCTURES IN SEISMIC AREAS: THEORETICAL FORMULATION AND VALIDATION ON EXPERIMENTAL RESULTS

RELATORE
Dr. Enzo Martinelli
CORRELATORE
Dr. Matija Gams

CANDIDATO
Gerardo Carpentieri
Matr. 0620100179

Anno Accademico 2010/2011

Ad Anna, Sabina e Gerardo,

faro nella nebbia e consiglio nella scelta.

Contents

Lists of figures

Lists of tables

Forewords

This Thesis completes the two-year Master Course in Civil Engineering at the University of Salerno and reports some of the results obtained during an internship period at the ZAG (Slovenian National Building and Civil Engineering Institute) in Ljubljana under the supervision of Dr. Matija Gams who is also co-tutor of this thesis.

The work is intended at formulating and validating design–oriented models for analysing the seismic response of masonry structures. Since modelling those structures is a challenging open issue, this research aims at providing designers with simplified methods which could be employed for ordinary design purpose. In particular this work explores the possibility to analyse masonry walls with frames modelling. This purpose is attained by either modelling the masonry walls with finite element programs or using simplified methods.

The chapter 1 introduces the key aspects of the mechanical response of existing buildings in Italy and in Europe, and focuses on the seismic response of masonry structures. The typical damage suffered by those structures in recent earthquake events are outlined and the most common strengthening techniques briefly described.

Chapter 2 proposes both an overview of the evolution of the seismic codes in Italy and a thorough description of the key documents currently in force for seismic design of new masonry structures and assessment of existing ones. Thus, the Italian Code of Standards for Structures in Seismic areas as well as the relevant Eurocodes are examined with the aim of pointing out the main provisions about the key subject of this thesis which is mainly intended at

describing the most common design-oriented analysis method for structures under seismic actions.

Since the thesis actually investigates several alternative methods for seismic analysis of masonry structures under seismic actions, chapter 3 outlines the results of some experimental tests already available in the scientific literature. The experimental results under consideration have been mainly carried out at ZAG during the last years. They could be possibly employed for assessing the accuracy of the above mentioned methods.

The following two chapters represent somehow the core of the thesis. They propose various analysis methods for masonry structures. Although several methods are actually available in the scientific literature this work focuses on those which can actually be employed by practitioners in the ordinary engineering activities. Thus, chapter 4 describes different approaches which can be possibly followed by using an ordinary FEM package. Both 2D- and frame-elements are employed for implementing alternative numerical models aimed at performing either linear or nonlinear seismic analyses. A couple of case-studies are modelled according to those approach, as the results of relevant experimental tests are available in the scientific literature and can be utilised in the following chapter for a possible validation.

Moreover, chapter 5 propose a novel frame-like model for analysing 2D masonry façades under seismic actions. It is intended at implementing the capacity models actually adopted by the seismic codes currently in force in Italy and Europe for simulating the nonlinear behaviour of both walls and spandrels. The stiff panel zones is also implemented in those elements and the nonlinear behaviour is actually implemented according to a “lumped” approach. Thus, a couple of nonlinear springs are considered for simulating the possible failure in bending, whereas another couple of shear springs models the failure in sliding shear. The model is implemented in a numerical code developed in MatLab® and is firstly employed for pointing out some of

the key aspects of the seismic response of masonry structures under seismic actions.

Then, the results of the numerical simulations carried out through the numerical models presented in both chapter 4 and 5 are presented in chapter 6 with the aim of comparing those numerical simulations with experimental results already available in the scientific literature and outlined in chapter 3. The simulation carried out by means of the frame-like model implemented in SAP2000® is in rather good agreement with the experimental results considered in this study. As a matter of principle, the lack in modelling the shear-normal force interaction in simulating the possible sliding-shear failure is the key drawback of the model under consideration. In fact, this flaw is not relevant for the considered comparison, as masonry generally fails in bending in the considered case-study. However, this possible drawback is overcome by the novel numerical model presented in chapter 5. This is the main achievement of the present thesis and can be used in numerically-efficient (and thus design-oriented) simulations of masonry structures by implementing all the capacity models ideally considered by the structural codes currently in force in both Italy and Europe. According to those documents the proposed model can be employed in performing nonlinear static (pushover) analysis for determining both seismic capacity and demand of masonry structures under seismic excitation. The possible extension of the present model to the case of fully 3D structures as well as the implementation of a numerical routine for performing nonlinear time-history analyses are among the next developments of this research.

1. Introduction and description of the purpose

1.1 Motivation

Many existing buildings in Italy and in various European countries are made of masonry structures. As shown in the Table 1.1, produced by ISTAT (Italian National Institute of Statistics) [1], more than 60% of existing buildings are made of masonry.

Table 1.1: Residential buildings for type of material used for the structure [1].

Material type	Residential buildings	[%]
Masonry	6903982	61,5
Reinforced concrete	2768205	24,7
Other	1554408	13,8
Total	11226595	100,0

The housing stock under consideration (two significant examples are in Figure 1.1) is very diversified. It includes both popular structures of low interest and historical buildings characterised by a significant cultural value and often regarded as “cultural heritage”.

Figure 1.1: A popular masonry structure (to the left) and Iside’s Temple at Pompei (to the right).

Most of the existing masonry are made of bricks or natural stones (see Figure 1.2). Those two materials can be also combined in different ways. The housing stock also includes buildings of different ages, in many cases more than a century. This means that cannot be regarded as a unique structural typology, but require, in principle, different dedicated testing, analysis and design methods.

From this point of view, the existing codes, which are derived from historical norms, they will be described in detail and discussed in the next chapter, always distinguish between new structures and existing structures. In particular, the analysis methods for existing structures are more affected by uncertainties because of the numerous unknowns about the section's geometry and the materials' strength.

The same wall material, moreover, is in fact heterogeneous and almost never equivalent to an isotropic material. The masonry is made up of elements of considerable size (bricks or stones) connected by mortar joints.

Figure 1.2: Stone masonry (Roman ruins of Abellinum, on the left) and brick masonry (Forum of Rome, on the right).

Thus determining the actual properties of masonry (including tensile strength, compressive strength, ductility, constitutive law, rigidity of the elements), by experimental tests is often a complicated issue.

The execution of those tests (see Figure 1.3) is, therefore, very expensive and requires specialised staff and large areas in advanced testing laboratories.

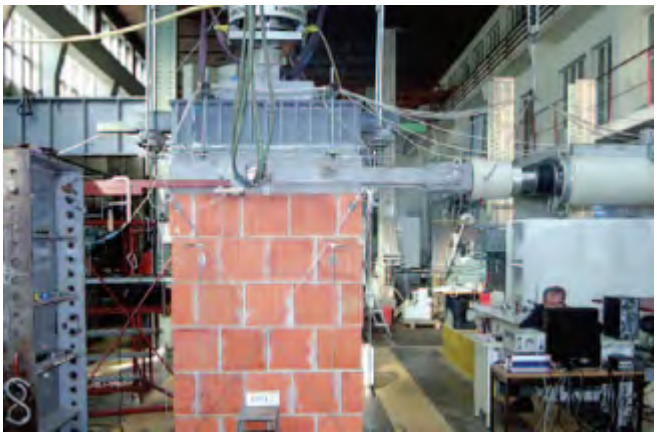

Figure 1.3: Masonry wall during a cyclic lateral resistance test at ZAG [2].

The masonry structures in the past were often realised according to the rules of good practice that has been obtained from observation of the results produced in similar structures. In practice, especially for multi secular structures, they were not done the analysis but they follow the "rules of art", which was known by tradition. The result of the work carried out this way is not necessarily wrong. Indeed, many of the structures of the past are well realised and still in use nowadays. However, damages in masonry structures often arise after exceptional events wich overstress the structures. Earthquakes can be a class of those damaging events.

Figure 1.4: Church of Santa Maria del Suffragio, before and after L'Aquila earthquake in 2009, M 5,9 [3].

Constructions in seismogenic zones, in fact, are almost regularly destroyed by the earthquakes (as shown in Figure 1.4). This causes from one side the damage in terms of loss of human lives and other direct economic losses (for the construction collapse) and indirect (other loss resulting from the collapse).

The major innovation of the modern analysis methods in seismic zones is the so–called "seismic microzonation" (shown in Figure 1.5). This was introduced with the current technical norm. In practice hazard parameters have been defined point–by–point basis in all the Italian territory. This result was achieved by means of a "seismic hazard map" by the Geophysics and Vulcanology National Institute [4]. This work has allowed a major step forward in seismic analysis.

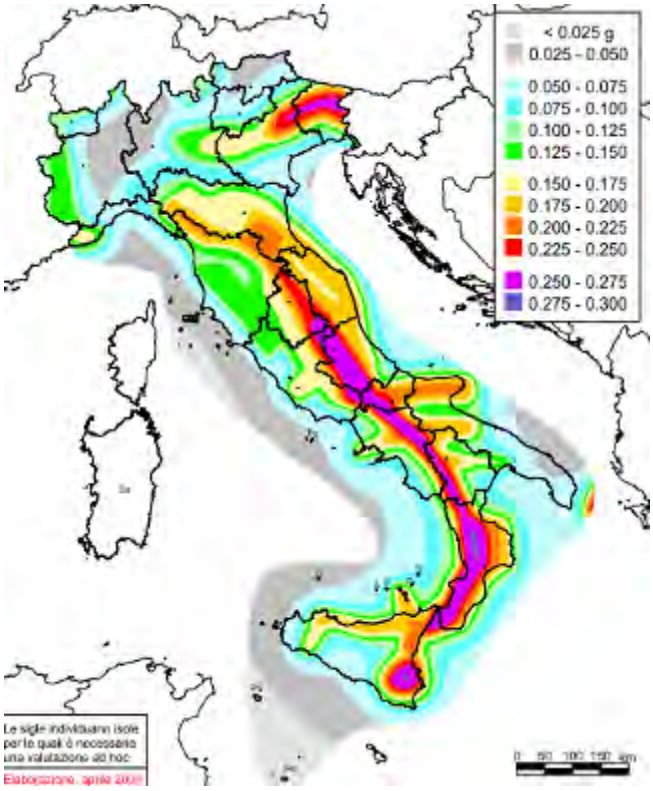

Figure 1.5: Seismic hazard map of the National territory [4].

In fact, they have been abandoned the previous seismic macrozone of the Italian territory, where they had set a few parameters of seismic hazard for large areas of Italian territory. The old methods, in fact, did not allow to take into due account local site properties. This leads to unnecessarily oversized projects in some areas, improperly disadvantaged. The seismic analysis on masonry structures, often, present additional problems because they relate to existing structures. This fact require an interdisciplinary knowledge. Work on masonry structures, for example, cannot ignore the knowledge of the historical and cultural context.

The interventions have the following characteristics:

1) reversibility: the intervention must be removed without damage to other structures;
2) compatibility: the intervention must use materials similar to those of the original;
3) minimization: the intervention must be little invasive.

The safety evaluation of an existing building is necessary when there is a degradation of structural and non-structural evident as a result of:

1) seismic events;
2) action of wind and snow;
3) subsidence in the foundation;
4) fires;
5) change of use.

To proceed to work on these structures and to reduce the uncertainties of the analysis is essential to achieve a good level of knowledge through the execution of a research on:

1) materials used for masonry;
2) geometry: dimensions of the wall panels;
3) types and structural characteristics of floors and roofs;
4) type and size of foundations;

5) reference standards and analysis methods used at the time of realization.

For historical and cultural buildings is necessary to refer to the specifications of Legislative Decree No. 42 in 22/01/2004 entitled "Code of the cultural heritage and landscape" [5].

1.2 Typical seismic–induced damages

To proceed a correct action on a building and to give an opinion on the security is necessary an investigation of the instability and an appropriate level of general knowledge of the existing structure.

The first and most important thing to do, to obtain the information necessary to evaluate the level of damage that it has suffered a structure in time, is the reading of the crack (see Figure 1.6).

Figure 1.6: Partial collapse in a masonry building after L'Aquila earthquake [3].

A high level of damage, with very large and thick cracks and partial collapse, is a sure sign of unfitness for the use of the existing structure. The presence, however, of minor damage is certainly a good sign, but should not prejudice the execution of an accurate investigation. In particular, if the structure has some minor damage, it is not said that it is practicable. This is true, in particular, if these minor damages are not arising as a result of a seismic event.

The primary purpose of the investigation of the damage is, therefore, to determine the practicability of a structure and it takes the necessary steps to recover a static (or retrofitting).

Figure 1.7: Interventions on a Church in L'Aquila to prevent other damages [3].

The investigation of the damage must ensure the capacity or not of the existing structure to withstand future load levels in safety, including the seismic action (see an example in Figure 1.7). The current Italian technical standards [6], in particular, requires that, under the earthquake, the structure maintains the "performances". The seismic testing in combination with the current rule, then, is not only an "verification of strength" of the membering sections but it is a "performance verification". In agreement with the results offered by American standards, NTC 2008 [6] defines, in fact, several limit states in relation to the seismic performance that the structure must ensure in according to its importance.

The Figure 1.8 contains some typical levels of damage defined by the "National Group for Defense from Earthquakes" of the CNR in the "Handbook of census card damage". The Figure 1.8 sets out the main types of cracks that can appear (usually not simultaneously) in a traditional masonry building after a seismic event.

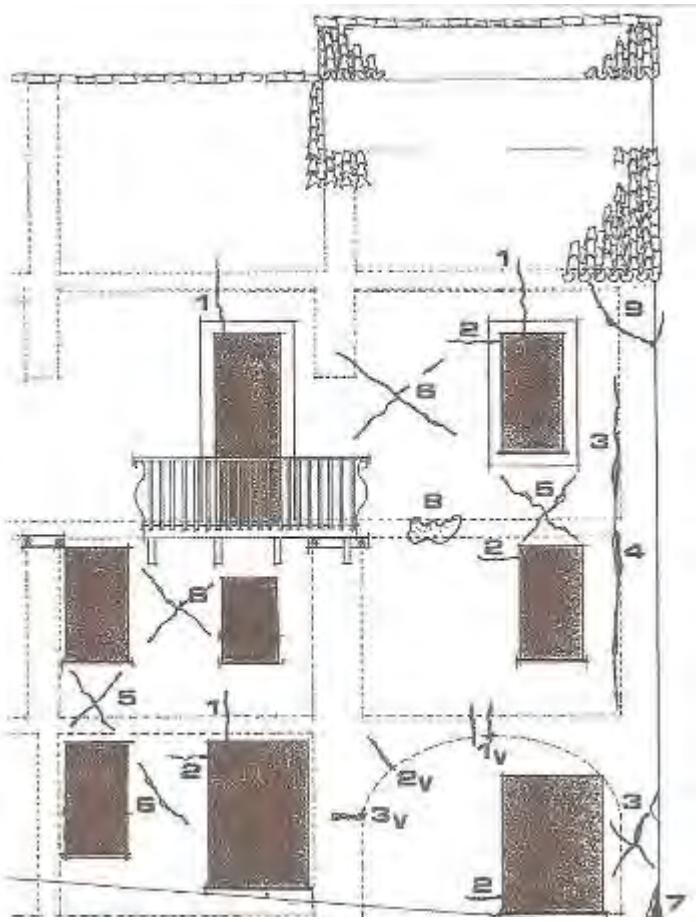

Legend

1 – Flexural cracks on door and windows beams;
2 – Flexural horizontal cracks on the top of the walls;
3 – Small cracks in the intersection between walls;
4 – Important cracks in the intersection between walls;
5 – 6 Diagonal shear cracks on piers and spandrels;
7 – Flexural cracks in the elements for compression failure;
8 – Failure for impact between more elements;
9 – Failure in the connection between two walls;
1v – 2v Cracks in the vaults;
3v – Cracks in the bottom of the vaults.

Figure 1.8: Framework of possible cracks in masonry building [7].

1.2.1 Observed damage

On existing structures it is, therefore, possible to use the previous criteria to make a classification of the level of damage. This is particularly useful when, after a seismic event, it is necessary to coordinate rescue operations and identify areas requiring evacuation, the buildings to shore up, the structures that are uninhabitable and evacuation, especially the work more appropriate to restore a level of optimal security.

In the following there are some examples of classifications as a result of various earthquakes and reported from [8].

Figure 1.9: Examples 1 [8].

Figure 1.10: Example 2 [8].

In the Figure 1.9 there are some lesions in the vertical spandrel between the two apertures and connection to transversal wall to the left (Damage Level A. Mild). The next case in Figure 1.10 shows vertical and diagonal lesion at the architrave with strengthening structure (Damage Level: A. Mild).

In the next situations it's possible to see more critical damages of the masonry structures after earthquake.

Figure 1.11: Examples 3 [8].

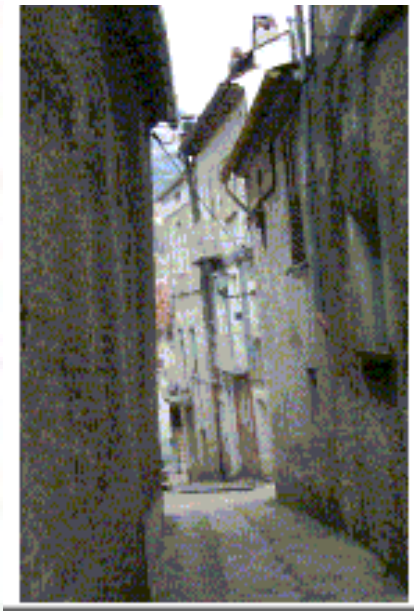

Figure 1.12: Example 4 [8].

In the Figure 1.11 it's notable some vertical lesions along the vertical connection between two buildings (Damage Level: A. Mild). In the Figure 1.12 there are an outside lead of an existing building in an old historic center (Damage Level: A. Mild).

Figure 1.13: Examples 5 [8].

Figure 1.14: Example 6 [8].

In Figure 1.13 some vertical lesions with separation from the adjacent building, horizontal and diagonal lesions at the floor level, partial collapse of the roof are present (Damage Level B - C . Medium - Severe). In the case of Figure 1.14 there are vertical and diagonal lesions almost the entire wall and lesion nearly horizontal at the level of the attic (Damage Level: C. Severe).

Figure 1.15: Example 7 [8].

Figure 1.16: Example 8 [8].

The Figure 1.15 shows a diagonal lesion in a masonry walls with dislocation at the base. (Damage Level: C - D. From serious to very serious).

In the Figure 1.16, some lesions of the vertical masonry walls on the second floor connected to horizontal lesions can be seen. To the right there are the formation of a large wedge of masonry displaced of more than 10 cm. (Damage Level D. Very serious).

Figure 1.17: Examples 9 [8].

Figure 1.18: Example 10 [8].

In the Figure 1.17 a partial collapse of a sack masonry in correspondence of old openings for extended release of the external face can be seen. Moreover a severe diagonal lesion with dislocation of several centimeters it's present in this case (Damage Level: D. Very serious). In the last case of Figure 1.18 there is a severe dislocation on the attic level floor beam for push of the roof (Damage Level: D. Very serious).

1.3 Technical solutions for strengthening

Existing masonry structures often undergo structural upgrading operations aimed at possibility achieving one of the aimed at the following objectives [6]:

- local repairing on isolated elements which are in need for an enhancement of their capacity;
- strengthening, intended at enhancing the global safety of structures up to relevant threshold values (see Figure 1.19);
- retrofitting: aimed to achieving the security levels provided by the present rules.

Figure 1.19: Strengthening of a vault with CFRP [3].

The different types of intervention on masonry structures can be classified, according to the structure that must be strengthened, in:

1) interventions on vertical structures (walls, piers, spandrels);
2) interventions on horizontal structures (floors, roofs, arches and vaults);
3) interventions on the foundations.

Often strengthening interventions on existing structures use innovative material like FRP (Fiber Reinforced Polymer) (see Figure 1.19).

Those elements allow to improve, i.e., the ultimate resistance in piers or in spandrels both in shear and in flexural. The FRP materials include the applications of plate elements, by paste, both in vertical direction (for improve the flexural resistance) and in horizontal direction (for improve the shear resistance).

In the past, other strengthening techniques were used, in particular:

1) injections of reinforced mortar (Figure 1.20);
2) reinforced plaster (Figure 1.21);
3) tie–beams and cables in steel (Figure 1.22);
4) reinforced concrete beams on the top of the walls.

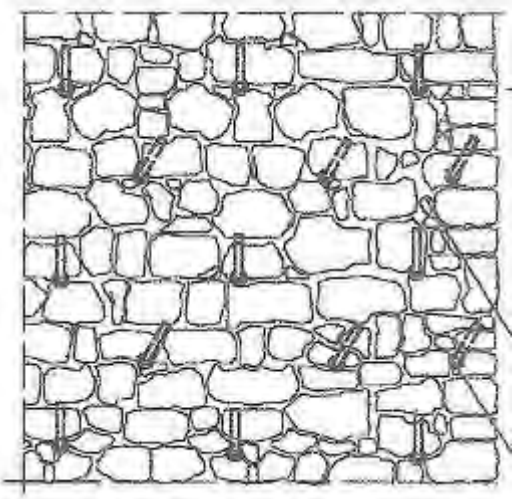

Figure 1.20: Scheme of a diffused injections in a masonry wall [7].

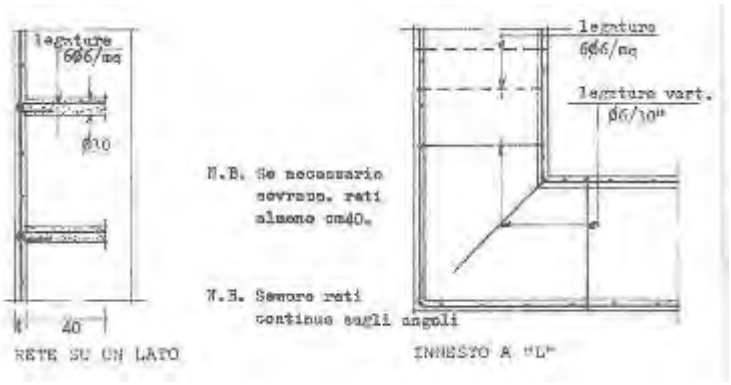

Figure 1.21: Design of a reinforced plaster [7].

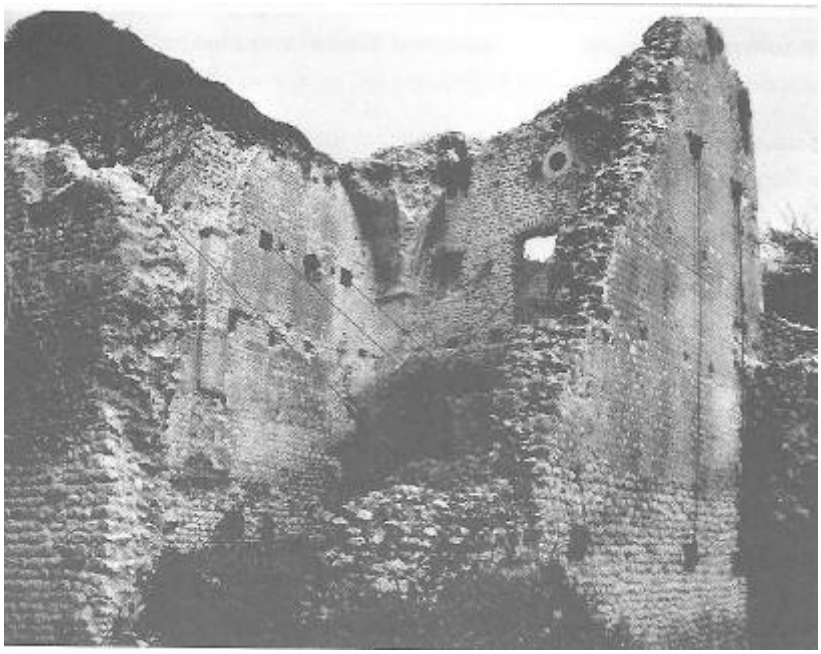

Figure 1.22: Tie–beams for vertical wall in Ninfa – Latina [7].

2. Codes for Masonry Structures

2.1 Historical evolution

In history many different technical documents, more or less sophisticated and scientifically–based have followed each other. Most of the seismic rules, on masonry structures but also on other kinds of structures, were made after the most destructive earthquakes occurred on the mostly of Italian territory.

Of all this material, the structural designer should not make a passive study and accept the requirements as they are imposed but he should study with a critical spirit the policies that have followed each other in time.

In particular, Structural Engineers should give priority to "his own technical and scientific knowledge" [9] and must apply it to works that are so designed as to meet the current codes provisions and, if possible, also the provisions of the previous rules which may be easily taken as the "rules of good practice".

Technical standards are analysed in this study after introducing the following typologies:

1) National Standards, which include both rules applicable throughout the Italian territory and local regulations issued by the regions or other administrative bodies;
2) European Standards, issued by the CEN (European Committee for Standardization) and reviewed by UNI (Italian Organization for Unification) for the application on the Italian territory;
3) International Standards, they are all the documents produced by organizations recognised as valid by the international scientific and technical point of view.

They include the standards and guidelines produced by FEMA [10][11] (Federal Emergency Management Agency) or ATC [12] (Applied Technology Council).

In the following paragraphs, there are the most important historical legal documents issued since the last century and are shown below the current Italian and European norms.

All the paragraphs set out some of the most significant requirements of the codes under consideration, both in terms of concepts and specific formulas. They also try to perform a critical comparison between the various documents that have occurred in time, making significant developments in the analysis of seismic and non-seismic masonry structures and the main differences.

The first law and the first research in the field of construction in seismic zones dates back to 1627, after an earthquake occurred in Campania and struck the Benevento area (4500 victims).

Thus, the "The Beneventan baroque System", that included a wooden skeleton with rectangular meshes, was introduced [9].

At first this method was applied only to the structures to rebuild after the collapse of the earthquake of 1627. After another earthquake in 1783 that struck Messina and Calabria (32000 victims), the previous construction system was improved by the engineer General Gian Battista Mori and also imposed on new buildings.

In the following centuries, regulations and seismic studies in the field were refined and updated and many other technical documents were produced with almost regular basis after every major earthquake.

2.1.1 Royal Decree No. 193 of 18/04/1909

This law [13] is the first modern technical standard in the field of earthquake resistant buildings. It was formulated in response to the earthquake occurred on 28/12/1908. In following years, they were also adopted other standards, including:

- Royal Decree No. 1080 of 06/09/1912: "Obligatory technical and hygienic standards for repair, reconstruction and new construction of public and private buildings in the municipalities affected by the earthquake of 28/12/1908 or other previous";
- Royal Decree No. 665 of 09/05/1920;
- Royal Decree No. 1705 of 16/11/1921;
- Royal Decree No. 1475 of 27/10/1922.

In these codes firstly the "good rules of building in seismic zone" have been defined. Limits were introduced especially in terms of height of buildings, which may not exceed 10 m, to ensure the requirement of monolithic. In particular, two types of walls can be used:

1) traditional masonry: building designed by giving the carrying capacity to load bearing walls, which must be resistant to in–plane and out–plane and, therefore, must have a suitable thickness;
2) reinforced masonry or animated: the wall is made by using a space frame structure with a reinforced concrete which involves the insertion of columns at intersections between masonry walls or beams or floor beams between the walls and floor systems.

However, the law of 1912, greatly limited the application of the first type of masonry and focuses on new construction technique of the r.c.. In particular, the use of ordinary masonry buildings up to only two floors, 7 meters high and without basements was imposed.

2.1.2 Royal Decree No. 2229 of 16/11/1939

One of the most important laws in the building and construction industry is certainly the Royal Decree No. 2229 of 1939 [14]. This legislation, referring explicitly to the reinforced concrete structures, were prepared by the National Research Council (CNR).

This rule also introduces the obligatory to annex the executive project, drawn up and signed by an engineer or a registered architect. The Standard also requires that the document must contain all of the detailed design information useful in defining the project in its entirety and in the definition the state of stress.

Afterwards, they are introduced the “minimum” performance required of the structural elements used, in particular the cement concrete and reinforcing bars. These mechanical properties must be verified and certified in recognised laboratories of structures.

In this standard is also required that, before starting work, the complaint is the start of work, which must include the detailed design of the works to be realised.

This document is also very important because it introduces essentially, the figures of the "project manager", the "design manager", the "builder" and the "tester".

In subsequent articles they have been reported the requirements regarding the mechanical characteristics of the conglomerate, in particular the size of aggregate (gravel or crushed stone) and the quality of the binder.

With regard, however, to the analysis of r.c. membering they are introduced the basic principles of "admissible stress method" which shall be applied using the principles of Science of Construction.

The requirements contained in this legislation, during the years, have evolved into the present knowledge up to the current requirements of the Guidelines on the concrete produced by CNR.

2.1.3 Law No. 64 of 02/02/1974

This law [15] is entitled "Provisions for buildings with special requirements for buildings in seismic zone" and is still current. The law in question was promulgated in response to the earthquake of Ancona in 1974.

In practice, this law has been followed by several decrees, the first of which was the Ministerial Decree No. 39 of 03.03.1975 [16].

This standard introduces for the first time the concept of "seismic equivalent" to conduct the seismic analysis of structures by applying actions to the level of floor systems. The seismic action was regarded as "equivalent" to the effect produced by the displacement of the ground.

This analysis, which is now known as Linear Static Analysis (ASL), provides for the use of response spectra in terms of pseudo spectral acceleration to define, at the natural period of vibration of the structure, the maximum acceleration possible. This acceleration is then used to define the action to be applied to the structure.

For more complex buildings and with higher periods of vibration, this rule already introduced the dynamic analysis, which have evolved to the present day with the modal analysis.

With regard to masonry buildings, the law and subsequent decrees required that the horizontal forces, assumed the hypothesis of rigid floor systems, shall be distributed among the various macro seismic resistant elements according to their vertical stiffness.

In addition, the concepts of stiffness and mass centers were introduced, resulting in the definition of eccentricity.

One of the greatest innovations was the introduction of the possibility of considering also the vertical seismic action, mainly due to the vibrating motion, that undertake not only the structures but also cantilevered structures and the horizontal members pushing with span than more 20 m.

Finally, this document includes the instructions on the operations of consolidation of crumbling structures, but without suggesting any of the methods in particular.

Compared to earlier standards, the Law No. 64 of 1974 provided clear statements of the methods used for the analysis of structures in seismic areas.

However, the earthquake is a ground motion imposed on the basis of the structure, or it is an event that affects the structure "from the low" rather than "from the top" how assumed in the linear static analysis procedure. This assumption is acceptable when the most important is the first among all the modes of vibration.

If this is the case, the seismic shear at the base of the structure can be shared between the different floor systems so similar to the first modal form, or in proportion to the masses of floor systems and, especially, marked by the height of the foundation.

2.1.4 Commentary No. 21745 of 30/07/1981

2.1.4.1 General comments

In general, masonry walls can be classified as follows:

- squat walls: characteristics of mostly few floors buildings (low rapport height/thickness) and operating mainly to the shear. In these types of buildings there are continuous floor spandrels, between the various openings, very rigid and approximated to the rigid transverse. In this way, the masonry wall can then be modelled as a shear–type frame (Figure 2.1a);
- slim walls: characteristics especially for buildings with more than four floors. In these cases the collapse for the horizontal actions in the wall's planes is usually at the first floor of the spandrels (shear failure with diagonal cracks) and then the masonry walls for the combined effect of bending and shear (Figure 2.1b).

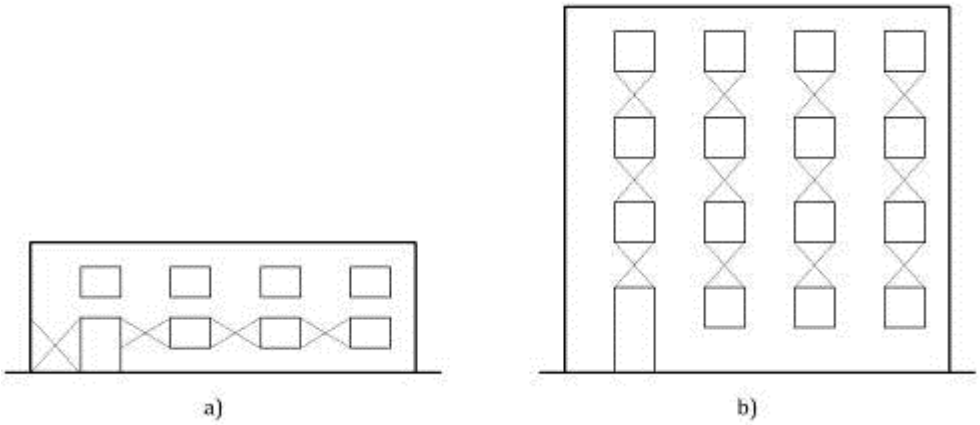

Figure 2.1: Collapse mechanisms [17].

2.1.4.2 The POR method

This Commentary [17] is widely known as it introduced the so–called POR method [18], which has been widely used for analysing masonry structures.

It is often possible to model the walls as plan elastic frames subjected to horizontal actions at the levels of the floors. The POR method is, therefore, a simplified method for analysing the behaviour of a wall under actions in its plan. The key assumptions underlying this method are:

1) infinitely rigid floor spandrels;
2) crisis of the pier with diagonal cracks;
3) negligible increases in normal stresses in piers because horizontal actions.

The third hypothesis is acceptable for a low-rise buildings. Therefore, the POR method is allowed, according to the Ministerial Decree 16/01/1996 [19], only to buildings up to three floors.

The technical document reports instructions taken as a reference for the repair and strengthening of masonry buildings damaged by the earthquake in 1980 that struck the Irpinia. Some of the most important provisions of this point are reported in the following.

The compressive shear strength of masonry can be identified using the Table 2.1.

Table 2.1: Masonry's mechanical characteristics [17].

Type of masonry	τ_k [t/m^2]	σ_k [t/m^2]
Non reinforced and non-damaged masonry		
Full bricks with "bastard mortar".	12	300
Standard block (with provisions of DM 03/03/1975) (29x19; 19 cm) with "bastard mortar".	8	250
Clay or concrete block with "bastard mortar".	18	300
Stone masonry (with brick layers the τ_k value can be incremented of the30%): a) stone in bed conditions; b) stone a few squat and well made; c) sandwich stone masonry in good conditions.	 2 7 4	 50 200 150
Tuff elements of good quality.	10	250
New masonry		
Full bricks with circular hole and cement mortar with $R_m \geq 1450$ t/m^2.	20	500
Double holed bricks UNI ratio empty/full = 40% and cement mortar with $R_m \geq 1450$ t/m^2.	24	500
Reinforced masonry		
Full bricks or squat stone with reinforced plaster of minimum 3 cm thickness.	18	500
Injected stone, sandwich masonry with two reinforced concrete slabs of minimum 3 cm thickness.	11 11	300 300

The shear and axial compressive elastic moduli can be define as follows:

$$G = 1100 \cdot \tau_k \,; \tag{2.1}$$

$$E = 6 \cdot G \,. \tag{2.2}$$

Moreover, the seismic action can be evaluated by the relation:

$$F = \beta \cdot C \cdot W_i \,, \tag{2.3}$$

where:

- C is the coefficient of seismic intensity, evaluated by the expression:

$$C = \frac{S-2}{1000} \,; \tag{2.4}$$

- S is the degree of seismic activity;
- β is the coefficient of the structure, usually equal to 4;
- W_i is the total weight of the building at the time of the earthquake.

In particular, three seismic zones were defined and the following values provided for S:

- to earthquake zones with degree of seismic activity S = 12, it has: β C = 0,40;
- to earthquake zones with degree of seismic activity S = 9, it has: β C = 0,28;
- to earthquake zones with degree of seismic activity S = 6, it has: β C = 0,16.

2.1.4.2.1 The wall

In the Figure 2.2, a single masonry wall, subjected to action in its plane, is considered. For the Commentary [17], the element arrives to the collapse with diagonal shear lesions.

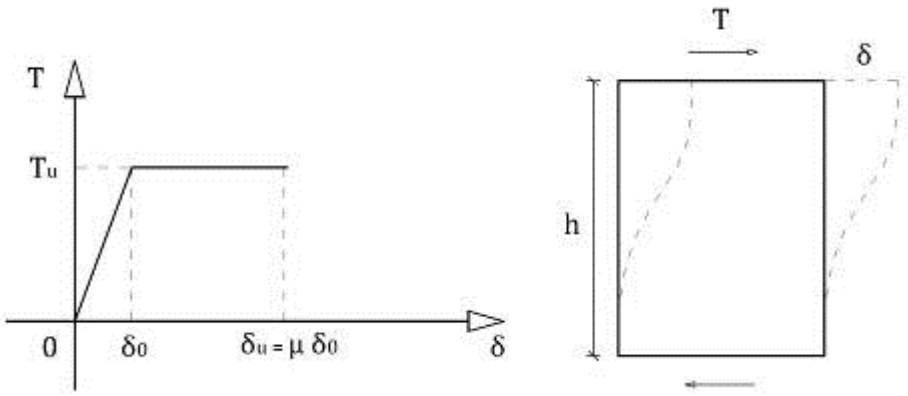

Figure 2.2: Panel's pseudo constitutive behaviour [17].

According to the Commentary in object, the ultimate shear action is determined by the relation:

$$T_u = A \cdot \tau_k \cdot \sqrt{1 + \frac{\sigma_0}{1{,}5 \cdot \tau_k}}, \tag{2.5}$$

where:

- A = t b is the area of the cross section of the masonry panel;
- t, b and h are the panel's dimension (see Figure 2.3);
- τ_k is the shear strength;
- σ_0 is the normal stress at the base of the panel due to vertical loads.

Finally, for the panel, there is an elastic plastic perfect relationship, characterised by the following equations:

- elastic tract: $T = k_o \cdot \delta$ for: $\delta < \delta_0$; (2.6)
- plastic tract: $T = T_u$ for: $\delta_0 < \delta < \delta_u$. (2.7)

where:

- δ_0 is the limit elastic displacement;
- δ_u is the ultimate displacement, function of the panel's ductility.

The two previous displacements are obtained from relations:

$$\delta_0 = \frac{T_u}{k_0}; \tag{2.8}$$

$$\delta_u = \mu \cdot \delta_0 . \tag{2.9}$$

μ is the ductility factor, defined in the Table 2.2.

Table 2.2: Ductility factors [17].

Type of masonry	Ductility factor - μ
Non reinforced stone masonry	1,5
Injected stone masonry	1,5
Existing brick masonry	1,5
New brick masonry	2,0
Stone or brick masonry with tie beam	2,0

The stiffness of the linear elastic range is given by:

$$k_0 = \frac{G \cdot A}{1{,}2 \cdot h} \cdot \frac{1}{1 + \frac{1}{1{,}2} \cdot \frac{G}{E} \cdot \left(\frac{h}{b}\right)^2}, \tag{2.10}$$

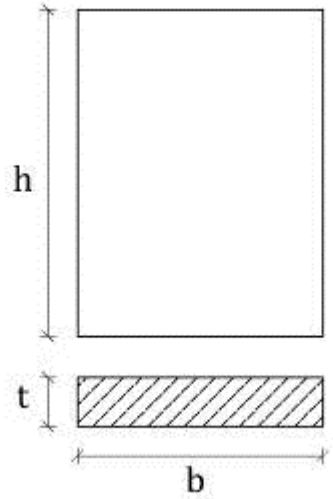

Figure 2.3: Panel's geometry [17].

2.1.4.2.2 The frame

The general masonry panel (or frame) can be modelled like a frame-like structure that is made of different element, shortly exposed in the Figure 2.4.

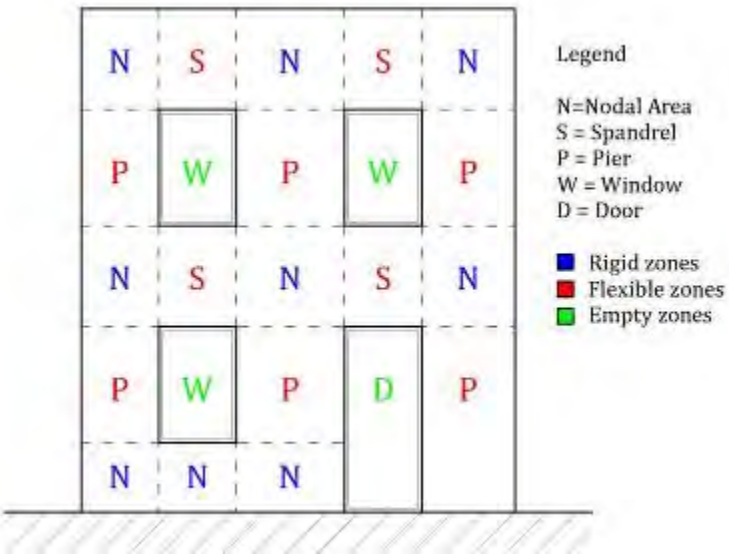

Figure 2.4: Modelling of a wall with POR method.

Now consider a generic wall consisting of three piers and subject to action F in its plan (see Figure 2.5). This wall can be simulated as three separate masonry walls connected by penduli. All the building piers, for the congruence, will be subjected to the same lateral displacement δ. It's possible to get the curve shear–total displacement of the wall from the notes of each septum. In a similar way, the system can be schematised with a shear–type frame, like the following one.

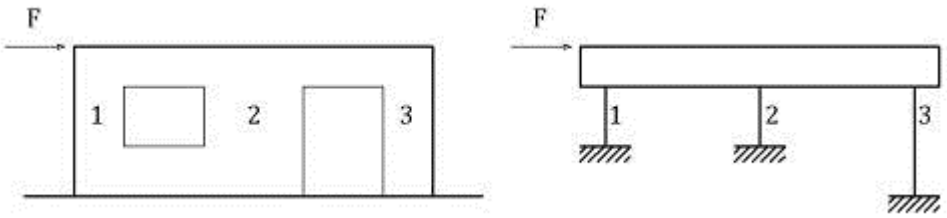

Figure 2.5: Modelling of a structure facade [17].

The elastic-perfectly plastic behaviour of every pier has done by the following relations:

- elastic tract: $T_i = k_{o,i} \cdot \delta_i$ for: $\delta_i < \delta_{0,i}$; (2.11)
- plastic tract: $T_i = T_u$ for: $\delta_{0,i} < \delta_i < \delta_{u,i}$. (2.12)

With: i=1,2,3.

The behaviour curve of the whole structure is obtained graphically as illustrated in following Figure 2.6 and is characterised by:

- ultimate displacement equal to the minimum displacement between the ultimate minimum of all piers:

$$\delta_{u,\min} = \min\left\{\delta_{u,1}; \delta_{u,2}; \delta_{u,3}\right\}. \quad (2.13)$$

- elastic limit displacement coincides with the displacement to the elastic limit minimum between that of all piers:

$$\delta_{0,\min} = \min\left\{\delta_{0,1}; \delta_{0,2}; \delta_{0,3}\right\}. \quad (2.14)$$

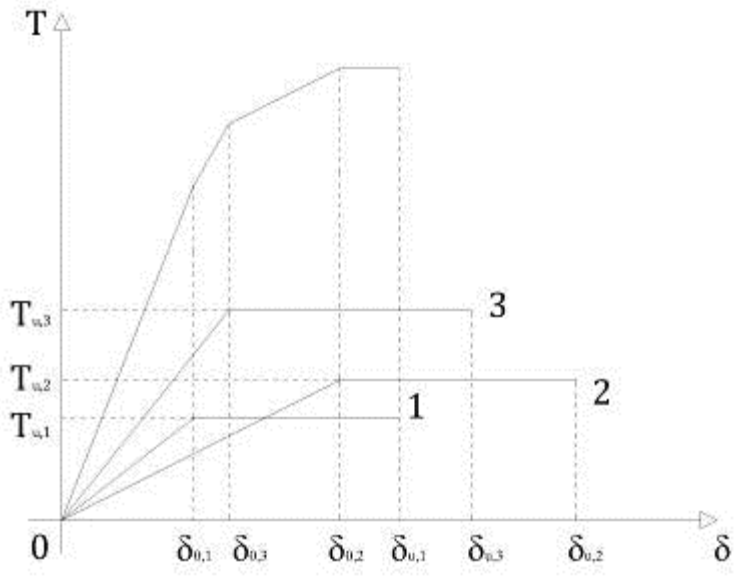

Figure 2.6: Shear–displacement behaviour of the wall.

Assuming: $\delta_{0,1} < \delta_{0,3} < \delta_{0,2}$ the previous curve can be draw. The behaviour of the wall will then be described by the following relationships:

- for: $0 < \delta < \delta_{0,1}$ it has: $T = \left(k_{0,1} + k_{0,2} + k_{0,3}\right) \cdot \delta$ (2.15)
- for: $\delta_{0,1} < \delta < \delta_{0,3}$ it has: $T = T_{u,1} + \left(k_{0,2} + k_{0,3}\right) \cdot \delta$ (2.16)
- for: $\delta_{0,3} < \delta < \delta_{0,2}$ it has: $T = T_{u,1} + T_{u,3} + \left(k_{0,2}\right) \cdot \delta$ (2.17)
- for: $\delta_{0,2} < \delta < \delta_{u,min}$ it has: $T = T_{u,1} + T_{u,2} + T_{u,3}$ (2.18)

Finally, from overall wall's relations, it can see that:

- the elastic tract ends when the elastic limit is reached, as lesser of all piers;
- traits intermediates are elastic-plastic and have decreasing stiffness;
- the plastic tract is limited by the ultimate displacement, as minimum of all piers.

2.1.5 Ministerial Decree 20/11/1987

This law [20] contains provisions about the design, execution and testing of masonry structures in non–seismic zone.

The topics that define the analysis procedures are the follows:

- it is defined the type of mortars and the elements (natural or artificial) that constitute the walls, including all mechanical properties;
- they are defined construction details to ensure box behavior of structure including the minimum thickness required of the masonry walls;
- it defines a method of sizing simplified approach for small and simple masonry structures;
- it is permitted to use both the method of verifying with admissible stresses and the limit state verification method;
- it is prescribed verification of masonry walls both flexural and sliding shear failure.

In the code in question they are then specified some important details of the methods adopted for the consolidation of the buildings (existing) in masonry. In practice, the consolidation is required when there is a change (with extensions, elevations, changes of use) of the existing structure.

This standard, respect to previous that deal the seismic problem, mainly produces some helpful tips for planning with "law of the art" both new structures and to address the problems of existing structures. However, in the case of buildings in seismic zones, is necessary but not sufficient to verify the specifications contained in this standard but it must be taken to guard against an earthquake.

2.1.6 Ministerial Decree 16/01/1996

For many years, these two documents [19][21] have been applied for the analysis of structures in seismic zones. The main importance of Ministerial Decree 1996 [19] derives by the possibility to use both admissible stresses method and Ultimate Limit States (ULS) method. Also, the concept of reinforced masonry structure was introduced.

A major innovation of this decree compared to the previous is a new design of masonry structures. They were, in fact, changed the indications on the strength of materials and the minimum thickness of the wall.

For smaller and simpler structures, this rule allows a much simpler design, which would exclude from the consideration and conduct a real seismic verification. It should, however, in these cases, follow a set of stringent structural details that often cannot be satisfied and would affect the architectural design and appearance of the building, which should aim to having a box–behaviour.

The Commentary No. 65 [21] imposes to consider a q-factor equal to 2,0 for masonry buildings and new construction. This leads us to consider the analysis of seismic action, new walls, substantially equal to half of what it should be considered for existing masonry structures, of the same characteristics.

2.1.7 O.P.C.M. No. 3274 of 2003 and O.P.C.M. No. 3431 of 2005

The Ordinance of the President of the Council of Ministers No. 3274 of 20/03/2003 [22] is entitled "First elements on the general criteria for national seismic classification and technical standards for construction in seismic zones". Of particular importance is Annex 2 of this Ordinance that contains "Technical standards for the design, seismic evaluation and adaptation of buildings".

This Ordinance, after a period of overlap with the previous Ministerial Decree 1996 [19], however remained in force, was updated later and corrected by the next two years after Ordinance No. 3431.

As for Annex 2 they should be considered, as regards the masonry, Chapter 8 for new structures and Chapter 11 for existing structures.

These laws have a special value because they apply both to new and existing structures that need modifications. In addition, these documents shall apply to all strategic buildings and to infrastructure projects, which are necessary for civil protection interventions during and after earthquakes. For all these buildings, Ordinance No. 3274, provided the evaluation of the level of vulnerability.

This code is a revolution compared to previous seismic standards with regard to the analysis and verification of construction submitted to the earthquake. In fact, this document introduces the latest research results in the range of earthquake engineering.

With regard to existing structures, however, the Ordinances distinguish two main types of intervention on the buildings in seismic areas:

1) intervention for improvement: it involves performing of one or more works on the individual structural elements of the building with the purpose to achieve a higher degree of security but it doesn't substantially change the overall behaviour;

2) seismic retrofitting intervention: it involves performing a series of operations sufficient to make the building able to resist to seismic action.

Regarding the seismic analysis, introduces the concept and the equations necessary to obtain the response spectrum in terms of acceleration, for the definition of seismic actions.

In addition, similar to what is stipulated by the existing rules, important indications for definition of the q-factor that must be used to take into account the dissipative capacity of the structure were introduced.

Ultimately, the seismic action applied to the generic floor is:

$$F_i = F_h \cdot \frac{z_i \cdot W_i}{\sum\left(z_j \cdot W_j\right)}, \tag{2.19}$$

where:

- the seismic design base shear is:

$$F_h = S_d\left(T_1\right) \cdot \lambda \cdot \frac{W}{g}; \tag{2.20}$$

- W_i and W_j are the weights at the i and j floors;
- z_i and z_j are the heights of floors i and j from foundations;
- $S_d(T_1)$ is the ordinate of the design response spectrum at the fundamental period of vibration corresponding to the first modal form;
- W is the weight of the combined seismic construction;
- λ is a factor that depends by the number of plans and that is 0,85 up three floors and 1,00 over three floors.

2.2 Overview of the codes currently in force in Europe

The regulatory framework currently existing include:

1) "Approval of new technical regulations for Construction" – D.M. Infrastructure of the 14/01/2008 [6];
2) Commentary No. 617 of 02/02/2009 of the Higher Council of Public Works – “Guidelines for application of new technical regulations for Construction” [23].

They are also in force:

3) Law No. 1086 of the 1971 entitled “Rules for the discipline of works in normal and precompressed reinforced cement conglomerate, and metal structure” [24];
4) Law No. 64 of the 1974 entitled “Measures for buildings with special requirements for seismic zones” [25].

For existing masonry structures they must also be applied documents produced by the CNR for the methods of application of FRP materials:

5) “Guidelines for the design, execution and control of static works of consolidation through the use of fiber–reinforced composites” - CNR - DT 200/2004 - Revision 2008 [26];
6) “Guidelines for the design, implementation and testing of interventions for strengthening of reinforced concrete structure, r.c.p. and masonry using FRP” of the Higher Council of Public Works [27].

Finally, to structures of historical and cultural interest, they must be considered the requirements of:

7) “Guidelines for seismic risk assessment and mitigation of cultural heritage with regard to technical standards for construction” made by the High Council of Public Works in 2006 [5].

2.2.1 National codes: NTC 2008 and Commentary No. 617

The NTC 2008 say that the load-bearing masonry construction must be designed to resist both vertical and horizontal actions. The topic of masonry is dealt by the standard as follows:

- in paragraph 4.5: civil and industrial constructions;
- in paragraph 7.8: design for seismic forces;
- in paragraph 8.7.1: evaluation and design in presence of existing structures for seismic actions;
- in paragraph 11.10: materials and products for structural use.

2.2.1.1 Material properties

The walls can be realised with the use of such artificial elements (bricks, Table 2.3, or concrete, Table 2.4) or natural elements (stones). The brick elements are classified in according to the percentage of hole.

Table 2.3: Classification of brick elements [6].

Elements	Percentage of hole φ	Area of the hole cross section f
Full	$\varphi \leq 15\%$	$f \leq 9\ cm^2$
Semi full	$15\% < \varphi \leq 45\%$	$f \leq 12\ cm^2$
Holed	$45\% < \varphi \leq 55\%$	$f \leq 15\ cm^2$

Table 2.4: Classification of concrete elements [6].

Elements	Percentage of hole φ	Area of the hole cross section f	
		$A \leq 900\ cm^2$	$A > 900\ cm^2$
Full	$\varphi \leq 15\%$	$f \leq 0{,}10\ A$	$f \leq 0{,}15\ A$
Semi full	$15\% < \varphi \leq 45\%$	$f \leq 0{,}10\ A$	$f \leq 0{,}15\ A$
Holed	$45\% < \varphi \leq 55\%$	$f \leq 0{,}10\ A$	$f \leq 0{,}10\ A$

In paragraph 4.5.4 they are defined the following minimum thicknesses:

- masonry with full artificial resistant elements: 150 mm;
- masonry with artificial and semi full resistant elements: 200 mm;
- masonry with hollow resistant elements: 240 mm;
- square stone masonry: 240 mm;
- listed stone masonry: 400 mm;

- not square stone masonry: 500 mm.

The conventional slenderness, useful for controlling second order effects, is defined as:

$$\lambda = \frac{h_0}{t}, \tag{2.21}$$

where:

- h_0 is the free length of inflection;
- t is the thickness of the wall.

The design values of the compressive and shear strengths can be evaluated as follows:

$$f_d = \frac{f_k}{\gamma_M}; \qquad f_{vd} = \frac{f_{vk}}{\gamma_M}, \tag{2.22}$$

where:

- f_k is the characteristic compressive strength of masonry;
- f_{vk} is the characteristic shear strength of masonry, as estimated by the relationship:

$$f_{vk} = f_{vk0} + 0{,}4 \cdot \sigma_n; \tag{2.23}$$

- f_{vk0} is the characteristic strength shear in the absence of axial force;
- σ_n is the mean normal stress;
- γ_M is the partial safety factor of the material (see Table 2.5).

The document defines two classes of wall execution, 1 and 2. The first class is one that involves the use of better qualified staff and better controls on materials.

Table 2.5: Values of γ_M coefficient [6].

Material	Execution class	
	1	2
Masonry with resistant elements of Class I, mortar with guaranteed performance	2,0	2,5
Masonry with resistant elements of Class I, mortar with prescribed performance	2,2	2,7
Masonry with resistant elements of Class II, all types of mortar	2,5	3,0

For the verifications to ULS, the regulations defines a reduced unitary resistance of project referred to structural element like:

$$f_{d,rid} = \Phi \cdot f_d \,. \tag{2.24}$$

The reductive coefficient is defined in the Table 2.6 as a function of slenderness ratio and eccentricity m.

Table 2.6: Φ coefficient values with the assumption of hinged joints [6].

Slenderness λ	Eccentricity factor m = 6 e / t				
	0,0	0,5	1,0	1,5	2,0
0	1,00	0,74	0,59	0,44	0,33
5	0,97	0,71	0,55	0,39	0,27
10	0,86	0,61	0,45	0,27	0,16
15	0,69	0,48	0,32	0,17	---
20	0,53	0,36	0,23	---	---

The free span of inflection can be:

$$h_0 = \rho \cdot h\,, \tag{2.25}$$

where:

- ρ is a factor which takes into account the effectiveness of the constraint of orthogonal walls;
- h is the height of the entire plan.

The coefficient of eccentricity is defined as:

$$m = 6 \cdot \frac{e}{t}\,. \tag{2.26}$$

Where “e” is the total eccentricity due to eccentricity of vertical loads, the tolerances of execution and the horizontal actions.

The eccentricity of the total vertical loads are:

$$e_{s1} = \frac{N_1 \cdot d_1}{N_1 + \sum N_2}\,; \quad e_{s2} = \frac{\sum N_2 \cdot d_2}{N_1 + \sum N_2}\,; \tag{2.27}$$

where:

- e_{S1} is the eccentricity of the resultant of the loads transmitted from the walls of the upper floors from the mid-plane of the wall to be tested;
- e_{S2} is the eccentricity of the support reactions of the floors above it in the verification section;
- N_1 is the load transmitted from the wall above assumed centered to the wall;
- N_2 is the support reaction of the floors above the wall to be tested;
- d_1 is the eccentricity of N_1 compared to the median plane of the wall to be tested;
- d_2 is the eccentricity of N_2 compared to the median plane of the wall to be tested.

The eccentricity due to the tolerance execution has assumed:

$$e_a = \frac{h}{200}. \tag{2.28}$$

The eccentricity due to the horizontal actions, hypothesised perpendicular to the wall, is:

$$e_v = \frac{M_v}{N}, \tag{2.29}$$

where:

- M_v is the maximum bending moment due to the horizontal actions;
- N is the normal stress in the verification section.

The previous eccentricity must be combined to obtain:

$$e_1 = |e_s| + e_a; \qquad e_1 = \frac{e_1}{2} + |e_v|; \tag{2.30}$$

must result:

$$e_1 \le 0{,}33 \cdot t; \qquad e_2 \le 0{,}33 \cdot t; \tag{2.31}$$

Technique norms [6][23] allows, for simple structures, a simplified verification to admissible stresses, by imposing:

$$\gamma_M = 4{,}2. \tag{2.32}$$

For simplified sizing of the structure, the following limitations must be respected:

a) the walls must be continuous from foundation to the extremities;
b) the inter-floor height must be less than 3,5 m;
c) the maximum number of floors is three to ordinary masonry and four to reinforced masonry;
d) the building's plan should be inscribed in a rectangle with a ratio between the shorter side and longer side not less than 1/3;
e) slenderness of the wall never exceeding 12;
f) variable load on the floors less than 3,00 kN/m^2.

The simplified verification is to investigate that it is:

$$\sigma = \frac{N}{0{,}65 \cdot A} \leq \frac{f_k}{\gamma_M}. \tag{2.33}$$

where:

- N is the vertical load at the base of each floor of the building which is the sum of permanent and variable loads (assuming $\gamma_g = \gamma_q = 1$);
- A is the total area of load-bearing walls on the same floor.

In the case of walls under horizontal actions, simplified verification can only be done if, in addition to the above conditions, they are fulfilled the following requirements:

a) regular structure in plan and elevation;
b) along the two directions in plan must be at least two walls with an overall length, exclusive of openings, each not less than 50% of the size of the building in the same direction. In addition, the distance between the two masonry walls must be greater than 75% of the size of the building at

orthogonal direction to the walls. Finally, 75% of the vertical loads must be carried by earthquake resistant walls;

c) in each direction they must be present earthquake resistant walls at intervals not exceeding 7 m, which may be increased to 9 m for reinforced masonry;

d) for each floor, the ratio of the area of cross section of the walls and the gross floor area not less than indicated in the Table 2.7.

Table 2.7: Area resistant walls in each orthogonal direction to simple constructions [6].

Pick ground acceleration S a_g		≤0,07g	≤0,1g	≤0,15g	≤0,20g	≤0,25g	≤0,30g	≤0,35g	≤0,40g	≤0,45g	≤0,4725g
Type of structure	Number of floor										
Ordinary masonry	1	3,5 %	3,5 %	4,0 %	4,5 %	5,0 %	5,5 %	6,0 %	6,0 %	6,0 %	6,5 %
	2	4,0 %	4,0 %	4,5 %	5,0 %	5,5 %	6,0 %	6,5 %	6,5 %	6,5 %	7,0 %
	3	4,5 %	4,5 %	5,0 %	5,5 %	6,0 %	6,5 %	7,0 %			
Reinforced masonry	1	2,5 %	3,0 %	3,0 %	3,0 %	3,5 %	3,5 %	4,0 %	4,0 %	4,5 %	4,5 %
	2	3,0 %	3,5 %	3,5 %	3,5 %	4,0 %	4,0 %	4,5 %	5,0 %	5,0 %	5,0 %
	3	3,5 %	4,0 %	4,0 %	4,0 %	4,5 %	5,0 %	5,5 %	5,5 %	6,0 %	6,0 %
	4	4,0 %	4,5 %	4,5 %	5,0 %	5,5 %	5,5 %	6,0 %	6,0 %	6,5 %	6,5 %

The geometry of the earthquake resistant walls, as indicated in paragraph 7.8.1.4 of the NTC 2008 [6], must respect the requirements listed in the Table 2.8, where:

- h' is the maximum height of the openings adjacent to the wall;
- l is the length of the wall.

It must be for each floor:

$$\sigma = \frac{N}{A} \leq 0{,}25 \cdot \frac{f_k}{\gamma_M}. \tag{2.34}$$

Table 2.8: Geometric requirements of earthquake resistant walls [6].

Type of structures	t_{min}	$(\lambda=h_0/t)_{max}$	$(l/h')_{min}$
Ordinary masonry, made with stone squat elements	300 mm	10	0,5
Ordinary masonry, made with artificial elements	240 mm	12	0,4
Reinforced masonry, made with artificial elements	240 mm	15	Whatever
Ordinary masonry, made with stone squat elements, in sites in zone 3 and 4	240 mm	12	0,3
Masonry made with artificial semi full elements, in sites in zone 4	200 mm	20	0,3
Masonry made with artificial full elements, in sites in zone 4	150 mm	20	0,3

The legislation [6], in paragraph 7.8.2, defines the safety verifications to be used to masonry structures. In the next part they are shown the relationships that permit to define:

- ultimate moment;
- shear strength.

In paragraph 11.10, they are defined the checks of the mechanical properties of the walls and the resistance of the masonry constituents, as well as various types of stone available.

The Table 2.9 shows the types of mortar and their strengths.

Table 2.9: Classes of mortars with guaranteed performance [6].

Class	M 2,5	M 5	M 10	M 15	M 20	M d
Compressive strength [N/mm^2]	2,5	5,0	10,0	15,0	20,0	d
d is a compressive strength greater than 25 N/mm^2 declared by the producer.						

The types of mortars with prescribed composition are shown in the following Table 2.10.

Table 2.10: Classes of mortars with prescribed composition [6].

Class	Type of mortar	Compositions				
		Cement	Air lime	Hydraulic lime	Sand	Pozzolana
M 2,5	Hydraulic	-	-	1	3	-
M 2,5	Pozzolana	-	1	-	-	3
M 2,5	Bastard	1	-	2	9	-
M 5	Bastard	1	-	1	5	-
M 8	Cement	2	-	1	8	-
M 12	Cement	1	-	-	3	-

The characteristic compressive strength of masonry can be determined using the following equation having known experimental results:

$$f_k = f_m - k \cdot s\,, \tag{2.35}$$

where:

- f_m is the mean resistance;
- s is the mean quadratic discard;
- k is a coefficient that depends on the number of samples (Table 2.11).

Table 2.11: Coefficient k values [6].

n	6	8	10	12	20
k	2,33	2,19	2,10	2,05	1,93

The law defines the characteristic resistance values depending by the type of mortar and characteristic resistance of the used element (see Table 2.12 and Table 2.13).

Table 2.12: f_k values for masonry with artificial element full and semi-full (in N/mm²) [6].

Characteristic compressive strength f_{bk} of the element N/mm²	Type of mortar			
	M 15	M 10	M 5	M 2,5
2,0	1,2	1,2	1,2	1,2
3,0	2,2	2,2	2,2	2,0
5,0	3,5	3,4	3,3	3,0
7,5	5,0	4,5	4,1	3,5
10,0	6,2	5,3	4,7	4,1
15,0	8,2	6,7	6,0	5,1
20,0	9,7	8,0	7,0	6,1
30,0	12,0	10,0	8,6	7,2
40,0	14,3	12,0	10,4	-

Table 2.13: f_k values for masonry with natural element full and semi-full (in N/mm²) [6].

Characteristic compressive strength f_{bk} of the element N/mm²	Type of mortar			
	M 15	M 10	M 5	M 2,5
2,0	1,0	1,0	1,0	1,0
3,0	2,2	2,2	2,2	2,0
5,0	3,5	3,4	3,3	3,0
7,5	5,0	4,5	4,1	3,5
10,0	6,2	5,3	4,7	4,1
15,0	8,2	6,7	6,0	5,1
20,0	9,7	8,0	7,0	6,1
30,0	12,0	10,0	8,6	7,2
40,0	14,3	12,0	10,4	-

The characteristic compressive strength in natural elements is obtained from the mean resistance:

$$f_{bk} = 0{,}7 \cdot f_{bm} \,. \tag{2.36}$$

The characteristic shear strength in the absence of normal stress can be obtained from the mean using the following relationship:

$$f_{vk0} = 0{,}7 \cdot f_{vm} . \tag{2.37}$$

The characteristic shear strength above can be obtained from the Table 2.14, depending on the type of element resistance and the resistance of the mortar.

Table 2.14: Characteristic shear resistance in absence of normal stress f_{vk0} (in N/mm²) [6].

Type of element	Characteristic compressive strength f_{bk} of the element [N/mm²]	Class of mortar	f_{vk0} [N/mm²]
Full or semi full brick	$f_{bk} > 15$	M 10 ≤ M ≤ M 20	0,30
	$7{,}5 \le f_{bk} \le 15$	M 5 ≤ M ≤ M 10	0,20
	$f_{bk} \le 7{,}5$	M 2,5 ≤ M ≤ M 5	0,10
Concrete, calcium silicate, autoclaved cement, natural squat stone	$f_{bk} > 15$	M 10 ≤ M ≤ M 20	0,20
	$7{,}5 \le f_{bk} \le 15$	M 5 ≤ M ≤ M 10	0,15
	$f_{bk} \le 7{,}5$	M 2,5 ≤ M ≤ M 5	0,10

Finally, the secant modulus of elasticity is:

$$E = 1000 \cdot f_k , \tag{2.38}$$

and the shear secant modulus of elasticity is:

$$G = 0{,}4 \cdot E . \tag{2.39}$$

With regard to the existing masonry buildings, Commentary No. 617 [23] defines, in the Appendix C8A, the levels of knowledges (LC) reported in the Table 2.15. These levels are obtained through detailed investigations and tests on samples of material. With increasing of the quality of these investigations the level of knowledge rises (from first to third) and decreases the value of the confidence factor (FC) which is proportional to the uncertainties of the analysis.

It is possible distinguish the following situations:

1) LC1 as "limited level of knowledge";

2) LC2 as "adequate level of knowledge";

3) LC3 as "accurate level of knowledge".

By knowing the level of knowledge (defined in Table 2.15) it's possible to use the Table 2.16 and Table 2.17 for to obtain the strength, elastic modulus and other properties for existing masonry structures.

Table 2.15: Levels of knowledges [6].

Level of knowledges	Geometry	Structural detail	Material properties	Analysis methods	FC
LC1	Investigation about masonry, vaults, floors, staircases, load, foundation, crack pattern.	Limited on site verification	Limited on site investigation. Strength: minimal value of Tab. C8A2.1. Elastic modulus: mean value of Tab. C8A2.1.	All	1,35
LC2		Complete on site verification	Extensive on site investigation. Strength: mean value of Tab. C8A2.1. Elastic modulus: mean value of the tests or of the Tab. C8A2.1.		1,20
LC3			Exhaustive on site investigation. CASE A Strength: mean of the value of the test. Elastic modulus: mean value of the tests or of the Tab. C8A2.1. CASE B Strength: if mean experimental value is between mean value in Tab. C8A.2.1, mean value in Tab. C8A.2.1; is mean experimental value greater than maximum extreme of the Tab. C8A.2.1, this one; if mean experimental value less than C8A2.1, mean experimental value. Elastic modulus: like LC3 CASE A. CASE C Strength: if mean experimental value is between mean value in Tab. C8A.2.1 or greater, mean value in Tab. C8A.2.1; if mean experimental value less than C8A2.1, mean experimental value. Elastic modulus: like LC3 CASE A.		1,00

Table 2.16: Reference values of mechanical parameters [23].

Type of masonry	f_m [N/cm^2]	τ_0 [N/cm^2]	E [N/mm^2]	G [N/mm^2]	W [kN/m^3]
	Min - Max	Min - Max	Min - Max	Min - Max	
Irregular stone masonry	100	2,0	690	230	19
	180	3,2	1050	350	
Few squat stone masonry	200	3,5	1020	340	20
	300	5,1	1440	480	
Regular stone masonry	260	5,6	1500	500	21
	380	7,4	1980	660	
Soft stone masonry (tuff, limestone)	140	2,8	900	300	16
	240	4,2	1260	420	
Squat stone masonry	600	9,0	2400	780	22
	800	12,0	3200	940	
Masonry with full brick and lime mortar	240	6,0	1200	400	18
	400	9,2	1800	600	
Masonry with semi full brick and cement mortar	500	24	3500	875	15
	800	32	5600	1400	
Masonry with semi full brick	400	30,0	3600	1080	12
	600	40,0	5400	1620	
Masonry with semi full brick without vertical mortar joints	300	10,0	2700	810	11
	400	13,0	3600	1080	
Masonry with concrete elements	150	9,5	1200	300	12
	200	12,5	1600	400	
Masonry with semi full concrete elements	300	18,0	2400	600	14
	440	24,0	3520	880	

Legend

Reference values of mechanical parameters (minimum and maximum) and mean specific weight for different types of masonry, refer to the following conditions: low mortar characteristics, lack of complaints (listature), vestments simply linked or bad combined, unconsolidated masonry, textures (in the case of regular elements) in a art's rule manner.

f_m = mean masonry compressive strength;

τ_0 = mean masonry shear strength;

E = modulus of elasticity mean value;

G = modulus of elasticity tangential mean value;

W = mean weight per unit volume of masonry.

Table 2.17: Correction factors of the mechanical parameters [23].

Type of masonry	Good mortar	Thickness of mortar < 10 mm	Masonry with layers of bricks	Transversal connections	Bed internal masonry	Injections of mortar	Reinforced plaster
Irregular stone masonry	1,5	-	1,3	1,5	0,9	2,0	2,5
Few squat stone masonry	1,4	1,2	1,2	1,5	0,8	1,7	2,0
Regular stone masonry	1,3	-	1,1	1,3	0,8	1,5	1,5
Soft stone masonry (tuff, limestone)	1,5	1,5	-	1,5	0,9	1,7	2,0
Squat stone masonry	1,2	1,2	-	1,2	0,7	1,2	1,2
Masonry with full brick and lime mortar	1,5	1,5	-	1,3	0,7	1,5	1,5

Legend

Correction factors of the mechanical parameters to be applied in the presence of: good or very good mortar characteristics, thin joints, recourse or listature, systematic transversal connections, especially bad and/or large internal core; consolidation by injection of mortar, plaster, consolidation with reinforced plaster.

The level of knowledge acquired is a function of: knowledge of structural geometry, knowledge of construction details, knowledge of materials.

The knowledge of structural geometry consists on the investigation of the size of all elements: walls, floors, roofs, stairs, vaults and foundations' building and in the design and interpretation of crack pattern.

The knowledge of structural details derived from the study of:

- quality of the links between vertical walls;
- quality of connections between floors and walls and presence of any floor beams;
- existence of architraves with good load–bearing capacity;
- existence of pushing elements and any elimination elements of the push;
- existence of elements with heightened vulnerability;
- types of masonry.

The knowledge of materials requires: the measurement of the mechanical characteristics of mortar joints and elements (stone or gravel), the investigation of texture and staggering of the joints, the investigation of the presence of any transversal links.

For details of construction are distinguished:

- limited on-site verifications: operations are based on visual investigation of a sample, with removal of the plaster, essays on the walls and the detachable.;
- extensive and comprehensive on–site verifications: investigations are based on visual investigation, with removal of the plaster, stripped of detachable between vertical walls and between walls and floors. The examination is extended to the entire building.

For the investigation of materials they can be distinguished:

- limited on-site investigations: they are information accessible through the data on the existing technical literature at the time of construction and

using the above Tables 2.15 – 2.17. Also in this case it must remove the plaster and to find the elements used and the strength of the mortar;

- extensive on-site investigations: they compared to previous investigations, but they also required a strength test on any type of existing masonry. In addition but not as a substitute for destructive tests they can be used the non-destructive investigation techniques;
- exhaustive on-site investigations: they compared to previous operations, the experimental tests are carried out in order to evaluate the mechanical properties of masonry. Experimental tests are conducted on-site or in the laboratory on undisturbed samples.

2.2.1.2 Seismic actions

According to the NTC 2008 [6], the limit states that can be considered in earthquake combination are:

1) Operativity Limit State (OLS);
2) Damage Limit State (DLS);
3) Preservation of Life Limit State (PLS);
4) Collapse Prevention Limit State (CLS).

The first two limit states are Service Limit States (SLS, Table 2.18), the other ones are the Ultimate Limit States (ULS, Table 2.19). For each of the previous limit states they are defined the seismic action (in the form of spectrum of demand) and performance that the structure must ensure.

Table 2.18: Performance of the Service Limit State [6].

Operativity Limit State (OLS)
A result of the earthquake, the building as a whole, including the structural elements, non-structural elements, relevant equipment to its function does not suffer significant damage and interruption of use.
Damage Limit State (DLS)
A result of the earthquake, the building as a whole, including the structural elements, non-structural elements, equipment relevant to its function, is damaged should not put users at risk and not compromise significantly the capacity of strength and rigidity against vertical and horizontal actions, but remaining immediately usable after the interruption of use of some equipment.

In any case, to carry out interventions on existing structures, a good level in advanced knowledge (LC) must be reached.

The investigation of the damage levels (see Table 2.20) consists mainly in the observation and understanding of lesions and collapse that may affect, in most cases:

1) load bearing and no load-bearing walls (internal divisions and external);
2) vaults and arcs;
3) floors and horizontal elements of any type;
4) roofs.

Table 2.19: Performance of the Ultimate Limit State [6].

Preservation of Live Limit State
A result of the earthquake the building suffered cracks and collapse of nonstructural components and plant components and significant structural damage which is associated with a significant loss of stiffness against horizontal actions, the construction preserves a part of the resistance and stiffness for vertical actions and a safety margin against collapse for horizontal seismic actions.
Collapse Prevention Limit State
Following the earthquake, the building suffered serious cracks and collapses of nonstructural components and plant and serious damage of structural components, the building still has a margin of safety measures vertical actions and a small safety margin against collapse due to horizontal actions.

Both for the choice of method of analysis and for to evaluate the q-factor adopted, the regularity of the structure must be checked. The following Table 2.21 summarises, for a generic structure under consideration, the conditions of regularity in plan and height.

Table 2.20: Damage levels [6].

Damage level	Masonry walls	Vaults	Floors	Ceiling
A - Small	Each cracks, 1 mm thickness.	Cracks until of 2 mm thickness without tie beams; until of 1 mm thickness with tie beams.	Cracks parallel to the beams and with 1 mm thickness.	Fall of a few roof tiles on the border.
B - Middle	Cracks of types 1 – 2 – 3, until 4 mm thickness. Cracks of types 4 – 5 – 6, until 2 mm thickness.	Cracks of types 1v and 2v, until 4 mm thickness, without tie beams and until 2 mm with tie beams. Cracks 1v – 3v without tie beams.	Cracks like A case until 4 mm. Damages of the wood floors in secondary structures.	Damages of the secondary structures. Displacement of the main beams until 4 mm.
C – Serious	Cracks of types 1 – 2 – 3, until 8 mm thickness. Cracks of types 4 – 5 – 6, until 4 mm thickness. Damages of types 7 – 8 – 9.	Cracks of types 1v and 2v, until 8 mm thickness, without tie beams and until 4 mm with tie beams. Several cracks 1v – 3v without tie beams.	Several separation between floors and walls. Damages like 8 but more big. Some collapse in the elements of the secondary structures.	Damages of the secondary structures. Displacement of the main beams until 40 mm.
D – Very serious	More damages of the case C.	More damages of the case C.	Some collapse of the main structure. General collapse in the elements of the secondary structures. Several separation between floors and walls.	Some partial collapse. Fall of the main beams.

Table 2.21: Regularity requirements [6].

REGOLARITY IN PLACE OF THE STRUCTURE	
The plant configuration is compact and approximately symmetric about two orthogonal directions, in relation to the distribution of mass and stiffness.	YES or NOT
The relationship between the sides of a rectangle that is inscribed on the building is less than 4.	YES or NOT
No returns or projections of any size exceeds 25% of the total size of the building in the corresponding direction.	YES or NOT
The floors can be considered infinitely rigid in their plan respect to the vertical elements and sufficiently resistant.	YES or NOT
REGOLARITY IN HEIGTH OF THE STRUCTURE	
All vertical resistant systems (such as frames and walls) extend throughout the height of the building.	YES or NOT
Mass and stiffness remain constant or change gradually, without abrupt changes from base to top of the building (the mass change from floor to floor does not exceed 25%, the stiffness is not reduced from one floor to the overlying more than 30 % and does not increase more than 10%) for stiffness can be considered regular in high the structures with walls or cores in concrete or masonry and cores of constant section in the height or with upwind steel frames, which has given at least 50% of the seismic base.	YES or NOT
In frame structures designed in CD "B" the relationship between effective resistance and strength required by the analysis is not significantly different for different floors (the ratio between the actual and the required resistance, defined at a generic floor must not differ more than 20% determined from the analogous relationship to another floor) can be done except the last floor of frame structures of at least three floors.	YES or NOT
Any constrictions of the horizontal section of the construction occur in a gradual way from one floor to the next, respecting the following restrictions: for each return floor does not exceed 30% of the size corresponding to the first floor, or 20% of the size corresponding to the horizontal elements immediately below. One exception is the last floor of at least four floors of buildings for which there are no limitations to shrinkage.	YES or NOT

The analysis of seismic forces is done using the requirements of the NTC 2008. The code [6] for buildings with characteristics of regularity in plan and height, in view of an equivalent static analysis, allows us to consider a distribution of seismic forces along the height congruent with the first modal shape of the building. For this reason, the seismic actions to be applied at each level can be obtained using the following relationship:

$$F_{hi} = F_h \cdot \frac{z_i \cdot W_i}{\sum_j z_j \cdot W_j}, \tag{2.40}$$

where:

- F_h is the design base shear, amounting to:

$$F_h = S_d(T_1) \cdot \lambda \cdot \frac{W}{g}; \tag{2.41}$$

- z_i and z_j are the quotas of the masses i and j (floor) from the plane of the foundations;
- $S_d(T_1)$ is the ordinate of the response spectrum of design;
- T_1 is the period of vibration of the structure;
- λ is a coefficient equal to 0,85 for structures up to three floors and where $T_1 < T_c$ and equal to 1,00 for the other cases;
- W is the weight of the structure in seismic combination;
- g is the acceleration of gravity.

The natural period of vibration can be obtained with the simplified relation:

$$T_1 = C_1 \cdot H^{3/4}. \tag{2.42}$$

For regular structures in height, it can take:

$$k_R = 1. \tag{2.43}$$

For ordinary masonry buildings with two or more existing floors it is (Par C8.7.1.2, see Table 2.22):

$$\frac{\alpha_u}{\alpha_1} = 1{,}5. \tag{2.44}$$

Table 2.22: Values of q_0 for different structural types [6].

Structural typology	q_0
Ordinary masonry buildings	2,0 α_u / α_1
Reinforced masonry buildings	2,5 α_u / α_1
Reinforced masonry buildings designed with GR	3,0 α_u / α_1

The q–factor is, finally:

$$q = k_R \cdot q_0 \,. \tag{2.45}$$

The structure factor will allow to pass from the elastic response spectrum to the design response spectrum, and it has used for the analysis of spectral acceleration needed for the analysis of the seismic action.

The seismic analysis according to NTC 2008 may be conducted from the knowledge of the geographical coordinates of the structure to be analysed, for example:

Latitude	40,9228	°
Longitude	14,7837	°

Interpolating the values in Table 1, Appendix B of the NTC 2008, the following parameters of seismic hazard reported in Table 2.23 can be obtained.

Table 2.23: Seismic hazard parameters [6].

Limit state		T_R	a_g	F_0	T^*_c
		[years]	[g]	[]	[s]
SLS	Operativity	30	0,053	2,343	0,282
	Damage	50	0,069	2,320	0,310
ULS	Life safety	475	0,193	2,372	0,367
	Collapse prevention	975	0,249	2,434	0,377

The nominal life of the structure (Table 2.24) is an index of the number of years that the structure can support without the need of extraordinary maintenance work. Based on this value, the return period of seismic action can be calculated.

Table 2.24: Nominal life for different types of building [6].

Types of buildings		Nominal life V_N [years]
1	Provisional buildings	≤ 10
2	Ordinary buildings	≥ 50
3	Big buildings	≥ 100

Table 2.25: Values of the use coefficient [6].

Use class	I	II	III	IV
Use factor C_U	0,7	1,0	1,5	2,0

The reference period is:

$$V_R = c_u \cdot V_N . \tag{2.46}$$

Where C_U is the use coefficient reported in Table 2.25.

The probability of overcoming during the reference period is indicated by P_{VR} and indicates what is the probability that in a number of years equal to the return period the real seismic event is more than the design seismic event (see Table 2.26).

Table 2.26: Probability of overcoming at vary limit state considered [6].

Limit state		P_{VR}: Probability of overcoming in the reference period V_R
Service Limit State (SLS)	OLS	81 %
	DLS	63 %
Ultimate Limit State (ULS)	PLS	10 %
	CLS	5 %

The return period of the seismic action is considered:

$$T_R = -\frac{V_R}{\log(1 - P_{VR})} . \tag{2.47}$$

The category of subsoil (show in Table 2.27 and Table 2.28) and the stratigraphy (see Table 2.29) express the geological characteristics of the place where there is the building to verify. Those factors (shows in Table 2.30 and Table 2.31) are very important because the geological nature of the soil and subsoil can affect the propagation and possible amplification of seismic waves in the transition from the hypocenter to the epicenter.

Table 2.27: Category of subsoil [6].

Category	Description
A	Emerging rock masses or very rigid soil
B	Fine grain consisting soil
C	Fine grain mildly consisting soil
D	Fine grain low consisting soil
E	Type C or D soils with thickness not more than 20 m

Table 2.28: Additional category of subsoil [6].

Category	Description
S1	Soils with VS30 < 100 m/s
S2	Soils susceptible of liquefaction

Table 2.29: Topographical category [6].

Category	Characteristics of the topographical surface
T1	Surface with inclination i ≤ 15°
T2	Surface with inclination i > 15°
T3	Surface with inclination 15° ≤ i ≤ 30°
T4	Surface with inclination i > 30°

The equations of the traits of the elastic response spectrum are:

- $S_e(T) = a_g \cdot S \cdot \eta \cdot F_0 \cdot \left[\frac{T}{T_B} + \frac{1}{\eta \cdot F_0} \cdot \left(1 - \frac{T}{T_B}\right)\right]$ for $0 < T < T_B$; (2.48)
- $S_e(T) = a_g \cdot S \cdot \eta \cdot F_0$ for $T_B < T < T_C$; (2.49)
- $S_e(T) = a_g \cdot S \cdot \eta \cdot F_0 \cdot \left(\frac{T_C}{T}\right)$ for $T_C < T < T_D$; (2.50)
- $S_e(T) = a_g \cdot S \cdot \eta \cdot F_0 \cdot \left(\frac{T_C \cdot T_D}{T^2}\right)$ for $T_D < T$, (2.51)

where:

- $S = S_S \cdot S_T$; (2.52)
- $\eta = \sqrt{\frac{10}{(5+\xi)}} \geq 0{,}55$; (2.53)
- $T_C = C_C \cdot T_C^*$; (2.54)
- $T_B = \frac{T_C}{3}$; (2.55)

- $T_D = 4{,}0 \cdot \frac{a_g}{g} + 1{,}6$. (2.56)

Table 2.30: Expressions of S_S and C_C [6].

Subsoil category	S_S	C_C
A	1,00	1,00
B	$1{,}00 \le 1{,}40 - 0{,}40 \cdot F_0 \cdot \frac{a_g}{g} \le 1{,}20$	$1{,}10 \cdot \left(T_C^*\right)^{-0{,}20}$
C	$1{,}00 \le 1{,}70 - 0{,}60 \cdot F_0 \cdot \frac{a_g}{g} \le 1{,}50$	$1{,}05 \cdot \left(T_C^*\right)^{-0{,}33}$
D	$1{,}00 \le 2{,}40 - 1{,}50 \cdot F_0 \cdot \frac{a_g}{g} \le 1{,}80$	$1{,}25 \cdot \left(T_C^*\right)^{-0{,}50}$
E	$1{,}00 \le 2{,}00 - 1{,}10 \cdot F_0 \cdot \frac{a_g}{g} \le 1{,}60$	$1{,}15 \cdot \left(T_C^*\right)^{-0{,}40}$

Table 2.31: Values of the topographic amplification coefficient [6].

Topographic category	Position	S_T
T1	-	1,0
T2	On the top of a mountain	1,2
T3	On the top of a mountain	1,2
T4	On the top of a mountain	1,4

To summarise, in the example:

$$S = S_S \cdot S_T = 1{,}2 \,. \tag{2.57}$$

The damping coefficient is usually assumed:

$$\xi = 5\ \%, \tag{2.58}$$

then:

$$\eta = \sqrt{\frac{10}{(5+\xi)}} = 1. \tag{2.59}$$

The period of start of the tract with constant speed is:

$$T_C = C_C \cdot T_C^* = 0{,}493 s \,. \tag{2.60}$$

The period of start of the trait with constant acceleration is:

$$T_B = \frac{T_C}{3} \,. \tag{2.61}$$

The period of start of the trait with constant displacement is:

$$T_D = 4{,}0 \cdot \frac{a_g}{g} + 1{,}6\,. \tag{2.62}$$

Using the equations of the traits previously set out, the following elastic response spectrum can be obtained (see Figure 2.7).

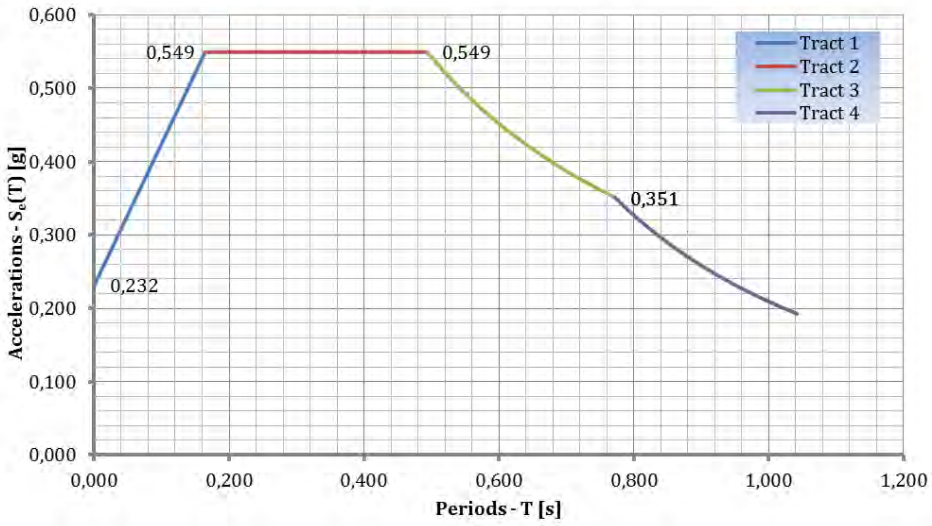

Figure 2.7: Typical Elastic response spectrum.

The design spectrum is obtained by scaling the elastic response spectrum with the q-factor, which replaces the coefficient η in the previous reports (see Figure 2.8).

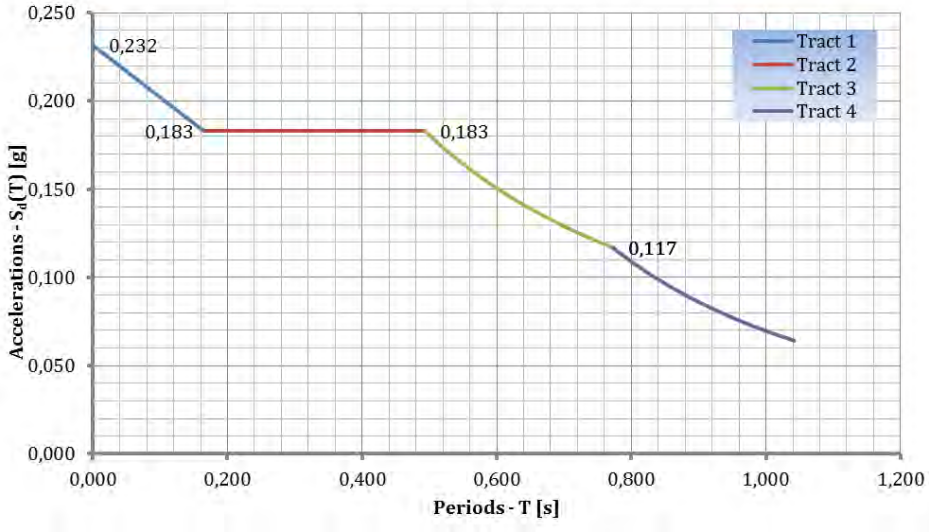

Figure 2.8: Typical Design spectrum.

The ordinate of the design spectrum, taken at the period T_1, is used for the analysis of the seismic action, provided that it is better than:

$$S_d(T_1)_{\min} = 0{,}2 \cdot a_g = 0{,}0386 \cdot [g] \quad (2.63)$$

2.2.1.2.1 Capacity models and ULS checks. Bending strength

The code [6] imposes to use the following expression, assuming a not linear distribution of compression, for calculating the ultimate bending moment of the wall panel:

$$M_u = \frac{1}{2} \cdot \sigma_0 \cdot t \cdot L^2 \cdot \left(1 - \frac{\sigma_0}{0{,}85 \cdot f_d}\right), \quad (2.64)$$

where:

- $\sigma_0 = \frac{P}{L \cdot t}$ is the normal stress averaged over the section;
- P is the vertical force perpendicular to the section in question;
- t is the thickness of the wall;
- L is the length of the wall;
- f_d is the design compressive strength.

All of this amounts to arguing for the maximum eccentricity of a load P always less than L/2:

$$e = \frac{M_u}{P} = \frac{M_u}{\sigma_0 \cdot t \cdot L} = \frac{1}{2} \cdot L \cdot \left(1 - \frac{\sigma_0}{0{,}85 \cdot f_d}\right). \tag{2.65}$$

The previous condition is often not checked on the upper floors of the structure due tallow values of vertical load P. In such cases a reinforced masonry with steel bars or FRP must be used.

2.2.1.2.2 Shear strength

The ultimate sliding shear in wall plan is evaluated using the following equation given in code [6]:

$$V_{Rd} = t \cdot D' \cdot f_{vd}, \tag{2.66}$$

where:

- $D' = 3 \cdot \left(\frac{L}{2} - e\right)$ is the length of the wall assuming a triangular distribution of compressive stresses;
- $e = \frac{M_{Ed}}{N_{Ed}}$ is the eccentricity of center of pressure;
- $f_{vd} = f_{vk0} + \mu \cdot \sigma_N$ analysis of the shear resistance of the masonry;
- $\mu = 0{,}4$ is the coefficient of friction;
- $\sigma_N = \frac{N_{Ed}}{t \cdot D'}$ is the average vertical stress on the compressed cross section.

The previous relationship provides a collapse of the panel to slide, and it is mostly used for new structures. For existing structures, however, the Commentary No. 617 [23] allows the possibility of evaluating a shear resistant very similar to the POR method [18], which provides a failure for diagonal cracking:

$$V_{Rd} = L \cdot t \cdot \frac{1{,}5 \cdot \tau_{0,d}}{b} \cdot \sqrt{1 + \frac{\sigma_0}{1{,}5 \cdot \tau_{0,d}}}\,, \tag{2.67}$$

where:

- L and t are the width and thickness of the wall;
- b = h/L is the ratio between the height and the width of the panel;
- $\tau_{0,d} = f_{vk0}$ is the shear strength of masonry;
- $\sigma_0 = N_{Ed}/(Lt)$ is the normal stress averaged over the whole panel.

2.2.1.3 Cultural heritage: Guidelines BBCC – DPC

These guidelines [5] deal with the assessment and mitigation the seismic risk faced by all those buildings which have a significant cultural interest. Italy, in particular, is full of such structures, which include for example, churches, monuments, historic and vintage buildings.

The protection of this heritage goes beyond the simple life safety objective but is aimed at preventing damage and protecting the building itself.

As proposed by these guidelines, in accordance with what is expected from the NTC 2008 [6], the following problems must be faced:

1) knowledge the building: to determine the mechanical properties of materials and geometric properties of the elements;
2) use of the most appropriate models for assessing the safety against seismic actions with the use of a static or dynamic analysis of linear or nonlinear types;
3) adoption of criteria needed for improving the seismic behaviour of the structure.

As regards the definition of seismic actions that must be considered, they are defined three different categories of importance of the buildings, for which an appropriate value of the probability of exceedance of the seismic action in the standard period of 50 years, with reference to ULS and DLS analysis, can be chosen in Table 2.32 or Table 2.33.

Table 2.32: Probability of exceedance in 50 years of seismic action (P) and factors of importance for the ULS verification γ_f of cultural heritage protection [5].

Use category	Important category					
	Limited		Middle		Elevated	
	P	γ_f	P	γ_f	P	γ_f
Occasional or not used	40 %	0,50	25 %	0,65	17 %	0,8
Frequent	25 %	0,65	17 %	0,80	10 %	1,0
Very frequent	17 %	0,80	10 %	1,00	6,5 %	1,2

Table 2.33: Probability of exceedance in 50 years of seismic action (P) and factors of importance for the DLS verification γ_f of cultural heritage protection [5].

Use category	Important category					
	Limited		Middle		Elevated	
	P	γ_f	P	γ_f	P	γ_f
Occasional or not used	90 %	0,50	80 %	0,65	65 %	0,8
Frequent	80 %	0,65	65 %	0,80	50 %	1,0
Very frequent	65 %	0,80	50 %	1,00	40 %	1,2

It is interesting to note that, for example, for the analysis of these types of structures must be used a factor of confidence equal to:

$$F_C = 1 + \sum_{k=1,4} F_{ck} \ . \tag{2.68}$$

Where the confidence factors (F_{ck}) depend on the degree of detail of the investigation, as shown in the Table 2.34.

Table 2.34: Definition of levels of depth investigations on different aspects of knowledge and confidence for partial factors [5].

Investigation on the geometry	Investigation of the detail	Mechanical propertied of the material	Soil and foundations
Complete $F_{C1} = 0,05$	Limited $F_{C2} = 0,12$	Use of disposable data $F_{C3} = 0,12$	Limited $F_{C4} = 0,06$
Complete with crack pattern $F_{C1} = 0,00$	Extensive $F_{C2} = 0,06$	Extensive $F_{C3} = 0,06$	Use of disposable data $F_{C4} = 0,03$
	Complete $F_{C2} = 0,00$	Complete $F_{C3} = 0,00$	Complete $F_{C4} = 0,00$

Based on the purpose to preserve the cultural heritage, the guidelines define three Levels of Evaluation (LV) corresponding to the different needs of seismic analysis:

1) valuation of the vulnerability of cultural heritage on a national scale;
2) design of seismic retrofitting on individual elements of construction;
3) design of seismic upgrading involving the behaviour of the whole product.

The following Table 2.35 shows the relationships between the finalities of the analysis, the levels of valuation and the analysis model.

Table 2.35: Summary for the evaluation of seismic capacity [5].

Analysis of the seismic hazard of the cultural heritage		
Scope of the analysis	Minimal level of evaluation	Analysis model
Evaluation of the seismic safety factor in national scale	LV1	Simplified models
Evaluation of the seismic safety of the single building	LV3	Complete local mechanisms of collapse
Design of intervention of seismic improve		
Scope of the analysis	Minimal level of evaluation	Analysis model
Local intervention on limited part of the building	LV2	Local mechanisms of collapse on a part of the building
Intervention on the whole building	LV3	Complete local mechanisms of collapse

The majority of cultural heritages are built of masonry and for this reason, the guidelines in question involves the execution of tests of strength and stability of masonry walls not only in–plane but also out–plan action. In particular, all the possible collapse mechanisms, especially for church facades, must be considered. Some of these are listed in the following Figure 2.9.

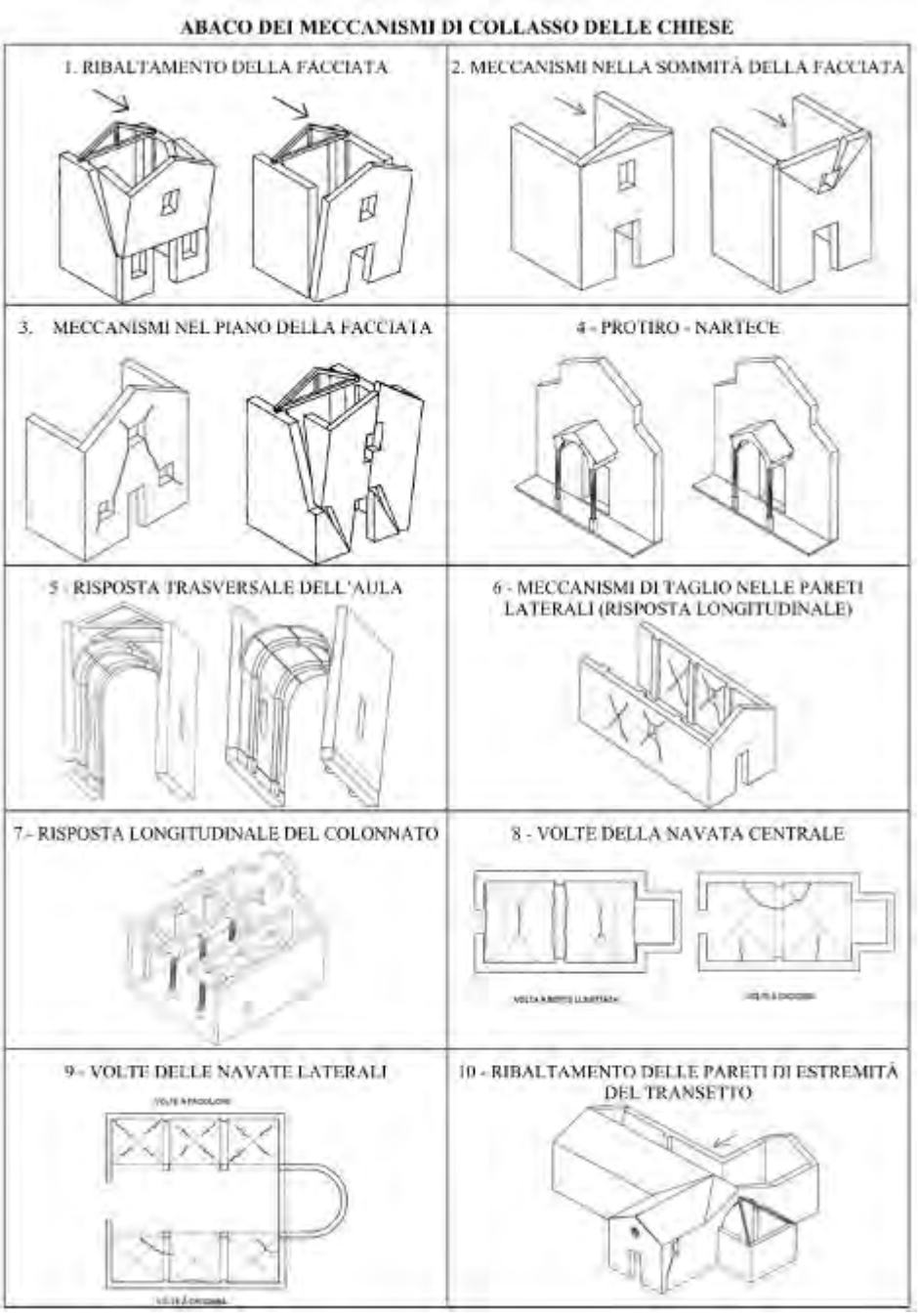

Figure 2.9: Abacus of some mechanisms of collapse of the churches [5].

2.2.2 European rules: Eurocodes

The Eurocodes are the standards produced by CEN (European Committee for Standardization) with the purpose of proposing a reference approval to structural design throughout the European Union.

Since the 1970 a series of harmonised technical rules has been issue for design of buildings under construction. Initially the purpose of Eurocodes was to be an alternative to national regulations, which eventually would have been substituted.

The Eurocodes programme consists of provides nine categories of documents, from the base of the design of structures to the design of aluminum structures.

Regarding the field of masonry, the interested Eurocodes are:

- Eurocode 6: it is dedicated to masonry carrying structures, reinforced or not and in natural or artificial elements;
- Eurocode 8: it is dedicated to the seismic aspect and connects to the other Eurocode depending on the material used.

In particular, the Eurocode 6 is composed of the following documents:

- UNI EN 1996-1-1:2006 Part 1-1: General rules for reinforced and unreinforced masonry structures [28];
- UNI EN 1996-1-2:2005 Part 1-2: General rules – Structural design for fire;
- UNI EN 1996-2:2006 Part 2: Design considerations, selection of materials and execution of masonry [29];
- UNI EN 1996-3:2006 Part 3: Simplified calculation methods for unreinforced masonry structures [30].

Eurocode 8, instead, contains useful information on the masonry in the following documents:

- UNI EN 1998-1:2005 Part 1: General rules, seismic actions and rules for buildings [31];
- UNI EN 1998-3:2005 Part 3: Assessments and retrofitting of buildings [32].

2.2.2.1 EuroCode 6

Eurocode 6 Part 1-1 [28] sets out general criteria for the design of either unreinforced and reinforced masonry buildings.

Design approach is always inspired to the Limit States method, which became consists in comparing the value of the design action and the design resistance:

$$E_d < R_d. \tag{2.69}$$

In a very general way, the stresses are obtained from the characteristic values and amplifying them with the appropriate factors. As regards, however, the design strengths, these can be obtained from the characteristic values reduced with the appropriate partial factors (see Table 2.36).

Table 2.36: Recommended values of γ_M [28].

Material		γ_M				
		Class				
		1	2	3	4	5
	Masonry made with	1,5	1,7	2,0	2,2	2,5
A	Units of Category I, designed mortar[a]	1,7	2,0	2,2	2,5	2,7
B	Units of Category I, prescribed mortar[b]	2,0	2,2	2,5	2,7	3,0
C	Units of Category II, any mortar[a-b-c]	1,7	2,0	2,2	2,5	2,7
D	Anchorage of reinforcing steel	1,15				
E	Reinforcing steel and prestressed steel	1,7	2,0	2,2	2,5	2,7
F	Ancillary components[c-d]	1,5 to 2,5				
G	Lintels according to EN 845-2					
a	[a] Requirements for designed mortars are given in EN 998-2 and EN 1996-2.					
b	[b] Requirements for prescribed mortars are given in EN 998-2 and EN 1996-2.					
c	[c] Declared values are mean values.					
d	[d] Damp proof courses are assumed to be covered by masonry γ_M.					
e	[e] When the coefficient of variation for Category II units is not greater than 25%.					

For the masonry material, the Eurocode 6 defines the geometrical requirements reported in Table 2.37 and the strengths for infills shows in the next Table 2.38.

Table 2.37: Geometrical requirements for Grouping of Masonry Units [28].

	Material and limits for Masonry Units							
	Group 1 (all materials)		Group 2		Group 3		Group 4	
		Units	Vertical holes				Horizontal holes	
Volume of all holes (% of the gross number)	≤ 25	Clay	> 25; ≤ 55		≥ 25; ≤ 70		> 25; ≤ 70	
		Calcium silicate	> 25; ≤ 55		not used		not used	
		concrete[b]	> 25; ≤ 60		> 25; ≤ 70		> 25; ≤ 50	
Volume of any hole (% of the gross volume)	≤ 12,5	Clay	each of multiple holes ≤ 2 gripholes up to a total of 12,5		each of multiple holes ≤ 2 gripholes up to a total of 12,5		each of multiple holes ≤ 30	
		Calcium silicate	each of multiple holes ≤ 15 gripholes up to a total of 30		not used		not used	
		concrete[b]	each of multiple holes ≤ 30 gripholes up to a total of 30		each of multiple holes ≤ 30 gripholes up to a total of 30		each of multiple holes ≤ 25	
Declared values of thickness of webs and shells (mm)	No requirement		web	shell	web	shell	web	shell
		Clay	≥ 5	≥ 8	≥ 3	≥ 6	≥ 5	≥ 6
		Calcium silicate	≥ 5	≥ 10	not used		not used	
		concrete[b]	≥ 15	≥ 18	≥ 15	≥ 15	≥ 20	≥ 20
Declared value of combined thickness[a] of webs and shells (% of the overall width)	No requirement	Clay	≥ 16		≥ 12		≥ 12	
		Calcium silicate	≥ 20		not used		not used	
		concrete[b]	≥ 18		≥ 15		≥ 45	

[a] The combined thickness is the thickness of the webs and shells, measured horizontally in the relevant direction. The check is to be seen as a qualification test and need only be repeated in the case of principal changes to the design dimensions of units.
[b] In the case of conical holes, or cellular holes, use the mean value of the thickness of the webs and the shells.

Table 2.38: Characteristic strengths of concrete infills [28].

Strength class of concrete	C12/15	C16/20	C20/25	C25/30, or stronger
f_{ck} [N/mm²]	12	16	20	25
f_{cvk} [N/mm²]	0,27	0,33	0,39	0,45

The characteristic compressive strength of unreinforced masonry is:

$$f_k = K \cdot f_b^{\alpha} \cdot f_m^{\beta}, \tag{2.70}$$

where:

- f_k is the characteristic compressive strength of the masonry in N/mm²;
- K is a constant that can be determined in accordance with the Table 2.39;
- α and β are constants;
- f_b is the normalised average compressive strength of masonry elements in N/mm²;
- f_m is the compressive strength of ordinary mortar, in N/mm².

Table 2.39: Values of K for use with general purpose, thin layer and lightweight mortars [28].

Masonry Unit		General purpose mortar	Thin layer mortar (bed joint ≥ 0,5 mm and ≤ 3 mm)	Lightweight mortar of density	
				600 ≤ ρ_d ≤ 800 kg/m³	800 ≤ ρ_d ≤ 1300 kg/m³
Clay	Group 1	0,55	0,75	0,30	0,40
	Group 2	0,45	0,70	0,25	0,30
	Group 3	0,35	0,50	0,20	0,25
	Group 4	0,35	0,35	0,20	0,25
Calcium silicate	Group 1	0,55	0,80	◊	◊
	Group 2	0,45	0,65	◊	◊
Aggregate concrete	Group 1	0,55	0,80	0,45	0,45
	Group 2	0,45	0,65	0,45	0,45
	Group 3	0,40	0,50	◊	◊
	Group 4	0,35	◊	◊	◊
Autoclaved Aerated Concrete	Group 1	0,55	0,80	0,45	0,45
Manufactured Stone	Group 1	0,45	0,75	◊	◊
Dimensioned Natural Stone	Group 1	0,45	◊	◊	◊
◊ Combination of mortar/unit not normally used, so no value given.					

The characteristic shear resistance of walls is:

$$f_{vk} = f_{vk0} + 0{,}4 \cdot \sigma_d \,, \tag{2.71}$$

where:

- f_{vk0} is the initial shear strength under zero axial load (see Table 2.40);
- σ_d is the design compressive stress perpendicular to the shear in membering level into consideration.

The Eurocode 6 imposes that f_{vk} should be lower than 0,065 f_b or f_{vlt}, where

- f_b is the resistance to compression of the standard elements of the masonry, for the direction of load application;
- f_{vlt} is the limit value of f_{vk}.

Table 2.40: Values of the initial shear strength of masonry [28].

Masonry units	f_{vk0} [N/mm²]			
	General purpose mortar of the Strength Class given		Thin layer mortar (bed joint ≥ 0,5 mm and ≤ 3 mm)	Lightweight mortar
Clay	M10 – M20	0,30	0,30	0,15
	M2,5 – M9	0,20		
	M1 – M2	0,10		
Calcium silicate	M10 – M20	0,20	0,40	0,15
	M2,5 – M9	0,15		
	M1 – M2	0,10		
Aggregate concrete	M10 – M20	0,20	0,30	0,15
Autoclaved Aerated Concrete	M2,5 – M9	0,15		
Manufactured stone and Dimensioned natural stone	M1 – M2	0,10		

Following the definition of the mechanical characteristics of masonry, Eurocode proceeds to set out the criteria to be used for verification both Ultimate Limit States and Service Limit States. Finally, the detail rules are also defined, including the minimum thickness of the walls, the minimum size of the reinforcements, the connections between the various wall elements.

2.2.2.2 EuroCode 8

The code [31] provides requirements for buildings and civil engineering projects in seismic zones and provides the rules for the representation of seismic actions and their combination with other actions, with the objective to ensure that in case of earthquake human lives are protected, the damages are limited and the major structures of civil protection remain operational.

Among all the existing codes on earthquake engineering, Eurocode 8 is certainly the most advanced ones. With regard to the seismic action, this can be calculated in a very similar way to the already shown in previous paragraphs 2.2.1.2. Firstly the Eurocode 8 defines the ground types in the Table 2.41.

Table 2.41: Ground types [31].

Ground type	Description of stratigraphic profile	Parameters		
		$v_{s,30}$ [m/s]	NSPT (blows 30cm)	c_u [kPa]
A	Rock or other rock-like geological formation, including at most 5 m of weaker material at the surface.	> 800	-	-
B	Deposits of very dense sand, gravel, or very stiff clay, at least several tens of metres in thickness, characterised by a gradual increase of mechanical properties with depth.	360 – 800	> 50	> 250
C	Deep deposits of dense or medium dense sand, gravel or stiff clay with thickness from several tens to many hundreds of metres.	180 – 360	15 – 50	70 – 250
D	Deposits of loose-to-medium cohesionless soil (with or without some soft cohesive layers), or of predominantly soft-to-firm cohesive soil.	< 180	< 15	< 70
E	A soil profile consisting of a surface alluvium layer with v_s, values of type C or D and thickness varying between about 5 m and 20 m, underlain by stiffer material with v_s > 800 m/s.			
S_1	Deposits consisting, or containing a layer at least 10 m thick, or soft clays/silts with a high plasticity index (PI > 40) and high water content.	< 100 (indicative)	-	10 – 20
S_2	Deposits of liquefiable soils, of sensitive clays, or any other soil profile not included in types A – E or S_1			

In particular, the elastic spectral acceleration can be defined as a function of return period. In contrast to the Italian standard NTC 2008 [6], the standard [31] fixed:

- the values of the vibration periods of the different tracts of the spectrum by knowing the category of subsoil (see Table 2.42 and Table 2.43);
- the value of spectral amplification factor, F_0, equal 2,5.

Table 2.42: Values of parameters of the elastic response spectrum recommended of Type 1 [31].

Ground type	S	T_B(s)	T_C(s)	T_D(s)
A	1,0	0,15	0,4	2,0
B	1,2	0,15	0,5	2,0
C	1,15	0,20	0,6	2,0
D	1,35	0,20	0,8	2,0
E	1,4	0,15	0,5	2,0

Table 2.43: Values of parameters of the elastic response spectrum recommended of Type 2 [31].

Ground type	S	T_B(s)	T_C(s)	T_D(s)
A	1,0	0,05	0,25	1,2
B	1,35	0,05	0,25	1,2
C	1,5	0,10	0,25	1,2
D	1,8	0,10	0,30	1,2
E	1,6	0,05	0,25	1,2

With the previous parameters it's possible to obtain different spectra that have a shape exposed in the Figure 2.10.

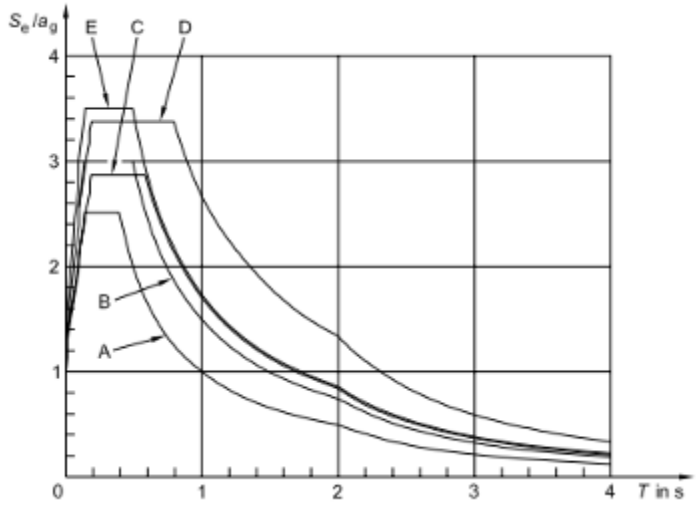

Figure 2.10: Recommended Type 1 elastic spectrum for soil types A through E (5% damping) [31].

The analysis method used for seismic analysis and verification of the structure depends explicitly on the regularity characteristics of the structure, as summarised in the Table 2.44. Compared to NTC 2008 [6], this represents a significant step forward that clarifies the differences between regular and irregular structures.

Table 2.44: Effects of structural regularity on analysis and seismic design [31].

Regularity		Allowed Simplification		Behaviour factor
Plan	Elevation	Model	Linear-elastic Analysis	(for linear analysis)
Yes	Yes	Planar	Lateral force[a]	Reference value
Yes	No	Planar	Modal	Decreased value
No	Yes	Spatial[b]	Lateral force[a]	Reference value
No	No	Spatial	Modal	Decreased value

[a] If the condition of 4.3.3.2.1(2)a is also met.
[b] Under the specific condition given in 4.3.3.1(8) a separate planar model may be used in each horizontal direction, in accordance with 4.3.3.1(8).

The simplest analysis method is the one that includes the application of a lateral horizontal forces distributed appropriately among the various vertical earthquake resistant element:

$$F_b = S_d(T_1) \cdot m \cdot \lambda \,, \tag{2.72}$$

where:

- $S_d(T_1)$ is the ordinate of the design spectrum for the period T_1;
- T_1 is the fundamental period of vibration of the building for a lateral motion in the considered direction;
- m is the total mass of the building above the foundation or on the top of a rigid base;
- λ is a correction factor, equal to 0,85 if $T_1 < T_{c2}$ and if the building has more than two plan or otherwise is equal to 1,00.

The fundamental period is equal to:

$$T_1 = C_t \cdot H^{3/4} \,, \tag{2.73}$$

where:

- $C_t = \frac{0{,}075}{\sqrt{A_c}}$ for structures with r.c. walls;
- C_t = 0,085 for steel spatial frame with rigid joints;
- C_t = 0,075 for concrete or steel spatial frames and rigid joints frames with eccentric upwind;
- C_t = 0,05 for all other structures;
- H is the building height in meters;
- $A_c = \sum \left[A_i \cdot \left(0{,}2 + \left(\frac{l_{wi}}{H} \right) \right)^2 \right]$ is the total effective area of shear walls on the first floor of the building, in m^2;
- A_i is the effective cross section area of the wall on the first floor of the building, in m^2;
- l_{wi} is the length of the i-th shear wall at the first floor in the direction parallel to the applied forces, in m, with the ratio l_{wi}/H not greater than 0,9.

With regard to masonry buildings, these are specifically dealt with in Chapter 9 of Part 1-1. In particular, the mechanical properties of the constituents of the wall and the factors for seismic analyses are defined. Among these factors, the most important is certainly the q-factor to be used, which is specified in the Table 2.45.

Table 2.45: Types of construction and the upper limit of the q–factor [31].

Type of construction	Behaviour factor q
Unreinforced masonry in accordance with EN 1996 alone (recommended for low seismicity cases).	1,5
Unreinforced masonry in accordance with EN 1998-1.	1,5 – 2,5
Confined masonry	2,0 – 3,0
Reinforced masonry	2,5 – 3,0

The main mechanism of earthquake resistant masonry buildings is made up of walls, which are sensitive to actions in their plan. These walls, for new buildings, should verify the following requirements of Table 2.46.

Table 2.46: Geometrical requirements recommended for shear walls [31].

Masonry type	$t_{ef,min}$ [mm]	$(h_{ef}/t_{ef})_{max}$	$(l/h)_{min}$
Unreinforced, with natural stone units.	350	9	0,5
Unreinforced, with any other type of units	240	12	0,4
Unreinforced, with any other type of units, in cases of low seismicity	170	15	0,35
Confined masonry	240	15	0,3
Reinforced masonry	240	15	No restriction
Symbols used have the following meaning: t_{ef} thickness of the wall (see EN 1996-1-1:2004); h_{ef} effective height of the wall (see EN 1996-1-1:2004); h greater height of the openings adjacent to the wall; l length of the wall.			

Finally, with regard to simple masonry buildings, simplified analysis are allowed, as prescribed in Eurocode 6. However, several limitations should be considered including those listed in the Table 2.47 with reference to the maximum number of floors.

With regard, instead, the existing masonry buildings, Part 3 of Eurocode 8 [32] must be used. This range is the most common for masonry structures, which are less made today, and for those that already exist, they are almost always outside the current parameters of verification.

The rule [32] provides criteria to assess the seismic performance of the single structures of existing buildings. The approach to select the necessary corrective measures and establish criteria for the design of adaptation measures is described.

Table 2.47: Number of floor recommended to be granted above the ground level and minimum area of shear walls for "simple masonry buildings" [31].

Acceleration at site a_g S		≤ 0,07 k g	≤ 0,10 k g	≤ 0,15 k g	≤ 0,20 k g
Type of construction	Number of storey (n)**	Minimum sum of cross-sections areas of horizontal shear walls in each dimension, as percentage of the total floor area per storey ($p_{A,min}$)			
Unreinforced masonry	1	2,0 %	2,0 %	3,5 %	n/a
	2	2,0 %	2,5 %	5,0 %	n/a
	3	3,0 %	5,0 %	n/a	n/a
	4	5,0 %	n/a*	n/a	n/a
Confined masonry	2	2,0 %	2,5 %	3,0 %	3,5 %
	3	2,0 %	3,0 %	4,0 %	n/a
	4	4,0 %	5,0 %	n/a	n/a
	5	6,0 %	n/a	n/a	n/a
Reinforced masonry	2	2,0 %	2,0 %	2,0 %	3,5 %
	3	2,0 %	2,0 %	3,0 %	5,0 %
	4	3,0 %	4,0 %	5,0 %	n/a
	5	4,0 %	5,0 %	n/a	n/a
* n/a means “not acceptable”.					
** Roof space above full storeys is not included in the number of storeys.					

The third part of Eurocode 8, therefore, first defines the methods for seismic analysis of existing structures and then provides specific rules for masonry structures in Appendix C.

As regards the methods of analysis they are affected by greater uncertainties of analysis from those used for new structures because they are not fully known material and geometry, which features will be determined by a detailed investigation. Depending on the type of investigations, a confidence factor useful to calculate the design values of resistance (see Table 2.48) can be defined.

Table 2.48: Knowledge levels and corresponding methods of analysis (LF: Lateral Force procedure, MRS: Modal Response Spectrum analysis) and confidence factors (CF) [31].

Knowledge Level	Geometry	Details	Materials	Analysis	CF
KL1	From original outline construction drawings with sample visual survey or from full survey	Simulated design in accordance with relevant practice and from limited in-situ inspection	Default values in accordance with standards of the time of construction and from limited in-situ testing	LF-MRS	CF_{KL1}
KL2		From incomplete original detailed construction drawings with limited in-situ inspection or from extended in-situ inspection	From original design specifications with limited in-situ testing or from extended in-situ testing	All	CF_{KL2}
KL3		From original detailed construction drawings with limited in-situ inspection or from comprehensive in-situ inspection	From original test reports with limited in-situ testing or from comprehensive in-situ testing	All	CF_{KL3}
NOTE: The values ascribed to the confidence factors to be used in a country may be found in its National Annex. The recommended values are CF_{KL1} = 1,35; CF_{KL2} = 1,20; CF_{KL3} = 1,00.					

The material characteristics are defined according to the method of analysis adopted in Table 2.49, which can be:

1) linear analysis;
2) nonlinear analysis;
3) q-factor approach.

Table 2.49: Values of material properties and criteria for analysis and safety verification [31].

<table>
<tr><td colspan="2" rowspan="2"></td><td colspan="2">Linear Model (LM)</td><td colspan="2">Nonlinear Model</td><td colspan="2">q-factor approach</td></tr>
<tr><td>Demand</td><td>Capacity</td><td>Demand</td><td>Capacity</td><td>Demand</td><td>Capacity</td></tr>
<tr><td rowspan="5">Type of element or mechanism (e/m)</td><td rowspan="2">Ductile</td><td colspan="2">Acceptability of Linear Model (for checking of $\rho_i = D_i/C_i$; Verification (if LM accepted):</td><td rowspan="5">From analysis. Use mean values of properties in model.</td><td rowspan="2">In terms of strength. Use mean values of properties divided by CF and by partial factor.</td><td rowspan="2">From analysis.</td><td rowspan="5">In terms of strength. Use mean values of properties divided by CF and by partial factor.</td></tr>
<tr><td>From analysis.</td><td>In terms of deformation. Use mean values of properties divided by CF.</td></tr>
<tr><td rowspan="3">Brittle</td><td colspan="2">Verifications (if LM accepted):</td><td rowspan="3">In terms of strength. Use mean values of properties divided by CF and by partial factor.</td><td rowspan="3">In accordance with the relevant Section of EN 1998-1:2004.</td></tr>
<tr><td>If $\rho_i \leq 1$: from analysis.</td><td></td></tr>
<tr><td>If $\rho_i > 1$: from equilibrium with strength of ductile e/m. Use mean values of properties multiplied by CF.</td><td>In terms of strength. Use mean values of properties divided by CF and partial factor.</td></tr>
</table>

With regard to the masonry walls, the Eurocode is used to calculate the basic resistant shears, that change to reflect the limit state considered, both with reference to the case of the walls subject to bending and the walls subject to shear.

The corresponding shear resistance of walls subject to bending is taken to be equal to:

$$V_f = \frac{D \cdot N}{2 \cdot H_0} \cdot \left(1 - 1{,}15 \cdot \nu_d\right), \tag{2.74}$$

where:

- D is the dimension in the horizontal plane of the wall;
- N is the normal action;
- H_0 is the distance between the section where is attained the capacity to bending and the contraflexure point;

- $\nu_d = \frac{N}{D \cdot t \cdot f_d}$ is the no-dimensional normal stress;
- t is the thickness of the wall;
- $f_d = \frac{f_m}{CF_m}$ is the design compressive strength of masonry;
- f_m is the average compressive strength of masonry;
- CF_m is the confidence factor of the wall.

The shear capacity of unreinforced masonry, however, is equal to:

$$V_f = f_{vd} \cdot D' \cdot t \,, \tag{2.75}$$

where:

- $f_{vd} = f_{vm0} + 0{,}4 \cdot \frac{N}{D' \cdot t} < 0{,}065 \cdot f_m$ is the shear strength of masonry in the presence of normal stress;
- f_{vm0} is the shear strength of masonry in the absence of normal stress;
- D' is the size of the compressed part of the section.

3. Analysis of masonry walls under in-plane earthquake induced actions

3.1 Failure modes of masonry panels subject to actions in their plane

This section outlines the key capacity models for simulate the relevant failure modes of masonry walls. The following notation is used for dimensions of a masonry panel:

- wall thickness: t;
- length: L;
- height: h;
- geometric slenderness of the wall in the plan:

$$\lambda = \frac{h}{L}. \tag{3.1}$$

A series of a simple capacity models is formulated by considering a generic masonry wall (see Figure 3.1), subjected to various restraint conditions, two vertical load N and one horizontal force V.

According to experimental observations [33] et al., the following aspects control the failure modes in masonry walls:

- geometrical parameters and particularly the slenderness;
- stress state: the vertical load has a significant effect on shear strength of masonry;
- mechanical properties: particularly bed component of the wall can influence the mode of failure (such as mortar).

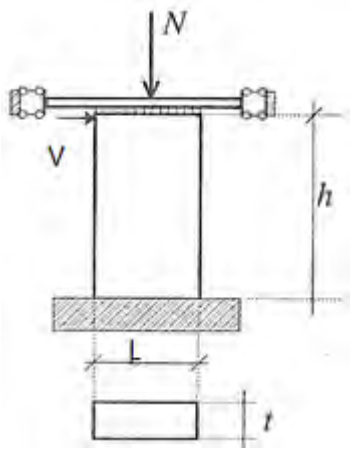

Figure 3.1: Load pattern and size of the masonry panel.

Thus, the following failure modes can occur in a masonry wall:

1) diagonal cracking: occur a shear failure with the formation of diagonal cracking, often along the beds of mortar but not always;
2) sliding shear: this kind of failure occurs when there is sliding along a horizontal bed of mortar, often at the base of the panel. This failure mode is typical for panels with low vertical loads, low shear strength of the mortar and low coefficient of friction (μ) between the base and wall;
3) flexural failure: masonry panels very high tend to fail in flexure which involves the opening of horizontal cracks at the base on the tensile side and a crushing of the compressed side.

The described types of failure are schematically represented in the following Figure 3.2.

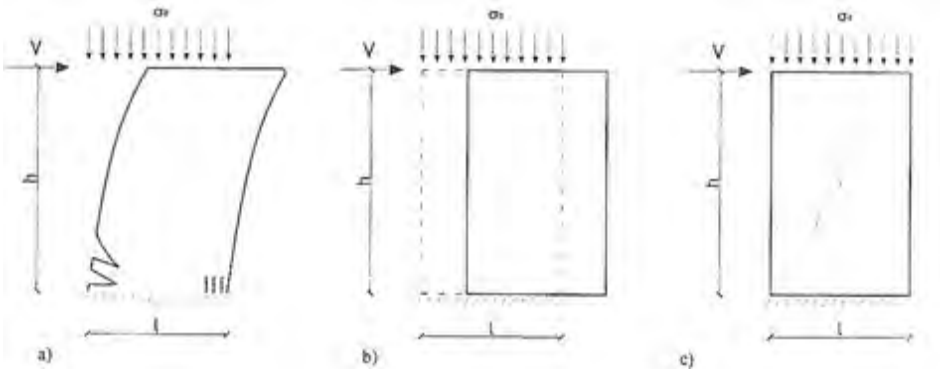

Figure 3.2: Possible collapse mechanisms [34].

Only diagonal shear collapse mechanism was considered in POR method [18] when the method was originally conceived. The other two mechanisms, however, were subsequently studied and it was found that their behaviours were very dependent by the extent of vertical load. Therefore, it is necessary to distinguish between the case of partially compressed section (low values of the normal load) from the case entirely compressed section (high values of the normal load).

The relationships of ultimate shear strength (V_u) of the panel subject to a constant normal action N are presented for each of the failure modes. They are derived by using the following assumptions for stresses in walls:

- mean shear stress: $$\tau = \frac{V}{L \cdot t};$$ (3.2)
- mean normal stress: $$\sigma = \frac{N}{L \cdot t}.$$ (3.3)

3.1.1 Diagonal shear failure

This failure mode is characterised by the formation of diagonal cracks in the panel. Because the panel has a rectangular cross section, shear stresses acting in the cross section have a quadratic distribution with the maximum at the central fiber (see Figure 3.3).

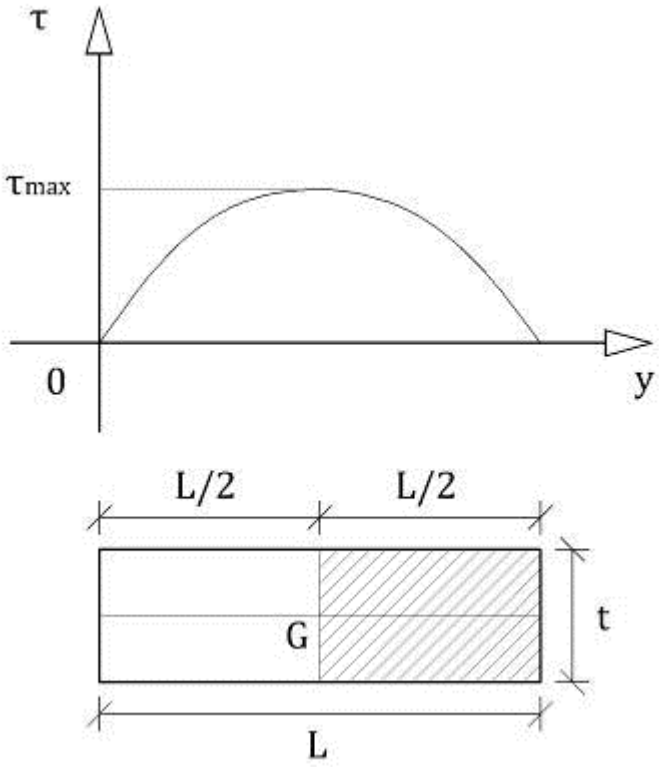

Figure 3.3: Evolution of tangential stresses in the section.

The presence of normal and shear stresses result in cracking which initiates from the central zone, where shear stresses attain their maximum value. The mean vertical stresses are assumed equal to:

$$\sigma = \frac{N}{L \cdot t}. \tag{3.4}$$

The scheme of the building panel is that of a beam fixed at the base and fixed to rotate at the top [35].

The ultimate limit state involves the formation of diagonal cracks perpendicular to the principal tensile direction that spread quickly from the center of the wall to the corners.

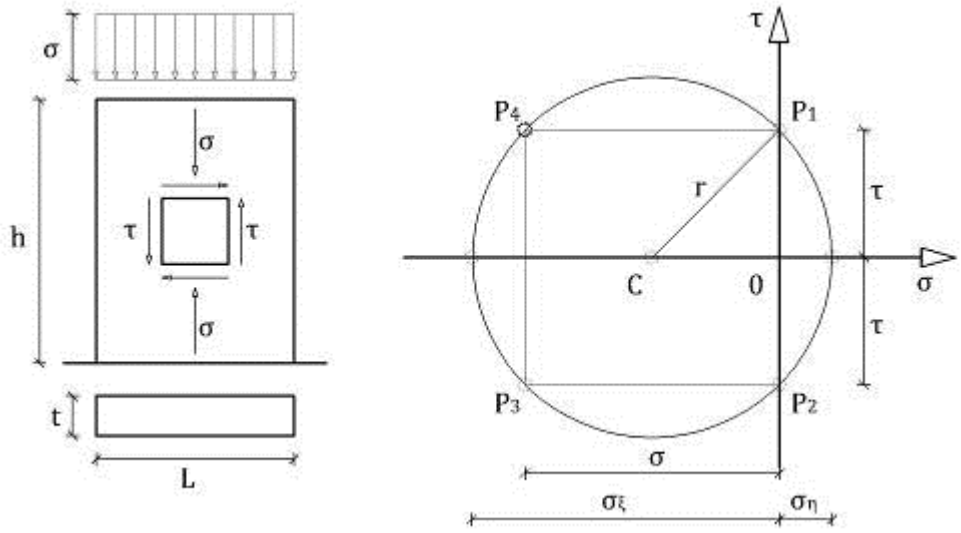

Figure 3.4: Stress state of a central element and the corresponding Mohr circle.

Consider a generic infinitesimal element at the center of the panel described in Figure 3.4, which is subject to a normal stress, and shear stress equal to:

$$\tau = \frac{V}{L \cdot t}. \tag{3.5}$$

Assuming this, four points (P_1, ..., P_4) of the Mohr circle, the center and the radius can be obtained. The center has coordinates:

$$x_c = \frac{\sigma}{2}; \tag{3.6}$$

$$y_c = 0. \tag{3.7}$$

The radius is:

$$r = \sqrt{\left(\frac{\sigma}{2}\right)^2 + \tau^2}. \tag{3.8}$$

The principal stresses σ_η and σ_ξ are of particular importance for the study of collapse mechanisms:

$$\sigma_\eta = \frac{\sigma}{2} - \sqrt{\left(\frac{\sigma}{2}\right)^2 + \tau^2}\ ; \tag{3.9}$$

$$\sigma_\xi = \frac{\sigma}{2} + \sqrt{\left(\frac{\sigma}{2}\right)^2 + \tau^2}\ . \tag{3.10}$$

At the center of the reference cross section, the maximum shear stress can be calculated using Jourawski formula:

$$\tau_{\max} = \frac{V \cdot S'}{I_G \cdot t} = \frac{V \cdot \left(t \cdot L^2/8\right)}{\left(t \cdot L^3/12\right) \cdot t} = \frac{3}{2} \cdot \frac{V}{L \cdot t} = 1{,}5 \cdot \tau\ , \tag{3.11}$$

where:

- S' is the moment of the part of the section above the central fiber or the half section in relation to the center of gravity:

$$S' = \left(t \cdot \frac{L}{2}\right) \cdot \frac{L}{4} = \frac{t \cdot L^2}{8}\ ; \tag{3.12}$$

- I_G is the moment of inertia of the entire section in relation to the center of gravity axis:

$$I_G = \frac{t \cdot L^3}{12}\ . \tag{3.13}$$

Thus, the maximum principal stresses can be determined as follows:

$$\sigma_{\eta,\max} = \frac{\sigma}{2} - \sqrt{\left(\frac{\sigma}{2}\right)^2 + \left(1{,}5 \cdot \tau\right)^2}\ ; \tag{3.14}$$

$$\sigma_{\xi,\max} = \frac{\sigma}{2} + \sqrt{\left(\frac{\sigma}{2}\right)^2 + \left(1{,}5 \cdot \tau\right)^2}\ . \tag{3.15}$$

3.1.1.1 Italian codes [6][23]

The ultimate condition is obtained when the principal tensile stress reaches the maximum value of the resistance, equal to 1,5 f_{vk0} (where f_{vk0} is shear strength under zero vertical load), the ultimate shear stresses associated with this failure are (τ_u):

$$\frac{\sigma}{2}-\sqrt{\left(\frac{\sigma}{2}\right)^2+(1{,}5\cdot\tau_u)^2}=-1{,}5\cdot f_{vk0}. \tag{3.16}$$

Rearranging the above equation (3.16) the following expression can be obtained:

$$\frac{\sigma}{2}+1{,}5\cdot f_{vk0}=\sqrt{\left(\frac{\sigma}{2}\right)^2+(1{,}5\cdot\tau_u)^2}\,, \tag{3.17}$$

then:

$$\left(\frac{\sigma}{2}+1{,}5\cdot f_{vk0}\right)^2=\left(\frac{\sigma}{2}\right)^2+(1{,}5\cdot\tau_u)^2, \tag{3.18}$$

After simple mathematical transformations, the following expression can be written:

$$(1{,}5\cdot f_{vk0})^2\cdot\left[1+\frac{\sigma}{1{,}5\cdot f_{vk0}}\right]=(1{,}5\cdot\tau_u)^2, \tag{3.19}$$

and the mean ultimate shear stress is:

$$\tau_u=f_{vk0}\cdot\sqrt{1+\frac{\sigma}{1{,}5\cdot f_{vk0}}}\,, \tag{3.20}$$

From the definition of ultimate shear stress given in (3.20, the ultimate shear associated with this mode of failure can be the following:

$$V_{ds}=L\cdot t\cdot f_{vk0}\cdot\sqrt{1+\frac{\sigma}{1{,}5\cdot f_{vk0}}}\,. \tag{3.21}$$

This equation (3.21) can be further modified to take into account the slenderness of the panel [23]:

$$V_{ds}=L\cdot t\cdot\frac{1{,}5\cdot f_{vk0}}{\lambda}\cdot\sqrt{1+\frac{\sigma}{1{,}5\cdot f_{vk0}}}\,. \tag{3.22}$$

In according to the Italian technical requirements [6], the value of the slenderness factor must be between 1,0 and 1,5.

Using the equation for shear strength, the value of the ultimate shear for different levels of vertical load at fixed mechanical properties and geometry panel can be obtained (see Figure 3.5).

This diagram shows that the mean stress of shear failure increases with the square root of vertical stress, until other mechanisms of collapse of the wall are triggered.

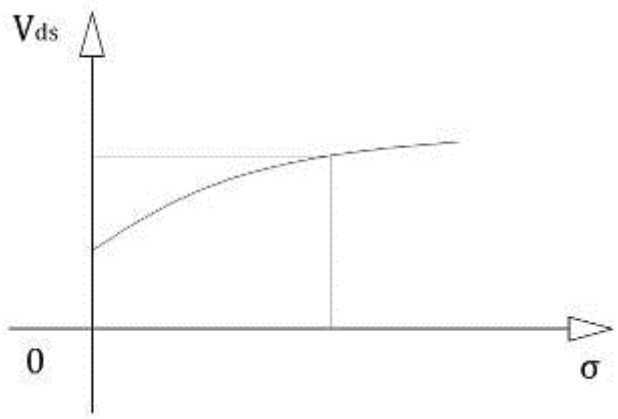

Figure 3.5: Variation of the ultimate diagonal shear as a function of the vertical compression.

3.1.1.2 Turnsek and Cacovic

One possible way to get Turnsek and Cacovic [35] formula is from the plane stress state:

$$\sigma_{1,2} = -\frac{\sigma_{xx} + \sigma_{yy}}{2} \pm \sqrt{\tau_{xy}^2 + \frac{\left(\sigma_{xx} - \sigma_{yy}\right)^2}{4}}. \tag{3.23}$$

By assuming:

$$\sigma_{xx} = 0; \qquad \sigma_{yy} = \sigma_0; \qquad \tau_{xy} = b \cdot \tau_0; \tag{3.24}$$

where:

- σ_0 is the vertical stress;
- τ_0 is the shear stress;
- $b = \frac{\tau_{xy}}{\tau_0}$ is equal to 1,5 for slenderness and 1,1 for squat piers.

The shear resistance becomes:

$$V_{\max} = A \cdot \frac{f_t}{b} \cdot \sqrt{1 + \frac{\sigma_0}{f_t}}, \tag{3.25}$$

where

- $f_t = \sigma_2$ is the max stress, or the tensile strength of masonry.

To calculate the ultimate shear, at the end, the following formula can be used:

$$V_{ds} = L \cdot t \cdot \frac{f_t}{b} \cdot \sqrt{1 + \frac{\sigma}{f_t}}, \tag{3.26}$$

where:

- f_t is the maximum shear resistance obtained by a diagonal shear test on a masonry wall (tensile strength);
- b is a shear stress distribution factor, which usually takes values between 1,0 and 1,5 and is a function of the slenderness panel.

In particular, according to [36], the b factor is:

$$b = 1{,}5 \quad \text{for:} \quad \frac{h}{L} \geq 1{,}5 \tag{3.27}$$

$$b = 1{,}0 \quad \text{for:} \quad \frac{h}{L} \leq 1{,}5 \tag{3.28}$$

$$b = \frac{h}{L} \quad \text{for:} \quad 1{,}0 \leq \frac{h}{L} \leq 1{,}5 \tag{3.29}$$

3.1.1.3 Other methods

Amongst other methods, the Mann and Müller [37] method is also well known. Two types of diagonal failure are considered: joint cracking and brick cracking. In this theory, the ultimate shear resistance depend from:

- brick geometry and strength;
- bonding type and friction coefficient;
- conditions of load.

The masonry material has the following properties:

- masonry is not homogeneous;
- masonry is made of different elements (bricks, bed joints, vertical joints).

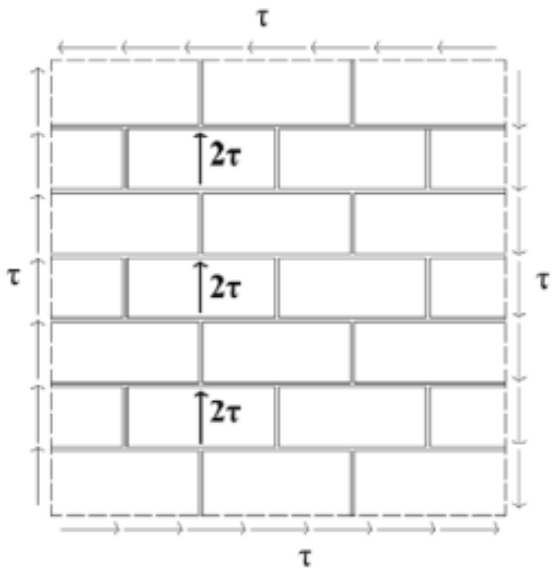

Figure 3.6: Bricks subjected to shear [37].

Mann and Müller determined, with testing, that stresses $\sigma_{xst} = \sigma_x$, $\sigma_y = 0$ and max $\tau_{st} = 2{,}3\ \tau$ occur at the centre of the brick (see Figure 3.6). The bricks crack as principal tensile stress σ_1 in the brick exceeds tensile strength $f_{t,b}$. From:

$$\sigma_1 = \frac{\sigma_x}{2} - \sqrt{\left(\frac{\sigma_x}{2}\right)^2 + (2{,}3 \cdot \tau)^2} = -f_{t,b}\,. \tag{3.30}$$

The failure criterion is given by:

$$\tau = \frac{f_{t,b}}{2{,}3} \cdot \sqrt{1 + \frac{\sigma_x}{f_{t,b}}}\,. \tag{3.31}$$

Finally, the ultimate diagonal shear is:

$$V_{ds} = \frac{f_{t,b} \cdot L \cdot t}{2{,}3} \cdot \sqrt{1 + \frac{\sigma_x}{f_{t,b}}}\,. \tag{3.32}$$

The brick tensile strength ($f_{t,b}$) is a function of the brick compressive strength ($f_{c,b}$):

- for clay units: $f_{t,b} = 0{,}025 \cdot f_{c,b}$ (3.33)
- for bricks with grip hole: $f_{t,b} = 0{,}033 \cdot f_{c,b}$ (3.34)
- for bricks without grip hole: $f_{t,b} = 0{,}040 \cdot f_{c,b}$ (3.35)

3.1.2 Sliding shear failure

The sliding shear collapse can possibly develop throughout a horizontal mortar bed failure, usually at the base of the panel. This mode of failure is typical for situations where mortar has low mechanical properties or there are low vertical loads, or at the upper floors of the structure.

The failure criteria, in this case, is expressed by the following equation:

$$f_{vk} = f_{vk0} + \mu \cdot \sigma', \tag{3.36}$$

where:

- f_{vk0} is the shear strength of the base of the wall in the absence of normal stress (it has the meaning of the cohesion between the blocks and mortar joints) and can be determined through a simple shear test on three bricks wall;
- μ is a coefficient of friction usually equal to 0,4;
- $\sigma' = \frac{N}{t \cdot D'}$ is the mean normal stress over the compressive zone of the wall;
- D' is the length of the compressed part of masonry, which can be obtained using the following formula (see also Figure 3.7):

$$D' = 3u = L \qquad \text{if:} \quad e < L / 6; \tag{3.37}$$

$$D' = 3u = 3 \cdot \left(\frac{L}{2} - e \right) \qquad \text{if:} \quad e > L / 6; \tag{3.38}$$

- $e = \frac{M}{N}$ is the value of the eccentricity of the axial force with respect to the center of gravity of the cross section and is equal to the ratio between the moment and the normal force applied.

At this point the shear resistance associated with this type of collapse is calculated as:

$$V_{ss} = D' \cdot t \cdot f_{vk}. \tag{3.39}$$

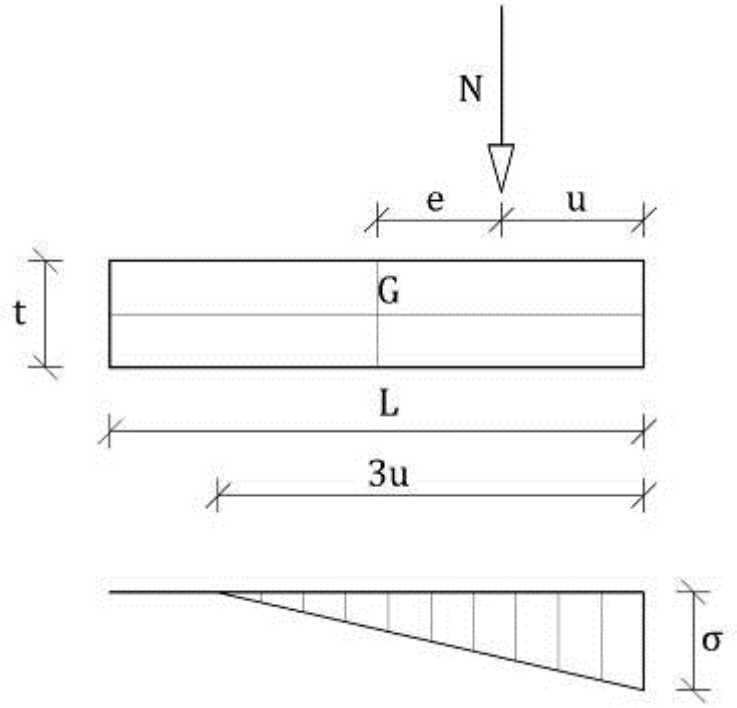

Figure 3.7: Cross section analysis.

The shear resistance for sliding should be linear for small eccentricity and nonlinear for large eccentricity. Substituting the expressions of various terms, in the case of large eccentricity:

$$V_{ss} = 3 \cdot \left(\frac{L}{2} - e \right) \cdot t \cdot \left(f_{vk0} + \mu \cdot \sigma' \right), \tag{3.40}$$

which becomes, after expressions for normal stress and the eccentricity (3.38):

$$V_{ss} = 3 \cdot \left(\frac{L}{2} - \frac{M}{N} \right) \cdot t \cdot \left(f_{vk0} + \mu \cdot \frac{N}{D' \cdot t} \right), \tag{3.41}$$

that is:

$$V_{ss} = 3 \cdot \left(\frac{L}{2} - \frac{M}{N} \right) \cdot t \cdot \left(f_{vk0} + \mu \cdot \frac{N}{3 \cdot \left(\frac{L}{2} - \frac{M}{N} \right) \cdot t} \right). \tag{3.42}$$

Currently this is the adopted formula by Eurocode 8.

3.1.3 Bending failure

The failure criteria which identify the limit load capacity of a masonry wall can consider different forms of the constitutive law of the masonry: linear, nonlinear (parabola-rectangle), stress block.

In the case of constant stress-deformations block diagram, the ultimate condition occurs when masonry reaches the maximum deformation, usually equal to [6]:

$$\varepsilon_{mu} = 0{,}0035. \tag{3.43}$$

Since it is generally assumed that cross section of the wall remains plane in its deformed configuration. The axial stress distribution is linear throughout the masonry section and the following value ε(x) can be determined for the axial strain developed by the masonry fiber at distance x from the most compressed side of the section (Figure 3.8):

$$\frac{\varepsilon_{mu}}{x_c} = \frac{\varepsilon(x)}{x_c - x} \quad \text{->} \quad \varepsilon(x) = \frac{\varepsilon_{mu}}{x_c} \cdot (x_c - x) \tag{3.44}$$

.

Then, if the stress-block distribution is assumed for compressive axial stresses, the position of the neutral axis can be easily evaluated by equilibrium:

$$\psi \cdot t \cdot x_c \cdot 0{,}85 \cdot f_c = N \quad \text{->} \quad x_c = \frac{N}{\psi \cdot t \cdot 0{,}85 \cdot f_c} \cdot \tag{3.45}$$

where:

- Ψ is a coefficient which generally ranges between 0,8 and 1,0;
- f_c is the compressive strength of the masonry.

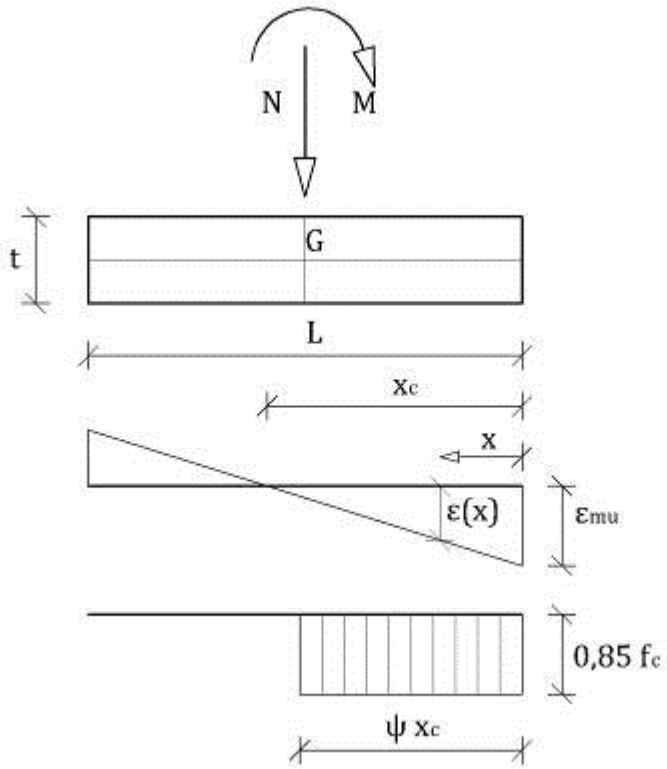

Figure 3.8: ULS analysis for buckling of a masonry cross section.

The Italian code [6] recommend to take a maximum compression strength for stress block equal to 0,85 f_c and $\psi = 1$.

Thus, the ultimate moment can be calculated as:

$$M_u = \psi \cdot t \cdot x_c \cdot 0{,}85 \cdot f_c \cdot \left(\frac{L}{2} - \psi \cdot \frac{x_c}{2} \right). \tag{3.46}$$

Substituting the expression of the neutral axis:

$$M_u = \psi \cdot t \cdot \left(\frac{N}{\psi \cdot t \cdot 0{,}85 \cdot f_c} \right) \cdot 0{,}85 \cdot f_c \cdot \left(\frac{L}{2} - \frac{\psi}{2} \cdot \frac{N}{\psi \cdot t \cdot 0{,}85 \cdot f_c} \right). \tag{3.47}$$

The following expression can be obtained for M_u after simple mathematical passages:

$$M_u = N \cdot \left(\frac{L}{2} - \frac{N}{2 \cdot t \cdot 0{,}85 \cdot f_c} \right) = \frac{1}{2} \cdot N \cdot L \cdot \left(1 - \frac{N}{L \cdot t \cdot 0{,}85 \cdot f_c} \right). \tag{3.48}$$

The previous can also be expressed in terms of average axial stress:

$$M_u = \frac{1}{2} \cdot N \cdot L \cdot \left(1 - \frac{\sigma}{0{,}85 \cdot f_c}\right) = \frac{1}{2} \cdot \frac{N}{L \cdot t} \cdot L \cdot t \cdot L \cdot \left(1 - \frac{\sigma}{0{,}85 \cdot f_c}\right). \quad (3.49)$$

Finally, the ultimate moment can be calculated as:

$$M_u = \frac{1}{2} \cdot \sigma \cdot t \cdot L^2 \cdot \left(1 - \frac{\sigma}{0{,}85 \cdot f_c}\right). \quad (3.50)$$

The maximum eccentricity that can be calculated for ultimate sliding shear is:

$$e = \frac{M_u}{N} = \frac{M_u}{\sigma \cdot t \cdot L} = \frac{L}{2} \cdot \left(1 - \frac{\sigma}{0{,}85 \cdot f_d}\right), \quad (3.51)$$

and the corresponding maximum curvature of cross section is:

$$\chi_y = \frac{\varepsilon_{mu}}{x_c}. \quad (3.52)$$

A corresponding shear force V_{bm} can be associated to the ultimate moment M_u once the wall boundary conditions are defined and a proper value of the shear length L_v is defined. In the case of doubly fixed wall $L_v = h/2$ and:

$$V_{bm} = \frac{2 \cdot M_u}{h}. \quad (3.53)$$

3.1.4 Comparison between different collapse mechanisms

The following three expressions for the ultimate shear have been determined in the previous section depending on the actual above three failure mechanisms under consideration:

- diagonal shear: $V_{ds} = L \cdot t \cdot \frac{1{,}5 \cdot f_{vk0}}{\lambda} \cdot \sqrt{1 + \frac{\sigma}{1{,}5 \cdot f_{vk0}}}$; (3.54)
- sliding shear: $V_{ss} = D' \cdot t \cdot f_{vd}$; (3.55)
- flexural shear: $V_{bm} = \frac{2 \cdot M_u}{h}$. (3.56)

The ultimate shear strength V_u is the smallest:

$$V = \min(V_{ds}, V_{ss}, V_{bm}). \tag{3.57}$$

It is possible to calculate the stiffness for the elastic range of the wall's response with the following formula, which takes into account both the bending stiffness and shear deformation:

$$k = \frac{1}{\frac{h^3}{12 \cdot E \cdot I} + \frac{\chi \cdot h}{G \cdot A}}, \tag{3.58}$$

where:

- $\frac{h^3}{12 \cdot E \cdot I}$ is the displacement in bending;
- $\frac{\chi \cdot h}{G \cdot A}$ is displacement in shear;
- $\chi = \frac{6}{5} = 1{,}2$ (in the case of rectangular cross section).

The previous relationship is identical to the following [17]:

$$k = \frac{G \cdot A}{1{,}2 \cdot h} \cdot \frac{1}{1 + \frac{1}{1{,}2} \cdot \frac{G}{E} \cdot \left(\frac{h}{L}\right)^2}. \tag{3.59}$$

The corresponding displacement can be defined at the conventional yield:

$$V = k \cdot \delta \qquad \text{->} \qquad \delta_y = \frac{V}{k}. \tag{3.60}$$

For the complete definition of the constitutive law of the wall panel (showed in Figure 3.9), the ultimate displacement can be defined as a product of the elastic limit displacement by a ductility factor:

$$\delta_u = \mu \cdot \delta_y. \tag{3.61}$$

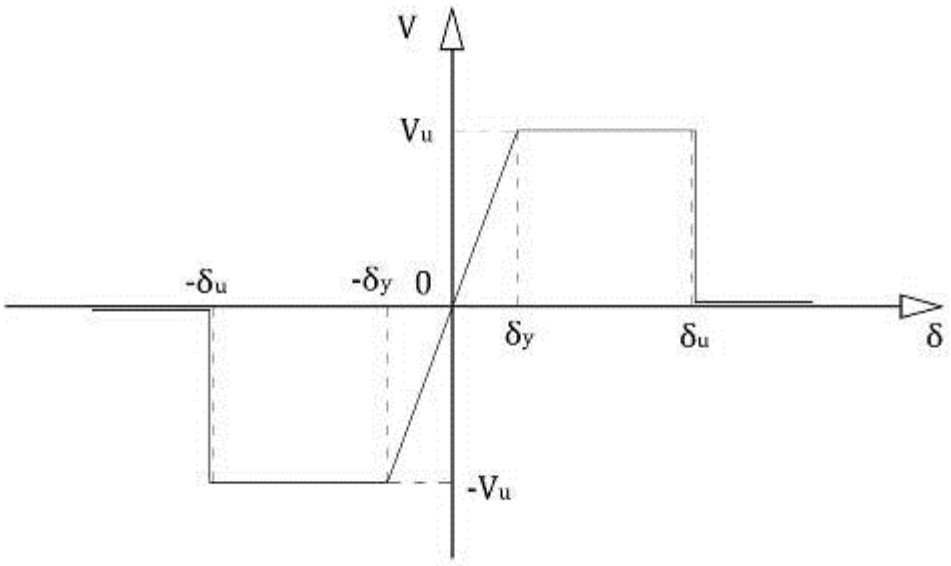

Figure 3.9: Bi-linear shear behaviour.

The ductility factor is defined as ratio between the ultimate displacement and the elastic limit displacement:

$$\mu = \frac{\delta_u}{\delta_y}. \tag{3.62}$$

It has prescribed in [17] value of ductility equal to:

- 1,5 for existing walls in good condition;
- 2,0 for existing reinforced walls.

Moreover, [6] fixes the value of ultimate displacement as a percentage of pier height as a function of different type of failure:

- 0,4% h for the shear failure mode (diagonal or sliding);

- 0,8% h for the flexural failure mode.

It is interesting that, if the geometrical and mechanical characteristics of the panel are fixed, the failure mode depends only on the axial force.

In the following Figure 3.10 there are the trends of three ultimate shear as a function of the normal force (in no-dimensional values with the use of a factor like Ltf_c). Usually, for small values of normal stress, sliding shear is critical; for intermediate values there is a diagonal cracking and for large values there is a flexural failure. These curves present the interaction diagram of the wall.

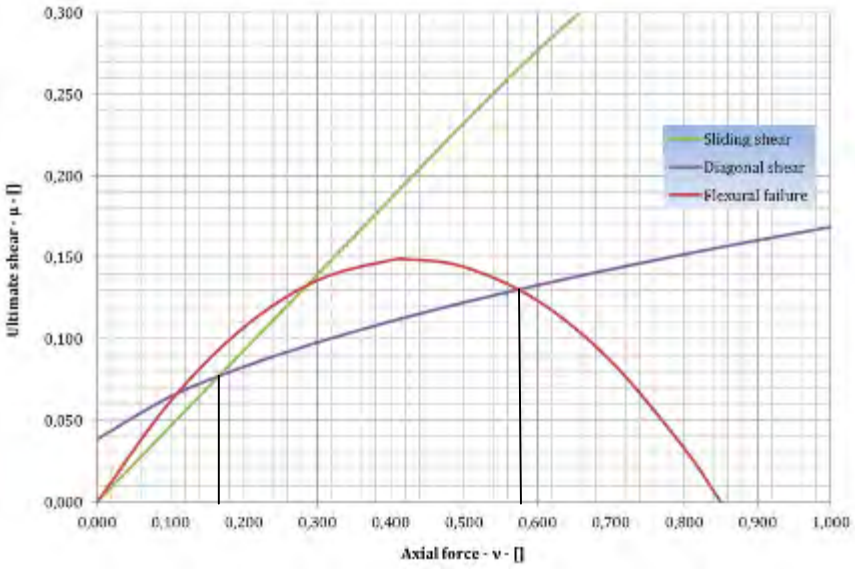

Figure 3.10: Variation of ultimate shear stress in relation to normal (FN) for the three collapse modes.

3.2 Classification

The behaviour of multi–storey structures is strongly influenced by the presence of spandrels. Indeed, according to the rigidity of the spandrels in relation to that of piers there are different static schemes of these ones. In practice, the models change from piers prevented to rotate at the top (infinitely rigid spandrels) to piers free to rotate to the top. In some analysis models the presence of spandrels in addition to the masonry walls are considered.

The methods of analysis can be:

1) one-dimensional models: the masonry walls and spandrels are shown as frame elements in nonlinear behaviour;
2) bi-dimensional models: they used finite elements or macro elements.

The one-dimensional models may require the use of:

a) infinitely rigid spandrels: POR method [18], RES method [38], Porflex method [34], floor spandrels method;
b) transverse with zero bending stiffness: independent piers models, piers coupled with penduli;
c) equivalent frames: SAM method [39].

The bi-dimensional models, as mentioned, use:

a) finite macro-elements: SISV model [40][41], MAS3d model [42][43];
b) finite elements: [44][45].

3.2.1 One-dimensional models: with rigid transverse

3.2.1.1 POR Method

One of the most popular simplified methods for the analysis of the walls behaviour for in-plane action is POR method [18]. In this method the possibility that piers collapsing producing a crisis for diagonal cracking are considered.

The method in question does the following assumptions:

1) infinite strength and stiffness of the floor spandrels;
2) piers crisis for diagonal shear;
3) negligible increases in piers of normal stress due to horizontal actions.

For the first hypothesis, the wall analysis models is reduced to a simple shear-type frame, as shown in the following example in Figure 3.11.

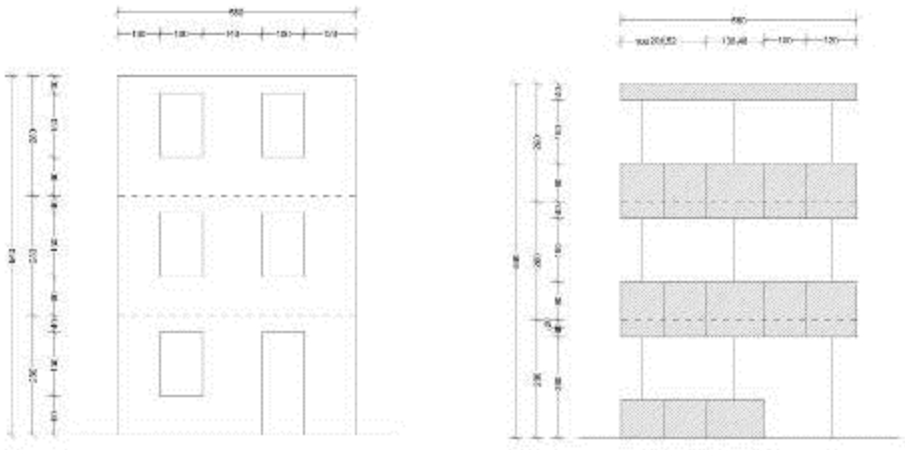

Figure 3.11: Real wall (on the left) and POR modelling.

In practice, the spandrels are replaced by rigid transverse and only piers are deformable elements. This first hypothesis is very forced, especially when in the considered structure they are not present stiffening elements such as architraves or spandrels with significant thickness (especially on the top floor) or floor beams.

However, this assumption produces acceptable results for structures with regular openings and made up by few floors. Manual analysis of the masonry walls can be done.

The second case involves a crisis in the piers only for diagonal cracking. This assumption is valid especially for squat piers, or with low slenderness ratios (height/length).

The more restrictive assumptions, however, is the third. The reason is that, especially for tall buildings, the horizontal seismic action can cyclical increase or decrease the normal stress in piers, especially the most perimetral.

The POR method was formulated, in the first place, with reference to a single piers wall and subjecting it to a quasi-static test with cyclic loading in its plane. From such tests, recording the top displacements in function of the base shear, it is possible to achieve nonlinear developments such as the Figure 3.12.

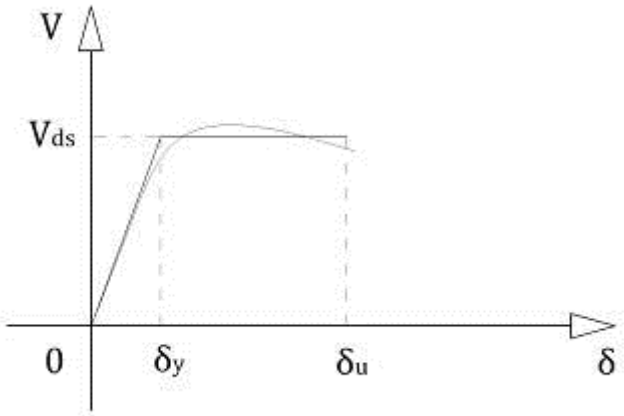

Figure 3.12: Constitutive law of a single masonry panel and relative idealisation.

However, this complicated relationship can be simplified by considering a conveniently elastic–perfectly plastic behaviour.

To calculate the ultimate shear, the following formula proposed by the NTC 2008 [6] and Commentary No. 617 [23], valid in the presence of non–zero vertical stress, can be applied:

$$V_{ds} = L \cdot t \cdot \frac{1{,}5 \cdot f_{vk0}}{\lambda} \cdot \sqrt{1 + \frac{\sigma}{1{,}5 \cdot f_{vk0}}} \,. \tag{3.63}$$

Alternatively the following formula, proposed by Commentary 21745 [17] can be used:

$$V_{ds} = L \cdot t \cdot f_{vk0} \cdot \sqrt{1 + \frac{\sigma_0}{1{,}5 \cdot f_{vk0}}} \,. \tag{3.64}$$

Finally, there is the following relationship proposed by Turnsek and Cacovic [35]:

$$V_{ds} = L \cdot t \cdot \frac{f_t}{b} \cdot \sqrt{1 + \frac{\sigma}{f_t}} \,. \tag{3.65}$$

where:

- f_t is the maximum shear strength, greater than f_{vk0}, obtained through a diagonal shear test on a masonry wall;
- b is a distribution shear stresses factor, which usually takes values between 1,0 and 1,5 and is a function of the slenderness panel.

In particular, according to Benedetti and Tomazevic [36], the b factor is:

$$b = 1{,}5 \qquad \text{for:} \qquad \frac{h}{L} \geq 1{,}5 \tag{3.66}$$

$$b = 1{,}0 \qquad \text{for:} \qquad \frac{h}{L} \leq 1{,}5 \tag{3.67}$$

$$b = \frac{h}{L} \qquad \text{for:} \qquad 1{,}0 \leq \frac{h}{L} \leq 1{,}5 \tag{3.68}$$

To define completely the previous relationship it is necessary to introduce a panel stiffness, which takes into account both the bending deformability and shear deformability:

$$\frac{1}{k} = \frac{1}{k_f} + \frac{1}{k_v}, \tag{3.69}$$

in the case of rectangular cross section:

$$k = \frac{1}{\frac{h^3}{12 \cdot E \cdot I} + \frac{\chi \cdot h}{G \cdot A}} \,. \tag{3.70}$$

Ultimately, the relationship of each panel is represented by the following equations:

$$V(\delta) = k \cdot \delta \quad \text{if:} \quad 0 \le \delta \le \delta_y = \frac{V_{ds}}{k} \tag{3.71}$$

$$V(\delta) = V_{ds} \quad \text{if:} \quad \delta_y \le \delta \le \delta_u = \delta_y \cdot \mu \tag{3.72}$$

where:

- μ is a ductility factor greater than one.

Turning, finally, to consider an entire wall, a shear-displacement relationship for each pier can be defined and then the superposition principle can be applied to obtain the curve for the entire wall.

In this case:

a) the maximum displacement of entire wall coincides with the minimum ultimate displacement among those of all the individual piers;
b) the elastic limit displacement coincides with the lowest elastic displacement of all piers;
c) the overall wall stiffness gradually decreases when the piers are plasticised.

Ultimately, for the wall exposed in the previous Figure 3.11, for example, the following behaviour of Figure 3.13 can be obtained.

From the previous diagram, the ultimate shear of the wall can be compared with the seismic shear applied to the structure to carry out a seismic verification. In particular:

$$V_u > F_h . \tag{3.73}$$

In particular, standards [46] requiring:

1) $\eta_e = \frac{V_e}{F_h} \ge 1{,}10$; (3.74)

2) $\eta_f = \frac{V_f}{F_h} > 1{,}15$; (3.75)

3) $\eta_u = \frac{V_u}{F_h} > 1{,}20$. (3.76)

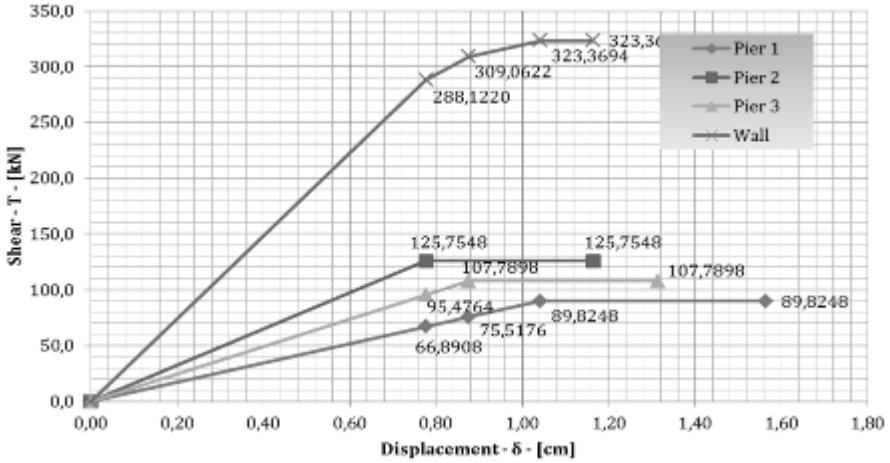

Figure 3.13: Constitutive law of a wall obtained by the POR method.

where:

- V_e is the minimum elastic shear of all masonry walls;
- V_f is the wall carrying capacity to the cracking limit, that is the shear corresponding to a displacement equal to 20% higher than that seen in the preceding point;
- V_u is the shear at the minimum ultimate displacement of all masonry walls.

The Commentary 21745 [17] and Ministerial Decree 16/01/1996 [19] include a verification solely on the ultimate wall strength, which must be greater than the design seismic base shear. Finally, the OPCM 3274 [22] has two modes of verification:

a) in the case of linear analysis a test of wall strength as the Ministerial Decree of 1996 is required;
b) in the case of nonlinear analysis, however, a displacement check both with reference to the Damage Limit State and with reference to the Ultimate Limit State is required.

3.2.1.2 RES Method

The RES method [38] (Equivalent Slenderness Ratio) represents an evolution of the POR method and was introduced to take into account the influence of geometric slenderness and floor spandrels on the evaluation of ultimate strength of multi–storey masonry walls.

Since the POR method is procedure with a check of each floor, the following hypotheses must be assumed:

1) all possible modes of collapse of the walls (diagonal cracking, shear sliding and bending) are possible;
2) the wall's slenderness must change for single pier to take into account the infinite stiffness of the spandrels.

In other words, for the second hypothesis, an intermediate behaviour between multi storey wall model (although with windows) and independent masonry walls connected by penduli model must be defined. The purpose is to overcome the applicability of the POR method to buildings of only two or three floors, which were summarised as the shear-type frame.

To take into account the different failure modes, the RES method introduces a correction factor k_t of the ultimate shear calculated with the POR. In particular:

$$\tau_u = \tau_{u,POR} \cdot k_t . \tag{3.77}$$

where:

- k_t is the correction factor which depends by the ratio between the ultimate shear ultimate corresponding to the three mode of collapse;
- τ_u is the no-dimensional ultimate shear of the wall panel;
- $\tau_{u,POR}$ is the no-dimensional ultimate shear for diagonal cracking crisis.

The RES method uses the following equation for calculating the optimal slenderness of masonry walls, in order to take into account the effective stiffness of the spandrels:

$$\lambda_{ott,i} = \lambda_p + \left[\left(\lambda_{m,i} - \lambda_p \right) \cdot \psi^{1,25 + \left(56,591 \cdot \frac{f_{vk0}}{f_{ck}} + 0,621 \right) \cdot \lambda_p} \right], \tag{3.78}$$

where:

- $\lambda_p = \frac{h_0}{B}$ is the slenderness of the full wall, disregarding the openings;
- $h_0 = \frac{2 \cdot M}{T}$ is double of the ratio between the moment and the base shear of the wall;
- B is the base length of the entire wall;
- $\lambda_{m,i} = \frac{h_0}{b_i}$ is the wall slenderness of the single pier;
- b_i is the base width of the pier;
- $\psi = \frac{h_v}{h_i}$ is the ratio between the height of the opening and the height of floor;
- f_{vk0} and f_{ck} are, respectively, the characteristic shear strength in the absence of normal stress and the characteristic compressive strength.

The previous report was obtained by performing several finite element simulations and the accuracy of the method has been checked by comparing with the computer code ADINA (see Figure 3.14).

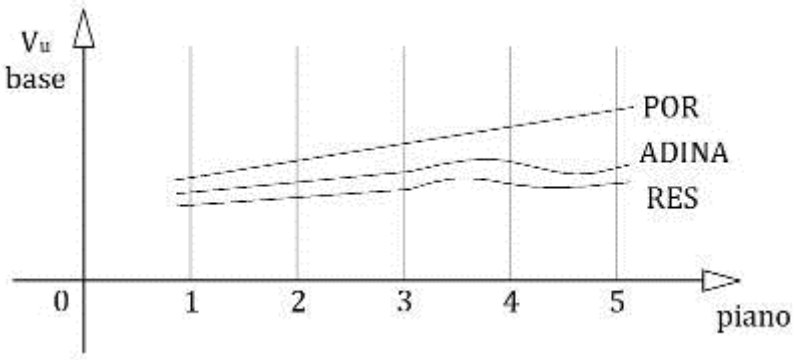

Figure 3.14: Comparison between approximate methods and sophisticated methods.

3.2.1.3 Porflex method

The Porflex method [34] serves to extend the POR method to structures with many floors and more complex but still preserving the simplicity of the method.

In this method they have been removed some of the simplifying assumptions by POR method, in particular:

- spandrels infinitely stiff but not infinitely deformable;
- piers failure for shear or bending;
- variable normal stress in piers.

For the first two assumptions, the Porflex method is certainly conservative compared to the POR method, or the Porflex method and gives results in terms of forces, lower than the POR method.

The scheme of the Porflex method wall is an equivalent frame of the masonry wall consists on rigid and deformable sections (shown in Figure 3.15).

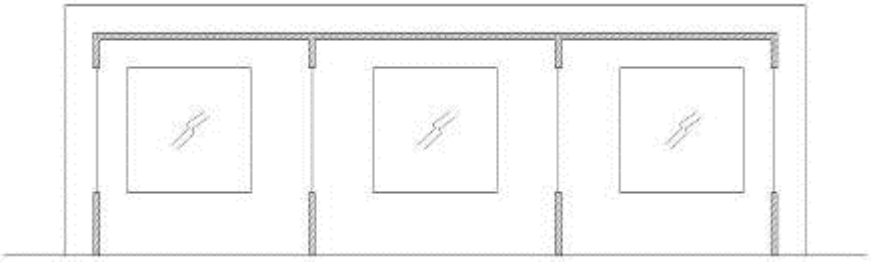

Figure 3.15: Equivalent frame of the Porflex method.

In this scheme, the piers have considered constrained in spandrels. In particular, there is a sliding interlocking until the stresses are lower than the failure condition and a hinge in the case of a shear or bending failure.

In particular, in this method they are taken the following constitutive laws shown in Figure 3.16:

a) rigid-fragile relationship for the normal and shear stresses into spandrels, that are infinitely stiff but not infinitely strong;
b) elastic-perfectly plastic relationship for shear behaviour of masonry walls, similar to what is assumed for the POR method;

c) elastic-fragile relationship for normal stresses behaviour, both in tensile and compressive stress.

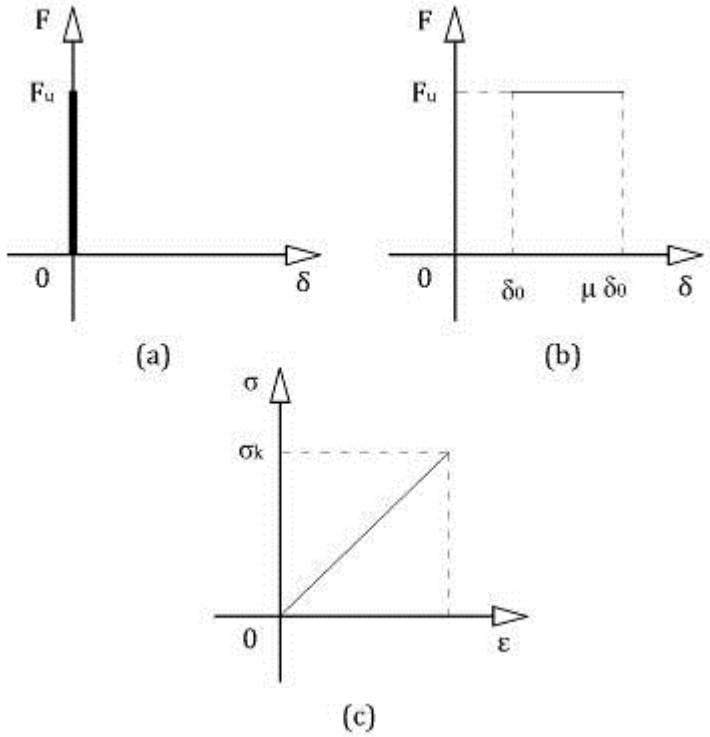

Figure 3.16: Constitutive laws of the resistant elements in Porflex.

In this method, in order to take also the spandrels as resistant elements, the masonry tensile strength must be assumed not zero. The reason is that, unlike piers, the wall spandrels have not subject to any normal stress and, therefore, there can be no equilibrium regardless of the tensile strength of masonry.

3.2.2 One-dimensional models: transverse with no-bending stiffness

3.2.2.1 Models with independent walls

In this case, the masonry walls behave as a strong independent element to each other and modelled as the frames fixed to the base (Figure 3.17).

This model is acceptable when the following two conditions occur:

1) floor spandrels, both material and size, are of very little strength and are therefore not a constraint for the masonry walls;
2) there are not floor beams and then the piers are independent on each other.

In this situation, seismic testing should be conducted separately for each piers.

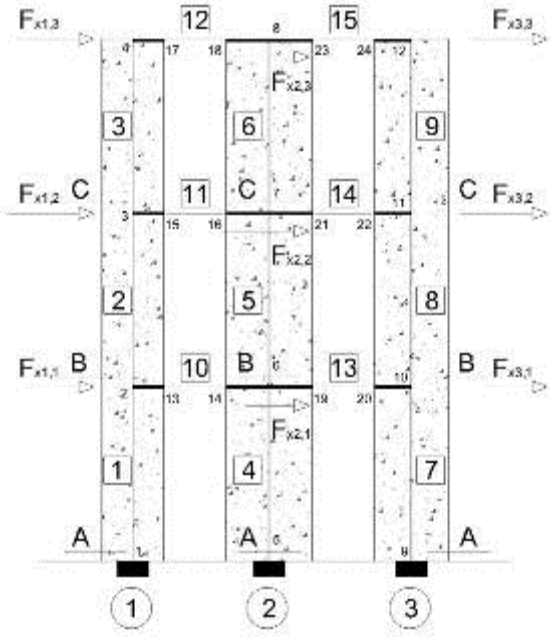

Figure 3.17: Wall model with transverse of nothing flexural stiffness and no floor beams.

The static model consists of different frames fixed at the base and subject to forces at the level of floor. For this reason, the characteristic of shear stress and the normal stress grow downward.

The bending moment, however, is linear. For this reason, for each independent piers, the check at each level taking into account all the possible collapse mechanisms must be executed.

For the model assumed in this case, there are large bending moments at the base and large slenderness of the wall. This often makes determinant the bending shear verification.

3.2.2.2 Models with walls linked by penduli

In this case there is a wall made of masonry piers connected together at each floor level, from inextensible penduli (Figure 3.18). This model is valid when it is possible to consider floor spandrels deformable and with very little strength and when the floor beams are very effective.

In this case, therefore, the penduli require an equality of displacements at each floor. For this reason, the seismic actions to apply to different piers, unlike the previous case, must be divided among piers according to their rigidity.

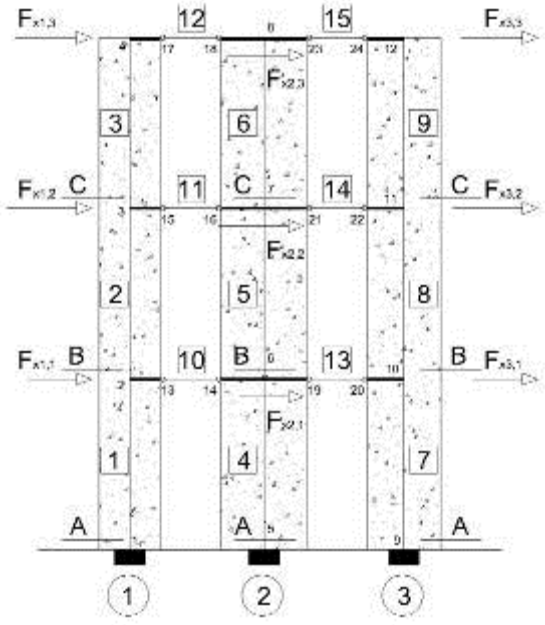

Figure 3.18: Wall model with transverse of nothing flexural stiffness and efficient floor beams.

In particular, for the generic piers is:

$$\{F\}_i = [K]_i \cdot \{\delta\}_i , \tag{3.79}$$

where:

- $\{F\}_i$ is the vector of the floor seismic forces relating to the piers “i”;
- $[K]_i$ is the stiffness matrix of translating of the piers “i”;
- $\{\delta\}_i$ is for the vector of the storey displacement of piers “i”.

For the entire wall must be:

$$\{F\} = \sum_i \{F\}_i = \sum_i [K]_i \cdot \{\delta\}_i = \sum_i [K]_i \cdot \{\delta\} = [K] \cdot \{\delta\}, \tag{3.80}$$

where:

- $\{F\}$ is for the vector of the floor seismic forces of the entire wall;
- $[K]$ is the stiffness matrix of the entire wall;
- $\{\delta\}$ is the vector of displacements of the entire wall.

The floor global displacements, for the presence of inextensible pendulums, are equal to floor displacement of individual frames.

Reversing the previous (3.80) the unknown displacements, which then enable the analysis of the actions of individual piers, can be obtained:

$$\{\delta\} = [K]^{-1} \cdot \{F\} = [D] \cdot \{F\}, \tag{3.81}$$

being:

- $[K]^{-1} = [D]$ the matrix of deformation of the entire wall.

The stiffness matrix of the entire wall can, therefore, be calculated from the stiffness matrix of individual masonry walls. This last, in turn, can be calculated, proceeding by columns, in two ways:

a) direct method: the generic piers is subjected to the unitary displacements of each floor and the relative shear can be calculated;
b) indirect method: the generic piers is subjected to the unitary action at each floor and can be calculated the floor displacements, which constitute

the terms of the matrix deformation, which can be inverted to obtain the stiffness matrix.

The indirect method presents, unlike the direct method, an extra step because it needs to invert the matrix of deformability.

However, the indirect method is used because it allows to work on a isostatic structure (frames subject to unitary forces), unlike the direct method, where the displacements to apply to each unit, whether by use of auxiliary constraints.

3.2.3 Equivalent frames models

A good model for analysis of a masonry structure must possess the following basic requirements:

1) it must include all the possible collapse mechanisms;
2) it must comply with all local and global equilibrium;
3) it must be reached the right balance between level of detail and ease of use;
4) it need to define the damage, for example according to the displacement.

The following paragraphs set out the methods based on the use of macro elements or finite elements, which generally provide excellent reliability, but are often expensive to apply.

For that reason today they are often used simplified models, especially with equivalent frames. In this model, the generic masonry structure is reviewed as a frame made up from truss items. Often, the model would involve the use of rigid offset in order to outline the nodal zones of intersections between piers and spandrels. The most important of these methods is no doubt the SAM method [39] that is shown below.

3.2.3.1 SAM method

This is an equivalent frame method developed by Magenes and Calvi in 1996 [39]. Initially this method was implemented for the analysing of plan walls. Then, for three-dimensional buildings, the algorithm was implemented in a nonlinear structural analysis code.

Consider the analysis of a multistory wall subjected to increasing horizontal actions and constant vertical loads (see Figure 3.19).

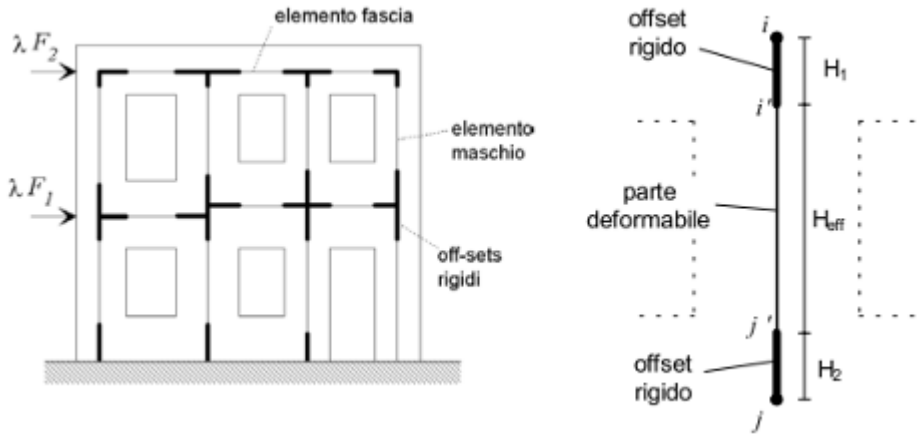

Figure 3.19: Schematic equivalent frame of a wall loaded in the plane [39].

It is possible modelling the wall as a frame consisting of:

- piers elements;
- spandrels elements;
- nodes elements.

Only the first two elements are modelled as elements with axial and shear deformation. The node elements are infinitely rigid and strong and they are modelled through the use of offset elements.

The piers elements are characterised by a certain effective length of the deformable part, which can be calculated with an appropriate formula proposed from Dolce [47] and exposed in Figure 3.20.

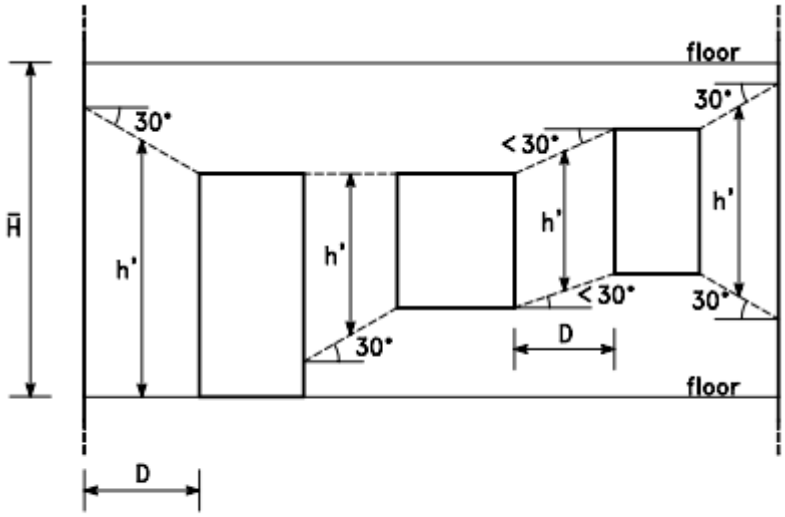

$$H_{eff} = h' + \frac{1}{3} D(\bar{H} - h')/h' \qquad \bar{H} = \text{altezza interpiano}$$

Figure 3.20: Effective length in piers [39].

For masonry walls they are provided the following failure mechanisms:

a) failure for bending: when the ultimate bending moment to the extreme sections of the deformable part is reached;
b) failure for shear with diagonal cracks: it happens when the ultimate value of the shear is reached, assumed to be equal to the minimum value among the diagonal shear associated with the failure of the mortar joints and the diagonal shear associated with the failure of the bricks;
c) it is assumed an elastic–plastic behaviour with a limit deformation;
d) failure for sliding shear: it occurs along a mortar bed of one of the extreme sections.

For the masonry element spandrels they are defined effective lengths similar to those of piers, but the possible failure mechanisms are only for bending and shear (see Figure 3.21). In particular, in the case of shear failure the different location of the mortar beds must be taken into account.

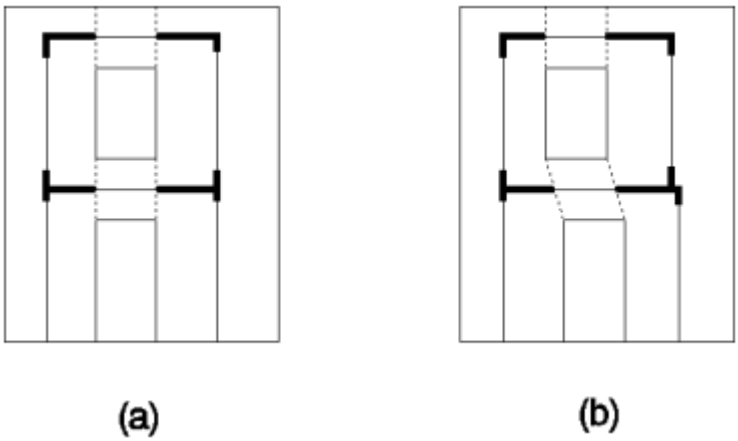

Figure 3.21: Definition of the effective length of the spandrel [39].

3.2.4 Bi–dimensional models

3.2.4.1 Models with macro–finite elements

The idea of using macro-elements is due to the search a discretisation of a generic wall as consisting of areas with a very pronounced damage (piers and spandrels) and areas that are preserved intact, in seismic combination, as if they should be rigid elements.

The entire wall is then modelled by an assembly of macro-elements opportunities connected with rigid blocks. Subsequently, these models allow to perform seismic analysis to evaluate the static and dynamic response of the wall.

The models with macro elements include:

- SISV model [40][41] (Settis Inclined with Variable Section) means any element of vertical masonry panel is modelled as a tensile zone not cooperating and a compression zone modelled as a variable section beam element (Figure 3.22);

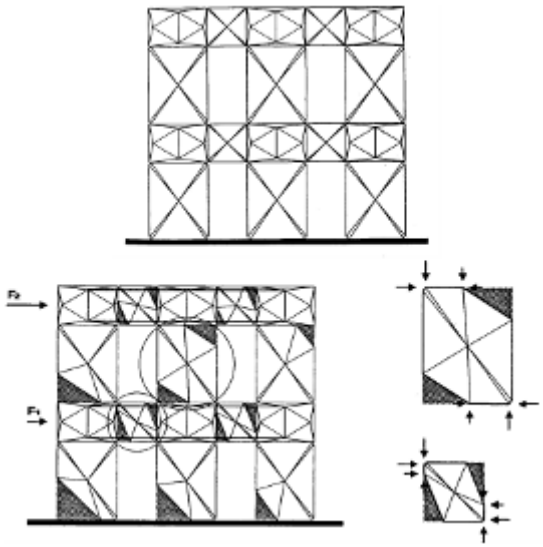

Figure 3.22: Model with finite element with variable geometry [39].

- MAS3D model [42][43]: it uses a panel element (shown in Figure 3.23) that does not respond to compression and is made from a compressed set of fans whose terminal faces are rigid and are not allowed interactions between the sides of the primary fans.

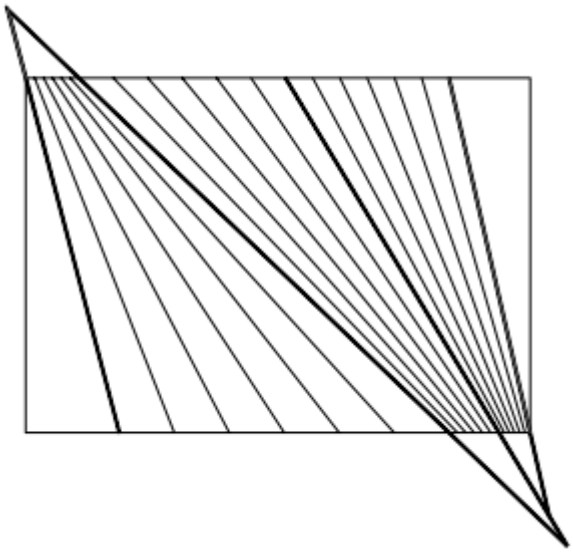

Figure 3.23: Multi–array element [39].

3.2.4.2 Finite Elements Models

The Finite Element Method (FEM) is a discretisation techniques which turns the partial differential equations of general structural problems to a set of algebraic equations.

As a first step, the body or structure is subdivided (discretised) in different subdomains called Finite Elements (see Figure 3.24). Those subdomains are connected to each other in some nodes which define a so-called mesh. The displacement of the nodes of the structural system are generally assumed as key unknown of the structural problem.

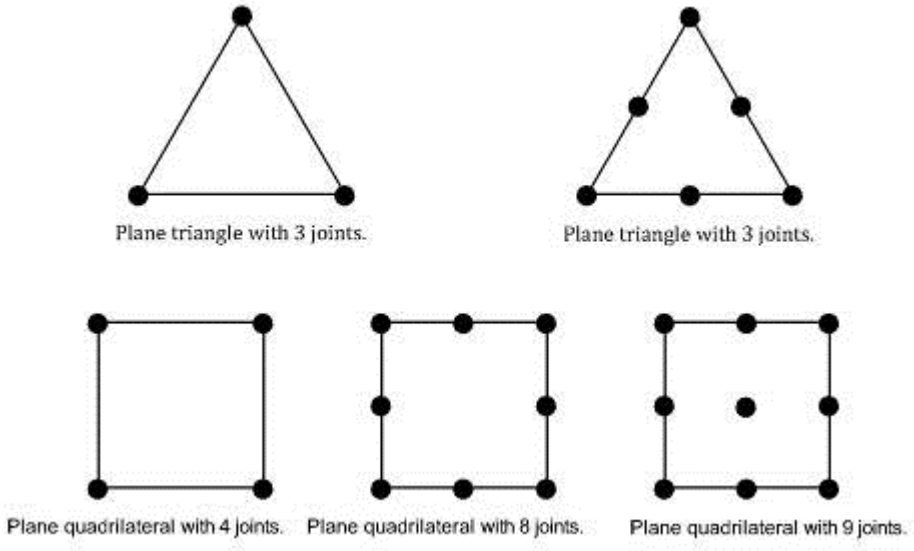

Figure 3.24: Bi-dimensional finite elements.

For the correct discretisation the following customs must be respected:

a) to avoid elements with irregular form: long and thin rectangles, flattened triangles;
b) to thicken the number of nodes in areas where stresses are concentrated;
c) to evaluate the accuracy of the results obtained by increasing the thickening and evaluating the convergence conditions.

3.3 Seismic analysis of masonry structures

The seismic analysis is intended at determining the effects (in terms of displacement, stresses and strains) induced by the earthquake shaking on the structure under consideration.

Firstly structural analysis under seismic actions may be linear: an elastic analysis is carried out considering the structure subjected to a set of static forces by considering a fixed value of the q–factor. It takes into account the dissipative capacity of structure and the damage capacity compatibly with the desired level of performance.

This factor can be defined as the following ratio (Figure 3.25):

$$q = \frac{F_e}{F_y} = \frac{\delta_e}{\delta_y}. \tag{3.82}$$

where:

- F_e is the elastic force of the structures modelled like an SDOF (Single Degree of Freedom) under seismic load;
- F_y is the limit elastic force of the system;
- δ_e and δ_y are the elastic displacement under seismic load and the elastic limit displacement.

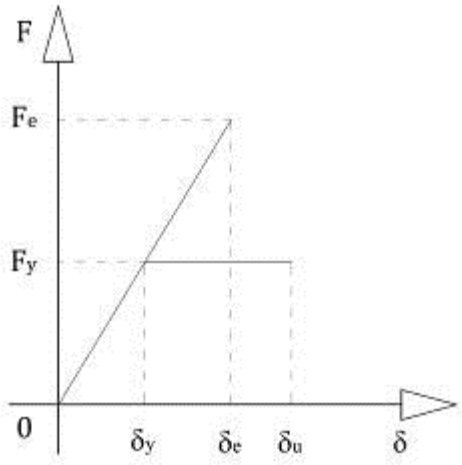

Figure 3.25: Transition from elastic behaviour to an elastic perfectly plastic behaviour.

The possible reduction of the elastic force F_e depends on the available ductility of the structures. It is clear that fragile structures ($\mu = 1$) should be designed for bearing elastically under action F_e. However, q-factor value can be determined with the following relationships:

$$q = \sqrt{2 \cdot \mu - 1} \qquad \text{if:} \qquad T < T_C ; \tag{3.83}$$

$$q = \mu \qquad \text{if:} \qquad T > T_C . \tag{3.84}$$

where:

- $\mu = \frac{\delta_u}{\delta_y}$ is the ductility of the structural system idealised as an elastic perfectly plastic behaviour and equal to the ratio between the ultimate system displacement and the plasticisation displacement;
- T is the fundamental structure period of vibration, properly represented as a SDOF system.

In particular, it was observed experimentally that the behaviour is represented in the following Figure 3.26.

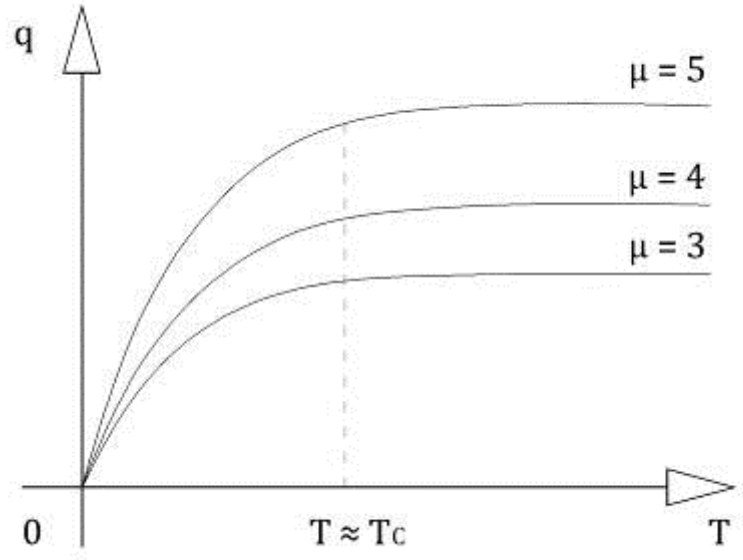

Figure 3.26: Change of the q–factor as a function of the vibration period for fixed values of ductility.

The two previous equations can be obtained from the following two principles:

a) in the case of short periods, so-called principle of "conservation of energy", which can equalise the area under the linear behaviour and the area subtended the bi–linear behaviour;
b) in the case of high periods, the principle of "equal displacement" is valid, and ultimate displacement of the elastoplastic structure is equal to the maximum displacement of the elastic structure.

In the first case (see Figure 3.25), an analytical relationship between the available ductility μ and the force reduction factor (q) can be obtained.

In particular, the equivalence of the energy shared by the elastic and inelastic system represented in Figure 3.25 leads to the following relationship:

$$\frac{1}{2}\cdot F_e \cdot \delta_e = \frac{1}{2}\cdot F_y \cdot \delta_y + F_y \cdot \left(\delta_u - \delta_y\right), \tag{3.85}$$

and, after dividing for $F_y\,\delta_y$ the (3.85):

$$\frac{1}{2}\frac{F_e \cdot \delta_e}{F_y \cdot \delta_y} = \frac{1}{2} + \frac{\delta_u}{\delta_y} - 1 = \mu - \frac{1}{2}. \tag{3.86}$$

Remembering the first definition of q–factor in (3.82) and multiplying for two the previous relationship (3.86), the following solution is obtained:

$$q = \sqrt{2\cdot\mu - 1}\,. \tag{3.87}$$

In the second case (shown in Figure 3.27), instead:

$$T > T_C\,. \tag{3.88}$$

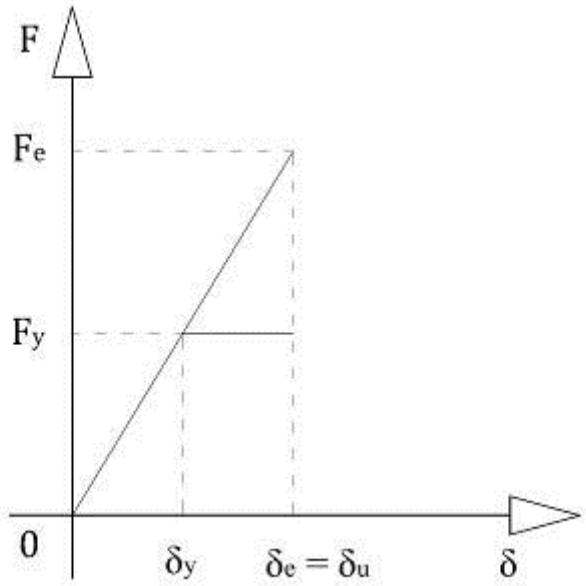

Figure 3.27: Case 2.

The q–factor, in this case, will be, for the principle of equality of maximum displacement:

$$q = \frac{F_e}{F_y} = \frac{\delta_e}{\delta_y} = \frac{\delta_u}{\delta_y} = \mu . \tag{3.89}$$

Seismic analysis of structures can then also be nonlinear, when they take into account the nonlinear capacity of the material and geometry. This type of analysis is used for dissipative systems, that have some capacity in plastic field and have a ductility greater than one.

A second classification of seismic analysis, in relation to how they will handle the equilibrium, distinguishes between:

- static analysis: they use lateral actions that must be applied to the structure for modelling the earthquake and in the analysis of stresses and deformations;
- dynamic analysis: to perform the structure modal analysis, the identification of the main modes of vibration and evaluation of the effects that produce.

3.3.1 Linear static analysis

The dynamic response to seismic actions can be studied using linear and nonlinear analysis on a standard three dimensional model. The analysis of the local effects can refer instead to models of isolated parts of the whole resistant organism.

The linear static analysis is based on applying static forces, which are supposed to be equivalent to the ones induced by the earthquake. This analysis is usually applied to buildings that look like regular period of oscillation that verifying with the relation:

$$T_1 < T_D . \tag{3.90}$$

This analysis procedure can be performed manually and it is also useful during the pre–sizing.

The linear static analysis can be applied to both regular buildings in height and irregular building. The regularity requirement is necessary to ensure that same oscillations are similar to those of a system with a single degree of freedom (SDOF: Single Degree of Freedom), with the involvement of the totality of the mass and with torsional oscillations limited. For irregular buildings any seismic reduction is possible.

The static analysis is conducted using rigid floor in the horizontal plane and obtaining the walls stiffness, taking into account both the flexural and the shear stiffness. The floors may be considered infinitely rigid in the horizontal plane if they are made about r.c. or if in steel or wood, but with a slab of minimum 4 to 5 cm thickness and well connected with shear connectors to the themselves beams.

The analysis model used for masonry structures is that of continue walls from the foundation to the top, linked for the translation purpose to the floors height. Ultimately they are a lot of walls fixed in the foundation subjected to proportional seismic forces by to their rigidities.

To define the seismic actions, the response spectra must be firstly defined. The NTC 2008 [6] provide a seismic classification of the national territory of a continuing nature. The parameters that characterise the seismicity of the site are derived from the latitude and longitude of the site.

Usually the buildings can be considered as consisting of vertical earthquake resistant macro-elements and substantially rigid floors and therefore each with only three degrees of freedom. With the modal analysis the modes of vibration must be find. The rule allows the use of simplified analysis, static analysis, which approximates the effects due only to the first mode of vibration.

Seismic actions that must be applied to the structure will be obtained as a product of the structural masses for the ordinate of the acceleration design spectrum, as defined by regulations. The static analysis can only be used for structures that are not excessively deformable and quite regular (like normal buildings for residential use). In these cases, the structure must have, therefore, a center of mass (point of application of seismic action) near enough to the center of stiffness, so to limit the rotations of the floor.

The seismic actions evaluation, induced in the structure vertical resistant panels' plane, is calculated by applying a distribution of equivalent static forces distributed along the height in a pseudo triangular waveform for the first mode of vibration:

$$F_i = F_h \cdot \frac{z_i \cdot W_i}{\sum z_j \cdot W_j}. \tag{3.91}$$

Having denoted by F_h the design base shear, amounting to:

$$F_h = S_d(T_1) \cdot \lambda \cdot \frac{W}{g}, \tag{3.92}$$

where:

- z_i and z_j are the quota of floors with respect to the start foundation;
- W_i and W_j are the weights of the floors of the building;

- $S_d(T_1)$ is the value of the design response spectrum calculated for the structure's vibration period;
- W is the total weight of the building;
- λ is the coefficient reductive, equal to 0,85 for structures with at least three floors and $T_1 < 2\,T_c$ and 1,00 in other cases.

The floor seismic forces calculated with the previous (3.91) will be applied in the floor's center of mass and will have an effective eccentricity with the walls' center of stiffness.

To the previous effective eccentricity, which depends on the real geometrical distribution of the masses, it need to add accidental eccentricity at least 5% of the maximum size of the building along the orthogonal direction to that seismic action.

Regarding the evaluation of the torsional effects of buildings with stiffness and mass distributed in an almost symmetrical in plan, an increasing factor δ can be used.

This factor considers the position of the single wall in relation to the geometric center of gravity of the building, and the maximum distance between two resistant element measured perpendicularly to the seismic direction:

$$\delta = 1 + 0{,}6 \cdot \frac{x}{L_e}, \tag{3.93}$$

where:

- x is the distance from the geometric building center of gravity and the generic wall, measured perpendicular to the seismic direction in question;
- L_e is the distance between the two most distant resistant walls, measured perpendicular to the seismic direction in consideration.

3.3.2 Nonlinear static analysis: N2 method

The structural analysis can be carried out on both linear and nonlinear models.

The nonlinear system capacity depends on material's nonlinearity, or the material capacity to deform in the plastic field.

Nonlinear static analysis are widely utilised for simulating the seismic response of structures. On the one hand, they allow for mechanical nonlinearity of materials (and possibly for geometrical non linearity) to be explicitly considered in structural analysis. On the other hand, they are reasonably cost-effective as a system of static forces is actually considered (instead of the base shaking induced by the earthquake event) for simulating the inertial seismic-induced actions on the structure under consideration.

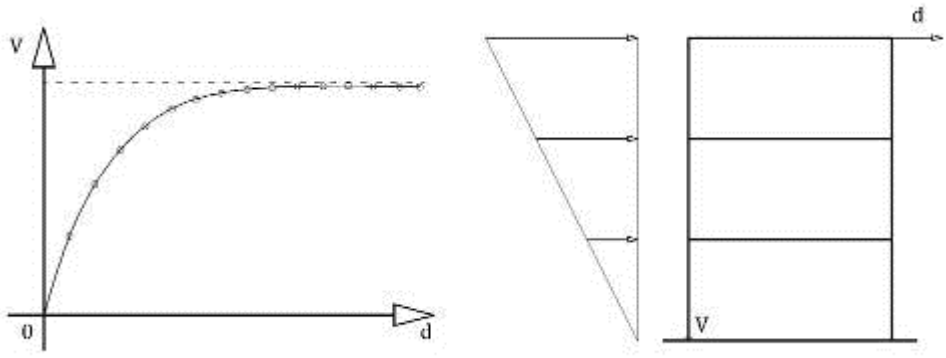

Figure 3.28: Scheme of pushover test.

Pushover analyses are generally based on two keys steps [48]:

- first of all the "capacity curve" (namely a curve relating the base shear force V to the top displacement induced on the structure and reported in Figure 3.28) is determined by considering the nonlinear behaviour of material and structure;
- based on key in formulations deriving by the "capacity curve" the displacement demand induced by the expected seismic event can be determined.

An intermediate step is actually needed for employing the “capacity curve” in determining the above mentioned displacement demand (or the so-called “performance point”) of a structure under seismic action. In particular, the “capacity curve” should be transformed into “capacity spectrum” which describes the behaviour of the so-called equivalent SDOF system.

Details about the conceptual meaning of this mathematical transformation are beyond the scope of this work and are omitted herein. They can be found in [48][49].

Figure 3.29 shows two ideal examples of capacity curve. The first one has been clearly derived by only considering non-linearity whereas the second one is also based in a geometrically nonlinear model which lead to a softening response of the structure under lateral loads.

Several contributions are already available in the scientific literature on this topic [48].

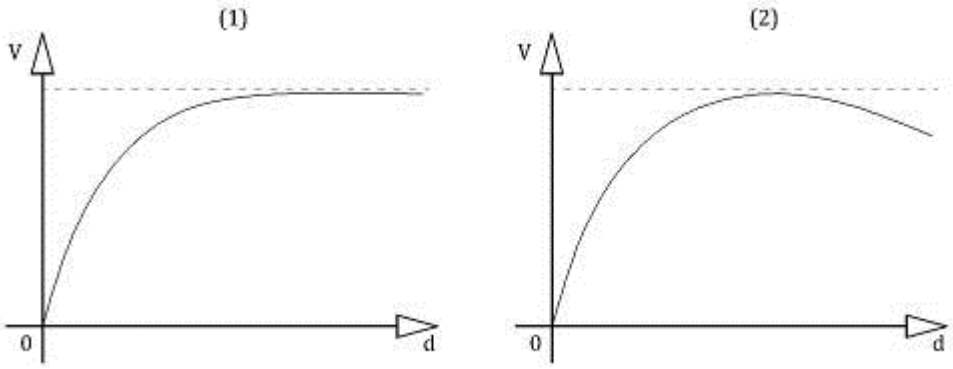

Figure 3.29: Comparison between the pushover curve obtained with test in force control (1) and that obtained in displacements control (2).

4. Analyses models through ordinary FEM codes

4.1 Introduction

In the following sections there are some applications about the frequent used models of masonry structures. The analyses that follows are presented both in the linear range and in the nonlinear range, by application of the principles exposed in the previous chapter 3.

The analyses models can use the following typologies of elements:

1) one-dimensional elements;
2) bi-dimensional elements;
3) three-dimensional elements.

The nonlinear analyses, shown in this chapter, are very important especially for the analysis about existing masonry structures because they permit to know the better work to do for improve the seismic strength.

4.2 Linear analyses

The linear analyses is a procedure that permits to understand the behaviour of a structure under some loads in the elastic range. This assumption doesn't permit the modelling of the real nonlinear capacity of the masonry structure but it has used in the Finite Elements codes (like SAP2000®) for to obtain the strain and the stiffness in an "elastic prediction". Those results can be used for to check the singles elements (i.e. piers or spandrels) with respect the relative strength domains, which are obtained by considering the nonlinear behaviour of the elements (failure modes exposed in chapter 3).

4.2.1 One-dimensional elements

The one-dimensional elements available in SAP2000® are the frame of type Finite Elements. These are appropriate for modelling the masonry walls with an equivalent frame, similar to what is done in the SAM method [39].

In particular for each frame element they are assigned some rigid offsets of appropriate length to predict the behaviour of the nodal areas.

The frame element can be a complete and correct modelling of a pier or a spandrel element of the real masonry wall with the definition of their cross section and the material properties.

The following Figure 4.1 shows the modelling of the wall subjected to both vertical and horizontal loads due to mass and earthquake.

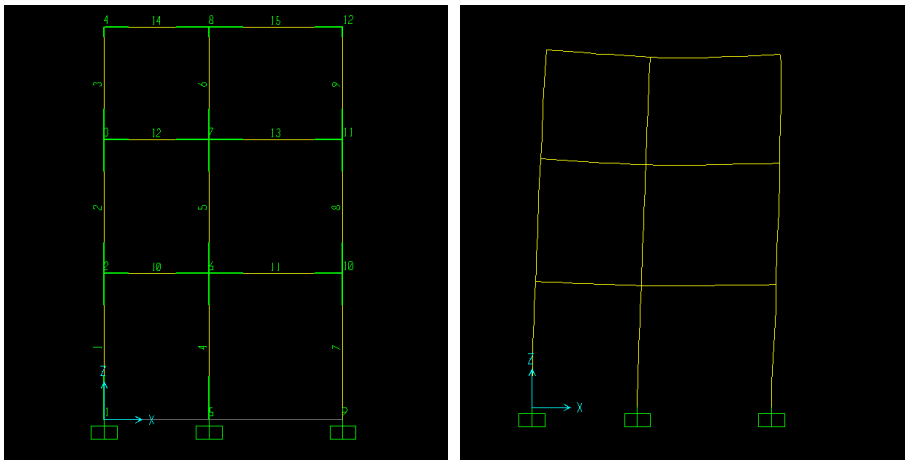

Figure 4.1: Frame model (on the left) and deformed shape (in the right).

4.2.2 Two-dimensional elements

The previous masonry wall can also analysed by using different type of Finite Element so-called shell elements. These elements are very useful for modelling the wall using a plane type elements, which are closest to the real structure. In fact, the real masonry element like a pier or a spandrel, frequently, have only one dimension (the thickness) negligible with respect the other dimensions (height and length).

The following Figure 4.2 shows the different solution obtained by the use of shell. In particular these elements are good for easily see the shear stress in the walls (shown in Figure 4.3).

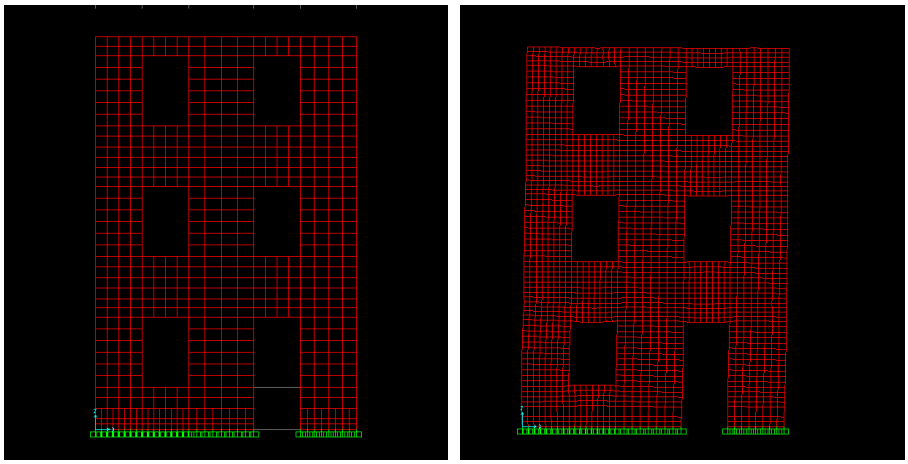

Figure 4.2: Shell model (on the left) and deformed shape (on the right).

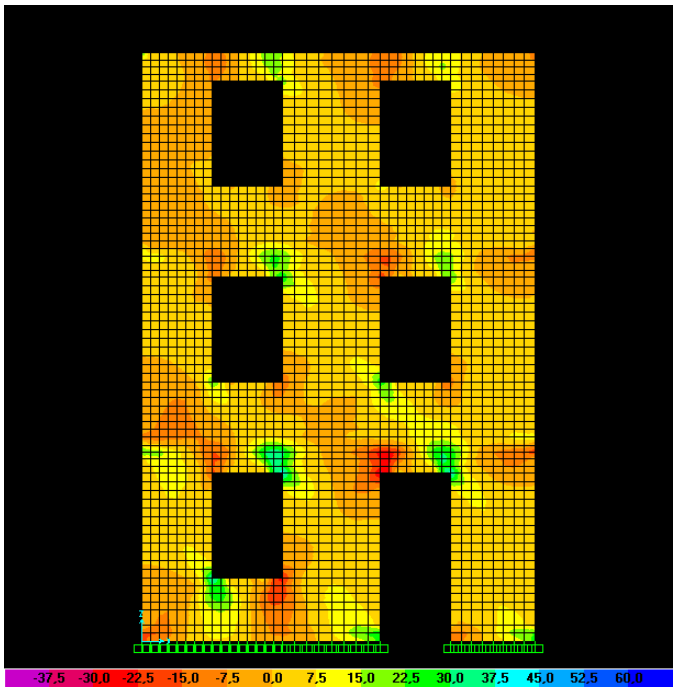

Figure 4.3: Resultant shear stress (F12) diagram.

4.2.3 Three-dimensional elements

The modelling of a masonry structure by the use of a three-dimensional elements is the more complete and complex way to analyse the masonry. This modelling is necessary when the walls have a thickness not negligible with respect the other dimension of the structures or when it needs to understand the behaviour of a single masonry panel subjected to a vertical and horizontal loads. In these modelling are possible the definition of the single elements that are in the masonry: bricks, mortar beds, cracks. This modelling include the first definition of the mesh and after is performed a pushover analysis [50].

4.3 Nonlinear analyses

The nonlinear analyses are used for modelling the real capacity of the masonry structure for to obtain the pushover curve, which can be used in the more complex analyses like N2 method [48]. The nonlinear analysis can be obtained in SAP2000® with the use of the following elements:

1) springs or hinges;
2) link elements.

4.3.1 Frame elements

There are finite elements like springs or hinges at the extremity of the frame elements with a behaviour described with the principles reported in [11]. These elements, however, are difficultly used for the masonry because cannot permit to define the real failure modes of walls.

However some springs, with variable stiffness, at the end of the elements can be used for the nonlinear analysis of the masonry structures. In particular, in the next chapter 5 a novel code which include these elements will be described.

4.3.2 Link elements

Link elements can be used for modelling the deformable part of the walls (like spandrels or piers) and for connect the nodal areas (which are modelled with rigid offsets frame elements). This modelling permits to define the real behaviour of the wall, by the assignment of the moment vs. rotation and shear vs. displacement diagrams (different for each link). At the end of the analysis is possible to obtain the pushover curve that can be used in the nonlinear analysis for to understand the damages of the structure.

At this point it is possible to analyse the previous masonry wall with the use of the link elements. The first step is the definition of the properties of each walls (see Table 4.1). It is assumed a constant and independent normal stress during the application of horizontal forces and equal to that due only to vertical loads present on the previous wall. For each element of the wall the size and the normal stress are identified.

Table 4.1: General parameters of piers and spandrels.

i	ID	t	L	h	N	σ_0
[]	[]	[mm]	[mm]	[mm]	[N]	[MPa]
1	M_F1_1000	500	1000	1500	76380	0,15
2	M_F1_1400	500	1400	1500	113800	0,16
3	M_F1_1200	500	1200	2400	99510	0,17
4	M_F2_1000	500	1000	1500	45800	0,09
5	M_F2_1400	500	1400	1500	67080	0,10
6	M_F2_1200	500	1200	1500	54990	0,09
7	M_F3_1000	500	1000	1500	14390	0,03
8	M_F3_1400	500	1400	1500	22410	0,03
9	M_F3_1200	500	1200	1500	17380	0,03
10	F_F1	500	1300	1000	0	0,00
11	F_F2	500	1300	1000	0	0,00
12	F_F3	500	200	1000	0	0,00
Legend: M = Pier; F = Spandrel; F1 = First floor; F2 = Second floor; F3 = Third floor.						

The ultimate bending moment and the ultimate shear (reported in Table 4.2) can be calculated, as defined in the preceding paragraphs 3.1.

The stiffness of each part can be obtained in Table 4.3, with the relationship reported in Commentary No. 21745 [17], which includes both the shear deformation and the flexural deformation. This stiffness is then used to calculate the displacements at the elastic limit and ultimate displacement.

For the shear behaviour, therefore, is defined an elastic perfectly plastic link. Instead, for extensional and flexural regime they are used indefinitely elastic links.

Table 4.2: Analysis of the ultimate shear.

i	ID	M_u	e	D'	σ_N	f_{vd}	V_{ss}	V_{bm}	b	V_{ds}	V_u
[]	[]	[Nmm]	[mm]	[mm]	[MPa]	[MPa]	[N]	[N]	[]	[N]	[N]
1	M_F1_1000	35902194,35	470,05	89,86	1,70	0,79	35494,24	47869,59	1,50	76325,62	35494,24
2	M_F1_1400	74581396,08	655,37	133,88	1,70	0,79	52883,53	99441,86	1,07	151890,21	52883,53
3	M_F1_1200	55822768,59	560,98	117,07	1,70	0,79	46242,88	46518,97	2,00	70093,67	46242,88
4	M_F2_1000	22077396,08	482,04	53,88	1,70	0,79	21283,53	29436,53	1,50	68588,14	21283,53
5	M_F2_1400	45191401,41	673,69	78,92	1,70	0,79	31172,47	60255,20	1,07	135535,91	31172,47
6	M_F2_1200	31808156,82	578,44	64,69	1,70	0,79	25554,18	42410,88	1,25	98776,55	25554,18
7	M_F3_1000	7113795,25	494,36	16,93	1,70	0,79	6687,12	9485,06	1,50	59603,97	6687,12
8	M_F3_1400	15490055,65	691,21	26,36	1,70	0,79	10414,06	20653,41	1,07	117794,67	10414,06
9	M_F3_1200	10309543,37	593,18	20,45	1,70	0,79	8076,59	13746,06	1,25	85871,05	8076,59
10	F_F1	0,00	-	-	-	-	-	-	0,77	139425,00	139425,00
11	F_F2	0,00	-	-	-	-	-	-	0,77	139425,00	139425,00
12	F_F3	0,00	-	-	-	-	-	-	5,00	3300,00	3300,00

Legend:
V_{ss} is the ultimate sliding shear;
V_{bm} is the ultimate flexural shear;
V_{ds} is the ultimate diagonal shear.

Table 4.3: Analysis of the shear behaviour.

i	ID	A	I	EA	GA	EI	k	δ_y	δ_u
[]	[]	[mm^2]	[mm^4]	[N]	[N]	[Nmm^2]	[N/mm]	[mm]	[mm]
1	M_F1_1000	500000	4,17E+10	3,63E+08	6,05E+07	3,03E+13	25608,47	1,39	2,08
2	M_F1_1400	700000	1,14E+11	5,08E+08	8,47E+07	8,30E+13	40584,77	1,30	1,95
3	M_F1_1200	600000	7,20E+10	4,36E+08	7,26E+07	5,23E+13	16205,36	2,85	4,28
4	M_F2_1000	500000	4,17E+10	3,63E+08	6,05E+07	3,03E+13	25608,47	0,83	1,25
5	M_F2_1400	700000	1,14E+11	5,08E+08	8,47E+07	8,30E+13	40584,77	0,77	1,15
6	M_F2_1200	600000	7,20E+10	4,36E+08	7,26E+07	5,23E+13	33141,23	0,77	1,16
7	M_F3_1000	500000	4,17E+10	3,63E+08	6,05E+07	3,03E+13	25608,47	0,26	0,39
8	M_F3_1400	700000	1,14E+11	5,08E+08	8,47E+07	8,30E+13	40584,77	0,26	0,38
9	M_F3_1200	600000	7,20E+10	4,36E+08	7,26E+07	5,23E+13	33141,23	0,24	0,37
10	F_F1	650000	9,15E+10	4,72E+08	7,87E+07	6,65E+13	60564,32	2,30	3,45
11	F_F2	650000	9,15E+10	4,72E+08	7,87E+07	6,65E+13	60564,32	2,30	3,45
12	F_F3	100000	3,33E+08	7,26E+07	1,21E+07	2,42E+11	2254,66	1,46	2,20

The deformed shape and the pushover curve (in Figure 4.5) obtained leading to the collapse the previous structure are shown in Figure 4.4,.

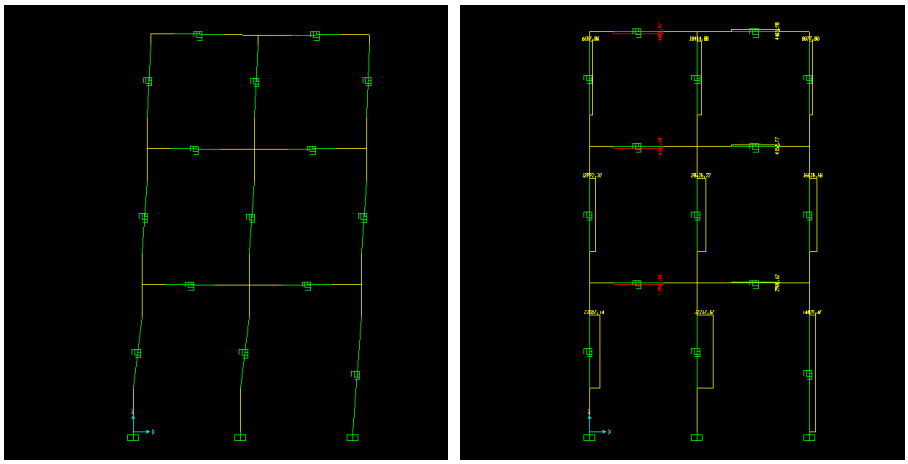

Figure 4.4: Last pushover step and relative shear diagram.

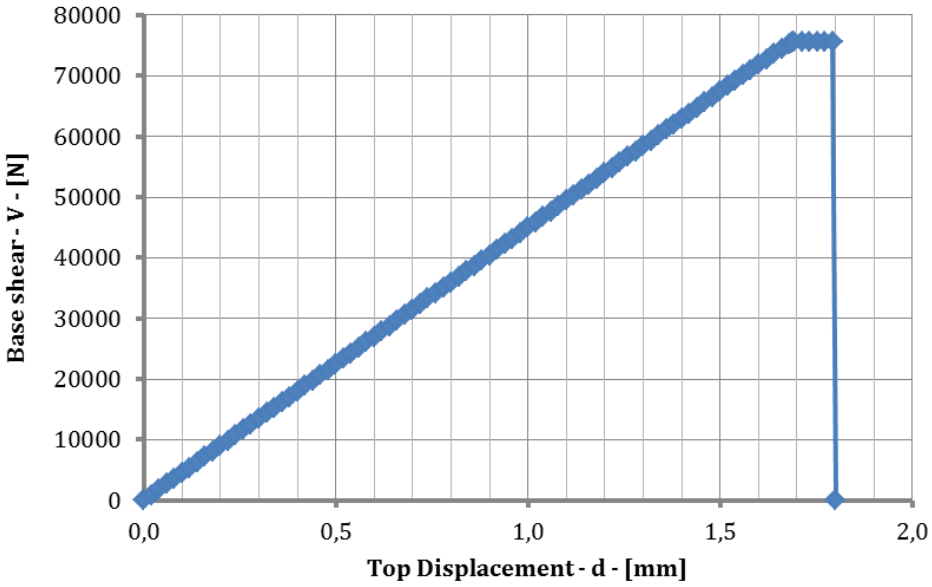

Figure 4.5: Pushover curve.

In the following Figures 4.6 – 4.8 and Tables 4.4 - 4.5, the representation of the characteristics of the stress in the deformable sections are reported.

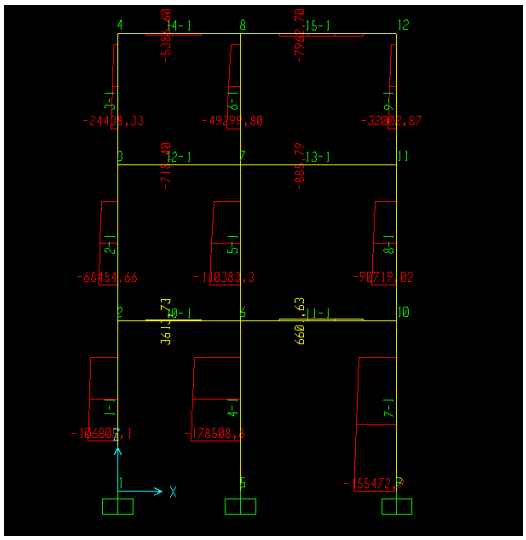

Figure 4.6: Axial force diagram.

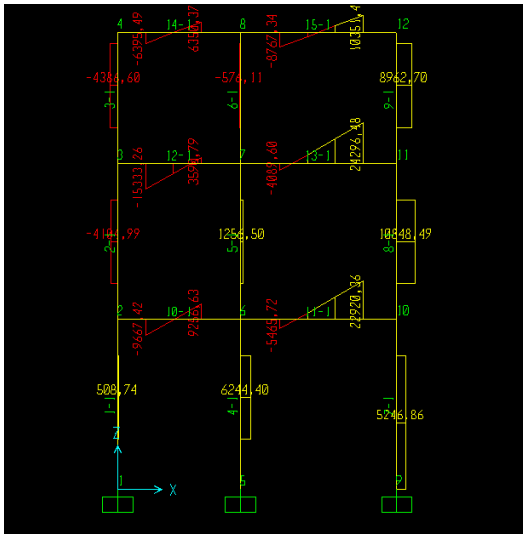

Figure 4.7: Shear force diagram.

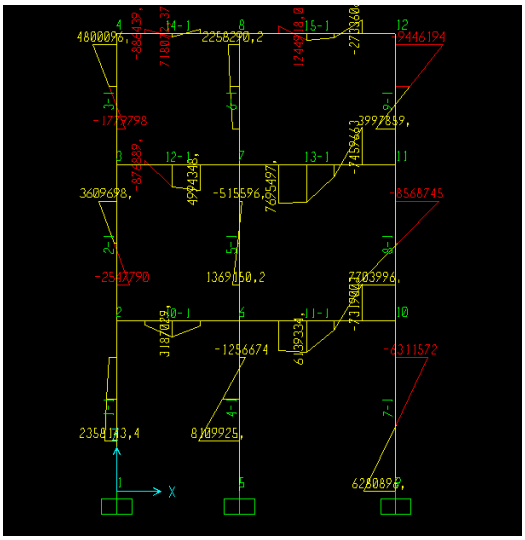

Figure 4.8: Moment diagram.

Table 4.4: Joint displacement.

Joint	U1	U2	U3	R1	R2	R3
Text	[mm]	[mm]	[mm]	Radians	Radians	Radians
1	0	0	0	0	0	0
2	0,003594	0	-0,02085	0	2,37E-06	0
3	0,008923	0	-0,03266	0	3,01E-06	0
4	0,01536	0	-0,03593	0	4,82E-06	0
5	0	0	0	0	0	0
6	0,004002	0	-0,02505	0	1,5E-06	0
7	0,008842	0	-0,03881	0	1,69E-06	0
8	0,013385	0	-0,04376	0	2,48E-06	0
9	0	0	0	0	0	0
10	0,004949	0	-0,02422	0	-1,7E-08	0
11	0,008715	0	-0,03737	0	-3,2E-07	0
12	0,009669	0	-0,04098	0	-2,2E-06	0

Table 4.5: Element forces in frames.

Frame	Station	P	V2	M3
Text	[mm]	[N]	[N]	[Nmm]
1	900	-106805	508,74	2358143
1	1650	-101657	508,74	1976589
1	2400	-96508,2	508,74	1595034
2	650	-68454,7	-4104,99	-2547790
2	1400	-63306,2	-4104,99	530954
2	2150	-58157,7	-4104,99	3609698
3	650	-24438,3	-4386,6	-1779798
3	1400	-19289,8	-4386,6	1510149
3	2150	-14141,4	-4386,6	4800096
4	900	-178509	6244,4	8109925
4	1650	-171301	6244,4	3426625
4	2400	-164093	6244,4	-1256674
5	650	-110383	1256,5	1369150
5	1400	-103175	1256,5	426777
5	2150	-95967,5	1256,5	-515596
6	650	-49299,8	-576,11	1394132
6	1400	-42091,9	-576,11	1826211
6	2150	-34884	-576,11	2258290
7	0	-155473	5246,86	6280896
7	1200	-145588	5246,86	-15338
7	2400	-135703	5246,86	-6311572
8	650	-90719	10848,49	7703996
8	1400	-84540,8	10848,49	-432374
8	2150	-78362,6	10848,49	-8568745
9	650	-32002,9	8962,7	3997859
9	1400	-25824,7	8962,7	-2724168
9	2150	-19646,5	8962,7	-9446194
10	500	3613,73	-9667,42	718826,9
10	1000	3613,73	-205,39	3187029
10	1500	3613,73	9256,63	924218,1
11	700	6601,63	-5465,72	5771982
11	1200	6601,63	3996,31	6139334
11	1700	6601,63	13458,34	1775672
11	2200	6601,63	22920,36	-7319003
12	500	-718,4	-15333,3	-876889
12	1000	-718,4	-5871,24	4424236
12	1500	-718,4	3590,79	4994348
13	700	-885,79	-4089,6	7695497
13	1200	-885,79	5372,43	7374790
13	1700	-885,79	14834,45	2323070
13	2200	-885,79	24296,48	-7459663
14	500	-5386,6	-6395,49	-886439
14	1000	-5386,6	-22,56	718072,4
14	1500	-5386,6	6350,37	-863882
15	700	-7962,7	-8767,34	-1545518
15	1200	-7962,7	-2394,41	1244918
15	1700	-7962,7	3978,52	848888,8
15	2200	-7962,7	10351,45	-2733606

5. A novel equivalent–frame analysis model

5.1 Introduction

The present model is based on a lumped-plasticity approach which allows for simulating the keys features of the nonlinear behaviour of structures basically corresponding to the various failure modes already described in section 3.1. The model is firstly formulated in the linear range. Section 5.2 presents analytical details about the closed-form expression of a 1D frame element which is employed in the model under consideration. Since it is intended at simulating the behaviour of both walls and spandrels it should also model the so-called panel zone. Thus, two fully rigid parts are introduced at the ends of this frame-like element, as commonly accepted in equivalent frame models for masonry structures.

Moreover, since this is a lumped-plasticity model, some springs components are introduced in the model for simulating the nonlinear behaviour of the materials. Thus, section 5.3 describes the key aspects of the process of those springs for realising a nonlinear procedure according to the secant method [45]. Some basic principles of the follow theory of plasticity are briefly recalled these in and their application to the case of masonry structures is also outlined.

Finally, details about numerical code developed in MatLab® are reported.

5.2 Frame element formulation

The masonry wall is modelled by the use of equivalent frame structures. Every frame (shown in Figure 5.1) uses deformable elements (for piers or spandrels), rigid elements (for the nodal zones), local springs (for modeling the nonlinear behaviour).

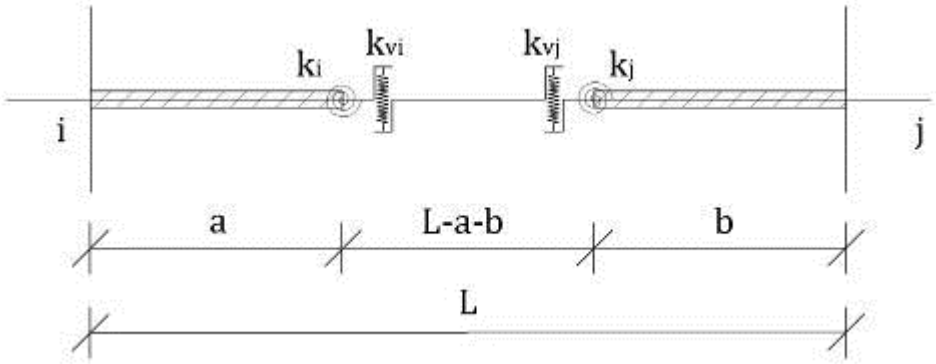

Figure 5.1: Truss element.

5.2.1 Description of the flexible part

The flexible tract is used for modelling the deformable part of the masonry wall. This element is, therefore, a simple frame with lumped releases at the end. For this element is simple to write the deformability coefficient:

$$\alpha_{ij} = \frac{L \cdot (1 - r_i - r_j)}{3 \cdot EI} + \frac{1}{k_i} + \frac{2}{[L \cdot (1 - r_i - r_j)]^2} \cdot \frac{1}{k_v} + \frac{\chi}{GA \cdot L}; \quad (5.1)$$

$$\alpha_{ji} = \frac{L \cdot (1 - r_i - r_j)}{3 \cdot EI} + \frac{1}{k_j} + \frac{2}{[L \cdot (1 - r_i - r_j)]^2} \cdot \frac{1}{k_v} + \frac{\chi}{GA \cdot L}; \quad (5.2)$$

$$\beta_{ji} = \frac{L \cdot (1 - r_i - r_j)}{6 \cdot EI} + \frac{2}{[L \cdot (1 - r_i - r_j)]^2} \cdot \frac{1}{k_v} - \frac{\chi}{GA \cdot L}. \quad (5.3)$$

At this point the coefficients of stiffness of only the deformable part are:

$$W_{ij} = \frac{\alpha_{ji}}{\alpha_{ij} \cdot \alpha_{ji} - \beta_{ij}^2}; \quad (5.4)$$

$$W_{ji} = \frac{\alpha_{ij}}{\alpha_{ij} \cdot \alpha_{ji} - \beta_{ij}^2}; \tag{5.5}$$

$$V_{ij} = \frac{\beta_{ij}}{\alpha_{ij} \cdot \alpha_{ji} - \beta_{ij}^2}; \tag{5.6}$$

$$U_{ij} = \frac{W_{ij} + U_{ji}}{L}. \tag{5.7}$$

5.2.2 Assembly of the rigid segments

It should be, however, calculate the moments at the ends of the frame, including the presence of the rigid traits. This can be done using a matrix operation that involves the use of a matrix of passage. The aim is to link the displacements of the external nodes (i and j) with the displacements of the internal nodes (i' and j'). Knowing the above factors the stiffness matrix of only the deformable part ($\underline{\underline{K}}'$) can be defined.

For the deformable part, it's valid a relationship like this:

$$\underline{f}' = \underline{\underline{K}}' \cdot \underline{v}' + \underline{f}'_0 . \tag{5.8}$$

The vector of nodal displacements of the deformable part will be:

$$v' = \left[u'_i, v'_i, \varphi'_i, u'_j, v'_j, \varphi'_j\right]^T . \tag{5.9}$$

The displacements of the deformable part obtained from the previous displacements at the ends of all the frame are:

$$u'_i = u_i; \tag{5.10}$$

$$v'_i = v_i + \varphi_i \cdot r_i \cdot L; \tag{5.11}$$

$$\varphi'_i = \varphi_i; \tag{5.12}$$

$$u'_j = u_j; \tag{5.13}$$

$$v'_j = v_j - \varphi_j \cdot r_j \cdot L; \tag{5.14}$$

$$\varphi'_j = \varphi_j . \tag{5.15}$$

Ultimately, the following transformation matrix is obtained:

$$\underline{v}' = \begin{bmatrix} u'_i \\ v'_i \\ \varphi'_i \\ u'_j \\ v'_j \\ \varphi'_j \end{bmatrix} = \begin{bmatrix} 1 & 0 & 0 & 0 & 0 & 0 \\ 0 & 1 & r_i \cdot L & 0 & 0 & 0 \\ 0 & 0 & 1 & 0 & 0 & 0 \\ 0 & 0 & 0 & 1 & 0 & 0 \\ 0 & 0 & 0 & 0 & 1 & -r_j \cdot L \\ 0 & 0 & 0 & 0 & 0 & 1 \end{bmatrix} \cdot \begin{bmatrix} u_i \\ v_i \\ \varphi_i \\ u_j \\ v_j \\ \varphi_j \end{bmatrix}. \quad (5.16)$$

Substituting v' in the previous report and multiplying the transpose of the transformation matrix:

$$\underline{f} = \underline{\underline{T}}^T \cdot \underline{f}' = \underline{\underline{T}}^T \cdot \underline{\underline{K}}' \underline{\underline{T}} \cdot \underline{v} + \underline{\underline{T}}^T \cdot \underline{f}'_0 + \underline{f}''_0. \quad (5.17)$$

Substituting again:

$$\underline{f} = \underline{\underline{K}} \cdot \underline{v} + \underline{f}_0 + \underline{f}''_0. \quad (5.18)$$

In fact to the previous has been added the vector of the nodal action present both on the deformable part and on the rigid part. In particular:

$$\underline{f}''_0 = \left[0, q \cdot r_i \cdot L, \frac{q \cdot r_i \cdot L^2}{2}, 0, q \cdot r_j \cdot L, -\frac{q \cdot r_j \cdot L^2}{2} \right]. \quad (5.19)$$

5.2.3 Final formulation

Ones obtained the stiffness matrix of each frame elements it is possible also to obtain the stiffness matrix of the entire structure [51]. This scope is reached by the rotation of the stiffness matrix of each frame element (with the passage from the local system to the global system). Every matrix is therefore assembled after a their expansion. At the end of this operation, the ultimate stiffness matrix can be obtained by the overwrite of the boundary conditions. Finally, this relation can be obtained:

$$\underline{F} = \underline{\underline{K}} \cdot \underline{s} + \underline{F}_0 , \tag{5.20}$$

where:

- $\underline{F}$ is the vector of the nodal forces of the entire structure;
- $\underline{K}$ is the stiffness matrix of the entire structure;
- $\underline{s}$ is the vector of the nodal displacements of the entire structure;
- $\underline{F}_0$ is the vector of the nodal actions of the entire structure.

The previous relation can be inverted to obtain the unknown displacement of the nodes:

$$\underline{s} = \underline{\underline{K}}^{-1} \cdot \left(\underline{F} - \underline{F} \right). \tag{5.21}$$

At this point, through simple relations, the strain on each frame elements can be obtained with the same relations of the section 5.2.2.

5.2.4 Validation within the linear range

In the following section there is a comparison between the results obtained by the MatLab® computer code and the modelling carried out in SAP2000® [52]. Firstly same tests were performed on simple structures and the results were compared in terms of nodal displacements, both in MatLab® code and in SAP2000®. In addition, for some cases have been obtained exact analytical solutions by solving the Timoshenko problem even using Mathematica.

The simple tests focused on three types of structures:

1) beam fixed at the base and subjected to a force on the top (Figure 5.2);
2) simply supported beam and subjected to a uniformly distributed load (Figure 5.3);
3) portal with one floor and a span with a distributed load on the beam and a horizontal force on the top (Figure 5.4);
4) masonry wall exposed in Commentary No. 21745 and described in the previous paragraph 2.1.4.

For each of the above types have been provided three cases:

1) structure with elastic beam elements;
2) structure with beams and rigid traits;
3) structure with beams, rigid traits and rotational and shear springs.

The tests are described in the following figures from which one can deduce the geometry and applied loads. In particular, the elastic moduli are equal to:

$$E = 726MPa\,; \qquad G = 279{,}23MPa\,. \tag{5.22}$$

The springs stiffness are equal to:

$$k_i = 10^9\,Nmm\,; \qquad k_{vi} = 10^9\,N/mm\,. \tag{5.23}$$

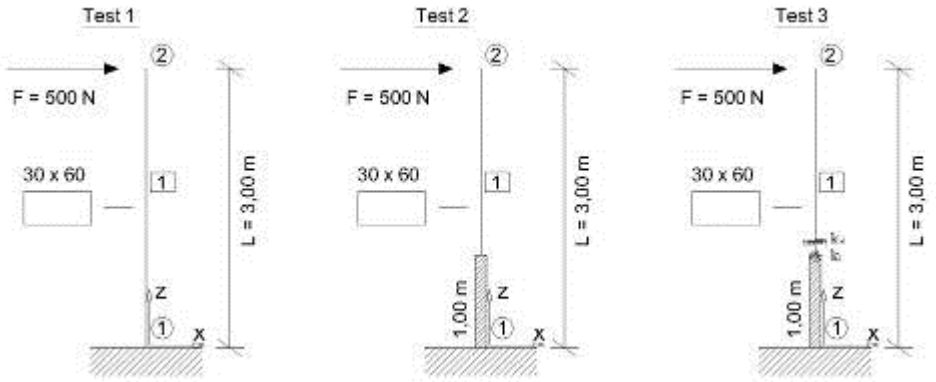

Figure 5.2: Test 1 – 2 – 3.

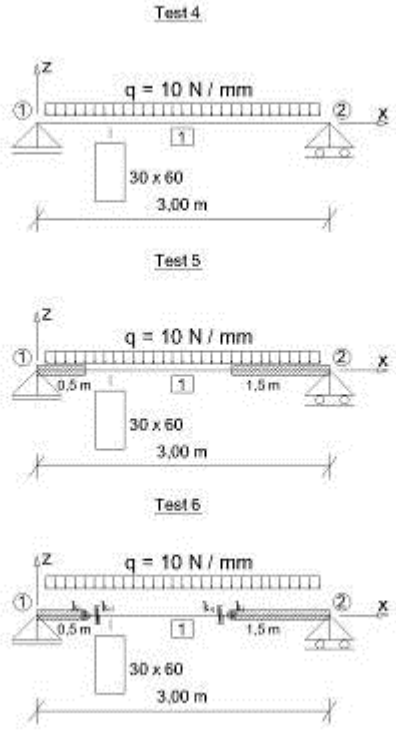

Figure 5.3: Test 4 – 5 – 6.

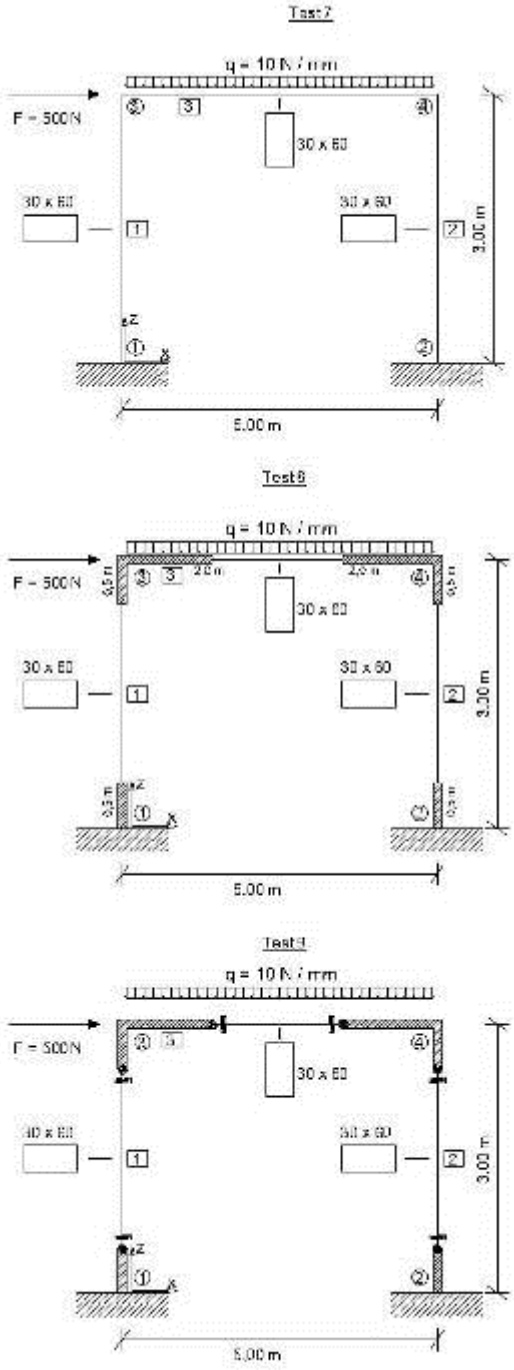

Figure 5.4: Test 7 – 8 – 9.

The differential problem of Timoshenko uses the following equations:

$$EI\frac{d^3\varphi}{dz^3}+q=0;\quad \frac{dv}{dz}=-\varphi+\chi\frac{EI}{GA}\cdot\frac{d^2\varphi}{dz^2}. \tag{5.24}$$

The shear and the moment are:

$$T=EI\cdot\frac{d^2\varphi}{dz^2};\qquad M=EI\cdot\frac{d\varphi}{dz}. \tag{5.25}$$

For the case of the beam fixed at the base and with a force to the end, the boundary conditions are:

$$v(z=0)=0;\qquad \varphi(z=0)=0. \tag{5.26}$$

$$M(z=L)=0;\qquad T(z=L)=F. \tag{5.27}$$

The solutions are:

$$v(z)=\frac{3\cdot F\cdot L\cdot z^2-F\cdot z^3}{6\cdot E\cdot I}+\frac{\chi\cdot F}{GA}\cdot z; \tag{5.28}$$

$$\varphi(z)=\frac{F\cdot x^2-2\cdot F\cdot L\cdot x}{2\cdot E\cdot I}; \tag{5.29}$$

$$M(z)=-F\cdot L+F\cdot x; \tag{5.30}$$

$$V(z)=F. \tag{5.31}$$

In the case of a beam with a uniform load, the conditions are:

$$v(z=0)=0;\qquad v(z=L)=0. \tag{5.32}$$

$$M(z=0)=0;\qquad M(z=L)=0. \tag{5.33}$$

The solutions are:

$$v(z)=\frac{q\cdot L^4}{24\cdot E\cdot I}\cdot\left[\frac{z}{L}-2\cdot\left(\frac{z}{L}\right)^2+\left(\frac{z}{L}\right)^4\right]+\beta\cdot\frac{q\cdot L^4}{2\cdot E\cdot I}\cdot\left[\frac{z}{L}-\left(\frac{z}{L}\right)^2\right]; \tag{5.34}$$

$$\varphi(z)=\frac{q\cdot L^3}{24\cdot E\cdot I}\cdot\left[-1+6\cdot\left(\frac{z}{L}\right)^2-4\cdot\left(\frac{z}{L}\right)^3\right]; \tag{5.35}$$

$$V(z)=q\cdot L\cdot\left(\frac{1}{2}-\frac{z}{L}\right); \tag{5.36}$$

$$M(z)=\frac{q\cdot L^2}{2}\cdot\left[\frac{z}{L}-\left(\frac{z}{L}\right)^2\right]. \tag{5.37}$$

where:

- $\beta = \chi \cdot \frac{E \cdot I}{G \cdot A \cdot L^2}$. (5.38)

The previous formulas can be used for check the results from the test 1 and 3 and they give the same numbers of the MatLab® and SAP2000® modelling. In the following Tables 5.1 – 5.3 are reported the comparisons for each test.

Table 5.1: Test 1-9.

Test	Joint	MatLab®			SAP2000®			Percentage changes		
		u	v	f_y	u	v	f_y	u	v	f_y
		[mm]	[mm]	[]	[mm]	[mm]	[]	[%]	[%]	[%]
1	2	1,1837	-0,1116	0,0006	1,1837	-0,1116	0,0006	0,00	0,00	0,00
2	2	0,3645	-0,1116	0,0003	0,3640	-0,1116	0,0003	0,14	0,00	-1,81
3	2	2,3690	-0,1116	0,0013	2,3692	-0,1116	0,0013	-0,01	0,00	0,00
4	1	0,0000	0,0000	-0,0038	0,0000	0,0000	-0,0038	-	-	0,00
4	2	0,0000	0,0000	0,0038	0,0000	0,0000	0,0038	-	-	0,00
5	1	0,0000	0,0000	0,0018	0,0000	0,0000	0,0018	-	-	0,00
5	2	0,0000	0,0000	-0,0018	0,0000	0,0000	-0,0018	-	-	0,00
6	1	0,0000	0,0000	0,0141	0,0000	0,0000	0,0142	-	-	-0,70
6	2	0,0000	0,0000	-0,0124	0,0000	0,0000	-0,0125	-	-	0,80
7	1	0,4544	-0,8688	0,0045	0,4544	-0,8688	0,0045	0,00	0,00	0,67
7	2	0,0645	-0,8741	-0,0043	0,0645	-0,8741	-0,0043	0,00	0,00	0,92
8	1	0,4006	-0,8683	0,0026	0,4006	-0,8683	0,0026	0,00	0,00	-0,38
8	2	-0,2359	-0,8745	-0,0026	-0,2355	-0,8745	-0,0026	0,17	0,00	-1,17
9	1	0,9349	-0,8685	0,0139	0,9370	-0,8685	0,0139	-0,22	0,00	0,07

Table 5.2: Test 10-11.

Test	Joint	MatLab®			SAP2000®			Percentage changes		
		u	v	f_y	u	v	f_y	u	v	f_y
		[mm]	[mm]	[]	[mm]	[mm]	[]	[%]	[%]	[%]
10	4	0,3763	-1,0023	-0,0002	0,3763	-1,0023	0,0002	0,00	0,00	0,02
10	5	0,3844	-1,1959	-0,0001	0,3844	-1,1959	0,0001	0,00	0,00	0,03
10	6	0,3934	-1,0799	0,0000	0,3934	-1,0799	0,0000	0,00	0,00	2,82
10	7	0,7362	-1,5602	-0,0002	0,7362	-1,5602	0,0002	0,00	0,00	-0,20
10	8	0,7397	-1,8455	-0,0001	0,7397	-1,8455	0,0001	0,00	0,00	0,22
10	9	0,7421	-1,6591	0,0000	0,7421	-1,6591	0,0000	0,00	0,00	-0,57
10	10	1,0788	-1,7242	-0,0003	1,0788	-1,7242	0,0003	0,00	0,00	0,14
10	11	1,0116	-2,0534	-0,0001	1,0116	-2,0534	0,0001	0,00	0,00	-0,12
10	12	0,9351	-1,8154	0,0000	0,9351	-1,8154	0,0000	0,00	0,00	0,01
11	4	0,1221	-1,0302	-0,0001	0,1243	-1,0324	0,0001	-1,78	-0,21	-0,52
11	5	0,1385	-1,1531	0,0000	0,1403	-1,1497	0,0000	-1,27	0,30	0,39
11	6	0,1651	-1,1064	0,0000	0,1661	-1,1086	0,0000	-0,60	-0,19	14,99
11	7	0,2729	-1,6064	-0,0001	0,2676	-1,6104	0,0001	1,96	-0,25	7,07
11	8	0,2719	-1,7777	0,0000	0,2685	-1,7709	0,0000	1,25	0,38	14,05
11	9	0,2682	-1,6997	0,0000	0,2660	-1,7043	0,0000	0,83	-0,27	8,10
11	10	0,4650	-1,7659	-0,0002	0,4259	-1,7719	0,0002	9,19	-0,34	10,23
11	11	0,3750	-1,9885	0,0000	0,3312	-1,9713	0,0000	13,24	0,87	-
11	12	0,2756	-1,8564	0,0001	0,2296	-1,8714	-0,0001	20,01	-0,80	-

Table 5.3: Test 12.

Joint	MatLab®			SAP2000®			Percentage changes		
	u	v	f_y	u	v	f_y	u	v	f_y
	[mm]	[mm]	[]	[mm]	[mm]	[]	[%]	[%]	[%]
4	8,19956	-0,86068	-0,00325	8,19513	-0,86373	0,00326	0,05	-0,35	-0,04
5	8,21489	-1,38848	-0,00103	8,21040	-1,38419	0,00102	0,05	0,31	0,41
6	8,23328	-0,97314	0,00008	8,22875	-0,97559	-0,00009	0,06	-0,25	7,23
7	14,43062	-1,34038	-0,00211	14,40649	-1,34616	0,00209	0,17	-0,43	1,04
8	14,42899	-2,14719	-0,00059	14,40532	-2,13908	0,00059	0,16	0,38	0,89
9	14,42596	-1,49028	0,00010	14,40271	-1,49493	-0,00010	0,16	-0,31	-0,58
10	17,45414	-1,47810	-0,00220	17,36101	-1,48587	0,00227	0,54	-0,52	-3,19
11	17,41224	-2,38628	-0,00019	17,31774	-2,37522	0,00011	0,55	0,47	-
12	17,36432	-1,63212	0,00159	17,26855	-1,63856	-0,00177	0,55	-0,39	-

5.3 Nonlinear behaviour

5.3.1 Introduction and general principles

In the classic formulation of the Finite Element problem the following hypotheses are assumed: linear and isotropic elastic material, small displacements.

Furthermore it is assumed that the nature of the boundary conditions remains unchanged during the application of loads. Under these assumptions, the equation of equilibrium which is used for static analysis of the problem is:

$$\underline{\underline{K}} \cdot \underline{u} = \underline{f} \,. \tag{5.39}$$

Where:

- $\underline{\underline{K}}$ is the stiffness matrix of the structure discretised with a Finite Element mesh;
- $\underline{u}$ is the vector of nodal displacements;
- $\underline{f}$ is the vector of loads.

In the case of linear analysis, the vector of displacement $\underline{u}$ is a linear function of the vector of loads $\underline{f}$. If it applies a load vector of the type $\alpha \cdot \underline{f}$ (multiplied by a constant factor, α) the solution of the problem in terms of displacements is equal to $\alpha \cdot \underline{u}$.

If the above property of linearity is not valid, there is the problem of a nonlinear analysis. The nonlinear case, in relation to the assumptions that are adopted can be classified as show in the Table 5.4.

In particular, in the case of masonry, the material has characteristics of nonlinearity (in terms of the constitutive low stress-strain). The main purpose of the study of a continuous body with the finite element method is to find a solution by equilibrium of the body subjected to external loads.

Table 5.4: Classification of nonlinear analysis [45].

Type of analysis	Description	Typical formulation used	Stress and strain measures
Materially-nonlinear-only	Infinitesimal displacements and strains; the stress-strain relation is nonlinear	Materially-nonlinear-only(MNO)	Engineering stress and strain
Large displacements, large rotations, but small strains	Displacements and rotations of fiber are large, but fiber extensions and angles changes between fibers are small; the stress-strain relation may be linear or nonlinear	Total Lagragian (TL) Updated Lagragian (UL)	Second Piola-Kirchhoff stress, Green-Lagrange strain Cauchy stress, Almansi strain
Large displacements, large rotations, and large strains	Fiber extensions and angle changes between fibers are large, fiber displacements and rotations may also be large; the stress-strain relation may be linear or nonlinear	Total Lagragian (TL) Updated Lagragian (UL)	Second Piola-Kirchhoff stress, Green-Lagrange strain Cauchy stress, Logarithmic strain

Each different nonlinearity must be studied in order to formulate appropriate methods that can be adopted to obtain a prediction of the nonlinear behavior of the structural system. In the case of nonlinearity caused from the mechanical properties of the material it may be convenient to switch to an incremental procedure:

$$\underline{\underline{\Delta K}} \cdot \underline{\Delta u} = \underline{\Delta f} \ . \tag{5.40}$$

In this way it's possible to adopt the simple linear solution in an iterative manner, but changing from one and the next step, the stiffness matrix of the system. In particular, when the load is applied on the structure and it has a progressive damage, the stiffness of the system decreases.

5.3.2 General principles

In this chapter a simple plan masonry structure shows in the Commentary No. 21745 is studied. This structure was discussed in the past, in very simply mode and providing a behaviour of equivalent shear type frame into the spirit of the POR method.

This modelling, in the previous paragraphs, has been improved taking:

1) plan spandrels not more infinitely rigid: in this way, it was possible to obtain a shear type frame made of frame elements with rigid ends of the lines that schematise the nodal areas;
2) collapse mechanism of masonry elements not only for diagonal shear but also for the sliding shear and flexural failure.

In the previously obtained modelling, however, the possibility of a normal stress model variable during the analysis has been considered. The assumption of constant axial forces, however, is acceptable in the case of small structures and with few floors.

Finally, the method of using the link elements has proved particularly suitable to model the plastic behaviour of wall elements and simple enough to apply.

For this reason, in the next chapter 6, also this type of modelling is applied to a structure that has been really tested in the laboratory and they are compared the results of this modelling with the related experimental results obtained during the test.

5.3.3 Application to the case of masonry

A nonlinear version of the program in MatLab® must be written. It must have concentrated deformation to simulate the progress of the damage in the elements (lumped plasticity).

Remaining firstly in an elastic structure, it needs to write the terms of the stiffness matrix of the structure in Figure 5.1, consisting of two rigid traits at the ends and once deformable with deformation concentrated at its ends (k_i and k_j for rotational stiffness, k_{vj} and k_{vi} for shear stiffness).

This problem can be solved, for example, by the method of unitary force. In particular the terms of the matrix deformation can be written. For example, by the application of a unitary moment at one end, and by knowing the moment diagram (triangular), the moment at the first spring can be obtained.

It must, therefore, to write the work done by the unitary action to derive the rotation, which will be the general term of matrix deformation. Alternatively the stiffness approach can be used. For example, by assigning an unitary rotation at one end (see Figure 5.5).

Multiplying this rotation (unitary) to the length of the trait, the vertical displacement of the trait is obtained (for example, amounted to "a"). The moments that are activated at the ends of the deformable section can be achieved. Knowing also the stiffness of the springs at the ends of the deformable section, through a decomposition and with the writing equilibrium relations, it can be identified the forces that are generated at the ends (moments and shear).

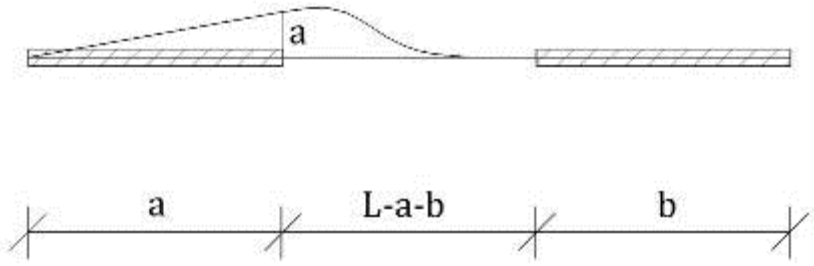

Figure 5.5: Scheme 1: unitary rotation at the joint i.

At this point the terms of the type W_{ij} can be obtained. Please note that W_{ij} is the moment that born in "i" to effect of an unitary rotation in "i". In practice, proceeding in this way, the stiffness matrix K as a function of the various concentrated stiffness can be written.

Since the structure is asymmetric in general, it needs assign a rotation at the other extreme and calculate the term W_{ji} (or simply need to swap the terms "a" and "b", length of rigid traits). Another model to consider is the one with the unitary translation of one of the two traits (shown in Figure 5.6).

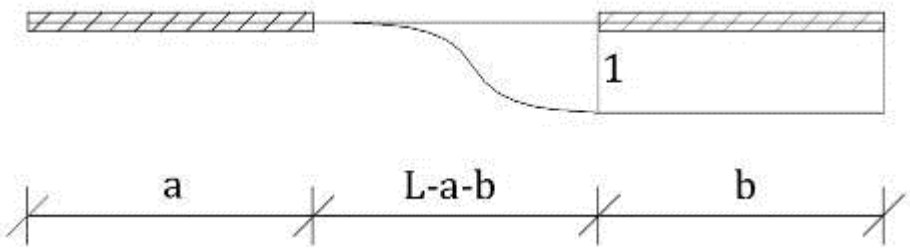

Figure 5.6: Scheme 2: unitary displacement at the joint j.

The objective is to generate a stiffness matrix for the frame m–th. This matrix, therefore, will depend on the size and stiffness of the traits:

$$\underline{\Delta f} = \underline{\underline{K}}\left(a, b, k_i, k_j, k_{vi}, k_{vj}\right) \cdot \underline{\Delta u} \,. \tag{5.41}$$

The terms "a" and "b" do not change during the analysis. Instead, k are parameters that vary according to the local stress state. It will be possible to relax this rigidity to take account the progressive damage in masonry of the various elements. Assigned displacement ($\underline{\Delta u}$), through the previous report, a forecast (prediction) of force ($\underline{\Delta f}$) can be obtained.

The idea is that, since a stress is performed an analysis with very large stiffness. Next, with an increment of load, for example, it comes at a point outside the domain (point i in Figure 5.7).

At this point there is a part that can describe in the linear range (i.e. that intra-domain, which is sufficient to describe the elastic response), and then it needs to find ways to relax the stiffness for return the first point reached in the domain. A rule type of normality can be used.

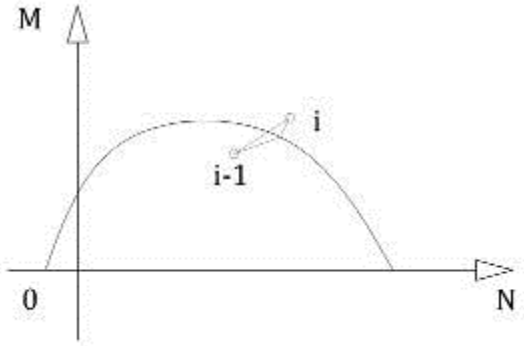

Figure 5.7: Behaviour near the domain.

For example, on the single element, the following increase in forces initially obtained using the elastic stiffness matrix is valid:

$$\underline{\Delta f} = \underline{\underline{K}}^{el} \cdot \underline{\Delta u}\,. \tag{5.42}$$

If it turns out that this increase of forces is excluded, there are two options. The first is to define a plastic, displacement leaving the elastic stiffness matrix:

$$\underline{\Delta f}^{NL} = \underline{\underline{K}}^{el} \cdot \left(\underline{\Delta u} - \underline{\Delta u}^{pl}\right). \tag{5.43}$$

It should, however, maintain the target that the state of the total stress is on the border:

$$F\left(\underline{f} + \underline{\Delta f}^{NL}\right) = 0\,. \tag{5.44}$$

When the point is not acceptable (outside the domain):

$$F\left(\underline{f} + \underline{\Delta f}\right) > 0\,. \tag{5.45}$$

In reality the previous procedure is impractical, and therefore might want to change the stiffness matrix in a matrix of tangent stiffness (secant on the step)

so that it preserves a fixed total displacement. The matrix can be obtained by relaxing the secant deformation concentrated:

$$\underline{\Delta f}^{NL} = \underline{\underline{K}}^{t} \cdot \underline{\Delta u} \,. \tag{5.46}$$

In the linear analysis of the single load step (Analysis.m) is also built the stiffness matrix (Stiffnessmatrix.m). This last function, based on data loaded before and the results from other functions, generates the matrix of element, the vector of actions, finds the nodes to which the element is connected, the inclination angle in the plan.

In the analysis will follow the next steps: generation of matrices, rotation matrices, matrix assembly, analysis of the nodal forces (equivalent to external forces multiplied by a multiplier factor), application of boundary conditions, matrix inversion, analysis of displacement, assignment of these displacements to the elements, strain analysis.

The nonlinear correction, before of all, must proceed incrementally. First must be apply the vertical load and then a process of incremental load for seismic actions. This thing can be done simply by assuming that the multiplier of the nodal action is variable. The nonlinear procedure must start from the elements with extreme rigid but without the springs (shown in Figure 5.8).

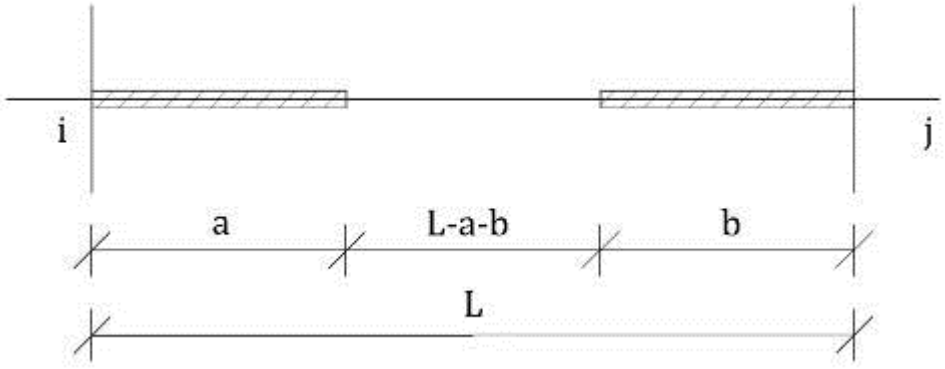

Figure 5.8: Frame in elastic range.

The nonlinear process might work, first making an elastic prediction and then a plastic correction. Starting from the elastic stiffness matrices of each element

(indicated with $\underline{\underline{K}}_{el}^{(e)}$), by an assembly operation, the elastic stiffness matrix of the structure ($\underline{\underline{K}}_{el}$) can be obtained.

Under initially only vertical loads will be possible to calculate the displacements (vertical):

$$\underline{v}_{el} = \underline{\underline{K}}_{el}^{-1} \cdot \underline{Q}_0 . \tag{5.47}$$

The vector of the vertical loads is obtained by assembling the individual elements:

$$\underline{Q}_0 = -\sum_e \underline{Q}_0^{(e)} . \tag{5.48}$$

The previous is a prediction of elastic displacements with elastic stresses, because each element can be calculated from the previous (with a process for extracting). The elastic displacements and the corresponding forecast in terms of forces are:

$$Q_{el}^{(e)} = K_{el}^{(e)} \cdot v_{el}^{(e)} + Q_0^{(e)} = \left[N_i, V_i, M_i, N_j, V_j, M_j\right]. \tag{5.49}$$

At this point it needs to understand if the obtained forces from the previous elastic prediction are admissible or must be changed to take into account the damage of structure. Therefore, eventual plastic correction should be considered. A check of the previous forecast must be conducted.

From the previous carrier it is possible to extrapolate the couples (N, M) and (V, N), assuming decoupled from mechanisms shear and flexural. However it is noteworthy that the check should be carried out in the end points of each beam (nodal actions indicated in Figure 5.9).

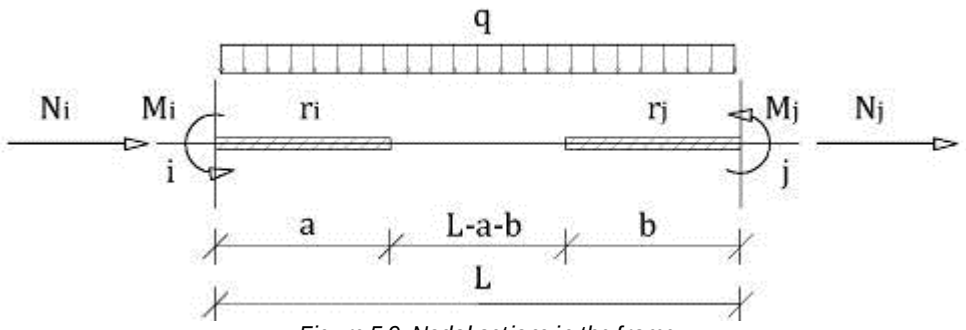

Figure 5.9: Nodal actions in the frame.

The problem is easily solved by calculating the stresses at the desired points, remembering that, in general, the laws of moment and normal force are, for example:

$$M(z) = -M_i + \left(\frac{M_i + M_j}{L} + \frac{q \cdot L}{2} \right) \cdot z - \frac{q \cdot z^2}{2}; \tag{5.50}$$

$$N(z) = N_i + p \cdot z\,. \tag{5.51}$$

At this point the couples that must be checked with the domains can be obtained:

$$\left(\overline{N}_i, \overline{M}_i\right), \qquad \left(\overline{N}_j, \overline{M}_j\right). \tag{5.52}$$

If the couples are internal to the previous domain do not need to change anything. If, instead, they are out of domain it needs to change something.

Only for vertical loads, in fact, should almost always be a situation within the domains. Only the floor spandrels, if it does not establish a minimum of reinforce, it could have a situation out of the domain.

If the point should be outside the domain it needs to be back inside by using appropriate techniques. It can be reasoned in a manner similar to the plasticity. It can first obtain a no-dimensional diagram μ, ν (Figure 5.10).

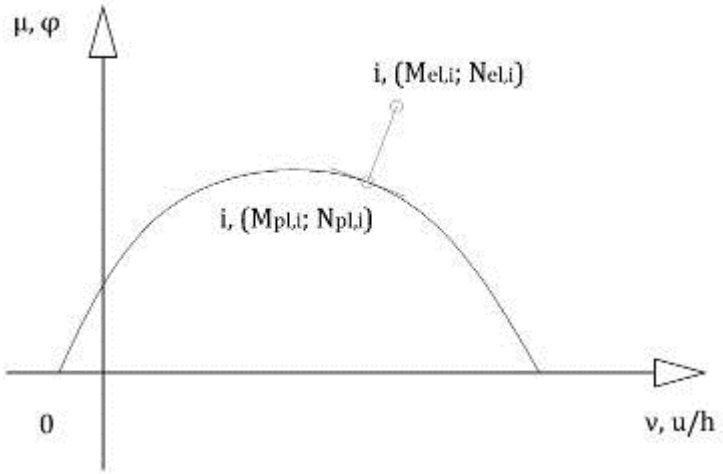

Figure 5.10: Elastic prediction and plastic correction.

In particular, in this case is:

$$\mu = \frac{M}{t \cdot l^2 \cdot f_m}; \tag{5.53}$$

$$\nu = \frac{N}{t \cdot l \cdot f_m}. \tag{5.54}$$

From the point of view of energy, the work is given by:

$$L = M \cdot \varphi + N \cdot u, \tag{5.55}$$

substituting:

$$L = t \cdot l^2 \cdot f_m \cdot \left[\mu \cdot \varphi + \nu \cdot \frac{u}{l} \right]. \tag{5.56}$$

If there is a point outside the borders of the domain it must return to the surface should follow the shortest route, or going perpendicular.

For the domain is known the equation of the curve, which is of type:

$$f = \mu - \frac{\nu}{2} \cdot (1 - \nu) = 0. \tag{5.57}$$

The normal unit vector can be calculated by the derivatives of the above function with respect to two variables:

$$\frac{\partial f}{\partial \nu} = \nu - \frac{1}{2}; \tag{5.58}$$

$$\frac{\partial f}{\partial \mu} = 1. \tag{5.59}$$

Consider the predicted elastic stresses out of the domain:

$$\left(\overline{N}_i^{el}, \overline{M}_i^{el}\right), \quad \left(\overline{N}_j^{el}, \overline{M}_j^{el}\right), \tag{5.60}$$

the characteristics of the stress that take into account the plastic correction are the following:

$$\left(\overline{N}_i^{pl}, \overline{M}_i^{pl}\right), \quad \left(\overline{N}_j^{pl}, \overline{M}_j^{pl}\right). \tag{5.61}$$

From the previous values, with a reverse, can be defined the moments and normal plastic stress to the end of the frame:

$$\left(N_i^{pl}, M_i^{pl}\right), \quad \left(N_j^{pl}, M_j^{pl}\right). \tag{5.62}$$

The previous values are present in a vector that must be obtainable from the following relationship:

$$\underline{Q}_{pl}^{(e)} = \underline{\underline{K}}_{pl}^{(e)} \cdot \underline{v}_{el}^{(e)} + \underline{Q}_{o}^{(e)}. \tag{5.63}$$

The idea is to find a secant stiffness matrix. Consider, for example, the following one dimensional loading process in Figure 5.11.

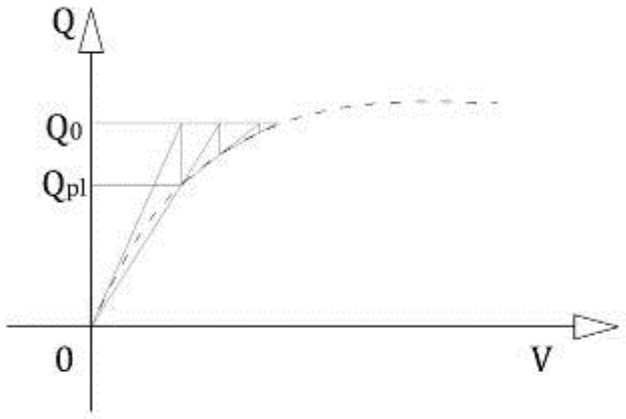

Figure 5.11: Analysis of the secant stiffness matrix.

At the beginning of the loading process is known force and initial stiffness. A certain displacement from the elastic forecast can be had. However the point has a force Q_0 too high which should be reduced until the force Q_{pl}. This

research, therefore, the new stiffness that corresponds to the force (which will be less than the previous).

A second step is reached, however, the force Q_0 to get the actual result (in terms of displacements) of nonlinear analysis. This can be done considering the initial stiffness matrix and applying the next increment of load in an iterative way.

5.3.4 Implementation of the numerical procedure

5.3.4.1 General comments

This section reports an analysis code created with MatLab® language. The major good thing of this code is the possibility to implement all the standard's prescription [6] about masonry. This standards, in fact, recommend to use a nonlinear implementation with the use of finite macro-elements. By the use of the following code, it's available a control about the failure of the elements both in sliding shear and in flexural. This checks can be done with a control of the relative displacement on the top of the deformable element in respect to the limit displacement defined by the [6] and exposed in section 3.1.4.

This code runs a nonlinear analysis of an object schematised as a frame with some rigid traits and spring with variable stiffness at the ends (i.e. Figure 5.12).

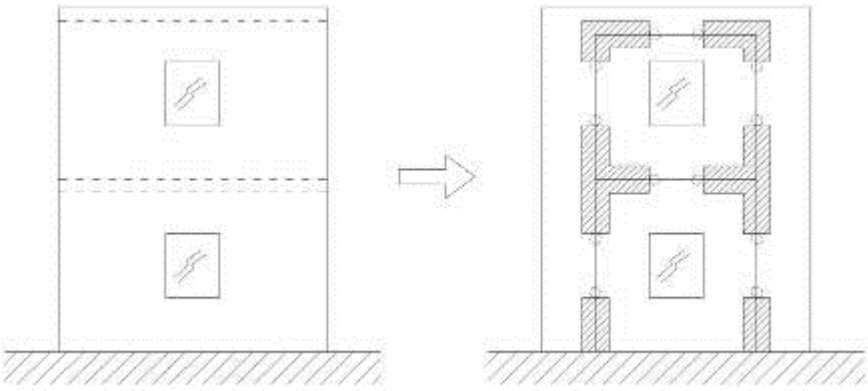

Figure 5.12: Real wall (on the left) and relative frame modelling.

These hinges have a certain behavior in a normal stress versus bending moment domain (useful to outline the flexural crisis), and in a shear versus normal stress domain (useful to outline the shear crisis).

5.3.4.2 Outline of the procedure

The program written in MatLab® analyses the same wall as described in Commentary No. 21745 (see Figure 5.13). In the Data folder there are the essential ingredients of a finite element model. First of all there are the coordinates of the nodes (Coords.txt) listed in Table 5.5. Initially the program was designed in a three-dimensional space. However now this program can be used for the analysis of two dimensional walls.

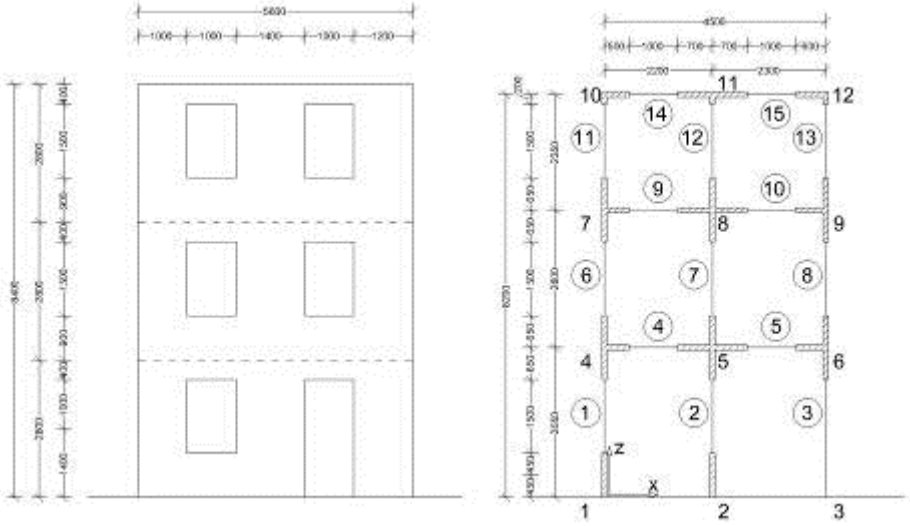

Figure 5.13: Wall prospect and relative frame model.

Table 5.5: Points' coordinates.

Point	x	y	z
	[mm]	[mm]	[mm]
1	0,0	0,0	0,0
2	2200,0	0,0	0,0
3	4500,0	0,0	0,0
4	0,0	0,0	3050,0
5	2200,0	0,0	3050,0
6	4500,0	0,0	3050,0
7	0,0	0,0	5850,0
8	2200,0	0,0	5850,0
9	4500,0	0,0	5850,0
10	0,0	0,0	8200,0
11	2200,0	0,0	8200,0
12	4500,0	0,0	8200,0

The displacements and the nodes uses the reference system shown in *Figure 5.14*. Moreover, in the Connectivity.txt file there are the nodes' index at the extremities of each frame (see Table 5.6).

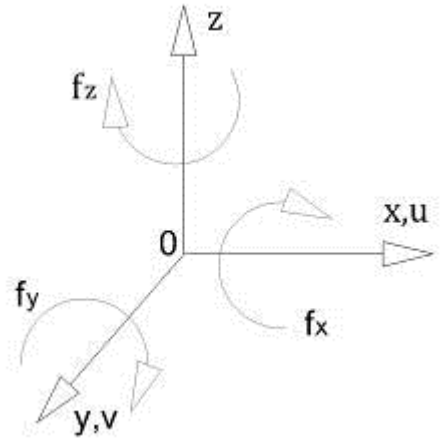

Figure 5.14: Coordinate and displacement system.

In the wall example of the Commentary, which was analysed using a method similar to the SAM method, there are three floors and two openings on each floor. The schematic equivalent frame consists of a three–storey frame and two bays. The coordinates of 12 nodes must be defined. Then there is the Frame.txt file that contains the elements properties (see Table 5.7).

Table 5.6: Truss connectivity.

Truss	i	j
1	1	4
2	2	5
3	3	6
4	4	5
5	5	6
6	4	7
7	5	8
8	6	9
9	7	8
10	8	9
11	7	10
12	8	11
13	9	12
14	10	11
15	11	12

For each element the size of t and L (rectangular section, thickness and length) are reported. Also f_c is defined and represents the maximum vertical compression stress. Then, the shear strength f_{v0} in the absence of compression, the friction factor (μ), the weight per unit volume (γ_g) can be defined. For the rigid tract, r_i and r_j, are the no-dimensional length and equal to:

$$r_i = \frac{a}{L}; \qquad r_j = \frac{c}{L}. \tag{5.64}$$

Table 5.7: Truss characteristics.

Truss	t	L	f_c	f_{v0}	μ	γ_g	r_i	r_j	q	E	G
	[mm]	[mm]	[MPa]	[MPa]	[]	[N/mm³]	[]	[]	[N/mm]	[MPa]	[MPa]
1	500	1000	3	0,11	0,4	0,000014	0,295	0,213	0	726	121
2	500	1400	3	0,11	0,4	0,000014	0,295	0,213	0	726	121
3	500	1200	3	0,11	0,4	0,000014	0,000	0,213	0	726	121
4	500	1300	3	0,11	0,4	0,000014	0,227	0,318	10	726	121
5	500	1300	3	0,11	0,4	0,000014	0,304	0,261	10	726	121
6	500	1000	3	0,11	0,4	0,000014	0,232	0,232	0	726	121
7	500	1400	3	0,11	0,4	0,000014	0,232	0,232	0	726	121
8	500	1200	3	0,11	0,4	0,000014	0,232	0,232	0	726	121
9	500	1300	3	0,11	0,4	0,000014	0,227	0,318	10	726	121
10	500	1300	3	0,11	0,4	0,000014	0,304	0,261	10	726	121
11	500	1000	3	0,11	0,4	0,000014	0,277	0,085	0	726	121
12	500	1400	3	0,11	0,4	0,000014	0,277	0,085	0	726	121
13	500	1200	3	0,11	0,4	0,000014	0,277	0,085	0	726	121
14	500	400	3	0,11	0,4	0,000014	0,227	0,318	10	726	121
15	500	400	3	0,11	0,4	0,000014	0,304	0,261	10	726	121

Table 5.7 reports an example of the input data required for describing the geometrical and mechanical parameters of the frames. In particular, q is the transverse load on the truss. Finally, the modulus of elasticity in compression (E) and shear (G) are displayed. Then there is the Connectivity.txt file that says which are nodes that connect each beam (see previous Table 5.6). Then there are the forces applied to the nodes (in Forces.txt file and reported in

Table *5.8*). Horizontal forces are applied, because the vertical loads have already been applied on the truss with distributed loads.

Table 5.8: Forces on the wall.

Point	F_x	F_y	F_z
1	0,0	0,0	0,0
2	0,0	0,0	0,0
3	0,0	0,0	0,0
4	1000,0	0,0	0,0
5	2000,0	0,0	0,0
6	1000,0	0,0	0,0
7	1000,0	0,0	0,0
8	2000,0	0,0	0,0
9	1000,0	0,0	0,0
10	1000,0	0,0	0,0
11	2000,0	0,0	0,0
12	1000,0	0,0	0,0

The last input is the file Restraints.txt. For each node, the degrees of freedom, active or bound, are imposed (Table 5.9).

Table 5.9: Boundary condition.

Bond	u	v	z	f_x	f_y	f_z
1	1	0	1	0	1	0
2	1	0	1	0	1	0
3	1	0	1	0	1	0
Legend: 0 = "free"; 1 = "fixed".						

Since the program is generally designed to operate in three dimensions, each node has six degrees of freedom. In particular, there are the three translations (u, v, z, respectively along x, y, z) and three rotations (f_x, f_y, f_z, respectively, around the three axes x, y, z). It requires a value of 1 if the degree of freedom is bound (or fixed) and 0 if the degree of freedom is free (or active) or if it's not defined. The program begins starting the file Main.m.

The program is designed to apply forces to steps. In practice, the analysis is done applying forces with a multiplication factor ($\Delta\lambda$). So, there are several load steps and, step by step, the displacements are added.

The program is done in this manner because it must use these first steps of elastic load to make a prediction. The purpose is to obtain, however, a nonlinear analysis. In this analysis, in a certain step, it can make a prediction and then adjust the elastic stiffness matrix, taking into account the constitutive laws in order to have the plastic correction.

In practice the stiffness must be reduced. For example, for to do the non-elastic analysis in a beam, the elastic prediction is to obtain the diagram of moments. At this point, knowing of the constitutive link of the beam, as curvature vs. moment of each section, it can be associated each moment (bi triangular diagram) to the value of the curvature (nonlinear diagram).

To calculate, at this point, the stiffness of the truss, that is its deformability (α_{ij}) it can integrate the curvatures for the unitary moment. For each step it is necessary to make an elastic prediction and then a correction to consider the plasticity.

It needs to change the K in an iterative cycle that reaches to convergence. After the analysis, in output, there are the displacements (three components of displacement for each node). The displacements are ordered as y, z, f. The displacements along z are negative, because downward.

The mechanical properties of materials are loaded separately for each beams. The code obtains the weights of the elements knowing volumes and specific weights. For this reason it can have displacement even without the vertical loads. Once loaded the data with the input functions it must use them in other functions. For example, the different stiffness matrix of each frame (file Assembly.m) must be assembled. The most important function is the one that performs the analysis (Analisys.m). StiffnessMatrix.m is the function delegated to write the stiffness matrix. Basically, the written code, generates the stiffness matrix for each element. This matrix is computed first in the local truss system. In this function, they are identified the indices of the nodes of each

truss (for uploading the file attempts Connectivity.txt). Then they are obtained the length and angle (in the two plan) of the truss.

In fact, knowing the indices of the nodes in ends of the truss, also the coordinates of these nodes are known. For to calculate the matrix of the truss, the shear stiffness (GA) and flexural stiffness (EI) must be obtained. In the following there are the coefficients of deformation used to define the matrix of the truss. Ultimately, this function provides, in addition to the stiffness matrix, the vector of loads equivalent to the forces, the indices to which the generic truss is connected and the angle of inclination.

The indexes are used to make the assembly, the angle is used to make the rotation. Then there is the function Rotation.m. This rotates the matrix related to each truss. Finally, Assembly.m is done with the assembly of the stiffness matrix of the individual truss (suitably expanded) to obtain the stiffness matrix of the whole structure. The assembly is done classically going to put the four minors in which is divided the stiffness matrix of each individual truss in the appropriate places of the stiffness matrix of the total structure.

The same is done for the vector of nodal forces. After the assembly, the forces are multiplied by the factor λ (called force multiplier). Only the nodal forces are multiplied by this factor (seismic actions applied to the various floors).

There is a table of type Restrain in which, for each node, it sees if they are bound or not (using the relative input file). If the node is bound to a certain degree of freedom, the stiffness matrix of the structure obtained previously (in its basic configuration) is overwritten in the line and column of the degree of freedom constrained. Basically it puts all zeroes except for a unitary term in the main diagonal (this is called the equation of constraint).

When the analysis is made, among other results, the displacements of the nodes corresponding to the applied forces are obtained. In fact, with an increase of forces, an increase of displacements is reached. Once it has done the analysis of the elements, it can pass to post processing. This is a table that,

for each element, reports the force vector. This table has got seven columns and as many rows as the elements.

In the first column there is the index of the element, in the other columns there are other forces. ElForceTable provides the result of all the nodal forces. This shows, for each element, the normal stress, shear and bending moment. The first step is the linear validation with different loads and forces, with rigid traits and normal traits, comparing the results obtained with a model made with SAP2000®.

The second thing to do is the validation of the plastic correction. Imagine to have put an increases of load. Firstly all the vertical loads must be applied. They are then placed horizontal seismic forces that are grown. A procedure in control of displacements can be done.

Suppose that in an ideal process of nonlinear load, it arrives to a certain extent. A tangent or secant stiffness matrix can be used. From this, it can impose a new increase of displacements and the elastic prediction can be obtained. For the i-th step of loading:

$$\Delta \underline{u_i^{el}} = \underline{\underline{K_{t,i}^{-1}}} \cdot \Delta \underline{\lambda_i} \underline{F} \qquad \text{->} \qquad \Delta \underline{F_i^{el,j}} \,. \tag{5.65}$$

The total forces of the element i–th at the step j-th are:

$$F_i^{el,j} = F_{i-1}^{el} + \Delta F_i^{el,j} \,. \tag{5.66}$$

At this point it needs to understand if these forces change or not the state of the structure. The problem can be solved by imagining that there is a beam with different sampling points (Gauss points). At these points can be obtained:

$$K = \int_0^L B^T \cdot C \cdot B dz \cong \sum_i W_i B^T C B(\xi_i) \,. \tag{5.67}$$

By solving the previous integral by a sum in quadrature, for each point k-th stress characteristics are known:

$$M_k, V_k, N_k. \tag{5.68}$$

A generic trait (rigid or deformable) is described by a certain surface domain both in the plan M-N and in the plan V-N (see Figure 5.15).

If the points are within the domain does not change anything and the state can be accepted without changing contributions to the stiffness.

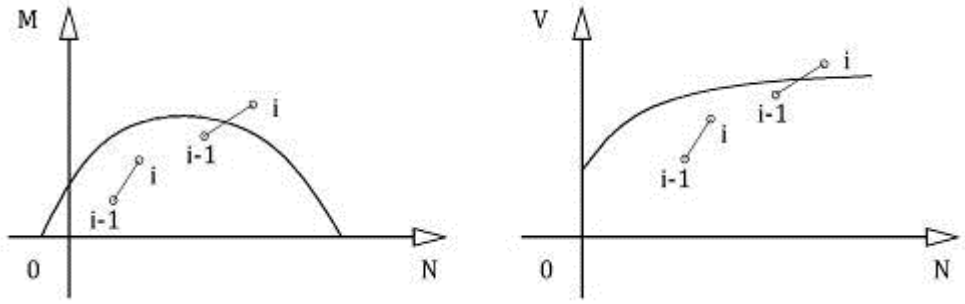

Figure 5.15: Behaviour of the wall during the load steps.

If at the generic iteration, it starts from an internal point and end outside the domain, the solution cannot be accepted. It is necessary to return the solution in the domain. The problem can be solved by assuming that there is an acceptable first part and a second part that must be changed. The plasticity must be taken into account so the end point returns into the domain.

The law of plastic flow can be used. A method that takes account of the crisis to sliding shear, diagonal shear and flexural failure is required. These two types of crises can be obtained directly from regulatory provisions exposed in section 3.1. A model frame which includes these two modes of crisis must be realised. A model with macro-elements will be used.

6. Validation of the proposed models

6.1 Introduction

This chapter aims at validating the model presented in chapters 4 and 5 by comparing the numerical simulations to a series of experimental results currently available in scientific literature. Those results generally derives by experimental tests results carried out at Slovenian National and Civil Engineering Institute (ZAG).

In the followings sections, the experimental data obtained from these tests are compared and interpreted for to be compared with the results that may be derived from the classical models of masonry. The innovative characteristic consists on the model used for the application of the two previous methods, which does not require the application of the classical Finite Element models or the application of commercial computational models for masonry structures (such as analysis code 3Muri, the SAM method [39] and others).

This study aims at describing the basic principles of seismic strength of masonry structures, review macro modelling approach to modelling masonry structures using frame-like models and compare the effectiveness of various approaches and modelling assumption by doing numerical simulation of seismic response of a masonry building, which was tested on a shaking table.

The results of numerical analyses are compared to experimental data obtained on a shaking table test, which was performed at ZAG at 1:4 scale. The tested structure was built using YTONG material (AAC masonry). The results validate our models and also expand our knowledge and confidence when assessing seismic response of masonry structures and in particularly confined masonry

structures built from AAC. For the modelling of the structure a simplified model based on frame and the use of link elements available in the Finite Element program SAP2000® (Version 14) [52] was used. These elements can be used to model structural elements such as piers and spandrels; because they provide the ability to define nonlinear behaviour. A model that possesses sufficient accuracy and ease of analysis is wanted. However, this structural model is not sophisticated enough to be able take into account the effect of variable normal forces on ultimate shear.

However, from experimental data and experience is known that these changes in normal stress due to seismic action can be neglected for small buildings (in terms of number of floors) and with some regularity in plan and elevation. This is also verified in this study in section 6.4.7.

This chapter start with the introduction about a description of behaviour of masonry under lateral loads and typical failure models. In the following, a common approach to modelling masonry using frame elements is presented as well as a description of one possible application in program SAP2000® using link elements. The methods for assessments of seismic strength are presented. Finally the building that is analysed is presented as well as the experiments on shaking table. The numerical analysis of the structure is presented, including pushover analysis, different approaches to modelling slabs and analysis of axial forces behaviour with comparisons of all the approach and methods.

The classical analysis methods prescribe the type of the mathematical model (with same simplifications) and the type of control of seismic strength and demand. The N2 method, on the other hand, only prescribes the way in wich seismic capacity and demand should be compared and the choice of the model of the structure is in essence arbitrary and left to the deigning engineering. One of the aims of this study is to see if there is an effect of the mathematical model on the results of the N2 method and how big these effects are.

6.2 Modelling masonry structures

The behaviour of multi–storey building is strongly influenced by the presence of spandrels of the floor. Indeed, according to the rigidity of the top spandrels in relation to that of piers a different static scheme of these ones is considered.

In practice, the modelling changes from piers prevented to rotate at the top (infinitely rigid spandrels) to piers free to rotate to the top. In some model analysis the presence of spandrels is taken into account in addition to the masonry walls, making it more precise and a better representation of the real behaviour of the wall.

6.2.1 Modelling based on frame elements

A model for masonry structure should address the following basic aspects:

1) it must include all the possible collapse mechanisms;
2) it must comply with all local and global equilibrium;
3) it must have the right balance between level of detail and ease of use;
4) it needs to have thresholds of damage defined, for example as a function of the displacement.

The following paragraphs describe a method that is based on the use of link elements which generally provide good reliability at low computational cost.

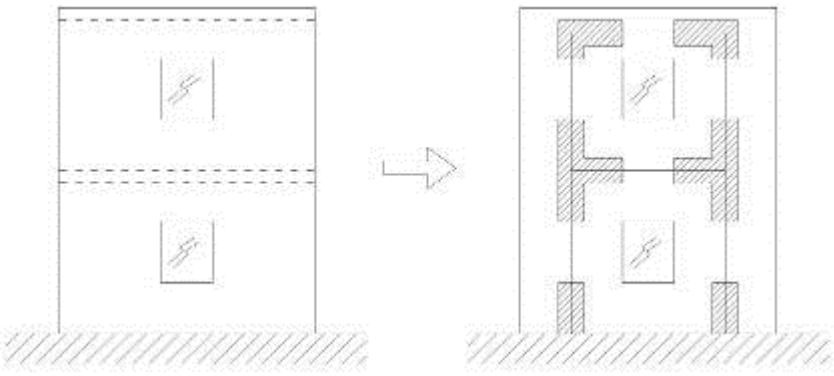

Figure 6.1: Modelling of a two level masonry wall with openings for the window.

Equivalent-frame models are generally considered for analysing masonry structures as they represent a trade-off between simplicity and accuracy (see Figure 6.1).

In this class of model, the generic brick structure is viewed as a frame made up from frame items. Often, the model would involve the use of rigid offset in order to outline the nodal zones of intersections between piers and spandrels. The most known of these methods is the SAM method [39]. If the wall geometry is sufficiently regular, it is possible to modelling a masonry wall as a frame consisting of:

a) pier elements;
b) spandrel elements;
c) node elements (rigid zones).

Only the first two elements are modelled as elements with axial and shear deformation. The nodal elements are assumed infinitely rigid and strong and are modelled through the use of offset elements. The pier elements are characterised by a certain effective length of the deformable part. Constitutive law for piers and spandrels is defined taking into account all three possible failure modes, which is shown in the following sections.

6.2.2 Modelling with link elements

The possible simulation of masonry macro-elements by means of equivalent frames has been recalled in section 6.2.1. A further design-oriented simplification can be achieved by simulating the same masonry elements through the so-called “link” element available in SAP2000®. The links can be employed in modelling the key aspects of the mechanical response of parts of the structure (either piers or spandrels, see Figure 6.2).

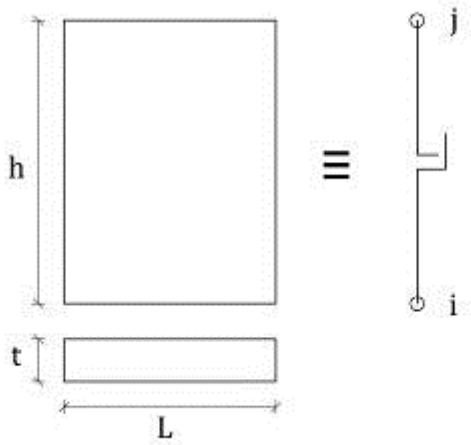

Figure 6.2: Modelling a deformable element through a link element.

In particular, link elements connect two nodes of the structural model and are characterised by a (generalised) force-displacement relationships which can be calibrated for simulating both stiffness and strength of masonry walls taking into account (through a simplified way) their relevant failure modes.

It is also possible to use these elements to represent the viscous behaviour of elements (dissipation). In defining the kind of behaviour of the link element, in a special box, the mechanical properties of this constitutive law can be assigned. Finally, the link element can be assigned to the structure both in punctual and linear form (link between two distant points). In the Figure 6.3 is possible to see the loading process that affects these elements.

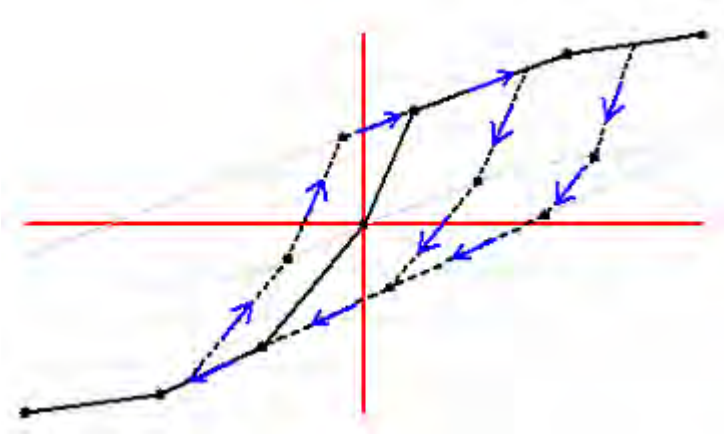

Figure 6.3: Loading process [52].

For each link element, used in the SAP2000® model the following three behaviours are defined:

1) for the shear in the wall plan it assumes an elastic perfectly plastic behaviour and the ultimate shear is assumed to be equal to the ultimate shear on diagonal cracking, as calculated in the previous chapter (Figure 6.4);
2) for the bending behaviour it assumes an elastic behaviour (Figure 6.5);
3) for the axial behaviour it assumes a linear elastic behaviour, following the analysis of the axial stiffness of the wall (EA), reported in Figure 6.6.

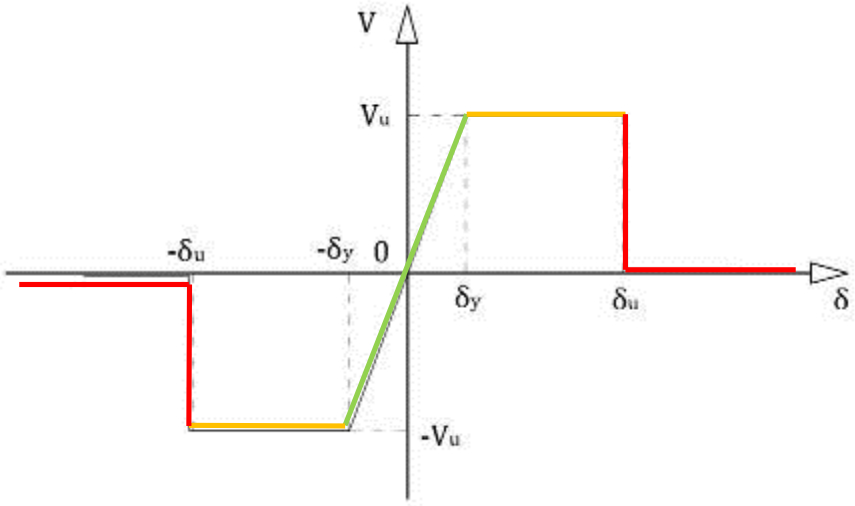

Figure 6.4: Shear behaviour.

For modelling of the structure, which will be presented later on, it will use a linear behaviour for axial force (N), nonlinear behaviour for shear (V) and linear behaviour for bending moment (M); with back–checking of axial forces.

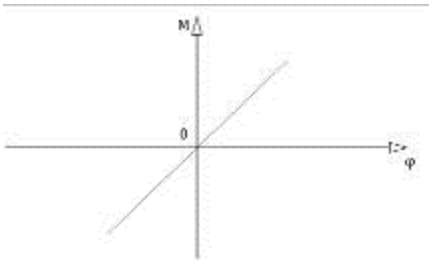

Figure 6.5: Rotation behaviour.

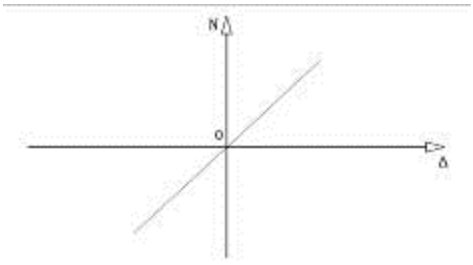

Figure 6.6: Axial behaviour.

In order to define the nonlinear generalised force–generalised displacement relationship, appropriate stiffness must be used. Stiffness for the axial force is EA, stiffness for shear is $\frac{1{,}2 \cdot h}{G \cdot A}$ and stiffness for buckling is $\frac{h^3}{12 \cdot E \cdot I}$.

6.3 Experiments on a shaking table

6.3.1 Physical modelling

The capacity of testing facilities, available at Slovenian National Building and Civil Engineering Institute (ZAG) does not permit the testing of seismic response of real size structures. By using the simple, uni-directional earthquake simulator, installed at ZAG, the models of buildings only can be tested. On the basis of experience, technology for producing AAC materials and capacity of the shaking table, it has been decided that the model built at 1:4 scale be tested. The modelling scale is relatively small, so that the buildings up to four storey high can be tested, but sufficiently large so that all relevant structural details can be reliably modelled.

Compared to the basic prototype, therefore, it was possible to build in scale models and using appropriate theories of modelling elements in scale and the mechanical and geometrical characteristics of the real structure from measurements made on the scaled structure can be obtained. In particular, scale factors listed in the Table 6.1 can be used.

If a general physical quantity, q_M, is measured on the models, the following correlation exists between the measured value on the model and the corresponding value on the prototype, q_P [53][54]:

$$q_{\mathrm{P}} = q_{\mathrm{M}} S_{\mathrm{q}} \tag{6.1}$$

where S_{q} is the scale factor for the given physical quantity.

Table 6.1: Scale factors in the case of the complete model similitude [55].

Physical quantity	Relationship	Scale factor
Length (l)	$S_L = l_P / l_M$	4
Strength (f)	$S_f = f_P / f_M = S_L$	4
Strain (ε)	$S_\varepsilon = \varepsilon_P / \varepsilon_M$	1
Sp. weight (γ)	$S_\gamma = \gamma_P / \gamma_M$	1
Displacement (d)	$S_d = S_L$	5
Force (F)	$S_F = S_L^2 S_f = S_L^3$	64
Time (t)	$S_t = S_L^{0.5}$	2
Frequency (ω)	$S_\omega = 1 / S_t$	0,5
Velocity (v)	$S_v = S_L / S_t = S_L^{0.5}$	2
Acceleration (a)	$S_a = S_v / S_t$	1

6.3.2 Prototype structure

The prototype buildings, investigated within the framework of this project, are typical residential buildings, built as confined masonry structures in YTONG system. As a prototype building, an idealised masonry building, with similar distribution of walls in plan and similar distribution of window and door openings along the height been selected (see Figure 6.7 and Figure 6.8).

The dimensions of the idealised prototype building, corresponding to the tested models, in the plan are 6,85 x 8,75 m, whereas the storey height amounts to 2,50 m. The prototype dimensions of the YTONG masonry blocks are 62,5/25/30 cm (length/height/thickness), according to the actual characteristics of model materials, the prototypes represent buildings, built with strength class 4 AAC masonry blocks. The walls are constructed according to YTONG technology rules, using YTONG paste for gluing the units.

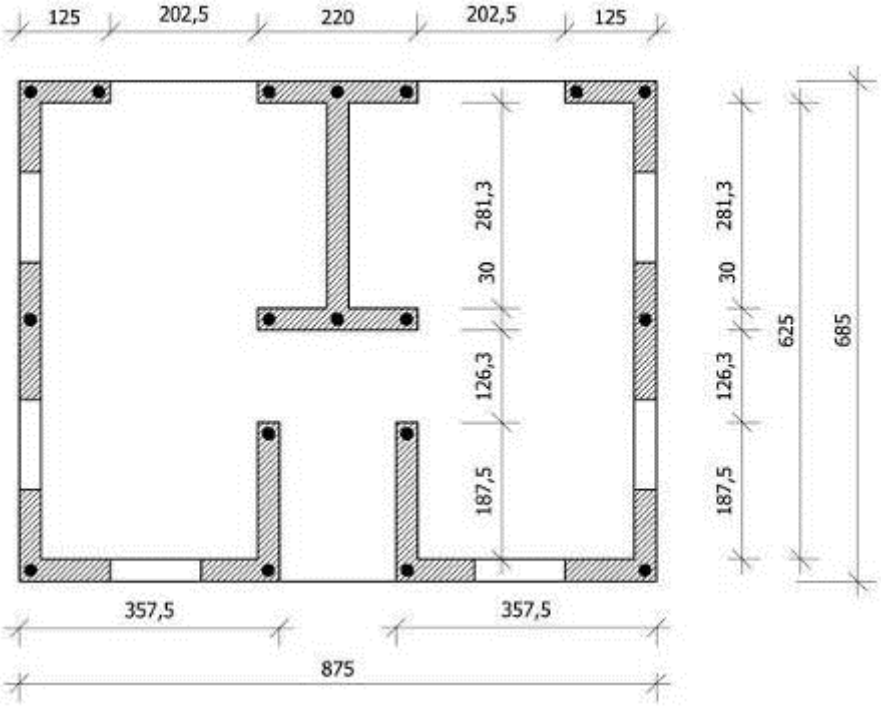

Figure 6.7: Dimensions of the idealised prototype building in plan and position of vertical confining elements [55].

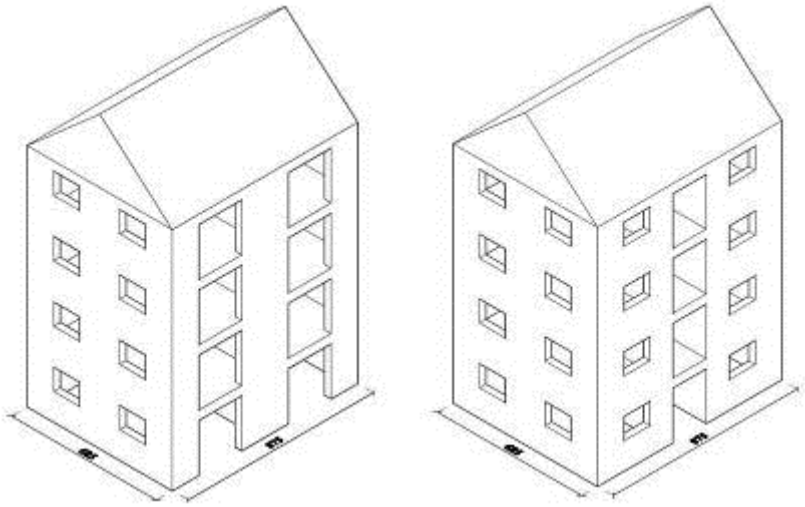

Figure 6.8: Isometric view on the prototype of the tested model M3 [55].

Prototype buildings are confined masonry structures with a system of vertical and horizontal confining elements, tie-columns and bond beams. The vertical confining elements are placed at all corners, wall intersections and at the free edges of window and door openings with an area of opening greater than 1,5 m^2 (SIST EN 1998-1), and where the distance between them would be greater than 5 m. The ties-columns are longitudinally reinforced with 4 Ø 14 mm diameter bars, whereas the cross section is commentary with 16 cm diameter. The placing of vertical confining elements in the case of the prototype, represented by model M3, is the same, however, the amount of steel is increased to 4 Ø 16 mm diameter bars, but the diameter of the cross section decreased from 16 cm to only 10 cm. Horizontal bond beams are reinforced with 4 Ø 12 mm diameter bars, located within the floors slabs on the top of all walls in each storey.

6.3.3 Physical models

The models have been built at 1:4 scale. The dimensions in plan have been 1,71 m by 2,19 m, with the storey height equal to 0,675 m. Taking into consideration the different thicknesses of floor structures, the height of model M3 was 2,65 m. The thickness of walls was 7,5 cm. The layout of models in plan and whereas the vertical sections are presented in the Figure 6.9 and Figure 6.10.

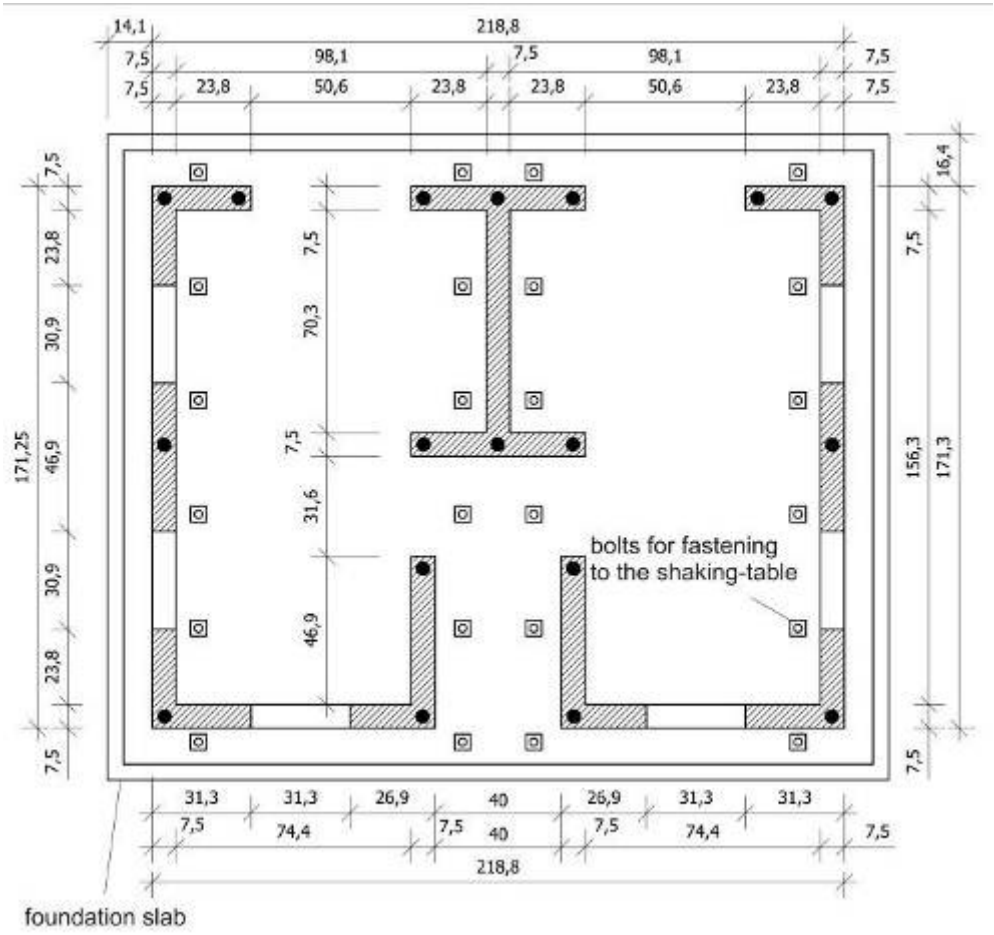

Figure 6.9: Dimensions of the models in plan [55].

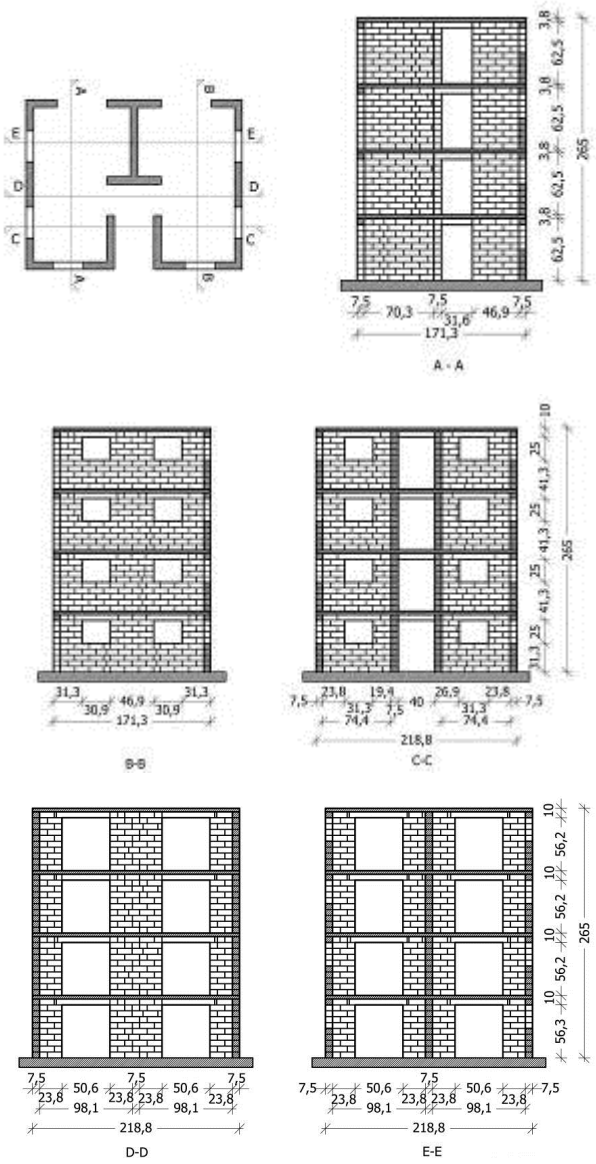

Figure 6.10: Plan and vertical sections of model M3 [55].

Before the shaking table tests, additional masses to compensate the missing live load on the floors and missing mass of the roof structure had to be fixed on the models' floors (see Table 6.2 and Figure 6.11).

Table 6.2: Model M3. Mass distribution at floor levels [55].

	1st storey [kg]	2nd storey [kg]	3rd storey [kg]	4th storey [kg]
walls	175	175	175	79
floor	406	406	406	406
weight	560	560	560	680
total	1141	1141	1141	1165
grand total	4588 kg			

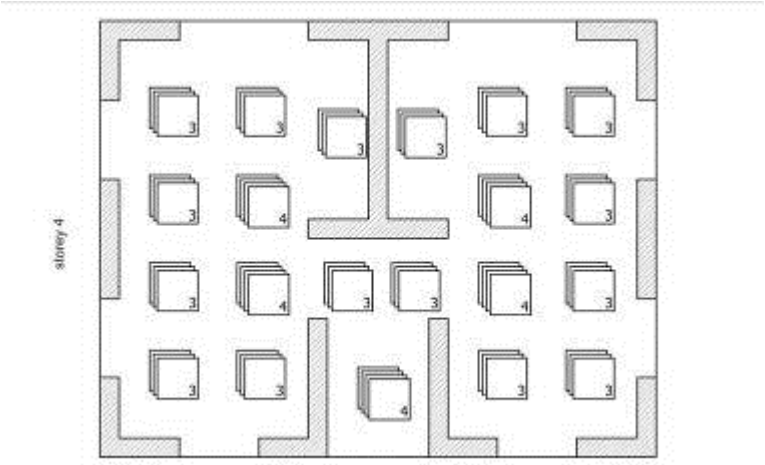

Figure 6.11: Distribution of weights on the floors of model M3 – fourth floor [55].

6.3.4 Model materials

6.3.4.1 Mechanical properties of prototype materials

When designing the models, the dimensions of AAC units and mechanical properties of units, mortar and masonry, as well as other materials used for the construction of buildings in YTONG system, listed on the official web–site of the company (Xella porobeton SI) and published in [55], have been considered as target values. The mechanical properties of YTONG masonry are summarised in the Table 6.3.

Table 6.3: Mechanical properties of YTONG masonry [55].

Strength class	Density [kg/m^3]	f_b [MPa]	f_{ck} [MPa]	f_t [MPa]	E [MPa]	G [GPa]
2	440	2,5	1,71	0,22	1200	480
4	500	5,0	3,14*	0,24*	2200*	880*
6	660	7,5	4,28	0,26	3000	1200

* interpolated

The meaning of the symbols listed in the previous table are as follows:

f_b - declared strength of the YTONG block,

f_{ck} - characteristic compressive strength of masonry,

f_t - average tensile strength of masonry (units glued on the bed joints and head joints),

E - modulus of elasticity,

G - shear modulus.

The dimensions of model masonry units, scaled at geometrical scale, were 15,6/6,3/7,5 cm (length/height/width). The compressive strength of units has been determined on cubes 6,3/6,3/6,3 cm, cut from the blocks. The values are given in the Table 6.4.

Table 6.4: Compressive strength of model YTONG blocks [55].

Model YTONG blocks	No. of specimens	20
	Average value (MPa)	1,73
	Coefficient of variation	13 %

The properties of the thin layer mortar (paste) for gluing the model masonry units have not been modelled because of technological difficulties. The dry part of the mortar is prepared in the factory. On the construction site, water is added and a special tool is needed to prepare and apply the paste. The results of tests for the determination of compressive and bending strength of thin layer mortar, obtained on cubes 7,07/7,07/7,07 cm and prisms 4/4/16 cm are given in Table 6.5.

Table 6.5: Compressive and bending strength of thin layer mortar used for the construction of model M3 [55].

Model M3	Compressive strength		Bending strength
	Cubes	Prisms	Prisms
No. of specimens	56	94	46
Average values (MPa)	13,05	12,39	4,84
Coefficient of variation	32 %	21 %	21 %

6.3.4.2 Masonry tests

In order to determine the mechanical properties of model masonry, 15 model walls have been tested, built as either plain or confined masonry walls. Among 9 confined masonry walls, 3 have been built with vertical confining elements (tie-column diameter 4 cm), 6 walls, however, have been built with the same tie-columns as in the case of model M3 (tie-column diameter 2,5 cm).

6.3.4.2.1 Compression tests of model masonry walls

The compressive strength of masonry has been determined on three specimens, denoted T1, T2 and T3 (see Figure 6.12). Whereas specimens T2 and T3 have been tested as plain masonry walls, without vertical confining elements, specimen T1 has been made with vertical tie–columns with 4 cm diameter.

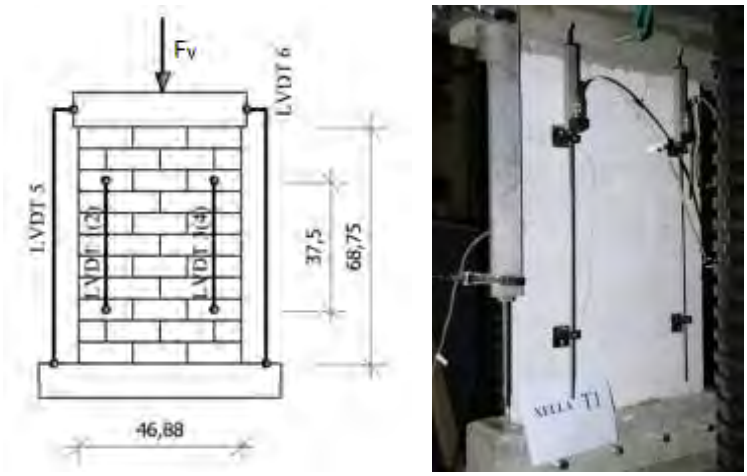

Figure 6.12: Dimensions and instrumentation of specimens for compression test (left); typical model wall at the end of compression test [55].

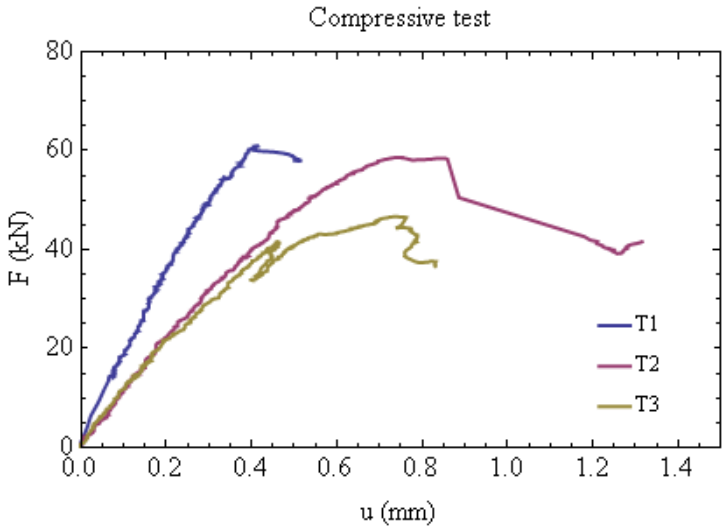

Figure 6.13: The results of compression tests [55].

As can be seen in Figure 6.13, the influence of vertical confining elements on the compressive strength of masonry is not essential. However, the reinforced concrete significantly increased the stiffness in compression (see Table 6.6).

Table 6.6: Results of compression tests of model masonry [55].

Specimen	Max. force [kN]	Compr. strength f_c [MPa]	Modulus of elasticity at 30% f_c [GPa]
T1 (tie-columns)	61,12	1,73	7,07
T2	58,64	1,66	4,14
T3	46,67	1,32	4,58
Average T2 and T3	52,66	1,49	4,36

6.3.4.2.2 Cyclic shear tests of model masonry walls

The parameters, which define the seismic behaviour of masonry walls, have been determined by subjecting the model walls to cyclic lateral load reversals at constant vertical preloading (see Figure 6.14). The walls have been tested as vertical cantilevers, fixed at the bottom into the horizontally moveable rigid platform of the shaking table, whereas the upper part of the walls could freely rotate, but was fixed in the horizontal direction. During the tests, the walls have been subjected to constant vertical load, acting on the bond–beam on the top of the walls, which induced compressive stresses in the walls equal to 20% of the masonry's compressive strength (0,20 f_c preloading). Horizontal load has been imposed in the shape of the programmed displacements of the shaking table, with step–wise increased amplitudes of displacements.

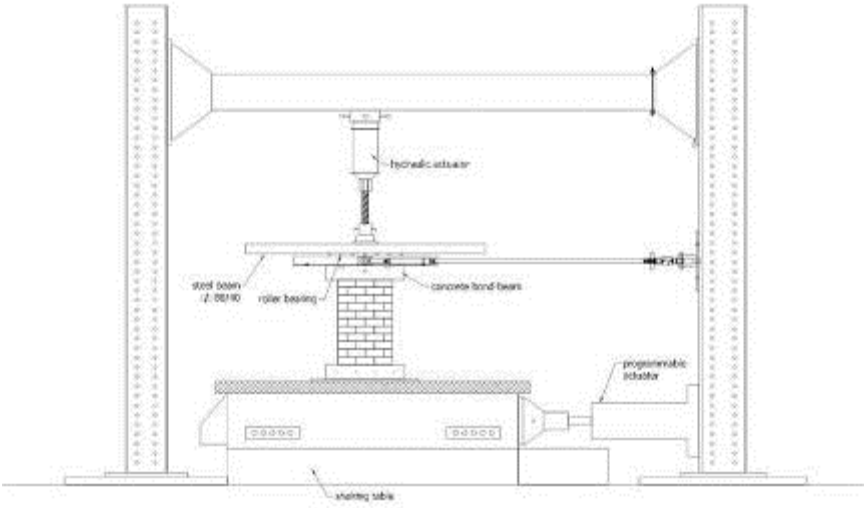

Figure 6.14: Test set–up for cyclic shear tests of model masonry walls [55].

At each amplitude step, the loading has been repeated three times in order to obtain information about strength and stiffness degradation at repeated load reversals. The programmed imposed horizontal displacement pattern is presented in the Figure 6.15, whereas the values of peak amplitudes at each step of testing are given in the Table 6.7. During the test, the velocity of increasing the displacements is kept constant.

Table 6.7: Imposed displacement pattern [55].

Phase	1	2	3	4	5	6	7	8	9	10
Displacement [mm]	0,25	0,50	0,75	1,00	1,50	2,00	2,50	3,00	4,00	5,00
Phase	11	12	13	14	15	16	17	18	19	20
Displacement [mm]	6,0	7,5	10,00	12,50	15,00	20,00	25,00	30,00	35,00	40,00

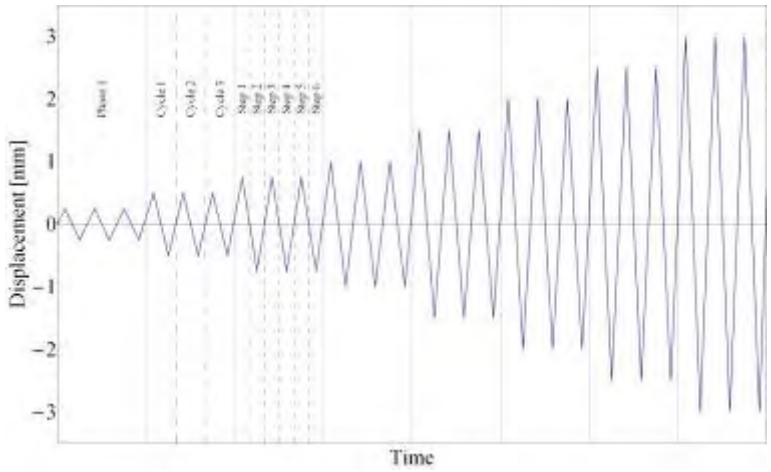

Figure 6.15: Imposed displacement pattern [55].

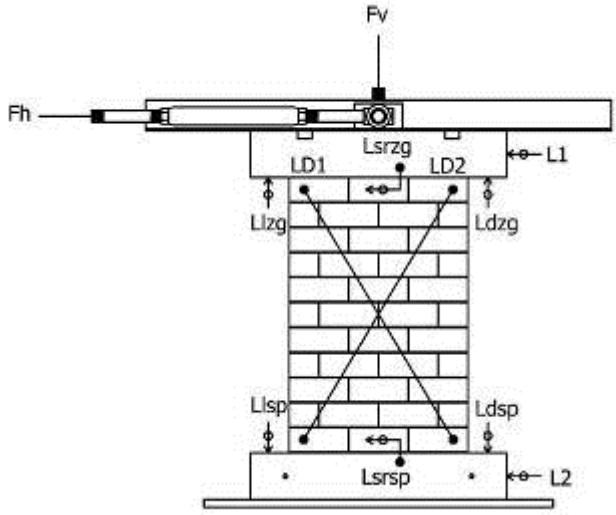

Figure 6.16: Instrumentation of model walls for shear tests [55].

All specimens have been instrumented with displacement and force transducers (shown in Figure 6.16). All together 10 model walls have been tested (Table 6.8). The notation and dimensions of specimens are presented, two groups of walls, as regards the dimensions of the walls and the size of vertical confining elements, have been tested (see Table 6.9 and Table 6.10).

Table 6.8: Designation and dimensions of model walls for cyclic lateral tests. l, h and t are length, height, and thickness of the walls, respectively [55].

Wall	*l* [cm]	*h* [cm]	*t* [cm]	Remark
X-1	47	70	7,3	Tie columns as M1
X-2	47	70	7,3	Plain masonry
X-3	47	70	7,3	Plain masonry
X-4	47	70	7,3	Plain masonry
X-5	47	70	7,3	Plain masonry
X-6	47	70	7,3	Tie columns as M1
X-7	47	58	7,4	Tie columns as M3
X-8	47	58	7,2	Tie columns as M3
X-9	47	58	7,2	Tie columns as M3
X-10	47	58	7,2	Tie columns as M3

Table 6.9: Resistance and displacements (rotation) at characteristic limit states [55].

	Damage limit			Maximum resistance			Design ultimate limit			Collapse		
Wall	d [mm]	F_h [kN]	Φ [%]	d [mm]	F_h [kN]	Φ [%]	d [mm]	F_h [kN]	Φ [%]	d [mm]	F_h [kN]	Φ [%]
X-1	2	3,90	0,27	36,61	5,18	4,94	-	-	-	36,61	5,18	4,94
X-2	1	2,08	0,13	4,28	3,19	0,57	16,12	2,47	2,16	30,00	1,79	4,02
X-3	1	2,24	0,13	3,21	3,15	0,43	9,92	2,49	1,33	12,53	1,62	1,68
X-4	1,5	2,21	0,20	4,61	3,26	0,61	29,55	2,80	3,92	50,26	2,34	6,67
X-5	1,5	1,89	0,20	5,19	3,34	0,69	20,12	2,51	2,68	60,97	1,72	8,11
X-6	1,5	4,11	0,20	9,18	5,00	1,22	12,18	3,81	1,61	30,01	2,39	3,97
X-7	1	4,41	0,16	5,02	5,79	0,80	6,75	4,31	1,08	30,01	1,52	4,79
X-8	1	4,24	0,16	3,95	6,47	0,64	3,95	6,47	0,64	3,95	6,47	0,64
X-9	0,75	4,10	0,12	5,37	6,61	0,84	5,37	6,61	0,84	5,37	6,61	0,84
X-10	1	4,19	0,16	4,42	6,32	0,71	8,00	4,58	1,28	30,01	2,83	4,80

Table 6.10: Resistance and displacement capacity of model walls [55].

	Damage limit		Design ultimate limit		Collapse	
Wall	F_h / $F_{h,max}$	Φ/ $\Phi_{H,max}$	F_h / $F_{h,max}$	Φ/ $\Phi_{H,max}$	F_h / $F_{h,max}$	Φ/ $\Phi_{H,max}$
X-1	0,75	0,05	1,00	1,00	1,00	1,00
X-2	0,65	0,23	0,78	3,76	0,56	7,00
X-3	0,71	0,31	0,79	3,09	0,51	3,91
X-4	0,68	0,33	0,86	6,41	0,72	10,89
X-5	0,57	0,29	0,75	3,88	0,51	11,75
X-6	0,82	0,16	0,76	1,33	0,48	3,27
X-7	0,76	0,20	0,74	1,35	0,26	5,98
X-8	0,66	0,25	1,00	1,00	1,00	1,00
X-9	0,62	0,14	1,00	1,00	1,00	1,00
X-10	0,66	0,23	0,72	1,81	0,45	6,79

As can be concluded on the basis of the observed failure mechanism of the plain masonry model walls, i.e. the walls without vertical confining elements, the shear resistance of the wall was greater than the flexural capacity of the walls' section at the foundation block because of the relatively high tensile strength but low compressive strength of AAC masonry (see Table 6.11). Consequently, the walls without vertical confining elements failed in bending (Figure 6.17). If confined, however, the flexural resistance is improved, so that the confined walls failed in shear. Since the tie–columns do not significantly improve the shear resistance of the walls (the area of concrete is small and the contribution of vertical reinforcement at shear is not significant), the confined

walls failed in shear with characteristic diagonal cracks developed in the walls.

Table 6.11: Failure mechanisms and resistance of the tested model walls [55].

Wall	Remark	Failure mode	$F_{h,max}$ [kN]
X-1	Tie columns as M1	shear	5,18
X-2	Plain masonry	flexural	3,19
X-3	Plain masonry	flexural	3,15
X-4	Plain masonry	flexural	3,26
X-5	Plain masonry	flexural	3,34
X-6	Tie columns as M1	shear	5,00
X-7	Tie columns as M3	flexural	5,79
X-8	Tie columns as M3	shear	6,47
X-9	Tie columns as M3	shear	6,61

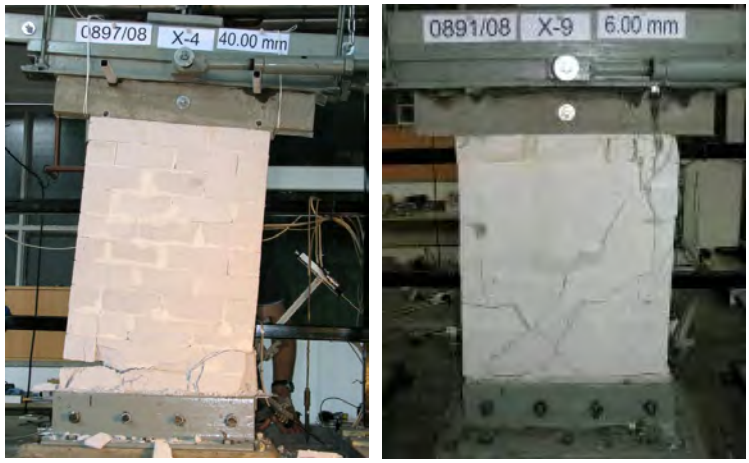

Figure 6.17: Flexural failure of a plain (left) and shear failure of a confined masonry wall (right) [55].

6.3.4.2.3 Diagonal compression test

Tensile strength of model masonry has been determined by means of diagonal compression test of wall prisms. The test set up is schematically presented in the Figure 6.18, where a typical specimen after the diagonal compression test is shown. The tensile strength is calculated by equation:

$$f_t = 0,45\frac{F_V}{A}, \tag{6.2}$$

where F_v is the maximum measure compressive force, and A is the cross–sectional area of the panel, determined by the length of the panel and the thickness of the wall.

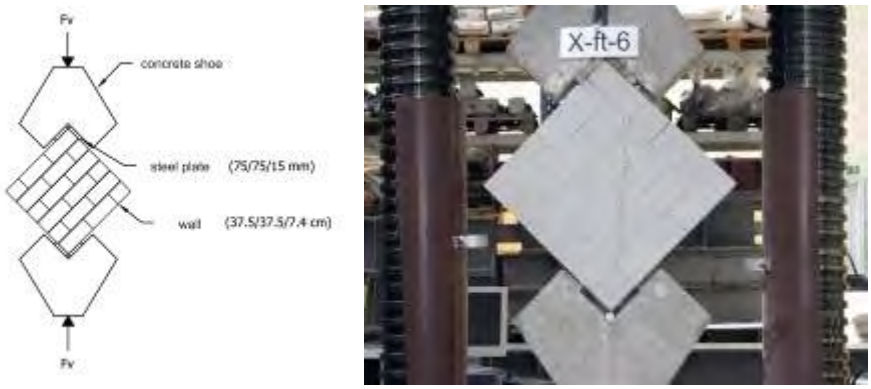

Figure 6.18: Test set–up for the diagonal compression test [55].

The conversion of the test results, obtained on the models, to the prototype in terms of resistance, displacement and energy dissipation capacity, is, fortunately not so complicated (see results in Table 6.12).

Table 6.12: Tensile strength of the model YTONG masonry [55].

Specimen	F [kN]	f_t [MPa]
X-ft-1	15,59	0,253
X-ft-2	12,32	0,200
X-ft-3	12,81	0,208
X-ft-4	17,30	0,281
X-ft-5	16,62	0,270
X-ft-6	17,23	0,279
Average	15,31	0,248

6.3.5 Shaking table and testing procedure

6.3.5.1 Shaking table

The shaking table, installed at Slovenian National Building and Civil Engineering Institute, is a simple testing facility, used for simulation of earthquake ground motion.

The facility consist of three main parts (shown in Figure 6.19):

- mechanical assemblage, consisting of a moveable steel box–type platform, on which the model is tested, and a steel box, fixed to the laboratory testing floor, which supports the moveable platform and controls the direction of motion. For this purpose, steel guide–rails with teflon slide–bearings, which prevent any lateral motion and rotation of the moveable platform, are fixed to the foundation box;
- hydraulic system which moves the platform, consisting of a two–way acting, programmable hydraulic actuator with a servo valve and hydraulic pump. On the one side, the actuator is fixed to a steel reaction walls, on the other, however, on the moveable platform;
- electronic system to control the intensity and time history of the motion of the platform

To drive the shaking table, a two–way acting, programmable actuator Schenk PL 160N of ± 160 kN force capacity at ± 125 mm stroke has been used. The dynamic capacity of the actuator in combination with the hydraulic pump used in this particular project made possible to model the frequency content and intensity of motion (accelerations) to fulfill the requirements of model similitude at the chosen technique of physical modelling and masses of models and the moveable part of the shaking table.

Figure 6.19: Shaking table with one of the models, ready for testing. Steel reaction wall and hydraulic actuator can be seen in front of the table [55].

The measurements, carried out within the calibration process of the facility, have indicates that the moveable platform is rigid enough to carry the bending effects, developed as a result of interaction between the model and the platform during the dynamic testing. Laboratory personal computer and home–made software have been used to control the shaking table motion.

6.3.5.2 Measurements and data acquisition

The models have been built of r.c. foundation slabs and transported from the construction site to the shaking table by means of laboratory crane. The foundation slabs have been fixed to the moveable platform by means of steel bolts.

The models have been instrumented with two sets of transducers (as can be seen in Figure 6.20):

- with accelerometers to measure the horizontal component of the absolute acceleration response in the direction of excitation. At each floor level, three instruments, in the middle and at both corners of the floor slab, have been fixed to floor structure at each floor level;
- with displacement transducers (LVDTs) to measure the absolute horizontal displacement response of the models in the direction of excitation, i.e. the displacements of the models with regard to the fixed testing floor. As in the case of the accelerometer, three displacement transducers, in the middle and at both corners of the floor slab, have been fixed to the floor at each floor level.

Whereas the accelerometers have been fixed directly to the floor slabs, the displacement transducers have been fixed to an outer rigid steel frame, which consisted of two columns and corresponding number of girders. The columns have been fixed to the testing floor. The calibration indicated that the effect of noise, transferred from the platform to the testing floor and to the displacement transducers' supporting frame did not affect the results of measurements to a great degree.

Besides, the motion of the shaking table has been controlled by measuring accelerations and displacements in the direction of motion.

Figure 6.20: Steel supporting frame to fix the displacement transducers during the testing of model M3 [55].

6.3.5.3 Modelling of the earthquake ground motion

N–S component of the Petrovac, Hotel Oliva ground acceleration record of the magnitude M_w = 6,9, Montenegro earthquake of April 15, 1979, with peak ground acceleration 0,43 g, has been used to drive the shaking table. The digitised acceleration time history data, the calculated displacement time history as well as the elastic response spectra, have been retrieved from the European Strong–Motion Database, ESM (see Figure 6.21).

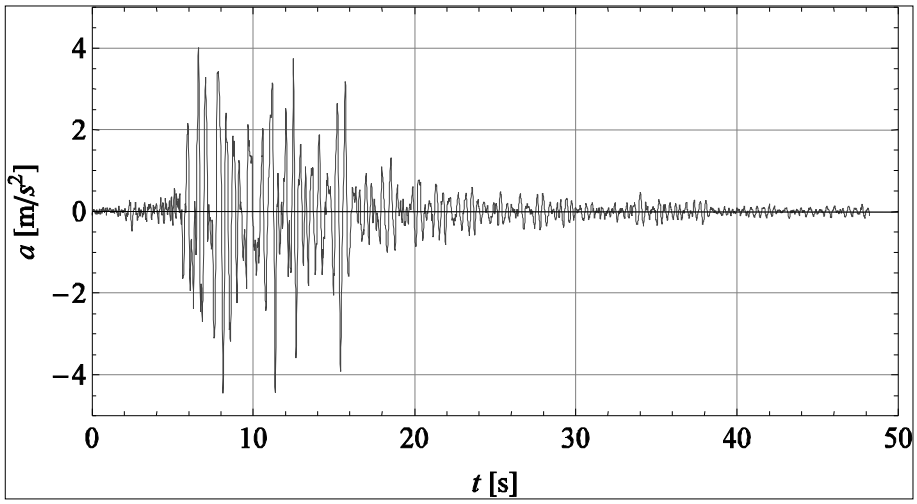

Figure 6.21: N-S component of the acceleration time history of the Montenegro, April 15, 1979 earthquake (Petrovac, Hotel Oliva record. Source: ESM database) [55].

In order to retrieve as many data as possible, the models are tested by subjecting them to a sequence of excitations with gradually increased intensity (see Table 6.13). In between, the propagation of eventual damage to models and changes in dynamic characteristics are followed. Each test run is named according to intensity of seismic excitation.

Table 6.13: Correlation between the maximum actual measured and programmed input displacements and accelerations of the shaking table motion during the testing of model M3 [55].

M3	Accelerations [ms^{-2}]		Ratio	Displacements [mm]		Ratio
	$a_{max,0}$	$a_{max,prg}$	$a_{max,0}/a_{max,prg}$	$d_{max,0}$	$d_{max,prg}$	$d_{max,0}/d_{max,prg}$
R005	0,24	0,22	1,11	0,61	0,57	1,07
R025	1,24	1,08	1,14	2,91	2,85	1,02
R050	2,45	2,16	1,13	5,75	5,70	1,01
R075	3,85	3,25	1,19	8,55	8,55	1,00
R100	5,02	4,33	1,16	11,37	11,40	1,00
R150	7,60	6,49	1,17	17,10	17,10	1,00
R200	10,10	8,65	1,17	21,99	22,81	0,96
R250	12,63	10,82	1,17	27,41	28,51	0,96

6.3.5.4 Testing procedures

All models have been tested with the same sequence of seismic excitations. In each testing phase:

- the model has been subjected to seismic excitation;
- by exciting free vibrations of the model with impact hammer, the first natural frequency has been determined;
- the models have been inspected and the damage to models' walls was identified and photographed.

The behaviour of models during shaking tests has been recorded with two video cameras.

6.4 Numerical analyses

6.4.1 Description of the modelling

Scale model M3 was modelled in SAP2000® using the following components:

1) link elements: to model the deformable zones, of walls parts between the openings and for the floor spandrels and parapets. They have a multi–linear elastoplastic behaviour;
2) rigid frame elements: were used to model the non-deformable and non-damageable areas, which are assumed infinitely stiff. For these elements a frame element with the definition of rigid length by rigid offset function of SAP2000® is defined;
3) shell elements for floor slabs.

In the next Figures 6.22 – 6.24 there are the modelling of each wall panels.

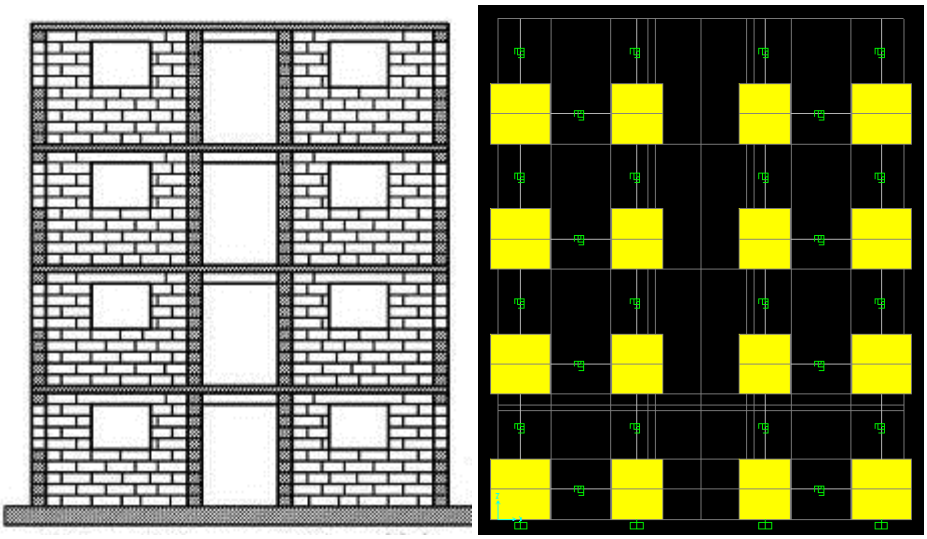

Figure 6.22: North wall and the model.

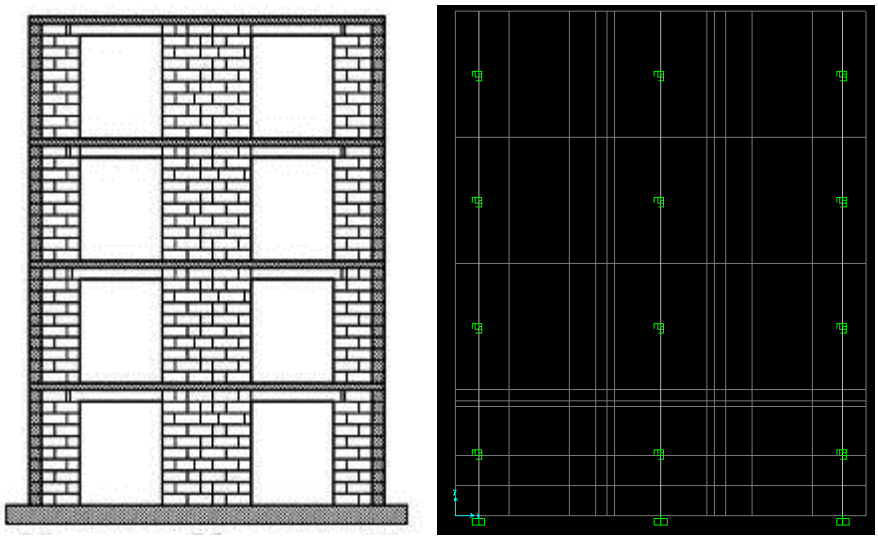

Figure 6.23: South side and the model.

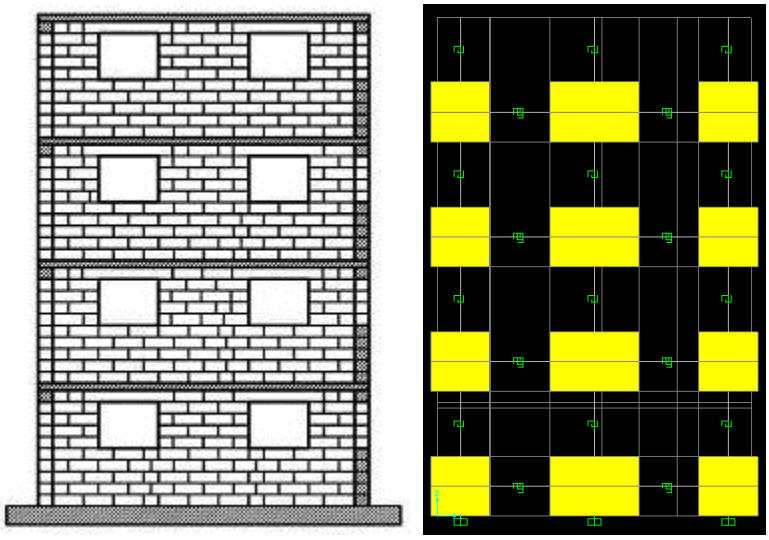

Figure 6.24: East and west side and their model.

For the floors modelling a shell element with 35 mm thickness has been assigned. The following Figure 6.25 shows a 3D view of the overall model obtained.

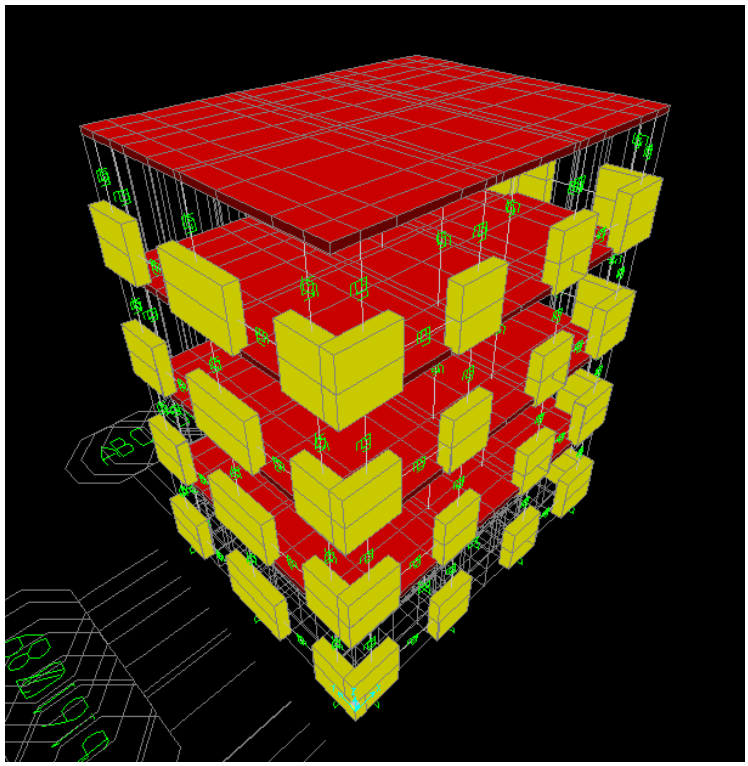

Figure 6.25: 3D view.

6.4.2 M3 model: geometric and mechanical properties

The principles exposed in previous paragraphs for the modelling of masonry are used to analyse the M3 model. In the Figure 6.26, the numbering of wall is schematised presented.

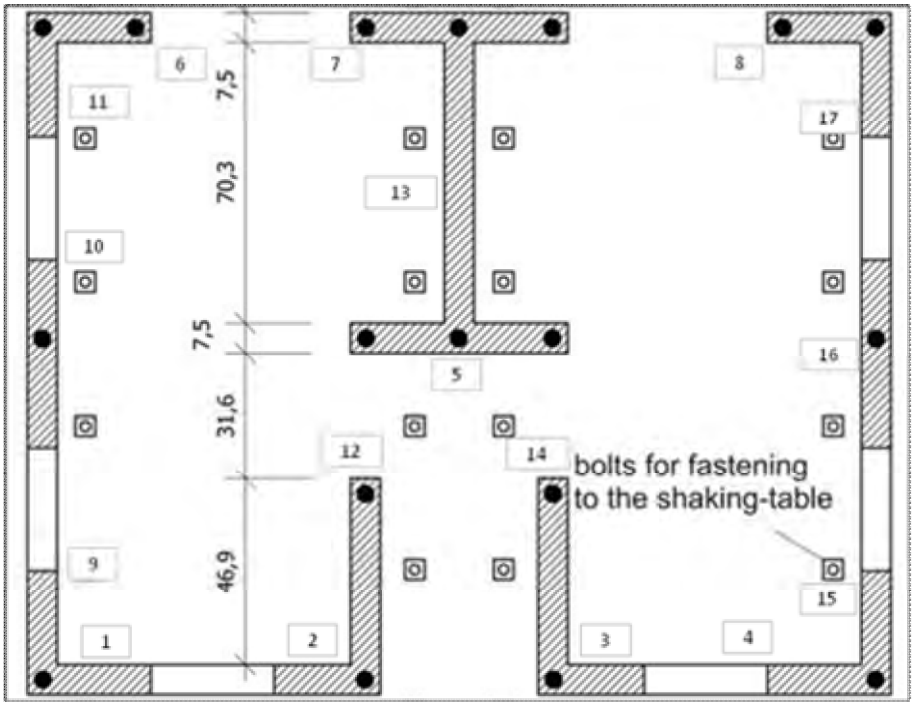

Figure 6.26: Numbering of masonry walls [55].

Geometrical and mechanical characteristics used in the following analyses are listed below.

1) Geometrical properties

t =	0,075	m	"thickness"
h_p =	0,3125	m	"height of the parapet"
h_b =	0,563	m	"height of the balcony"
h_w =	0,25	m	"height of the window"

2) Mechanical properties

f_c =	1490	kN/m²	=	1,49	MPa	"compressive strength"
f_t =	250	kN/m²	=	0,25	MPa	"shear strength (tensile)"
E =	7070000	kN/m²	=	7070	MPa	"modulus of elasticity"
G =	94000	kN/m²	=	94	MPa	"shear modulus"
ρ =	495,6	kg/m³				"density"
μ =	35					"ductility factor"

2) Load in plates

g_p =	2,56	kN/m²	"specific weight"

3) Load in roof

g_r =	2,86	kN/m²	"load on roof"

The reference generic masonry panel is shown in the Figure 6.27.

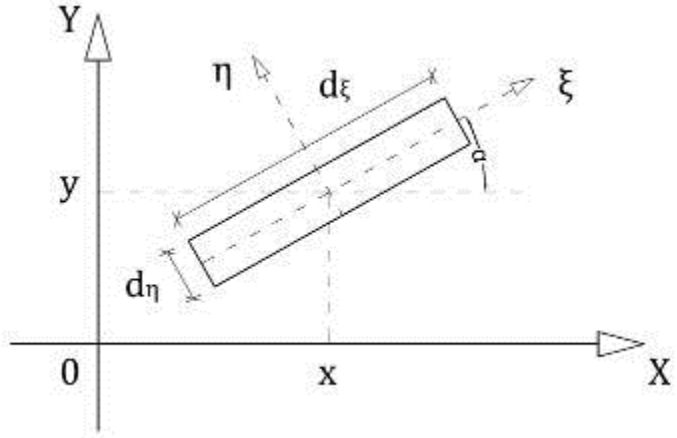

Figure 6.27: Reference system.

The following quantities are defined:

a) x and y are the center of gravity coordinates of the panel's cross section with respect to the global coordinate system;
b) ξ and η are the element's local axes exposed in the global coordinate system;
c) d_ξ and d_η are the width and thickness of the element, in ξ and η directions respectively;
d) h_ξ and h_η are the height of the element views in both directions, in direction ξ and η;
e) α is the clockwise positive angle from the horizontal to the ξ axis of the element.

For each masonry panel the vertical stress (σ) was computed by assuming simplified load distribution.

The stiffness in each of the local direction, is obtained using the following expressions:

$$K_{\xi} = \frac{G \cdot \left(d_{\xi} \cdot d_{\eta}\right)}{1{,}2 \cdot h_{\xi}} \cdot \frac{1}{1 + \frac{1}{1{,}2} \cdot \frac{G}{E} \cdot \left(\frac{h_{\xi}}{d_{\xi}}\right)}; \tag{6.3}$$

$$K_{\eta} = \frac{G \cdot \left(d_{\xi} \cdot d_{\eta}\right)}{1{,}2 \cdot h_{\eta}} \cdot \frac{1}{1 + \frac{1}{1{,}2} \cdot \frac{G}{E} \cdot \left(\frac{h_{\eta}}{d_{\eta}}\right)}. \tag{6.4}$$

In this situation diagonal shear cracking collapse for all masonry walls and in particular those in the first floor are predicted. The reason is due to the following aspects:

1) the sliding shear failure can be excluded (in particular in the first floor) because of the high value of normal vertical loads and the presence of mortar with good mechanical properties;
2) the flexural failure can be excluded due to the presence of the tie–column at the walls intersections, which constitute a very significant reinforcement and increase the ultimate moment resistance of the wall;
3) observation of the experimental response, where most walls failed in diagonal shear.

The shear strength for diagonal cracking in both direction was calculated using the following equation:

$$H_{\xi} = 0{,}9 \cdot d_{\xi} \cdot d_{\eta} \cdot \frac{f_t}{b} \cdot \sqrt{1 + \frac{\sigma}{f_t}}; \qquad H_{\eta} = 0{,}9 \cdot d_{\xi} \cdot d_{\eta} \cdot \frac{f_t}{b} \cdot \sqrt{1 + \frac{\sigma}{f_t}}. \tag{6.5}$$

Applying the previous relationships it's possible to obtain the results reported in the following Table 6.14 and Table 6.15.

Table 6.14: General data of the walls. Each floors.

i	x	y	d_ξ	d_η	h_ξ	h_η	α	K_ξ	K_η	b
[]	[m]	[m]	[m]	[m]	[m]	[m]	[rad]	[kN/mm]	[kN/mm]	[]
1	0,119	0,000	0,313	0,075	0,251	0,663	0,000	7,277	1,486	1,5
2	0,722	0,000	0,269	0,075	0,251	0,663	0,000	6,242	1,278	1,5
3	1,391	0,000	0,269	0,075	0,251	0,663	0,000	6,244	1,278	1,5
4	1,994	0,000	0,313	0,075	0,251	0,663	0,000	7,277	1,486	1,5
5	1,056	0,859	0,550	0,075	0,663	0,663	0,000	4,800	2,616	1,5
6	0,119	1,638	0,313	0,075	0,563	0,663	3,142	3,148	1,486	1,5
7	1,056	1,638	0,550	0,075	0,563	0,663	0,000	5,673	2,616	1,5
8	1,994	1,638	0,313	0,075	0,563	0,663	3,142	3,148	1,486	1,5
9	0,000	0,156	0,238	0,075	0,251	0,663	-1,571	5,502	1,130	1,5
10	0,000	0,819	0,469	0,075	0,251	0,663	-1,571	10,958	2,229	1,5
11	0,000	1,481	0,238	0,075	0,251	0,663	-1,571	5,502	1,130	1,5
12	0,819	0,272	0,469	0,075	0,563	0,663	1,571	4,815	2,230	1,5
13	1,056	1,248	0,703	0,075	0,663	0,663	-1,571	6,174	3,344	1,5
14	1,294	0,272	0,469	0,075	0,563	0,663	1,571	4,815	2,230	1,5
15	2,113	0,156	0,238	0,075	0,251	0,663	1,571	5,502	1,130	1,5
16	2,113	0,819	0,469	0,075	0,251	0,663	1,571	10,958	2,229	1,5
17	2,113	1,481	0,238	0,075	0,251	0,663	1,571	5,502	1,130	1,5

Table 6.15: Analysis of ultimate shear ultimate for diagonal cracking of the piers on each floor.

i	σ_1	σ_2	σ_3	σ_4	$H_{\xi,1}$	$H_{\eta,1}$	$H_{\xi,2}$	$H_{\eta,2}$	$H_{\xi,3}$	$H_{\eta,3}$	$H_{\xi,4}$	$H_{\eta,4}$
[]	[MPa]	[MPa]	[MPa]	[MPa]	[kN]	[kN]	[kN]	[kN]	[kN]	[kN]	[kN]	[kN]
1	0,062	0,046	0,031	0,016	3,925	0,157	3,828	0,119	3,728	0,081	3,625	0,041
2	0,074	0,056	0,038	0,019	3,443	0,161	3,344	0,123	3,242	0,083	3,136	0,043
3	0,074	0,056	0,038	0,019	3,444	0,161	3,345	0,123	3,243	0,083	3,137	0,043
4	0,062	0,046	0,031	0,016	3,925	0,157	3,828	0,119	3,728	0,081	3,625	0,041
5	0,110	0,083	0,057	0,030	7,428	0,477	7,146	0,368	6,851	0,254	6,544	0,136
6	0,081	0,061	0,041	0,022	4,045	0,203	3,923	0,156	3,796	0,107	3,665	0,057
7	0,081	0,061	0,041	0,022	7,120	0,358	6,904	0,274	6,681	0,188	6,450	0,100
8	0,081	0,061	0,041	0,022	4,045	0,203	3,923	0,156	3,796	0,107	3,665	0,057
9	0,083	0,062	0,042	0,021	3,083	0,158	2,987	0,121	2,887	0,082	2,784	0,043
10	0,088	0,066	0,044	0,023	6,127	0,328	5,929	0,251	5,722	0,171	5,507	0,089
11	0,083	0,062	0,042	0,021	3,083	0,158	2,987	0,121	2,887	0,082	2,784	0,043
12	0,136	0,103	0,070	0,037	6,551	0,491	6,263	0,381	5,963	0,264	5,646	0,142
13	0,068	0,051	0,035	0,018	8,915	0,385	8,681	0,294	8,439	0,202	8,191	0,106
14	0,136	0,103	0,070	0,037	6,551	0,491	6,263	0,381	5,963	0,264	5,646	0,142
15	0,083	0,062	0,042	0,021	3,083	0,158	2,987	0,121	2,887	0,082	2,784	0,043
16	0,088	0,066	0,044	0,023	6,128	0,328	5,929	0,251	5,722	0,171	5,507	0,089
17	0,083	0,062	0,042	0,021	3,083	0,158	2,987	0,121	2,887	0,082	2,784	0,043

To define element parameters included in the SAP2000® model, the following quantities of each macro elements are useful, as shows in the following Table 6.16 and Table 6.17:

- area of cross section: $A = d_\eta \cdot d_\xi$; (6.6)
- module of inertia in the direction of the storey axis: $I_\xi = \frac{d_\eta \cdot d_\xi^3}{12}$; (6.7)
- normal compressive force at the base: $N = \sigma \cdot A$; (6.8)
- location of the neutral axis: $x_c = \frac{N}{\psi \cdot d_\eta \cdot 0{,}85 \cdot f_c}$; (6.9)
- curvature at the ultimate moment: $\chi_y = \frac{\varepsilon_{mu}}{x_c}$. (6.10)

Table 6.16: Analysis of axial force and curvature at first and second floors.

i	A_1	N_1	x_{c1}	χ_{y1}	A_2	N_2	x_{c2}	χ_{y2}
[]	[m^2]	[N]	[mm]	[1/mm]	[m^2]	[N]	[mm]	[1/mm]
1	0,0234	1445,68	15,22	0,00023	0,0234	1086,71	11,44	0,00031
2	0,0202	1497,91	15,77	0,00022	0,0202	1127,03	11,87	0,00029
3	0,0202	1498,22	15,77	0,00022	0,0202	1127,27	11,87	0,00029
4	0,0234	1445,68	15,22	0,00023	0,0234	1086,71	11,44	0,00031
5	0,0413	4551,07	47,91	0,00007	0,0413	3441,66	36,23	0,00010
6	0,0234	1898,21	19,98	0,00018	0,0234	1434,77	15,10	0,00023
7	0,0413	3340,85	35,17	0,00010	0,0413	2525,19	26,58	0,00013
8	0,0234	1898,21	19,98	0,00018	0,0234	1434,77	15,10	0,00023
9	0,0178	1475,60	15,53	0,00023	0,0178	1111,13	11,70	0,00030
10	0,0352	3079,23	32,42	0,00011	0,0352	2318,40	24,41	0,00014
11	0,0178	1475,53	15,53	0,00023	0,0178	1111,26	11,70	0,00030
12	0,0352	4772,83	50,25	0,00007	0,0352	3610,02	38,01	0,00009
13	0,0527	3562,63	37,51	0,00009	0,0527	2692,56	28,35	0,00012
14	0,0352	4772,65	50,25	0,00007	0,0352	3609,92	38,00	0,00009
15	0,0178	1475,89	15,54	0,00023	0,0178	1111,35	11,70	0,00030
16	0,0352	3079,85	32,42	0,00011	0,0352	2318,87	24,41	0,00014
17	0,0178	1475,82	15,54	0,00023	0,0178	1111,49	11,70	0,00030

Table 6.17: Analysis of axial force and curvature at third and fourth floors.

i	A_3	N_3	x_{c3}	χ_{y3}	A_4	N_4	x_{c4}	χ_{y4}
[]	[m²]	[N]	[mm]	[1/mm]	[m²]	[N]	[mm]	[1/mm]
1	0,0234	727,80	7,66	0,00046	0,0234	368,83	3,88	0,00090
2	0,0202	756,20	7,96	0,00044	0,0202	385,33	4,06	0,00086
3	0,0202	756,36	7,96	0,00044	0,0202	385,41	4,06	0,00086
4	0,0234	727,80	7,66	0,00046	0,0234	368,83	3,88	0,00090
5	0,0413	2331,69	24,55	0,00014	0,0413	1222,26	12,87	0,00027
6	0,0234	971,23	10,22	0,00034	0,0234	507,79	5,35	0,00065
7	0,0413	1709,37	18,00	0,00019	0,0413	893,71	9,41	0,00037
8	0,0234	971,23	10,22	0,00034	0,0234	507,79	5,35	0,00065
9	0,0178	746,90	7,86	0,00045	0,0178	382,64	4,03	0,00087
10	0,0352	1557,42	16,40	0,00021	0,0352	796,27	8,38	0,00042
11	0,0178	746,86	7,86	0,00045	0,0178	382,64	4,03	0,00087
12	0,0352	2447,71	25,77	0,00014	0,0352	1284,96	13,53	0,00026
13	0,0527	1822,29	19,18	0,00018	0,0527	952,17	10,02	0,00035
14	0,0352	2447,63	25,77	0,00014	0,0352	1284,92	13,53	0,00026
15	0,0178	747,05	7,86	0,00045	0,0178	382,72	4,03	0,00087
16	0,0352	1557,74	16,40	0,00021	0,0352	796,44	8,38	0,00042
17	0,0178	747,01	7,86	0,00045	0,0178	382,72	4,03	0,00087

Assuming elastic-perfectly plastic behaviour for masonry panels and knowing the shear resistance V_{ds}, the stiffness ($K_{\xi} = k$) and the value of ductility of the panel (δ_y), the following displacements can be obtained:

- elastic limit displacement: $\delta_y = \frac{V_{ds}}{k}$; (6.11)
- ultimate displacement: $\delta_u = \mu \cdot \delta_y$. (6.12)

In the simplified model the resistance of wall panels out of their plan is neglected and only seismic excitation in the X direction is considered.

The panels perpendicular to this seismic load direction (or those disposed along y) will be subject to less stress in their plan that will be due to the eccentricity between the mass center of gravity of each floor and the stiffness center of gravity. The elements arranged along Y, in the case of an earthquake in the X direction, should be verified for action perpendicular to their plan, to prevent the occurrence of local collapse mechanisms. The results are shown in Tables 6.18 – 6.21.

Table 6.18: First floor. Diagonal shear parameters.

i	V_{ds}	k	δ_y	δ_u
[]	[kN]	[N/mm]	[mm]	[mm]
1	3,925	7277,282	0,539	18,879
2	3,443	6241,741	0,552	19,307
3	3,444	6244,108	0,552	19,306
4	3,925	7277,282	0,539	18,879
5	7,428	4800,191	1,548	54,163
6	4,045	3147,789	1,285	44,978
7	7,120	5673,476	1,255	43,921
8	4,045	3147,789	1,285	44,978
9	3,083	5502,290	0,560	19,611
10	6,127	10957,785	0,559	19,571
11	3,083	5502,290	0,560	19,610
12	6,551	4815,064	1,361	47,620
13	8,915	6174,301	1,444	50,535
14	6,551	4815,064	1,361	47,619
15	3,083	5502,290	0,560	19,611
16	6,128	10957,785	0,559	19,572
17	3,083	5502,290	0,560	19,611

Table 6.19: Second floor. Diagonal shear parameters.

i	V_{ds}	k	δ_y	δ_u
[]	[kN]	[N/mm]	[mm]	[mm]
1	3,828	7277,282	0,526	18,410
2	3,344	6241,741	0,536	18,751
3	3,345	6244,108	0,536	18,750
4	3,828	7277,282	0,526	18,410
5	7,146	4800,191	1,489	52,103
6	3,923	3147,789	1,246	43,614
7	6,904	5673,476	1,217	42,589
8	3,923	3147,789	1,246	43,614
9	2,987	5502,290	0,543	18,998
10	5,929	10960,138	0,541	18,933
11	2,987	5502,290	0,543	18,998
12	6,263	4814,004	1,301	45,534
13	8,681	6175,196	1,406	49,204
14	6,263	4814,004	1,301	45,534
15	2,987	5502,290	0,543	18,999
16	5,929	10960,138	0,541	18,934
17	2,987	5502,290	0,543	18,999

Table 6.20: Third floor. Diagonal shear parameters.

i	V_{ds}	k	δ_y	δ_u
[]	[kN]	[N/mm]	[mm]	[mm]
1	3,728	7277,282	0,512	17,928
2	3,242	6241,741	0,519	18,178
3	3,243	6244,108	0,519	18,178
4	3,728	7277,282	0,512	17,928
5	6,851	4800,191	1,427	49,956
6	3,796	3147,789	1,206	42,205
7	6,681	5673,476	1,178	41,213
8	3,796	3147,789	1,206	42,205
9	2,887	5502,290	0,525	18,366
10	5,722	10960,138	0,522	18,273
11	2,887	5502,290	0,525	18,366
12	5,963	4815,064	1,238	43,346
13	8,439	6174,301	1,367	47,837
14	5,963	4815,064	1,238	43,346
15	2,887	5502,290	0,525	18,366
16	5,722	10960,138	0,522	18,273
17	2,887	5502,290	0,525	18,366

Table 6.21: Fourth floor. Diagonal shear parameters.

i	V_{ds}	k	δ_y	δ_u
[]	[kN]	[N/mm]	[mm]	[mm]
1	3,625	7277,282	0,498	17,432
2	3,136	6241,741	0,502	17,587
3	3,137	6244,108	0,502	17,587
4	3,625	7277,282	0,498	17,432
5	6,544	4800,191	1,363	47,714
6	3,665	3147,789	1,164	40,749
7	6,450	5673,476	1,137	39,791
8	3,665	3147,789	1,164	40,749
9	2,784	5502,290	0,506	17,711
10	5,507	10957,785	0,503	17,588
11	2,784	5502,290	0,506	17,711
12	5,646	4815,064	1,173	41,042
13	8,191	6174,301	1,327	46,429
14	5,646	4815,064	1,173	41,042
15	2,784	5502,290	0,506	17,711
16	5,507	10957,785	0,503	17,589
17	2,784	5502,290	0,506	17,711

As regards the axial behaviour of the link elements a linear elastic behaviour is assumed. In particular, in SAP2000®, the following values of normal force (N) and its axial displacement (ΔL), obtained by the classical relationship (see Table 6.22 for the results) (6.13) are needed.

$$\varepsilon = \frac{\Delta L}{L} = \frac{N}{EA}. \tag{6.13}$$

Table 6.22: All floors. Axial behaviour.

i	EA	N	L	ε	Δ
[]	[kN]	[kN]	[mm]	[]	[mm]
1	165703,1	100000	250,50	0,60	151,17
2	142478,2	100000	250,50	0,70	175,82
3	142531,2	100000	250,50	0,70	175,75
4	165703,1	100000	250,50	0,60	151,17
5	291637,5	100000	662,50	0,34	227,17
6	165703,1	100000	563,00	0,60	339,76
7	291637,5	100000	563,00	0,34	193,05
8	165703,1	100000	563,00	0,60	339,76
9	125934,4	100000	250,50	0,79	198,91
10	248528,2	100000	250,50	0,40	100,79
11	125934,4	100000	250,50	0,79	198,91
12	248581,2	100000	563,00	0,40	226,49
13	372818,8	100000	662,50	0,27	177,70
14	248581,2	100000	563,00	0,40	226,49
15	125934,4	100000	250,50	0,79	198,91
16	248528,2	100000	250,50	0,40	100,79
17	125934,4	100000	250,50	0,79	198,91

As regards rotational behaviour of the section, the rotational stiffness is implicitly taken into account in the shear stiffness and a small numerical value was used in order to avoid singularity for the numerical procedure. Elastic rotational behaviour is assumed.

Finally, in the following Table 6.23 the masses and weights of each wall are presented:

- masonry mass for unit of volume: ρ;
- mass: $m = d_{\xi} \cdot d_{\eta} \cdot h_{\xi} \cdot \rho$; (6.14)
- weight: $W = m \cdot g$. (6.15)

Table 6.23: All floors. Mass and weight of the wall.

i	d_{ξ}	d_{η}	h_{ξ}	m	W
[]	[m]	[m]	[m]	[kg]	[N]
1	0,313	0,075	0,251	2,91	28,54
2	0,269	0,075	0,251	2,50	24,54
3	0,269	0,075	0,251	2,50	24,55
4	0,313	0,075	0,251	2,91	28,54
5	0,550	0,075	0,663	13,54	132,86
6	0,313	0,075	0,563	6,54	64,15
7	0,550	0,075	0,563	11,51	112,91
8	0,313	0,075	0,563	6,54	64,15
9	0,238	0,075	0,251	2,21	21,69
10	0,469	0,075	0,251	4,36	42,81
11	0,238	0,075	0,251	2,21	21,69
12	0,469	0,075	0,563	9,81	96,24
13	0,703	0,075	0,663	17,31	169,85
14	0,469	0,075	0,563	9,81	96,24
15	0,238	0,075	0,251	2,21	21,69
16	0,469	0,075	0,251	4,36	42,81
17	0,238	0,075	0,251	2,21	21,69

6.4.3 Structural model for N2 method

For the implementation of the N2 method the capacity curve of the structure must be obtained. This curve shows the base shear as a function of control point displacement, usually placed at the center of gravity at the top of the structure. In the finite element program SAP2000® was possible to model the structure. In particular, all the piers and the spandrels were considered to be deformable and they were modelled using the link element described above. The floors, however, were modelled using finite element with two dimensional shell. The floors, therefore, were modelled as a full slab. In the following analysis the behaviour of the structure and the final results of the analysis are highly dependent on the floor stiffness. For this reason, hereafter, an analysis with both deformable slab and infinitely rigid slab are performed. During the run of the pushover test, the computer program represents the evolution of the base shear as a function of the displacement of the control node (Figure 6.28).

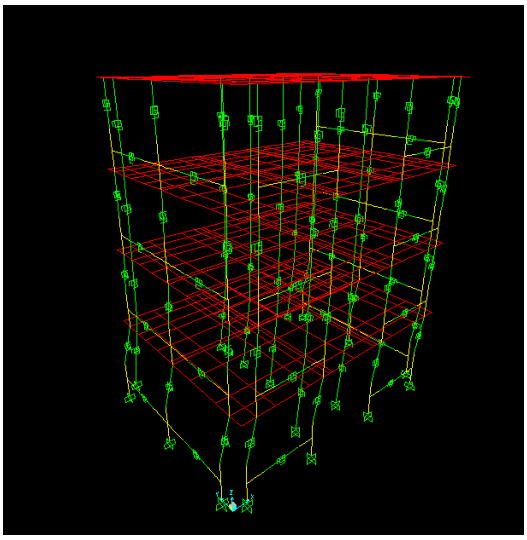

Figure 6.28: Deformation of the structure at a generic step load pushover analysis.

In this case, the pushover analysis were executed automatically in SAP2000® in displacement control. In particular, the load combination of pushover

analysis is nonlinear type and includes the performance of different load step maximum displacement of the control node. The load case of pushover starts by applying the vertical loads due to weight of only elements (frame and rigid link element) and the floor. At each loading step of this analysis it was possible to control the amount of shear and other stress characteristics in the link element (Figure 6.29 and Figure 6.30). In this way it is also possible to understand what elements are collapsed and in which range they are.

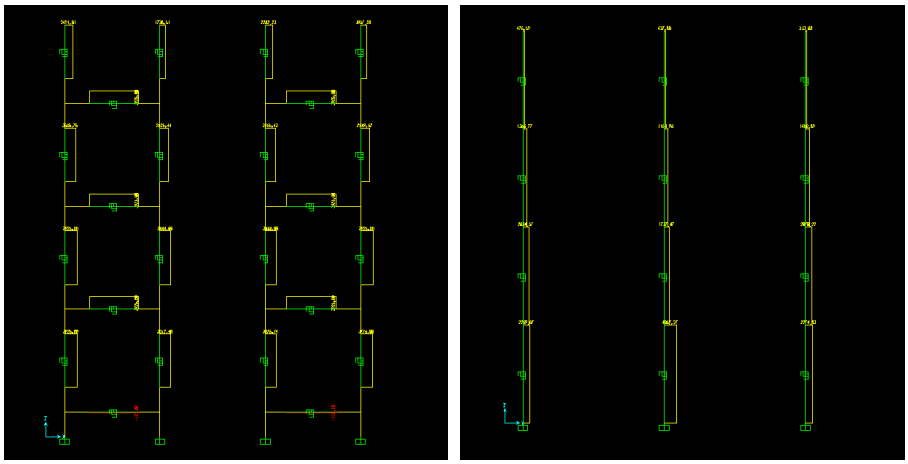

Figure 6.29: Shear in the link at Step 8 of the pushover with linear forces. North elevation (on the left) and south elevation (on the right).

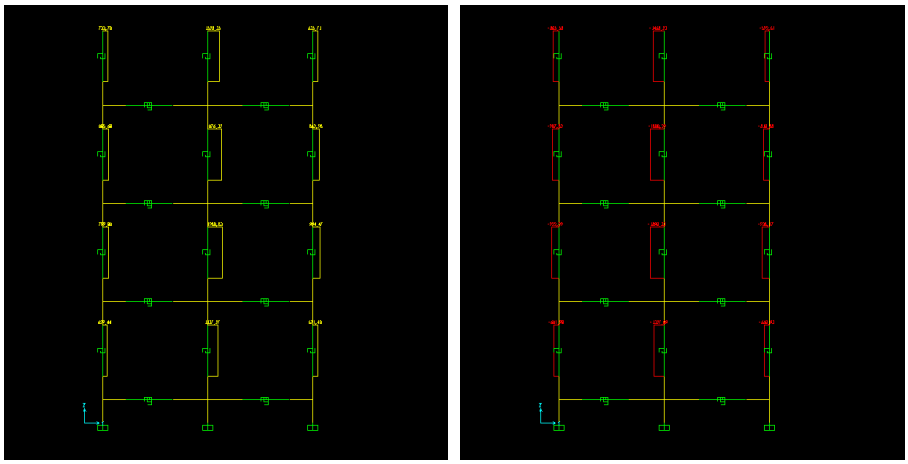

Figure 6.30: Shear in the link at Step 8 of the pushover with linear forces. East elevation (on the left) and west elevation (on the right).

6.4.4 Structural model for POR method

In this case, has been done a pushover test using a POR modelling and with the piers failure possibility only at the first floor of the building. Therefore, a pushover analysis of a structure with solely the first floor of M3 model must be run, as shown in the Figure 6.31.

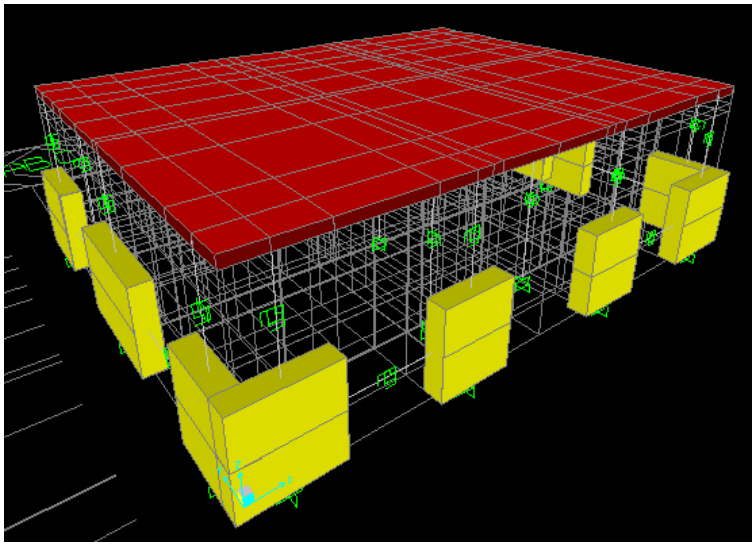

Figure 6.31: Structure used for the pushover analysis with the POR method.

The methods used to model the structure are the same as in the previous paragraph and provide, therefore, the use of a frame modelling of the structure that consists of equivalent frame with deformable and rigid parts. Unlike the previous case, however, this time is used only a portion of the structure, that of the first floor. Therefore, only piers and spandrels on the first floor can be damaged, while the rest of the structure above is preserved elastic during the test and can be approximated to a rigid body. In this model, then, interlocking bonds are assigned to the base of each piers and the control node of displacement is placed in the center of gravity of the first floor.

6.4.5 Application of N2 method

6.4.5.1 Data

For application of the N2 method are adopted the principles set out in the Fajfar's work [48]. This method is useful tool because it is based on a comparison of the structure's capacity curve with the demand curve.

In the following, the pushover analysis and subsequent implementation of the N2 method are performed for different values of the seismic demand in terms of spectral peak ground acceleration value and for different values of the floor's stiffness. In particular in case of flexible floor is considered a 35 mm concrete slab and run different analysis of the N2 method with three different values of the seismic demand. Later additional analysis is performed in the case of rigid floor, modelled using shell elements made of rigid material (with very large Young's modulus) in SAP2000®.

For the structure under investigation are known the following floor masses:

m_1 =	1141	kg	"first floor mass"
m_2 =	1141	kg	"second floor mass"
m_3 =	1141	kg	"third floor mass"
m_4 =	1165	kg	"fourth floor mass"

The fundamental period of vibration of the first modal shape, obtained from structure modal analysis of the structure is:

T_1 =	0,13	s	"period of the first modal form"

6.4.5.2 Seismic load and spectrum

Proceeding in a simplified way, the seismic demand can be defined by using spectrum provided in Eurocode 8. In particular, this rule provides possibility of using two types of spectra with the following values (Table 6.24 and Table 6.25).

Table 6.24: Values of type 1 spectrum [31].

Ground type	S	T_B(s)	T_C(s)	T_D(s)
A	1,0	0,15	0,4	2,0
B	1,2	0,15	0,5	2,0
C	1,15	0,20	0,6	2,0
D	1,35	0,20	0,8	2,0
E	1,4	0,15	0,5	2,0

Table 6.25: Values of type 2 spectrum [31].

Ground type	S	T_B(s)	T_C(s)	T_D(s)
A	1,0	0,05	0,25	1,2
B	1,35	0,05	0,25	1,2
C	1,5	0,10	0,25	1,2
D	1,8	0,10	0,30	1,2
E	1,6	0,05	0,25	1,2

In this case the Type 1 spectrum is used. Assuming a soil type B, the parameters of the spectrum can be defined. However, a scale factor must be taken into account in the case of model M3. In particular, for the periods of vibration, this factor is:

$$T_{scale} = 2 .$$

Ultimately it is necessary to halve the original values in the tables above and the new values are shown in the following Table 6.26 and Table 6.27.

Table 6.26: Scaled values of type 1 spectrum.

Soil	S	T_B [s]	T_C [s]	T_D [s]
A	1,00	0,08	0,20	1,00
B	1,20	0,08	0,25	1,00
C	1,15	0,10	0,30	1,00
D	1,35	0,10	0,40	1,00
E	1,40	0,08	0,25	1,00

Table 6.27: Scaled values of type 2 spectrum.

Soil	S	T_B [s]	T_C [s]	T_D [s]
A	1,00	0,03	0,13	0,60
B	1,35	0,03	0,13	0,60
C	1,50	0,05	0,13	0,60
D	1,80	0,05	0,15	0,60
E	1,80	0,03	0,13	0,60

In this case, the parameters used are:

S = 1,20 "soil type factor"

T_B = 0,08 s "start period of the trait with constant spectral acceleration"

T_C = 0,25 s "start period of the trait with constant spectral speed"

T_D = 1,00 s "start period of the trait with constant spectral displacement"

Assuming a typical value of the coefficient of viscous damping:

$$\xi = 5\%, \tag{6.16}$$

the following reduction factor can be defined:

$$\eta = \sqrt{\frac{10}{5+\xi(\%)}} = 1{,}00 \geq 0{,}55. \tag{6.17}$$

The analysis with the N2 method was performed for three values of peak ground acceleration:

a) $a_g = 0{,}25g$ "max value in Slovenia";

b) $a_g = 0{,}50g$ "exceptionally high";

c) $a_g = 1{,}29g$ "maximum value during the test on the M3 model".

The response spectra can be calculated for traits by using the following reports:

Trait 1: $$S_{ae}(T) = a_g \cdot S \cdot \left[1 + \frac{T}{T_B} \cdot (\eta \cdot 2{,}5) - 1\right] \quad \text{if:} \quad 0 \le T \le T_B ; \tag{6.18}$$

Trait 2: $$S_{ae}(T) = a_g \cdot S \cdot \eta \cdot 2{,}5 \quad \text{if:} \quad T_B \le T \le T_C ; \tag{6.19}$$

Trait 3: $$S_{ae}(T) = a_g \cdot S \cdot \eta \cdot 2{,}5 \cdot \left(\frac{T_C}{T}\right) \quad \text{if:} \quad T_C \le T \le T_D ; \tag{6.20}$$

Trait 4: $$S_{ae}(T) = a_g \cdot S \cdot \eta \cdot 2{,}5 \cdot \left(\frac{T_C \cdot T_D}{T^2}\right) \quad \text{if:} \quad T_D \le T . \tag{6.21}$$

The spectral displacement is obtained as:

$$S_{de}(T) = S_{ae}(T) \cdot \left[\frac{T}{2 \cdot \pi}\right]^2 . \tag{6.22}$$

By varying the three PGAs the following response spectra in Figures 6.32 – 6.34 are obtained.

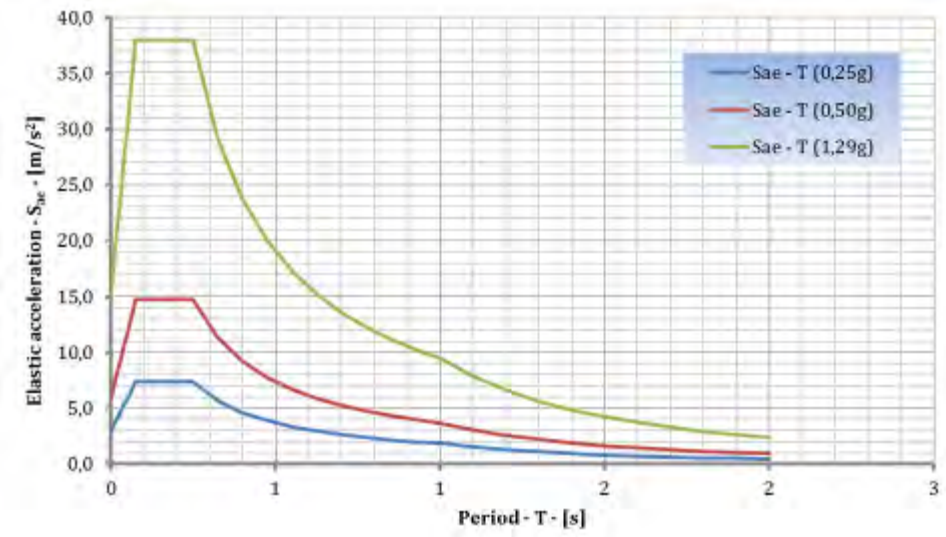

Figure 6.32: Elastic acceleration spectrum.

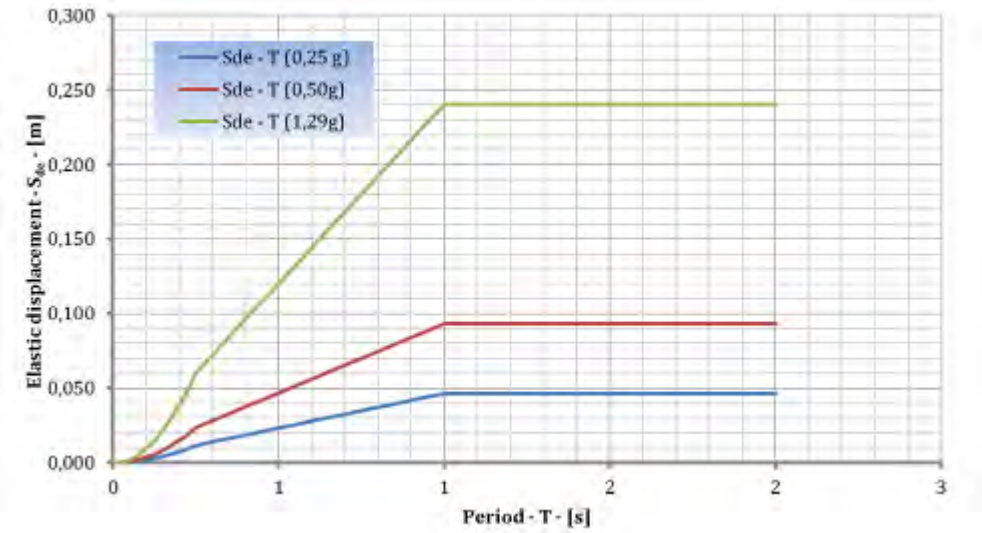

Figure 6.33: Elastic displacement spectrum.

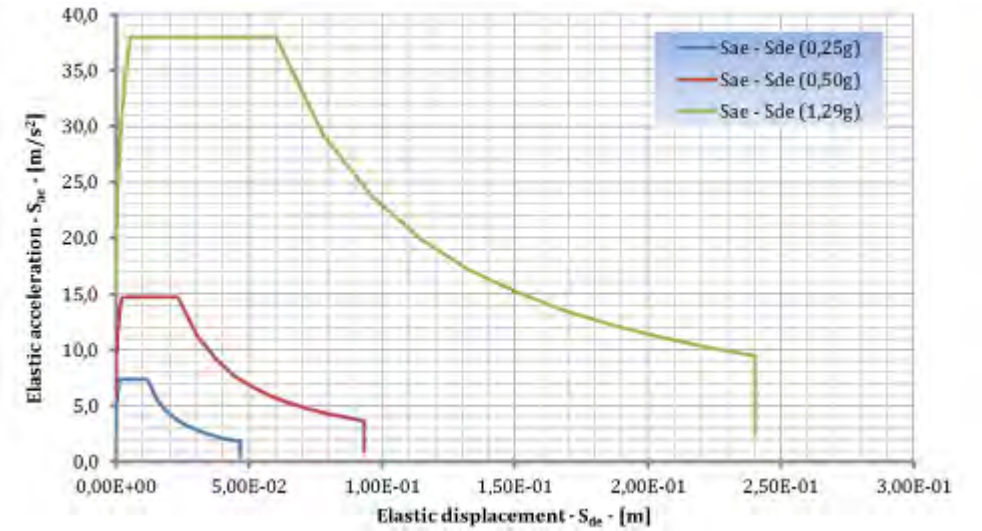

Figure 6.34: Elastic spectrum in AD format.

6.4.5.3 Pushover analysis

From the pushover analysis executed with uniform and linear distributions the following capacity curves in Figures 6.35 – 6.38 were obtained.

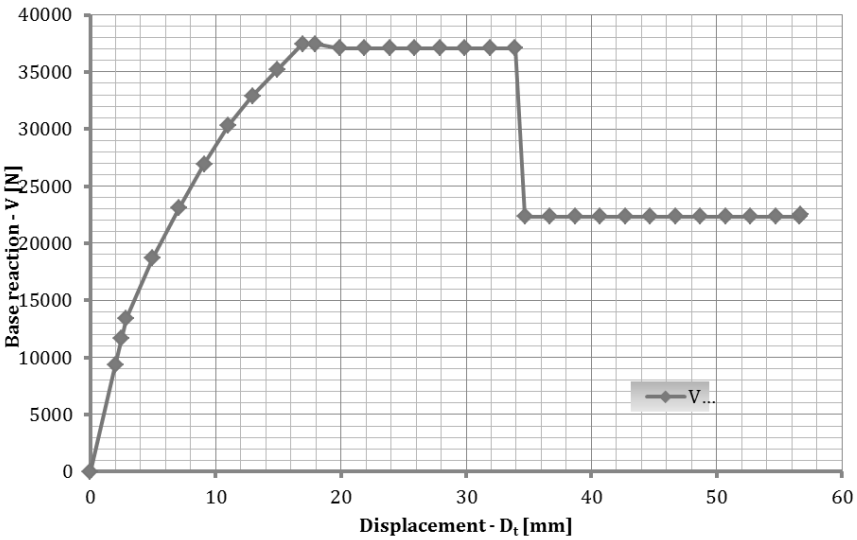

Figure 6.35: Pushover curve. N2 Method. Constant forces.

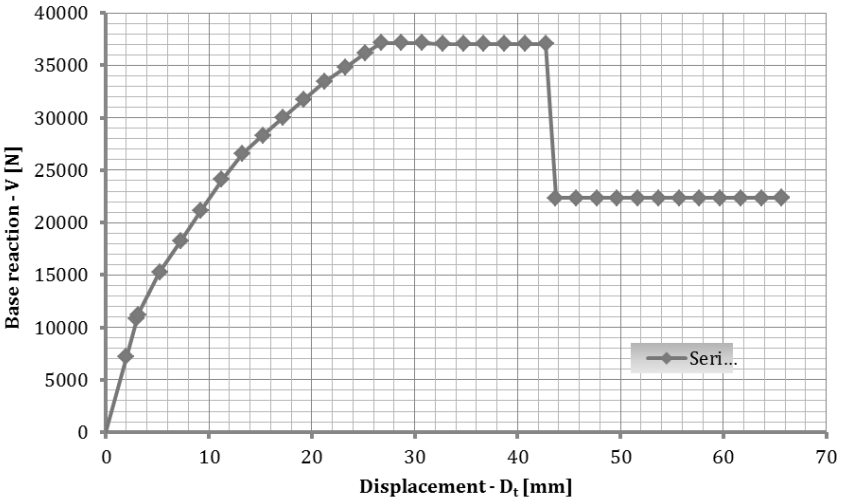

Figure 6.36: Pushover curve. N2 Method. Linear forces.

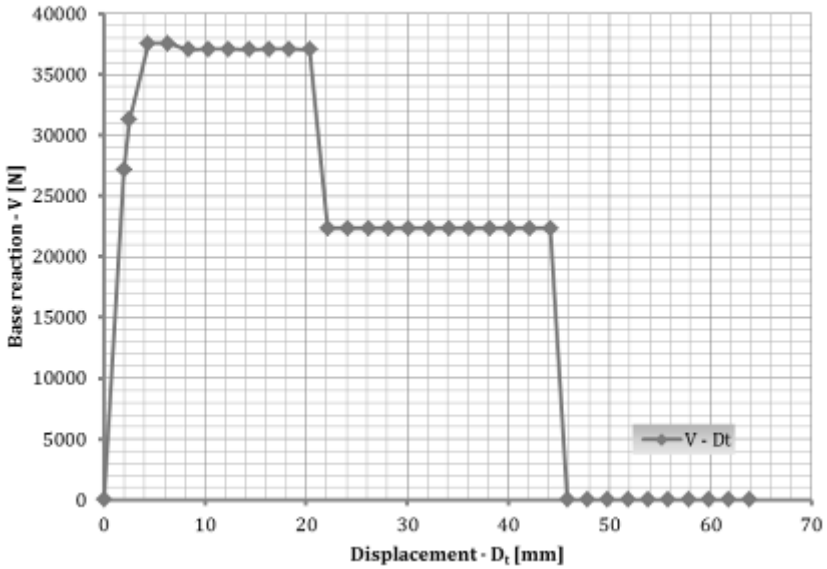

Figure 6.37: Pushover curve. N2 Method. Linear force. Rigid floors.

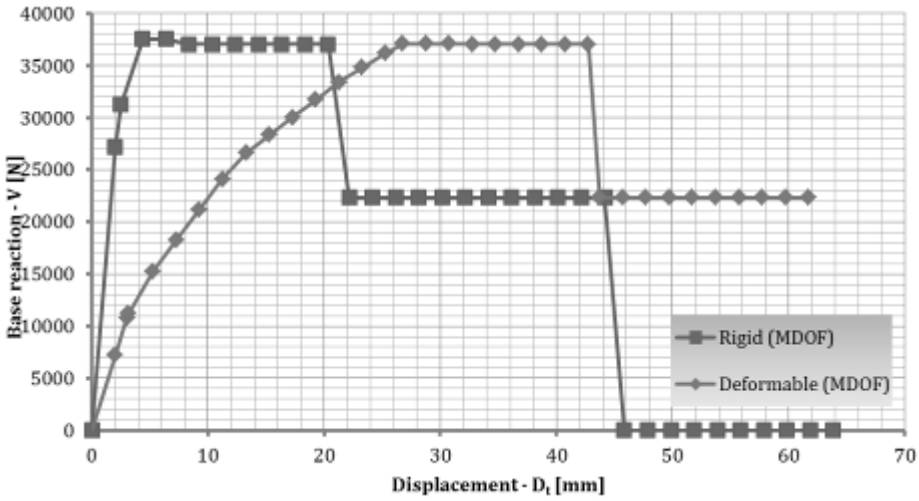

Figure 6.38: Comparison between flexible and rigid floors.

Assuming linear distribution of forces:

Φ_1 =	0,25	"first floor"
Φ_2 =	0,50	"second floor"
Φ_3 =	0,75	"third floor"
Φ_4 =	1,00	"fourth floor"

Using these the forces that are applied to different floors are:

$$\{P\} = [M]\{\Phi\} \quad \text{->} \quad P_i = m_i \cdot \Phi_i \quad \text{i = 1,2,3,4.} \tag{6.23}$$

6.4.5.4 Transformation to a SDOF system

At this point, to obtain the capacity curve and compare it with the demand curve (in the previous spectrum plan ADRS) is necessary to move from the real system MDOF to SDOF ideal system. SDOF system will have a mass equal to:

$$m^* = \sum_i m_i \cdot \Phi_i = 2876{,}5kg\,. \tag{6.24}$$

The general amounts of the SDOF system (force or displacement) can be obtained by dividing the relevant amount of the MDOF system to a scale factor:

$$Q^* = \frac{Q}{\Gamma}\,. \tag{6.25}$$

The transition factor is:

$$\Gamma = \frac{m^*}{\sum_i m_i \cdot \Phi_i^2} = 1{,}33\,. \tag{6.26}$$

By scaling forces and displacements of the pushover curve of the MDOF system, displacements and forces of the SDOF system can be obtained:

$$D^* = \frac{D_t}{\Gamma}; \qquad V^* = \frac{V}{\Gamma}\,. \tag{6.27}$$

In the Figure 6.39 and Figure 6.40, the SDOF capacity curves are presented for flexible and rigid floors.

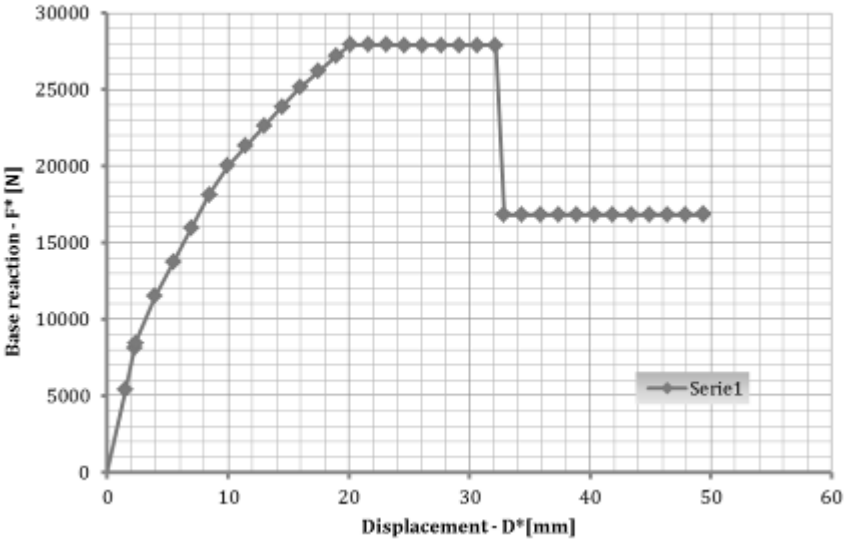

Figure 6.39: Pushover curve. N2 Method. Linear forces. SDOF system. Flexible floors.

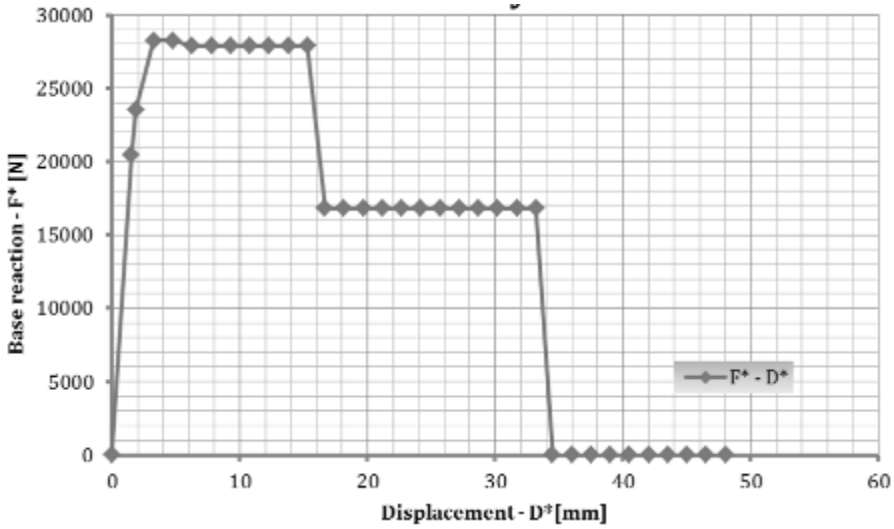

Figure 6.40: Pushover curve. N2 Method. Linear forces. SDOF system. Rigid floors.

6.4.5.5 Bilinear idealisation

In the next step a bi-linearization of the SDOF capacity curve assuming a linear perfectly plastic behaviour is performed. This can be done first by assuming a maximum force equal to:

$$F_y^* = 27919{,}88N\,. \tag{6.28}$$

The ultimate displacement will be:

$$D_u^* = 32{,}15mm\,, \tag{6.29}$$

in the rigid floor case:

$$F_y^* = 28237{,}93N\,, \quad D_u^* = 15{,}30mm\,. \tag{6.30}$$

In the linear part the elastic limit displacement value must be defined. Thus, the area under the two curves is the same (i.e., the dissipated energy must be constant). The idealisation is performed using trapezoidal integration rules. The length of the step, in terms of displacements, is:

$$\Delta u_i = D_{i+1}^* - D_i^*\,. \tag{6.31}$$

The area under the tract "i" will be:

$$A_i = \Delta u_i \cdot \frac{F_{i+1}^* + F_i^*}{2}\,. \tag{6.32}$$

The total area under the curve will be:

$$A_{real} = \sum_i A_i\,. \tag{6.33}$$

The area under the idealised curve is:

$$A_{id} = \frac{1}{2} F_y^* \cdot D_y^* + F_y^* \cdot \left(D_u^* - D_y^*\right). \tag{6.34}$$

By the equality of areas under the two curves, the following value for flexible floors:

$$D_y^* = 13{,}97mm\,. \tag{6.35}$$

For rigid floors:

$$D_y^* = 2{,}56mm\,. \tag{6.36}$$

Idealisation is graphically presented in the Figure 6.41 and Figure 6.42.

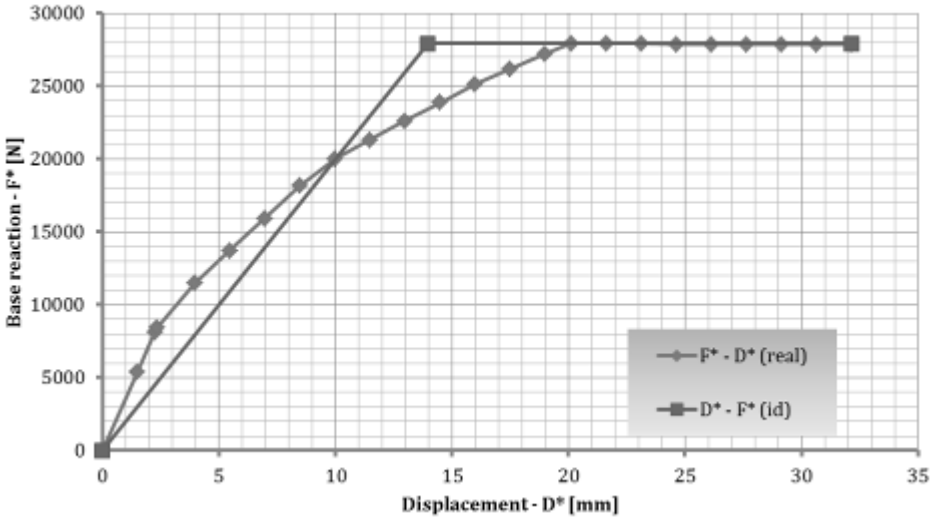

Figure 6.41: Pushover curve. Idealisation. SDOF system.

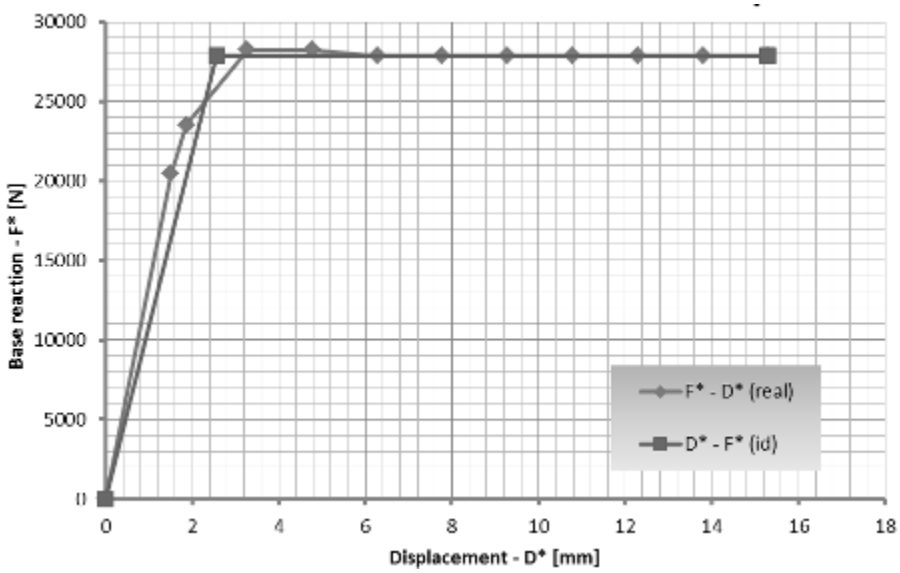

Figure 6.42: Pushover curve. Idealisation. SDOF system. Rigid floors.

6.4.5.6 Reduction factor

At this point the period of vibration of the SDOF system can be obtained:

$$T^* = 2 \cdot \pi \cdot \sqrt{\frac{m^* \cdot D_y^*}{F_y^*}} = 0{,}24s\,. \tag{6.37}$$

The capacity curve in the ADRS plan can be determined by dividing the force by the mass of the SDOF system:

$$S_a\left(D^*\right) = \frac{F^*\left(D^*\right)}{m^*}. \tag{6.38}$$

The maximum acceleration of the system is:

$$S_{ay} = \frac{F_y^*}{m^*} = 9{,}71\frac{m}{s^2}. \tag{6.39}$$

In the case of rigid floors:

$$T^* = 0{,}10s\,, \qquad S_{ay} = 9{,}82\frac{m}{s^2}. \tag{6.40}$$

The demand for the structure is not elastic demand spectrum, but this spectrum should be reduced to take into account the nonlinear capacity of structure and get the plastic demand spectrum.

The reduction factor is equal to the ratio between the maximum acceleration of the elastic response spectrum and maximum acceleration of the capacity spectrum of the structure:

$$R_\mu = \frac{S_{ae}}{S_{ay}}. \tag{6.41}$$

Once that reduction factor is obtained; the ductility of the system will be:

$$\mu = \left(R_\mu - 1\right) \cdot \frac{T_C}{T^*} + 1\,, \qquad \text{if: } T^* < T_C\,; \tag{6.42}$$

$$\mu = R_\mu \qquad \text{if: } T^* \geq T_C\,. \tag{6.43}$$

In the event that it proves $R_\mu < 1{,}0$ there is no reduction of the spectrum, and the plastic demand spectrum coincides with the elastic one. By varying the peak ground acceleration the following values in Table 6.28 are obtained.

Table 6.28: Values of reduction factor and ductility.

	0,25 g	0,50 g	1,29 g	Rigid
S_{ae} [m/s²]	7,36	14,72	37,96	37,96
R_μ	0,76	1,52	3,91	3,87
μ	1,00	1,54	4,05	8,06

Knowing the ductility, the whole demand spectrum can be defined. First is defined the reduction factor:

$$R_\mu = (\mu - 1)\cdot\frac{T}{T_C} + 1, \qquad \text{if: } T^* < T_C; \tag{6.44}$$

$$R_\mu = \mu, \qquad \text{if: } T^* \geq T_C. \tag{6.45}$$

The coordinates of each point of the spectrum demand are:

$$S_a = \frac{S_{ae}}{R_\mu}, \qquad S_d = \frac{\mu}{R_\mu}\cdot S_{de}. \tag{6.46}$$

The intersection of the scaled demand spectrum with bilinear capacity spectrum is the performance point.

SDOF system period of vibration defines the elastic spectral displacement:

$$S_{de} = S_{de}(T^*). \tag{6.47}$$

The SDOF system displacement demand is:

$$S_d = \frac{S_{de}}{R_\mu}\cdot\left[1 + (R_\mu - 1)\cdot\frac{T_C}{T^*}\right]; \qquad \text{if: } T^* < T_C; \tag{6.48}$$

$$S_d = S_{de}; \qquad \text{if: } T^* \geq T_C. \tag{6.49}$$

6.4.5.7 Demand for MDOF system

Finally, the demand for the MDOF system is:

$$D_t = \Gamma \cdot S_d \,. \tag{6.50}$$

In Table 6.29 the values of the displacements obtained for the three cases are presented.

Table 6.29: Displacement demand.

[mm]	0,25 g	0,50 g	1,29 g	Rigid
S_{de}	10,70	21,50	55,40	9,81
S_d	10,70	21,86	57,42	20,45
D_t	14,23	29,06	76,35	27,20

6.4.5.8 Graphical representation of capacity and demand

Graphical representation of capacity and demand are in the following Figures 6.43 – 6.46 for different cases that were analysed.

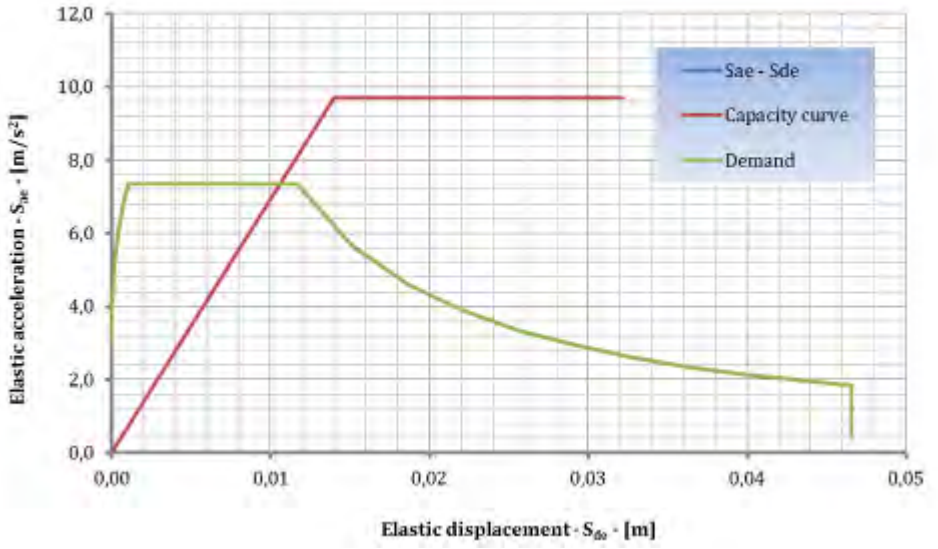

Figure 6.43: Result for a_g = 0,25 g.

As can be seen from the previous Figure 6.43 the model will respond elastically to the design earthquake with 0,25 g PGA.

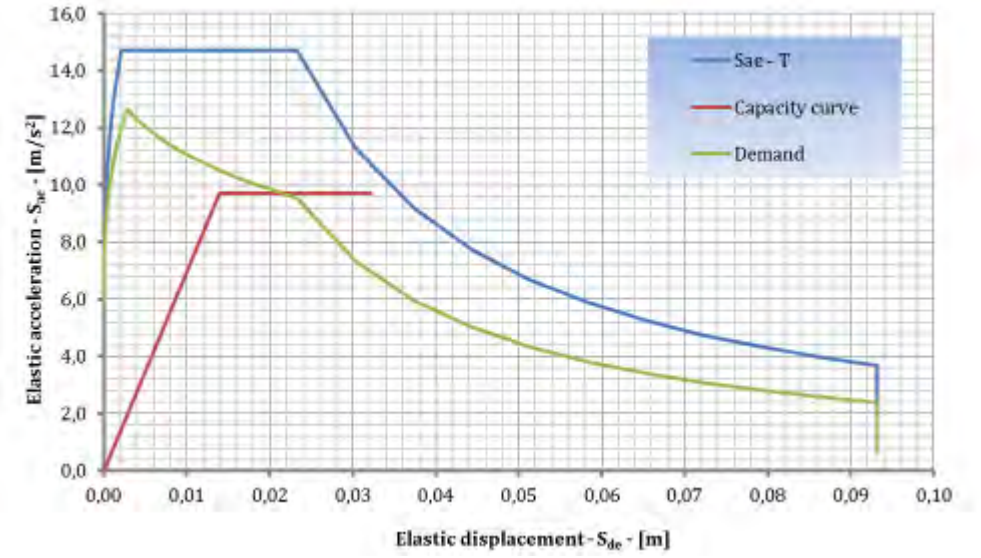

Figure 6.44: Result for a_g = 0,50 g.

The response to the design earthquake with 0,50 g PGA is in the plastic range, as can be seen in the previous Figure 6.44. The demand displacement for SDOF system is $\cong 0{,}022m$.

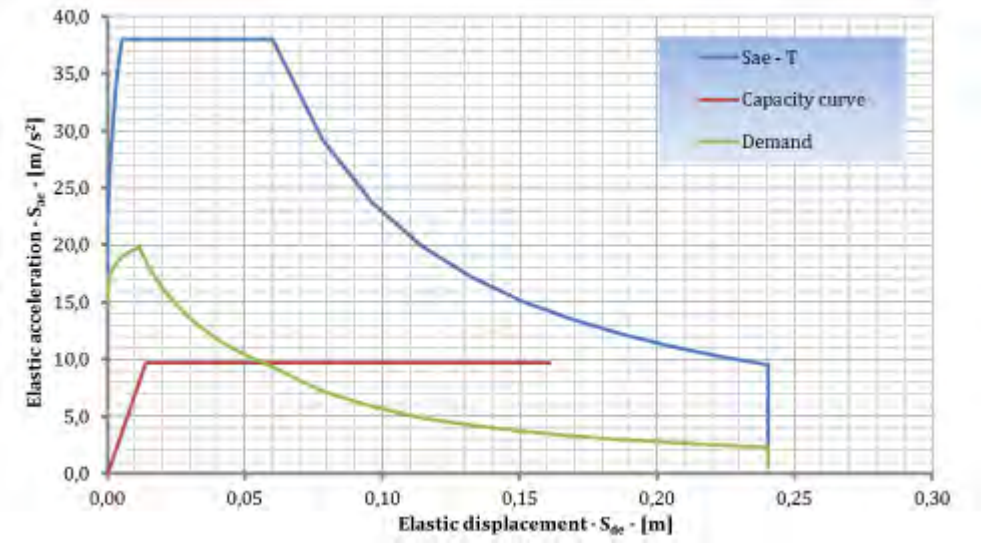

Figure 6.45: Result for a_g = 1,29 g.

The plastic displacement demand for the 1,29 g PGA design earthquake is $\cong 0{,}055m$.

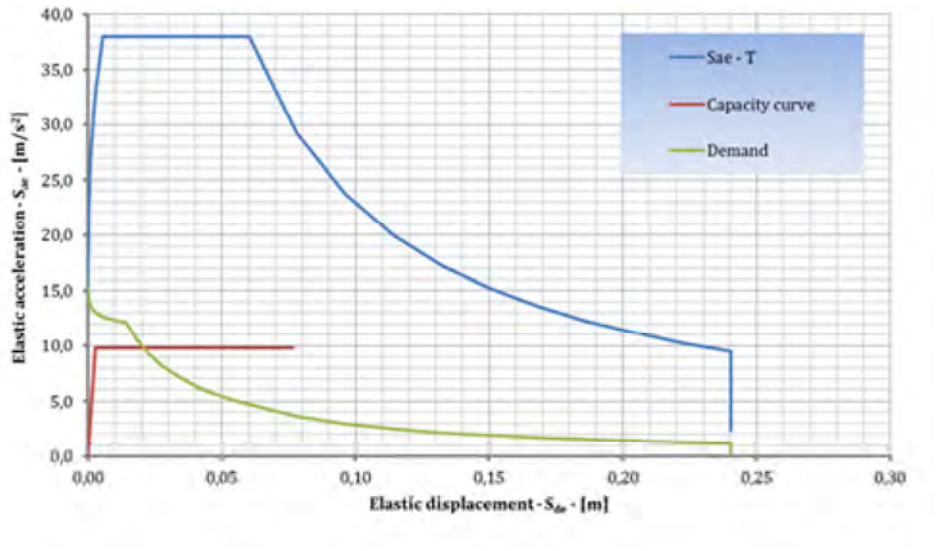

Figure 6.46: Result for rigid floors.

In case of rigid floors, the demand displacement is about the same at 0,043 m for SDOF system. Displacement demand increases with increasing of seismic demand. Knowing the displacement demand, it can trace back to the load step of the pushover analysis, and analyse damage (performance) of the structure.

In particular, the steps obtained are:

a) Step 9 for: a_g = 0,25 g, and: D_t = 14,23 mm;
b) Step 13 for: a_g = 0,50 g, and: D_t = 29,06 mm;
c) Step 36 for: a_g = 1,29 g, and: D_t = 76,36 mm;
d) Step 15 for: a_g = 1,29 g & Rigid floors, and: D_t = 27,20 mm.

6.4.5.9 Results

The result of the N2 method enable us to represented schematically the state of the structure for the given earthquake demand.

The following Figures 6.47 – 6.53 contain the link elements as rectangles of different colors according to the state in which they are:

- the green color indicates that the element remains in the elastic state;
- the orange color indicates that the element came in to plastic region;
- the red color indicates that the element is collapsed.

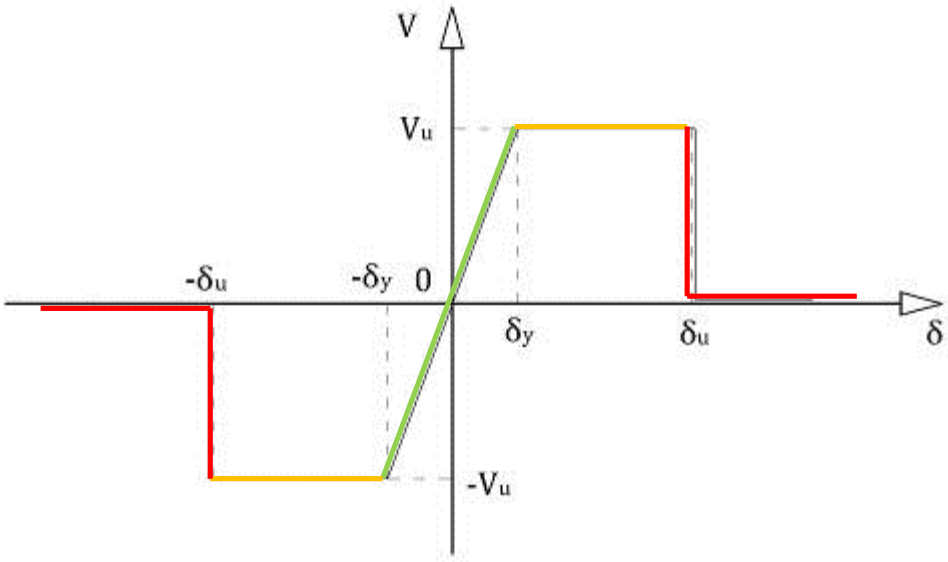

Figure 6.47: Link elements behaviour.

a) Step 9 (D_t = 14,23 mm) (a_g = 0,25 g)

The response is elastic.

b) Step 17 (D_t = 29,06 mm) (a_g = 0,50 g)

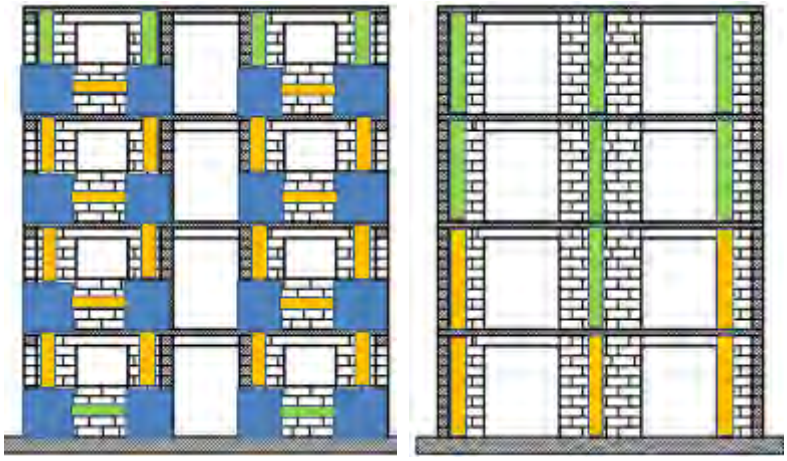

Figure 6.48: Status of link element in step 17 (29,06 mm). North elevation (on the left) and south elevation (on the right).

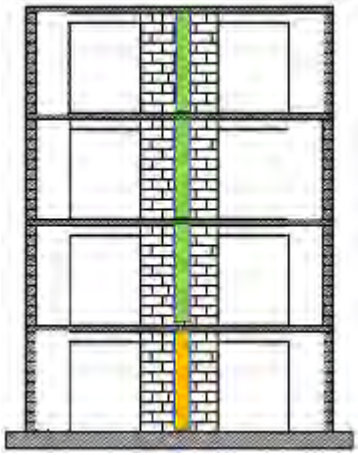

Figure 6.49: Status of link element in step 17 (29,06 mm). Central wall (number 5).

c) Step 23 (D_t = 76,36 mm) (a_g = 1,29 g)

The displacement demand is more than the maximum capacity displacement of the structure.

The collapse mechanism is represented in the following pictures.

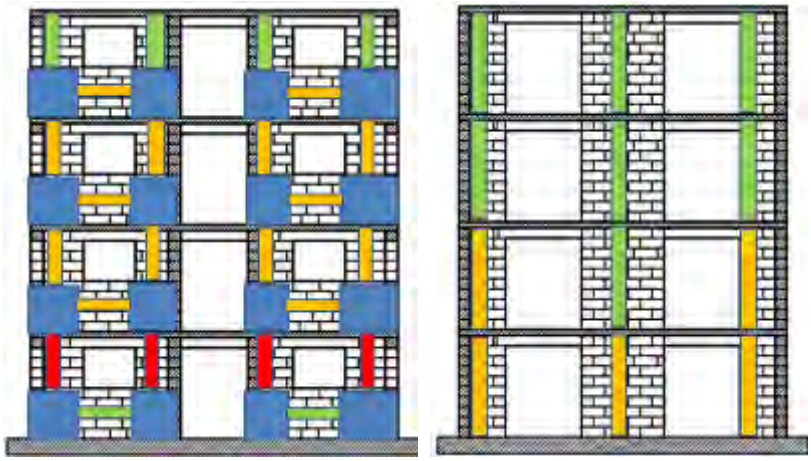

Figure 6.50: Status of link element in step 23 (42,75 mm). North elevation (on the left) and south elevation (on the right).

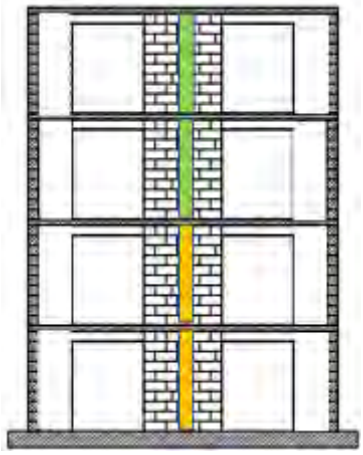

Figure 6.51: Status of link element in step 23 (42,75 mm). Central wall (number 5).

d) Step 15 (D_t = 27,20 mm) (Rigid floors case) (a_g = 1,29 g)

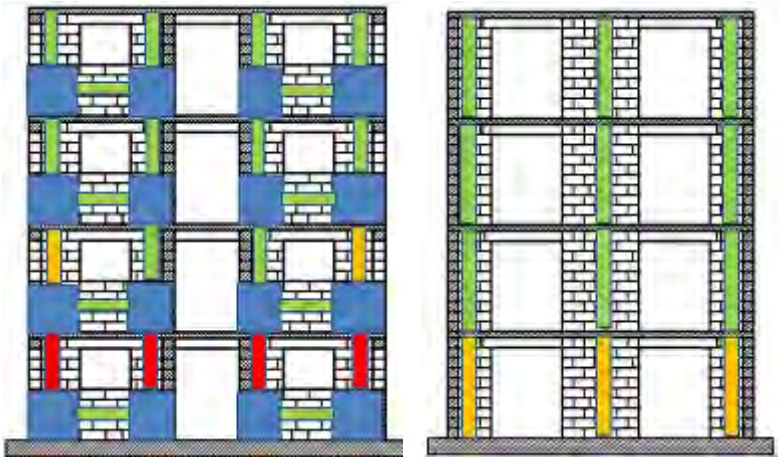

Figure 6.52: Status of link element in step 15 (27,20 mm) with rigid floors. North elevation (on the left) and south elevation (on the right).

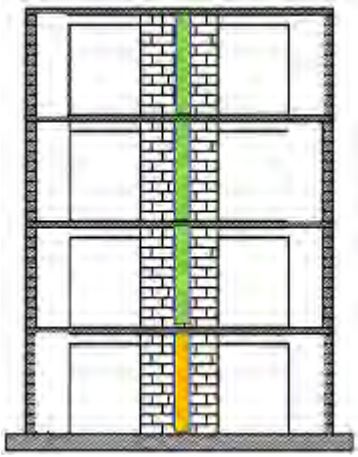

Figure 6.53: Status of link element in step 15 (27,20 mm). Central wall (number 5).

The previous Figures 6.47 – 6.53 show that the modelling with rigid slabs allows for a more localised damage on the first floor of the structure. In particular, it is possible to observe that, the demand for displacement has a plastification of all links on the first floor and the complete collapse of some of these. Compared to the more deformable floors where there is a low damage to upper floors, in fact almost all masonry walls are preserved in the elastic range.

6.4.6 N2 analyses with real spectra

In this section the results obtained from the previous method to the case where the demand is the actual response spectra of the ground excitation were time history of ground acceleration of R150 and R250 is presented in the following Figure 6.54 and Figure 6.55.

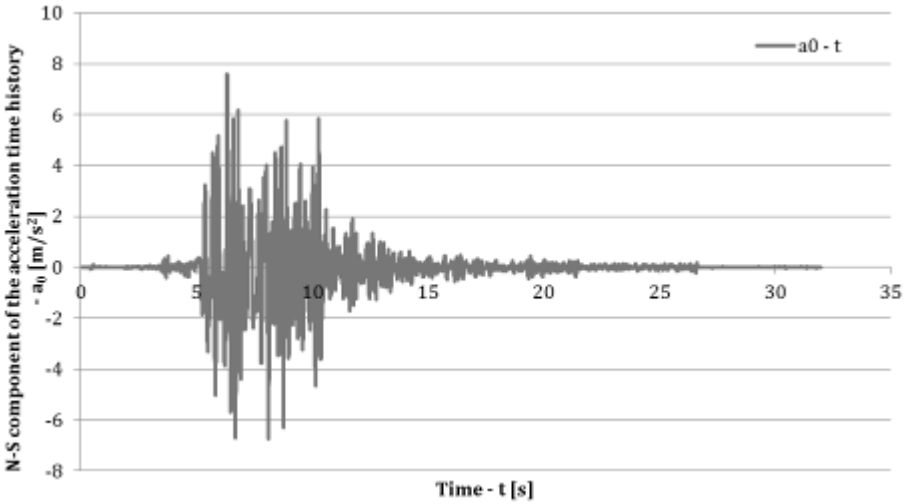

Figure 6.54: Modelled earthquake accelerogram for R150.

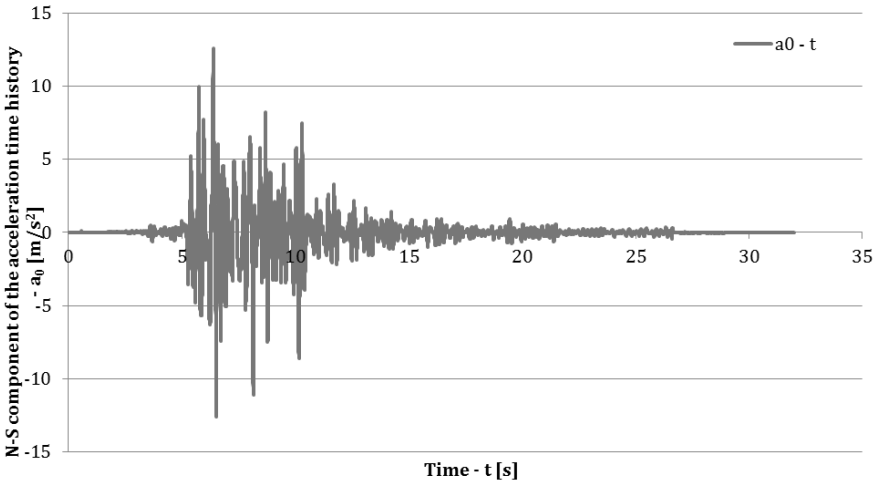

Figure 6.55: Modelled earthquake accelerogram for R250.

6.4.6.1 Analysis of response spectrum

From the time history of the ground acceleration, the elastic response spectra that must be used for the N2 analysis can be obtained. In particular, every point of the spectrum is characterised by a couple of values:

- S_{ae}: spectral acceleration, which is the maximum absolute acceleration of a SDOF system, at the given mass m, with stiffness k and viscous damping c;
- T: period of vibration of the SDOF system, which takes values ranging from 0 (infinitely rigid system) and ∞ (infinitely deformable system).

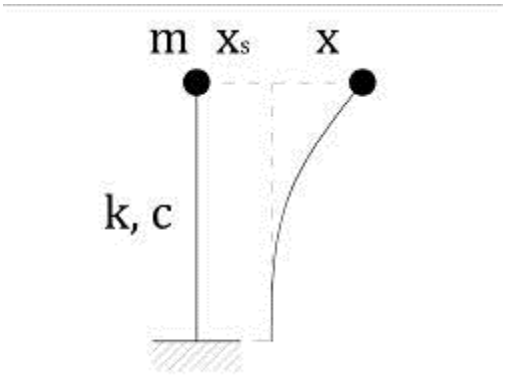

Figure 6.56: SDOF system.

For each point in the spectrum, the SDOF system (reported in Figure 6.56) first period of vibration must be determined:

$$T = \frac{2 \cdot \pi}{\omega}, \tag{6.51}$$

where ω is the natural pulse of vibration, equal to:

$$\omega_0 = \sqrt{\frac{k}{m}}. \tag{6.52}$$

It is also possible to obtain the relative damping, equal to the ratio between the actual and the critical damping of the structure:

$$\xi = \frac{c}{c_{cr}}. \tag{6.53}$$

where:

$$c_{cr} = 2 \cdot \sqrt{m \cdot k}\,. \tag{6.54}$$

The SDOF system is subjected to seismic motion at its base. Ultimately, three forces will act on the SDOF system:

- inertia force: by definition, the product of mass by acceleration:

$$F_I = m \cdot \left(\ddot{x} + \ddot{x}_s\right); \tag{6.55}$$

- force of viscous damping:

$$F_c = c \cdot \dot{x}\,; \tag{6.56}$$

- elastic force:

$$F_e = k \cdot x\,; \tag{6.57}$$

Applying the D'Alembert principle is possible to obtain the differential equation that governs the problem:

$$F_I + F_c + F_e = 0 \quad \text{->} \quad m \cdot \left(\ddot{x} + \ddot{x}_s\right) + c \cdot \dot{x} + k \cdot x = 0\,; \tag{6.58}$$

By solving this differential equation, the functions of the relative and absolute acceleration displacements and velocities can be calculated.

In particular:

$$m \cdot \ddot{x} + c \cdot \dot{x} + k \cdot x = -m \cdot \ddot{x}_s\,. \tag{6.59}$$

The associated homogeneous equation is:

$$m \cdot \ddot{x} + c \cdot \dot{x} + k \cdot x = 0\,, \tag{6.60}$$

by dividing by the mass:

$$\ddot{x} + \frac{c}{m} \cdot \dot{x} + \frac{k}{m} \cdot x = 0\,, \tag{6.61}$$

where:

$$\frac{c}{m} = 2 \cdot \xi \cdot \omega_0\,, \tag{6.62}$$

by substitution:

$$\ddot{x} + 2 \cdot \xi \cdot \omega_0 \cdot \dot{x} + \omega_0^2 \cdot x = 0\,. \tag{6.63}$$

The associated polynomial is:

$$\lambda^2 + 2 \cdot \xi \cdot \omega_0 \cdot \lambda + \omega_0^2 = 0. \tag{6.64}$$

The solutions are:

$$\lambda = -\xi \cdot \omega_0 \pm \sqrt{\xi^2 \cdot \omega_0^2 - \omega_0^2}\ . \tag{6.65}$$

There are the possible cases:

1) $\Delta = \xi^2 \cdot \omega_0^2 - \omega_0^2 > 0$, or: $c > c_{cr}$, or: $\xi > 1$; (6.66)

2) $\Delta = \xi^2 \cdot \omega_0^2 - \omega_0^2 = 0$, or: $c = c_{cr}$, or: $\xi = 1$; (6.67)

3) $\Delta = \xi^2 \cdot \omega_0^2 - \omega_0^2 < 0$, or: $c < c_{cr}$, or: $\xi < 1$. (6.68)

Looking at the third case, which is natural for buildings, the following solution, with real and imaginary parts is valid:

$$\lambda = -\xi \cdot \omega_0 \pm i \cdot \omega_0 \sqrt{1 - \xi^2}\ . \tag{6.69}$$

It can define:

$$\omega_d = \omega_0 \cdot \sqrt{1 - \xi^2}\ . \tag{6.70}$$

However, for normal building:

$$\xi \cong 0{,}05 << 1{,}00\ , \qquad \text{->} \qquad \omega_d \cong \omega_0. \tag{6.71}$$

Finally, the solution is:

$$x = e^{-\xi \cdot \omega_0 \cdot t} \cdot \left[c_1 \cdot \cos(\omega_d \cdot t) + c_2 \cdot \sin(\omega_d \cdot t)\right]. \tag{6.72}$$

The two constants can be obtained by the imposition of the initial conditions:

$$x(t = 0) = x_0; \tag{6.73}$$

$$\dot{x}(t = 0) = \dot{x}_0; \tag{6.74}$$

with the previous equation:

$$x = e^{-\xi \cdot \omega_0 \cdot t} \cdot \left[x_0 \cdot \cos(\omega_d \cdot t) + \frac{\xi \cdot \omega_0 \cdot x_0 + \dot{x}_0}{\omega_d} \cdot \sin(\omega_d \cdot t) \right]. \tag{6.75}$$

Only maximum absolute acceleration, coupled with the previously defined period of vibration, is a single point in the response spectrum.

It is therefore necessary to proceed iteratively to solve the dynamical problem of the simple oscillator many times. To do this a computer code was written in

the program Mathematica, which solves the above problem using a step–by–step process. The Figures 6.57 – 6.59 show the obtained response spectra.

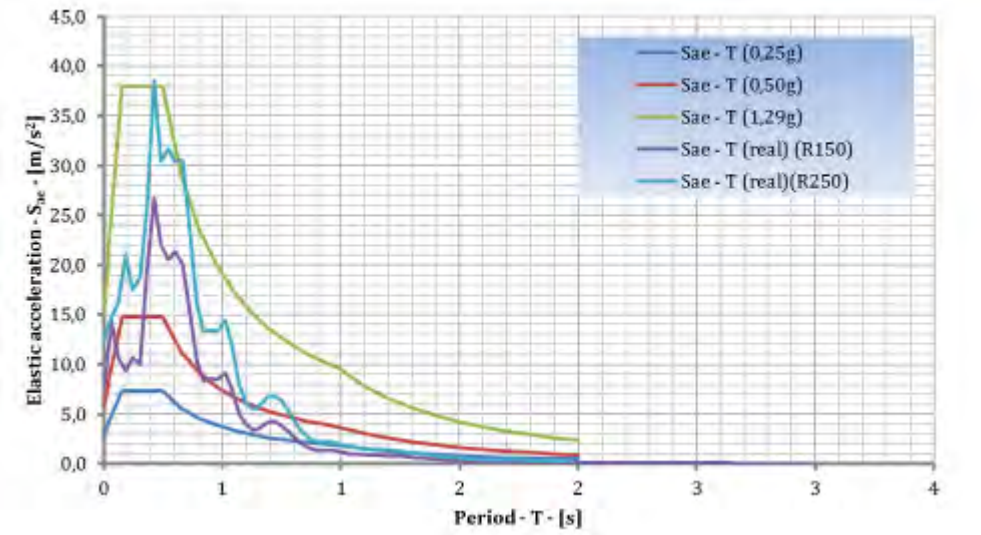

Figure 6.57: Real elastic acceleration spectrums and comparisons.

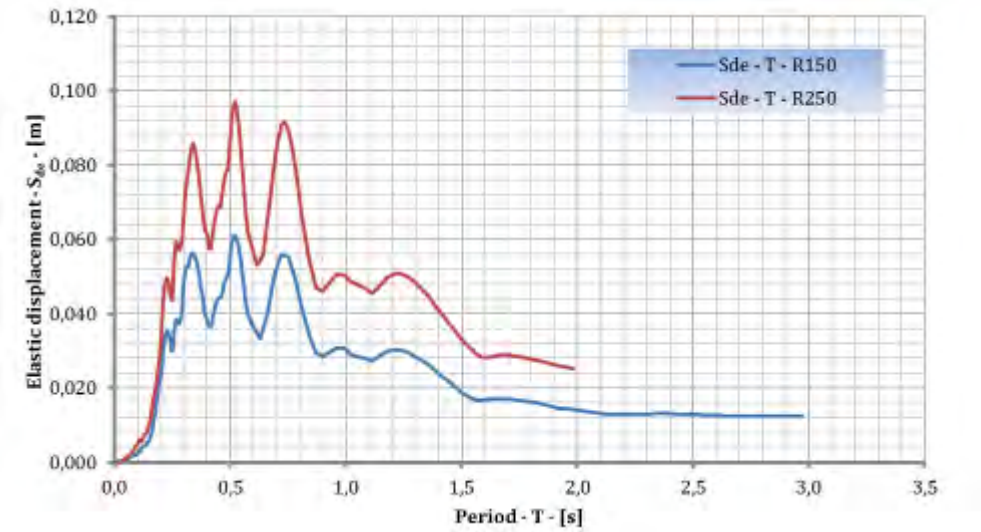

Figure 6.58: Real elastic displacement spectrum.

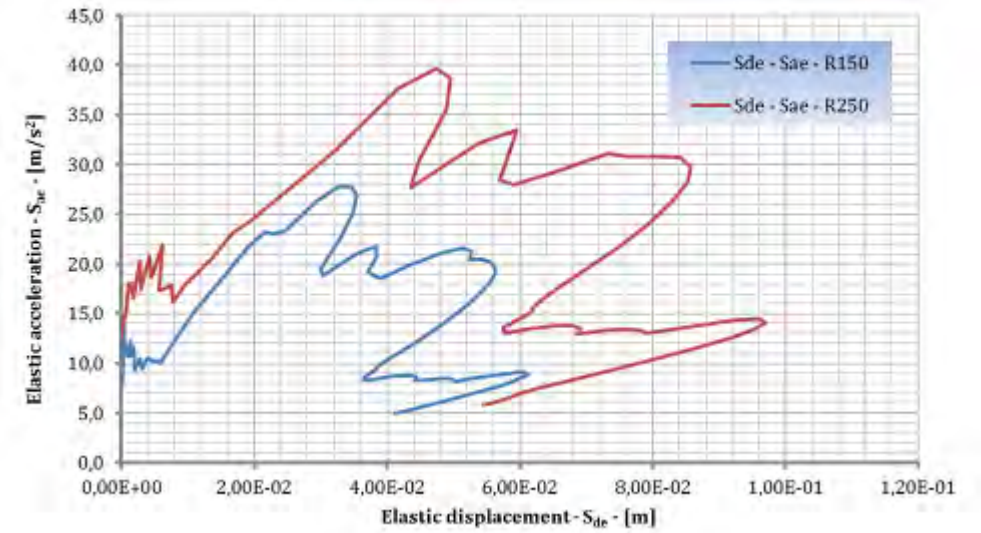

Figure 6.59: Real elastic spectrum in AD format.

In the following Table 6.30 and Table 6.31 the results of N2 method are reported. The period of vibration of the end of the tract with a constant spectral acceleration assumed was equal to:

$$T_C = 0{,}3s\,. \tag{6.76}$$

Next, using the above formulas for the structure and assuming a behaviour with rigid floor slabs, the results obtained are presented in the following tables.

Table 6.30: Ductility factor.

	R150	R250
S_{ae} [m/s²]	27,79	39,69
R_μ	2,83	4,04
μ	6,41	10,00

Table 6.31: Displacement demand.

[mm]	R150	R250
S_{de}	2,71	5,39
S_d	6,15	13,33
D_t	8,17	17,73

It should be noted that, for the analysis of the elastic displacement, a linear interpolation has been adopted:

$$S_{de} = S_{de1} + (T^* - T_1) \cdot \frac{S_{de2} - S_{de1}}{T_2 - T_1}. \quad (6.77)$$

In the Figures 6.60 – 6.62, the comparisons between the demand and the real capacity of the system under the two time histories are presented.

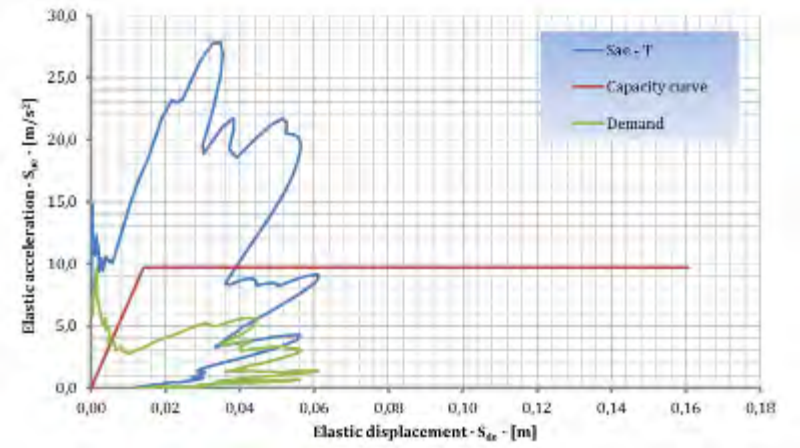

Figure 6.60: Capacity vs. demand for R150 and rigid floors.

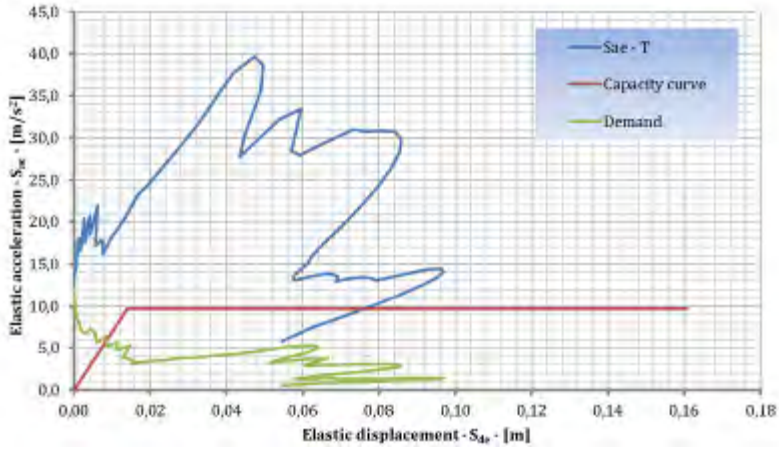

Figure 6.61: Capacity versus demand for R250 and rigid floors.

The results give an elastic response, which is in clear contrast to the observed collapse of the experimental model.

6.4.7 Evolution of the axial forces

The link elements used in the analysis conducted do not enable to define a variable behaviour depending on the value of axial force in the element. So a constant normal stress in each component is used and it must verified a posteriori that the changes in axial forces are not big.

During all the analysis the normal stress remains constant. This assumption is acceptable for small buildings, consisting of a maximum of 2 or 3 floors. The following Figure 6.62 show the numbering of link elements. Elements 1 to 8 are parallel to the direction of seismic loading.

These changes are measured from an initial value of normal stress (step 0) due only to vertical loads.

The variation of axial forces are shown in the following section. There are large variations in normal stress in most of the elements. Only the links belonging to the last two floors and links in baricentral position (i.e., 5 and 7) remain essentially unchanged.

This result is expected because of the height of the structure but in the next sections it will be shown that this fact does not lead to large errors when comparing the results of this model with experimental results.

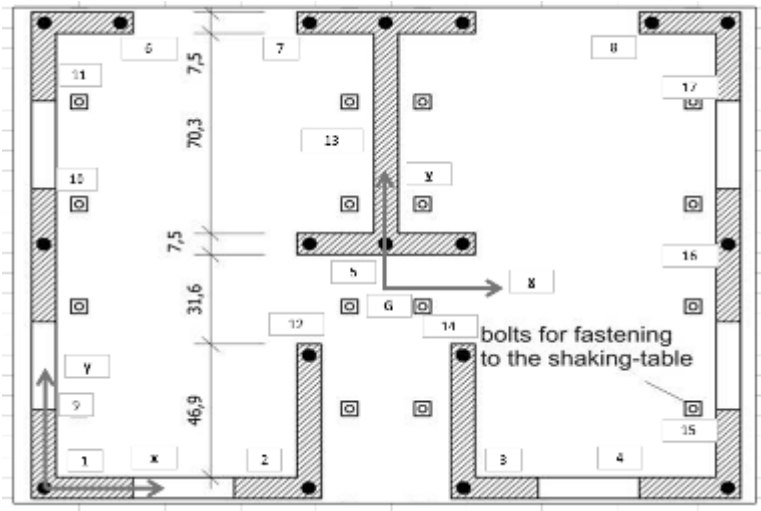

Figure 6.62: Plant and number of piers.

6.4.8 Manual analysis of the axial force from experiments

In the following tables mechanical parameters of masonry piers used to define the normal stresses are presented. In particular, first the center of gravity, which will be the origin of the new reference system, is obtained. For the general pier the following data are known (see Figure 6.63):

- x_i and y_i are the coordinate of center of gravity of the cross section of the wall with respect to global reference system with origin in O;
- d_{xi} and d_{yi} are the length and thickness of the pier.

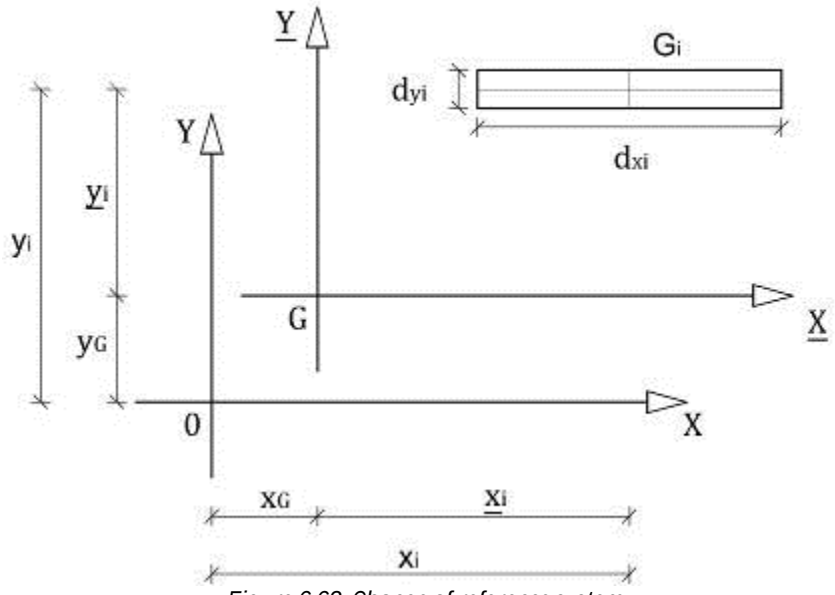

Figure 6.63: Change of reference system.

The following properties can be obtained in Table 6.32 and Table 6.33:

- area: $A_i = d_{xi} \cdot d_{yi}$; (6.78)
- static moment with respect to the x axis: $S_{xi} = A_i \cdot y_i$; (6.79)
- static moment with respect to the y axis: $S_{yi} = A_i \cdot x_i$; (6.80)
- coordinates of center of gravity:

$$x_G = \frac{\sum S_{yi}}{\sum A_i} = \frac{\sum A_i \cdot x_i}{\sum A_i}, \qquad y_G = \frac{\sum S_{xi}}{\sum A_i} = \frac{\sum A_i \cdot y_i}{\sum A_i}; \tag{6.81}$$

- coordinates of pier with respect to new reference system:

$$\underline{x}_i = x_i - x_G, \qquad \underline{y}_i = y_i - y_G; \tag{6.82}$$

- pier's moments of inertia with respect to new reference system:

$$I_{\underline{x}_i} = \frac{d_{xi} \cdot d_{yi}^3}{12} + A_i \cdot \underline{y}_i^2, \qquad I_{\underline{y}_i} = \frac{d_{yi} \cdot d_{xi}^3}{12} + A_i \cdot \underline{x}_i^2. \tag{6.83}$$

Table 6.32: Piers mechanical characteristics.

i	x_i	y_i	d_{xi}	d_{yi}	A_i	S_{xi}	S_{yi}	$\underline{x}_i$	$\underline{y}_i$	$I_{\underline{x}i}$	$I_{\underline{y}i}$
[]	[m]	[m]	[m]	[m]	[m²]	[m³]	[m³]	[m]	[m]	[m⁴]	[m⁴]
1	0,119	0,000	0,313	0,075	0,023	0,0000	0,0028	-0,937	-0,791	0,01468	0,02061
2	0,722	0,000	0,269	0,075	0,020	0,0000	0,0145	-0,334	-0,791	0,01262	0,00226
3	1,391	0,000	0,269	0,075	0,020	0,0000	0,0280	0,334	-0,791	0,01262	0,00226
4	1,994	0,000	0,313	0,075	0,023	0,0000	0,0467	0,938	-0,791	0,01468	0,02061
5	1,056	0,859	0,550	0,075	0,041	0,0355	0,0436	0,000	0,068	0,00021	0,00002
6	0,119	1,638	0,313	0,075	0,023	0,0384	0,0028	-0,937	0,846	0,01681	0,02061
7	1,056	1,638	0,550	0,075	0,041	0,0675	0,0436	0,000	0,846	0,02958	0,00002
8	1,994	1,638	0,313	0,075	0,023	0,0384	0,0467	0,938	0,846	0,01681	0,02061
9	0,000	0,156	0,075	0,238	0,018	0,0028	0,0000	-1,056	-0,635	0,00726	0,01996
10	0,000	0,819	0,075	0,469	0,035	0,0288	0,0000	-1,056	0,028	0,00067	0,03986
11	0,000	1,481	0,075	0,238	0,018	0,0264	0,0000	-1,056	0,690	0,00857	0,01996
12	0,819	0,272	0,075	0,469	0,035	0,0096	0,0288	-0,238	-0,519	0,01012	0,00263
13	1,056	1,248	0,075	0,703	0,053	0,0658	0,0557	0,000	0,457	0,01321	0,00217
14	1,294	0,272	0,075	0,469	0,035	0,0096	0,0455	0,237	-0,519	0,01012	0,00263
15	2,113	0,156	0,075	0,238	0,018	0,0028	0,0376	1,056	-0,635	0,00726	0,01996
16	2,113	0,819	0,075	0,469	0,035	0,0288	0,0743	1,056	0,028	0,00067	0,03986
17	2,113	1,481	0,075	0,238	0,018	0,0264	0,0376	1,056	0,690	0,00857	0,01996

The moments of inertia are:

$$I_{\underline{y}} = \sum I_{\underline{y}_i} = 0{,}2540 m^4 \ , \qquad I_{\underline{x}} = \sum I_{\underline{x}_i} = 0{,}1844 m^4 \ . \tag{6.84}$$

The total area of piers is:

$$\sum A_i = 0{,}4812 m^2 \ . \tag{6.85}$$

The total static moment are:

$$\sum S_{xi} = 0{,}3806 m^3 \ , \qquad \sum S_{yi} = 0{,}5082 m^3 \ . \tag{6.86}$$

The coordinates of the center of gravity, ultimately, are:

$$x_G = 1{,}056 m, \qquad y_G = 0{,}7910 m. \tag{6.87}$$

The normal stresses from pushover analysis with rigid floors, for each pier and each step of the analysis are in the Table 6.33. In particular, only shows the first 11 steps, or those that provide the highest level of achieved shear.

The results are also graphically show in Figure 6.64.

Table 6.33: Change of axial force in link element for rigid floors.

Step	1	2	3	4	5	6	7	8	9	10	11
i	ΔN_i										
[]	[N]										
1	3778,40	4289,52	4708,10	4708,16	4641,57	4641,69	4641,82	4641,57	4641,69	4641,82	4641,57
2	948,01	1083,96	1230,32	1230,34	1213,71	1213,74	1213,77	1213,71	1213,74	1213,77	1213,71
3	-945,89	-1081,34	-1227,76	-1227,79	-1211,20	-1211,23	-1211,26	-1211,20	-1211,23	-1211,26	-1211,20
4	-3777,95	-4289,19	-4707,78	-4707,84	-4641,24	-4641,36	-4641,49	-4641,24	-4641,36	-4641,49	-4641,24
5	2,38	2,75	2,90	2,90	2,86	2,86	2,86	2,86	2,86	2,86	2,86
6	2264,85	2658,41	3631,59	3631,73	3591,83	3591,90	3591,98	3591,83	3591,90	3591,98	3591,83
7	-0,13	-0,15	-0,36	-0,36	-0,36	-0,36	-0,36	-0,36	-0,36	-0,36	-0,36
8	-2265,38	-2659,03	-3632,24	-3632,38	-3592,47	-3592,55	-3592,62	-3592,47	-3592,55	-3592,62	-3592,47
9	2434,50	2846,37	3802,93	3803,07	3760,21	3760,29	3760,37	3760,21	3760,29	3760,37	3760,21
10	4604,77	5299,59	6419,79	6419,95	6338,86	6339,01	6339,16	6338,86	6339,01	6339,16	6338,86
11	3783,48	4296,48	4752,07	4752,13	4685,48	4685,61	4685,73	4685,48	4685,61	4685,73	4685,48
12	1129,34	1297,85	1533,58	1533,61	1513,72	1513,76	1513,79	1513,72	1513,76	1513,79	1513,72
13	1,55	1,80	1,95	1,95	1,92	1,92	1,92	1,92	1,92	1,92	1,92
14	-1127,33	-1295,43	-1531,48	-1531,51	-1511,66	-1511,69	-1511,73	-1511,66	-1511,69	-1511,73	-1511,66
15	-2435,07	-2847,04	-3803,55	-3803,69	-3760,82	-3760,90	-3760,98	-3760,82	-3760,90	-3760,98	-3760,82
16	-4607,21	-5302,44	-6422,53	-6422,69	-6341,55	-6341,71	-6341,86	-6341,56	-6341,71	-6341,86	-6341,56
17	-3788,31	-4302,13	-4757,52	-4757,58	-4690,85	-4690,97	-4691,10	-4690,85	-4690,97	-4691,10	-4690,85

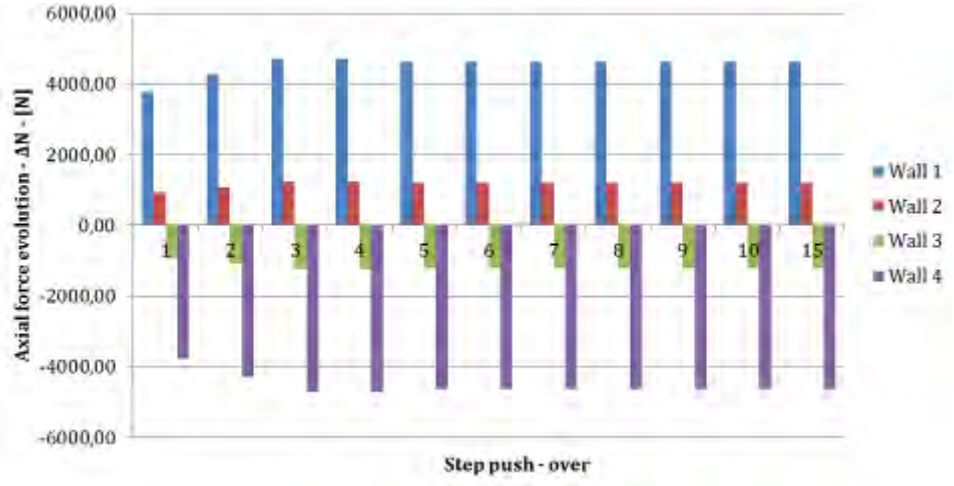

Figure 6.64: Change of axial force evolution. SAP2000® analysis.

In the analysis that follow it is used the resulting bending moments that are from the execution of tests on M3 model, which will be described in detail in the next paragraph. In particular, the bending moment was calculated for 10 points of the test, for which they are known by the Table 6.34, the values of the floor forces.

These points are the most important of the test, and those that constitute an overall behaviour of the constitutive law. Ultimately, for each step of loading, the bending moment is:

$$M = \sum_{i=1}^{4} F_i \cdot d_i \,. \tag{6.88}$$

The normal stress in each pier will be:

$$\sigma_i = \frac{M}{I_{\underline{y}}} \cdot \underline{x}_i + \sigma_0 \,. \tag{6.89}$$

By taking the normal compression stress as positive; σ_0 is the normal stress due to only vertical loads compression in step 0.

The normal stresses can be obtained by multiplying stress by the area of cross section of piers:

$$N_i = A_i \cdot \sigma_i \,. \tag{6.90}$$

Ultimately, the variations of normal stresses for all walls at each load step of pushover analysis can be defined. Starting from the initial normal stress due to vertical loads (N_0), used to obtain the resistance to shear of the panel, those variations are:

$$\Delta N_i = N_i - N_0 . \tag{6.91}$$

The results obtained by the application of the previous relationships are reported in the Tables 6.35 – 6.37 and in Figure 6.65.

Table 6.34: Analysis of the bending moment by the test on M3 model.

Step	F_1	F_2	F_3	F_4	d_1	d_2	d_3	d_4	M
	[N]	[N]	[N]	[N]	[m]	[m]	[m]	[m]	[Nm]
1	-1632,44924	-2299,3523	-2662,3215	-2697,4829	0,663	1,326	1,989	2,652	16580,337
2	-4464,77465	-4529,1915	-4605,1194	-4541,0273	0,663	1,326	1,989	2,652	30168,240
3	4616,612651	5282,5179	5403,8542	5891,0287	0,663	1,326	1,989	2,652	36436,707
4	-3823,85099	-5761,7414	-6033,6542	-5548,3224	0,663	1,326	1,989	2,652	36890,371
5	4959,861393	6399,4035	7005,7297	7101,7008	0,663	1,326	1,989	2,652	44542,104
6	-3390,73994	-4729,6703	-7305,2257	-9949,5206	0,663	1,326	1,989	2,652	49435,826
7	-3729,09208	-6584,703	-8206,6442	-9766,4676	0,663	1,326	1,989	2,652	53427,392
8	-7989,20841	-7986,3291	-8111,9463	-9153,9933	0,663	1,326	1,989	2,652	56297,769
9	434,055797	6935,3956	10464,879	14198,298	0,663	1,326	1,989	2,652	67952,645
10	-6975,42534	-10355,08	-11663,789	-12892,274	0,663	1,326	1,989	2,652	75745,132

Table 6.35: Axial stress in piers.

Step		1	2	3	4	5	6	7	8	9	10
i	σ_0	σ_i									
[]	[MPa]	[MPa]									
1	0,062	0,000	-0,050	-0,073	-0,074	-0,103	-0,121	-0,136	-0,146	-0,189	-0,218
2	0,074	0,052	0,035	0,026	0,026	0,016	0,009	0,004	0,000	-0,015	-0,025
3	0,074	0,096	0,114	0,122	0,123	0,133	0,139	0,145	0,148	0,164	0,174
4	0,062	0,123	0,173	0,196	0,198	0,226	0,244	0,259	0,269	0,313	0,341
5	0,110	0,110	0,110	0,110	0,110	0,110	0,110	0,110	0,110	0,110	0,110
6	0,081	0,020	-0,030	-0,054	-0,055	-0,083	-0,101	-0,116	-0,127	-0,170	-0,199
7	0,081	0,081	0,081	0,081	0,081	0,081	0,081	0,081	0,081	0,081	0,081
8	0,081	0,142	0,192	0,215	0,217	0,245	0,263	0,278	0,289	0,332	0,361
9	0,083	0,014	-0,043	-0,069	-0,071	-0,102	-0,123	-0,139	-0,151	-0,200	-0,232
10	0,088	0,019	-0,038	-0,064	-0,066	-0,098	-0,118	-0,135	-0,147	-0,195	-0,227
11	0,083	0,014	-0,043	-0,069	-0,071	-0,102	-0,123	-0,139	-0,151	-0,200	-0,232
12	0,136	0,120	0,108	0,102	0,101	0,094	0,090	0,086	0,083	0,072	0,065
13	0,068	0,068	0,068	0,068	0,068	0,068	0,068	0,068	0,068	0,068	0,068
14	0,136	0,151	0,164	0,170	0,170	0,177	0,182	0,186	0,188	0,199	0,207
15	0,083	0,152	0,208	0,234	0,236	0,268	0,288	0,305	0,317	0,365	0,398
16	0,088	0,157	0,213	0,239	0,241	0,273	0,293	0,310	0,322	0,370	0,403
17	0,083	0,152	0,208	0,234	0,236	0,268	0,288	0,305	0,317	0,365	0,398

Table 6.36: Axial force in piers.

Step	0	1	2	3	4	5	6	7	8	9	10
i	N_i										
[]	[MPa]										
1	-1445,68	-11,31	1164,19	1706,48	1745,73	2407,69	2831,05	3176,36	3424,68	4432,95	5107,08
2	-1742,08	-1058,00	-697,49	-531,17	-519,14	-316,12	-186,28	-80,38	-4,22	305,00	511,75
3	-1741,79	-1938,27	-2298,90	-2465,27	-2477,31	-2680,39	-2810,28	-2916,22	-2992,40	-3301,73	-3508,54
4	-1445,68	-2880,12	-4055,66	-4597,97	-4637,22	-5299,20	-5722,58	-6067,91	-6316,23	-7324,55	-7998,71
5	-2585,84	-4550,99	-4550,92	-4550,88	-4550,88	-4550,84	-4550,82	-4550,80	-4550,78	-4550,72	-4550,68
6	-1898,21	-463,83	711,67	1253,96	1293,21	1955,16	2378,52	2723,84	2972,15	3980,43	4654,56
7	-1898,21	-3340,76	-3340,69	-3340,66	-3340,66	-3340,62	-3340,59	-3340,57	-3340,56	-3340,50	-3340,46
8	-1898,21	-3332,65	-4508,19	-5050,50	-5089,75	-5751,73	-6175,11	-6520,44	-6768,77	-7777,08	-8451,24
9	-1941,58	-247,39	759,16	1223,50	1257,11	1823,92	2186,43	2482,11	2694,74	3558,09	4135,33
10	-2053,04	-655,39	1331,00	2247,37	2313,69	3432,28	4147,69	4731,20	5150,82	6854,62	7993,79
11	-1941,49	-247,32	759,23	1223,57	1257,18	1823,99	2186,50	2482,18	2694,81	3558,16	4135,40
12	-3181,55	-4227,62	-3780,82	-3574,69	-3559,78	-3308,17	-3147,25	-3016,00	-2921,61	-2538,37	-2282,13
13	-1583,45	-3562,52	-3562,44	-3562,39	-3562,39	-3562,34	-3562,31	-3562,28	-3562,26	-3562,19	-3562,13
14	-3181,43	-5317,71	-5764,40	-5970,47	-5985,38	-6236,92	-6397,80	-6529,02	-6623,38	-7006,52	-7262,69
15	-1941,97	-2704,15	-3710,73	-4175,09	-4208,69	-4775,53	-5138,05	-5433,74	-5646,38	-6509,76	-7087,02
16	-2053,45	-5503,78	-7490,23	-8406,64	-8472,96	-9591,59	-10307,02	-10890,56	-11310,19	-13014,05	-14153,25
17	-1941,87	-2704,08	-3710,66	-4175,02	-4208,63	-4775,46	-5137,98	-5433,67	-5646,31	-6509,69	-7086,95

M [Nm]	1,06	16242,94	29553,52	35694,05	36138,45	43634,02	48427,86	52337,96	55149,75	66566,76	74200,20

Table 6.37: Variation of the axial force in piers.

Step	1	2	3	4	5	6	7	8	9	10
i	ΔN_i									
[]	[N]									
1	1434,38	2609,88	3152,17	3191,41	3853,37	4276,73	4622,04	4870,36	5878,63	6552,77
2	439,91	800,42	966,73	978,77	1181,78	1311,62	1417,53	1493,68	1802,91	2009,66
3	-440,05	-800,68	-967,05	-979,09	-1182,18	-1312,06	-1418,00	-1494,18	-1803,51	-2010,32
4	-1434,43	-2609,98	-3152,29	-3191,54	-3853,52	-4276,90	-4622,22	-4870,55	-5878,86	-6553,02
5	0,09	0,16	0,19	0,19	0,23	0,25	0,28	0,29	0,35	0,39
6	1434,38	2609,88	3152,17	3191,41	3853,37	4276,73	4622,04	4870,36	5878,63	6552,77
7	0,09	0,16	0,19	0,19	0,23	0,25	0,28	0,29	0,35	0,39
8	-1434,43	-2609,98	-3152,29	-3191,54	-3853,52	-4276,90	-4622,22	-4870,55	-5878,86	-6553,02
9	1228,21	2234,76	2699,10	2732,71	3299,52	3662,03	3957,71	4170,34	5033,69	5610,93
10	2423,84	4410,23	5326,60	5392,92	6511,52	7226,92	7810,44	8230,05	9933,85	11073,02
11	1228,21	2234,76	2699,10	2732,71	3299,52	3662,03	3957,71	4170,34	5033,69	5610,93
12	545,20	992,01	1198,13	1213,05	1464,66	1625,58	1756,83	1851,22	2234,46	2490,70
13	0,11	0,20	0,24	0,24	0,29	0,33	0,35	0,37	0,45	0,50
14	-545,06	-991,75	-1197,81	-1212,73	-1464,27	-1625,14	-1756,36	-1850,72	-2233,86	-2490,03
15	-1228,25	-2234,83	-2699,19	-2732,80	-3299,63	-3662,16	-3957,85	-4170,48	-5033,86	-5611,12
16	-2423,93	-4410,38	-5326,79	-5393,11	-6511,74	-7227,17	-7810,71	-8230,34	-9934,20	-11073,40
17	-1228,25	-2234,83	-2699,19	-2732,80	-3299,63	-3662,16	-3957,85	-4170,48	-5033,86	-5611,12

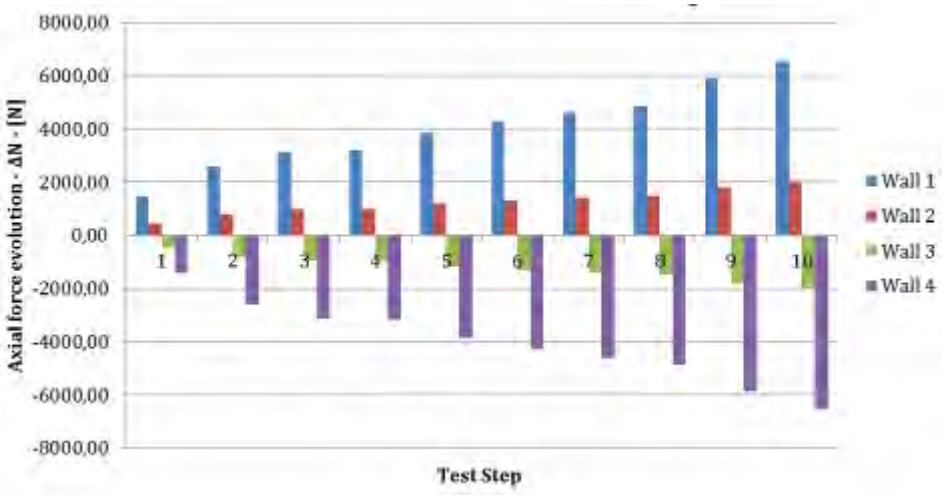

Figure 6.65: Axial force evolution by the test.

6.5 Comparisons between the methods and experimental data

In this section there are results obtained from shaking table tests of model M3 and then analyse them to obtain the force displacement curve that describes the real behaviour of the structure. The purpose is to make comparisons between the measured and simulated response of the structure.

6.5.1 Data acquisition

During the testing on shaking table experimental data was collected using different instruments such as accelerometers and LVDTs (see Figure 6.66). These data were recorded at regular time intervals of 0,00125 s. The model M3 has been subject to different levels of seismic action gradually increased to simulate different levels of performance that is required of the structure during an earthquake. In particular, these load levels are referred to as R150, R200 and R250.

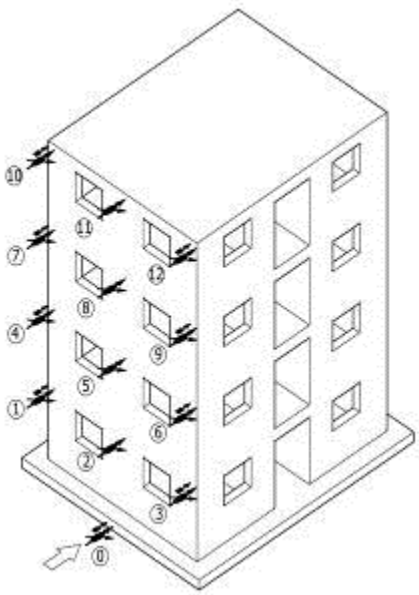

Figure 6.66: Axonometric of the measurement points of experimental data [55].

In each measuring point, shown in the previous figure, displacements and accelerations during the entire duration of the three tests were recorded. In total approximately 75.000 measurements were recorded at each point. List of displacement and acceleration measuring points is in Table 6.38.

Table 6.38: Name and type of experimental data collected during the test [55].

Position	Displacement	Acceleration
0	d_0	a_0
1	d_{1L}	a_{1L}
2	d_{1M}	a_{1M}
3	d_{1R}	a_{1R}
4	d_{2L}	a_{2L}
5	d_{2M}	a_{2M}
6	d_{2R}	a_{2R}
7	d_{3L}	a_{3L}
8	d_{3M}	a_{3M}
9	d_{3R}	a_{3R}
10	d_{4L}	a_{4L}
11	d_{4M}	a_{4M}
12	d_{4R}	a_{4R}

The following Figures 6.67 – 6.69 shows the state of the M3 model at the end of execution of the three seismic tests.

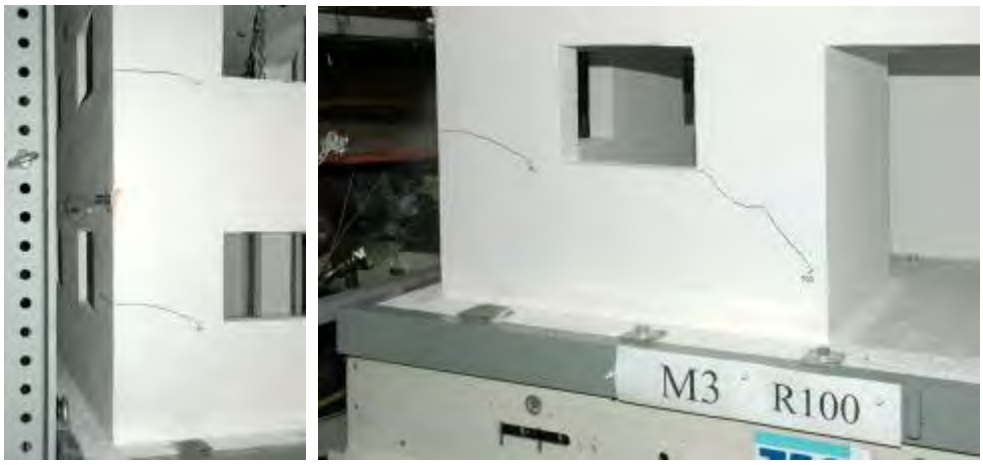

Figure 6.67: Cracks in the peripheral walls of model M3, observed after test run R100 *[55]*.

Figure 6.68: Typical diagonally oriented shear cracks in the walls of model M3 at maximum resistance after test run R150 [55].

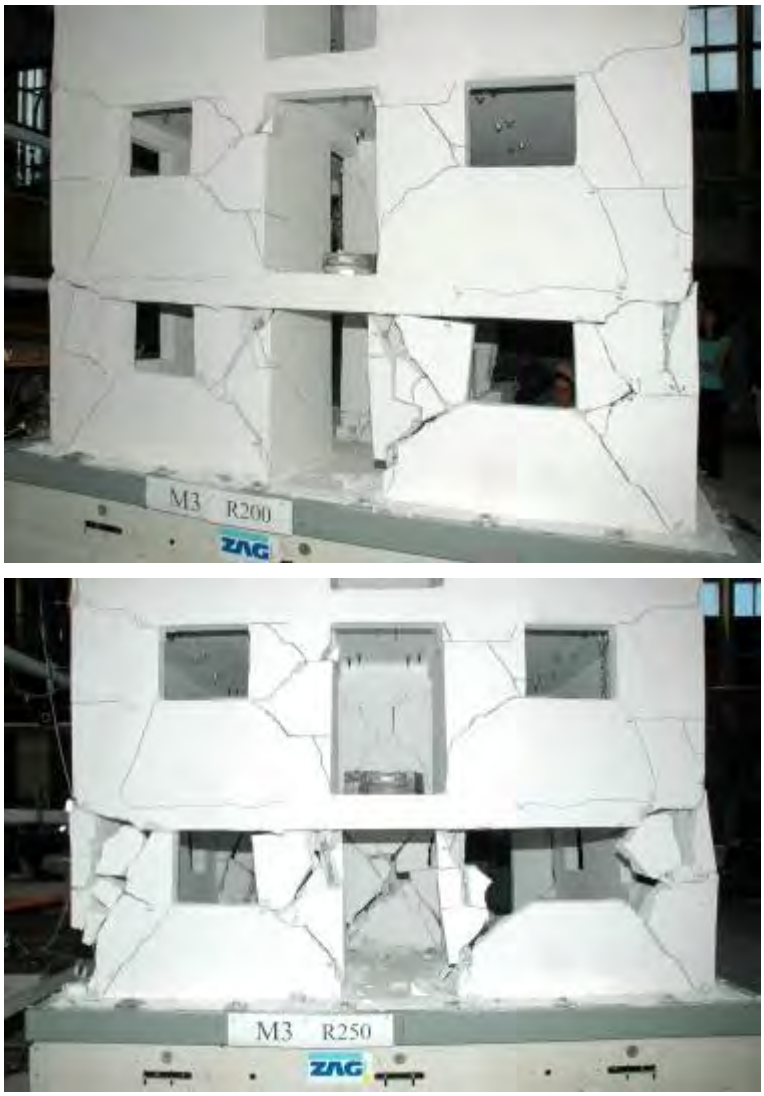

Figure 6.69: Severe damage to the walls in the ground floor and heavy damage to the walls in the first storey near collapse of model M3 after test run R250 [55].

6.5.2 Data analysis

The original purpose of the analysis of previous experimental data is to get the curves that show the evolution of the base shear as a function of displacement of a control node. In particular, the curves with reference displacements recorded on the top floor and with displacements recorded on the first floor are needed.

Firstly, the accelerations recorded at each level are the mean value of acceleration recorded on the right side and left side:

$$a_i = \frac{a_{iL} + a_{iR}}{2}, \qquad \text{for: } i = 1,...,4. \tag{6.92}$$

The equivalent inertial forces applied to each building floor are the product of mass multiplied by acceleration:

$$F_i = m_i \cdot a_i, \qquad \text{for: } i = 1,...,4. \tag{6.93}$$

The floor shear are the sum of forces in all floors:

$$V_i = \sum_{j=i}^{n} F_j, \qquad \text{for: } n = 4. \tag{6.94}$$

With regard to the displacements, the absolute displacements of each plan are assumed equal to the displacement recorded at the midpoint of each plan:

$$d_i = d_{iM}, \qquad \text{for: } i = 1,...,4. \tag{6.95}$$

6.5.3 Shear versus displacement curves

The following Figures 6.70 – 6.75, show the trends of the base shear curves in terms of the displacements on the top floor and the first floor.

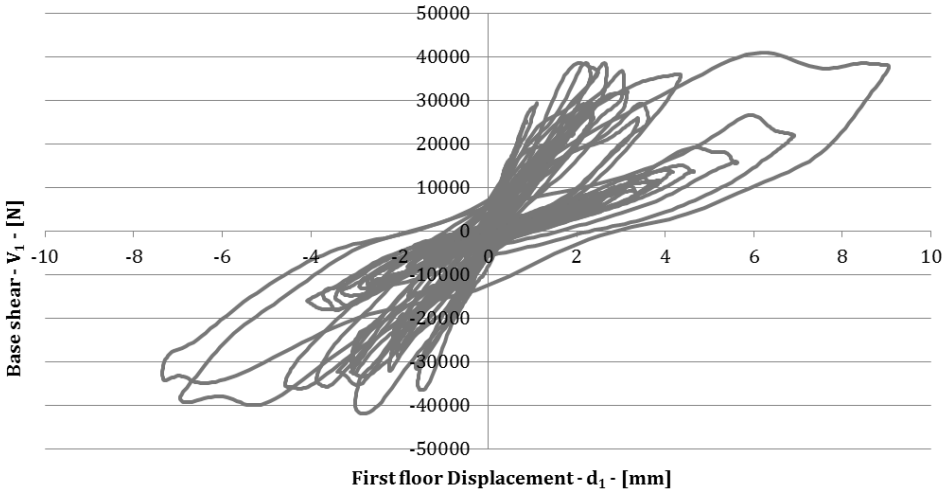

Figure 6.70: Base shear vs. first floor displacement. R150.

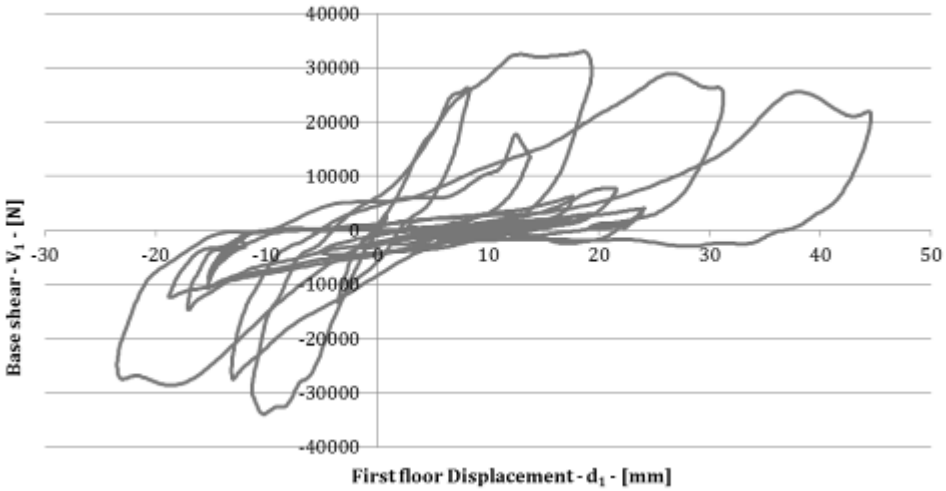

Figure 6.71: Base shear vs. first floor displacement. R200.

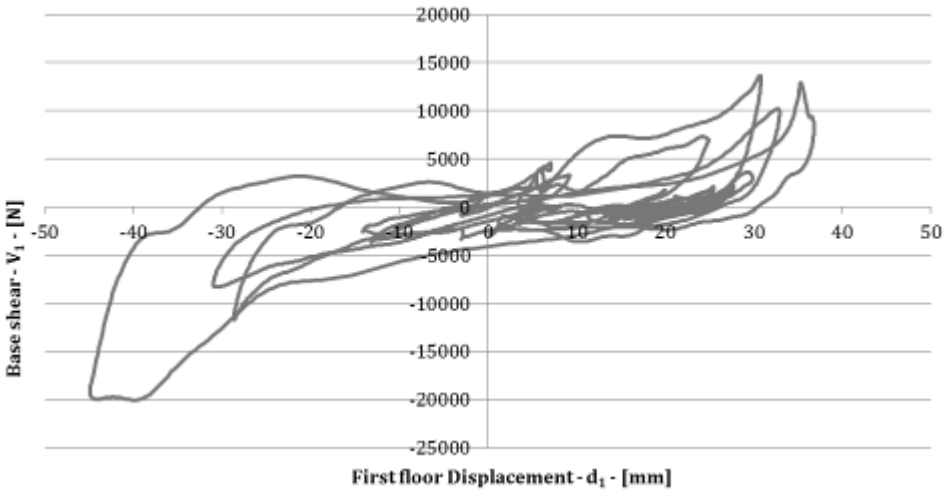

Figure 6.72: Base shear vs. first floor displacement. R250.

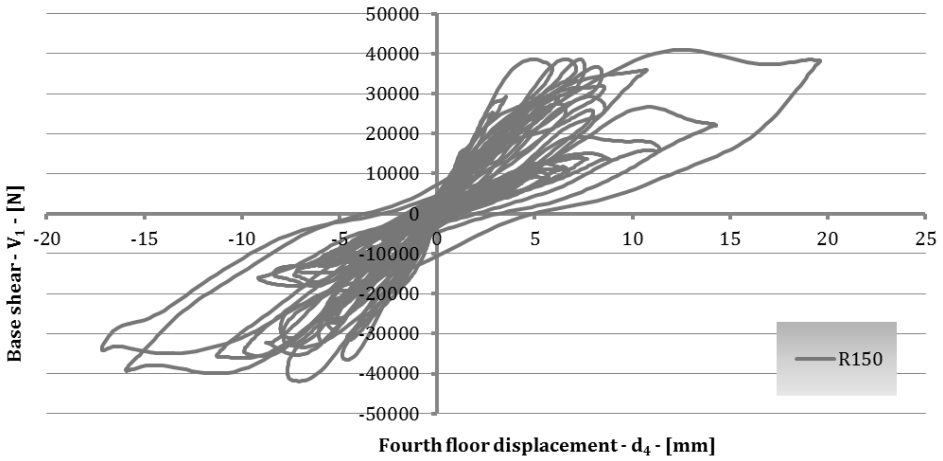

Figure 6.73: Base shear vs. fourth floor displacement. R150.

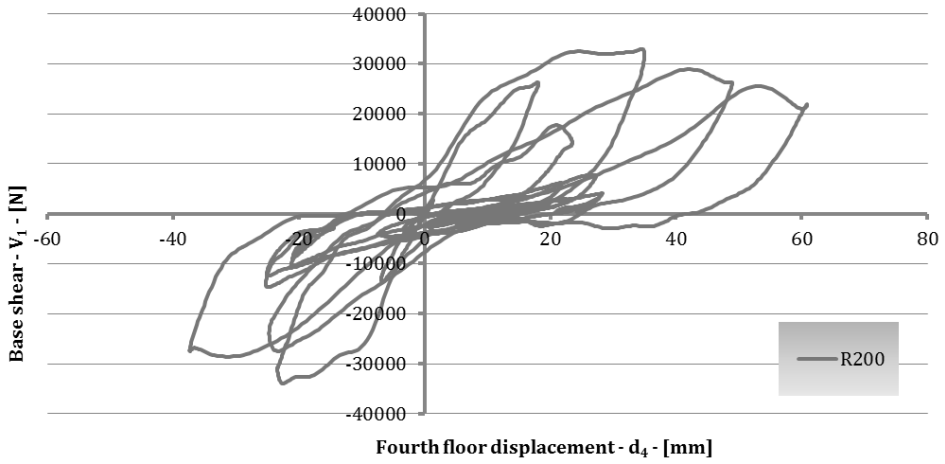

Figure 6.74: Base shear vs. fourth floor displacement. R200.

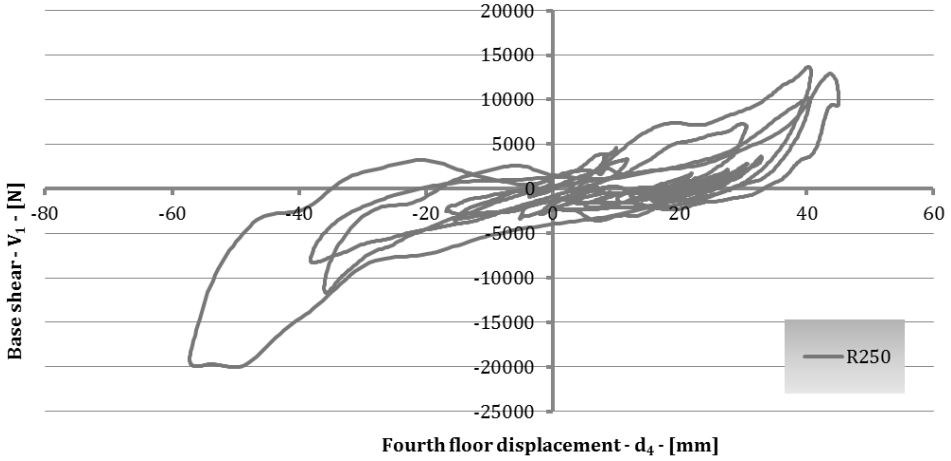

Figure 6.75: Base shear vs. fourth floor displacement. R250.

6.5.4 Idealisations

As can be seen by experimental data, a complex nonlinear behaviour was measured that cannot be used directly to make comparisons. The results, therefore, can be represented by a modelling.

These idealisations were obtained qualitatively and have been assumed to consist of several linear segments chosen so as to approximate the obtained experimental data (see Figure 6.76 and Figure 6.77).

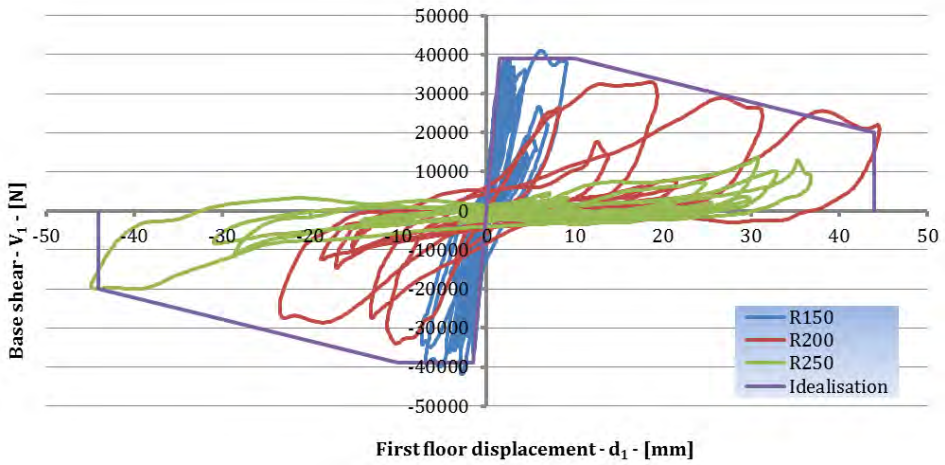

Figure 6.76: Base shear vs. first floor displacement Idealisation.

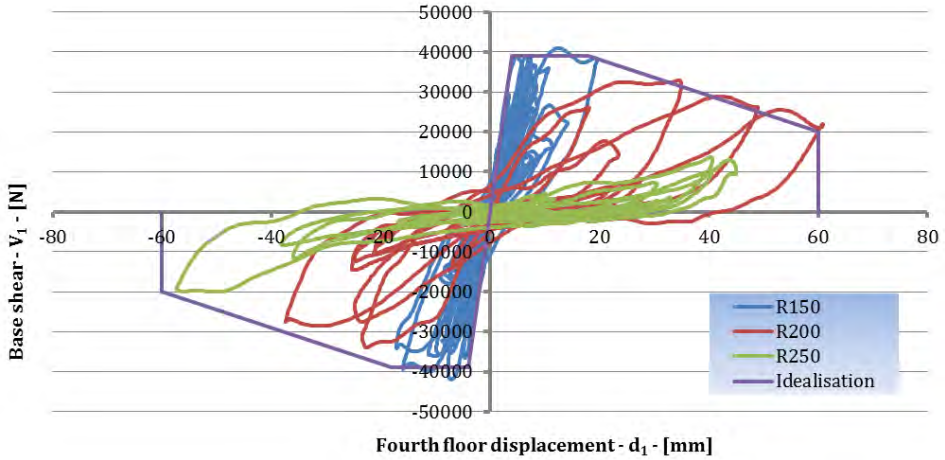

Figure 6.77: Base shear vs. fourth floor displacement Idealisation.

6.5.5 Comparisons

At this point a comparisons between the idealised curves of the real behaviour of the structure and the pushover curves can be done. Those curves were obtained measuring the displacements at the first (bottom idealisation) and top floor (top idealisation). The pushover curves were obtained previously by different mathematical model (see Figures 6.78 – 6.82).

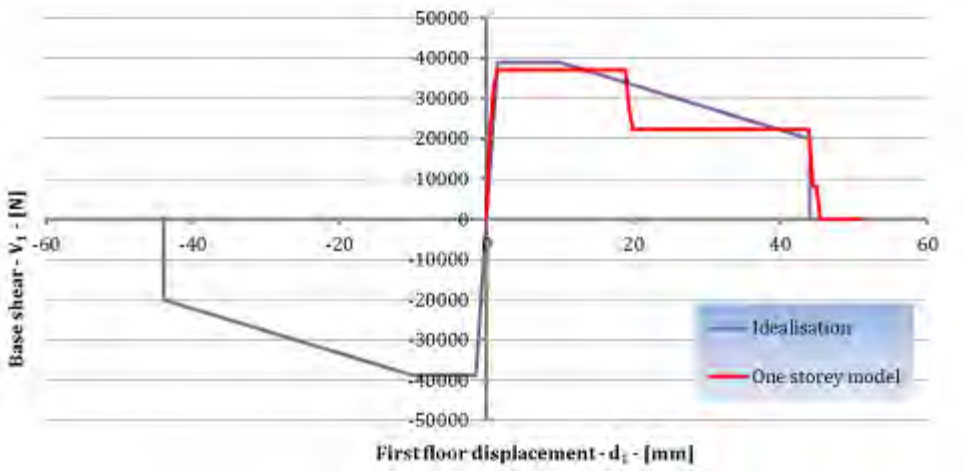

Figure 6.78: Comparison between experimental curve and one storey model.

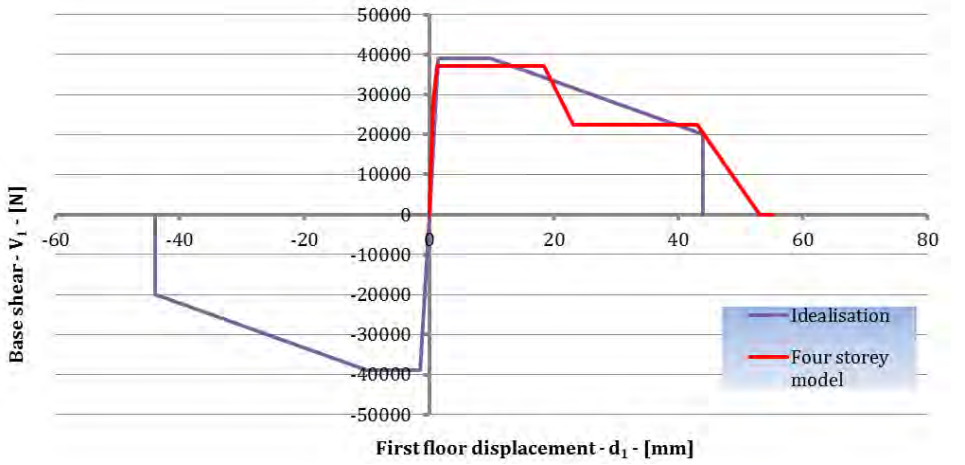

Figure 6.79: Comparison between experimental curve and four storey model with control displacement at the first floor slab.

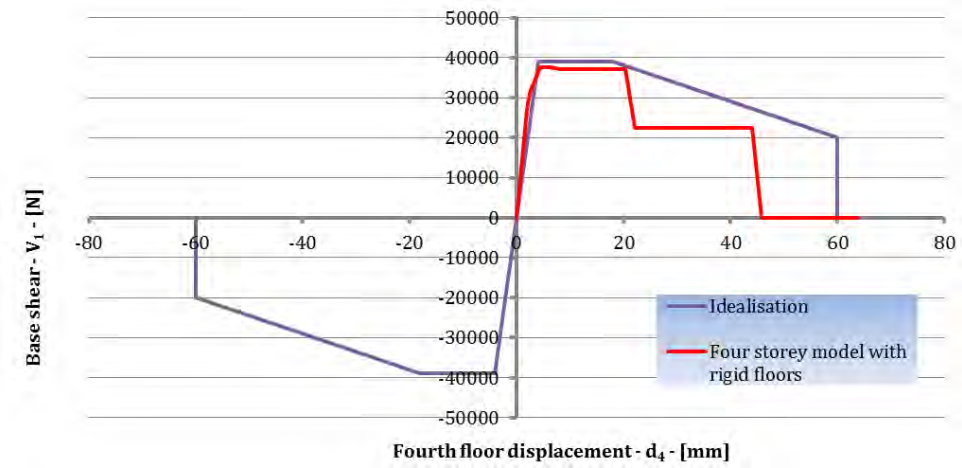

Figure 6.80: Comparison between experimental curve and four storey model with rigid floors and control displacement at the top of the structure.

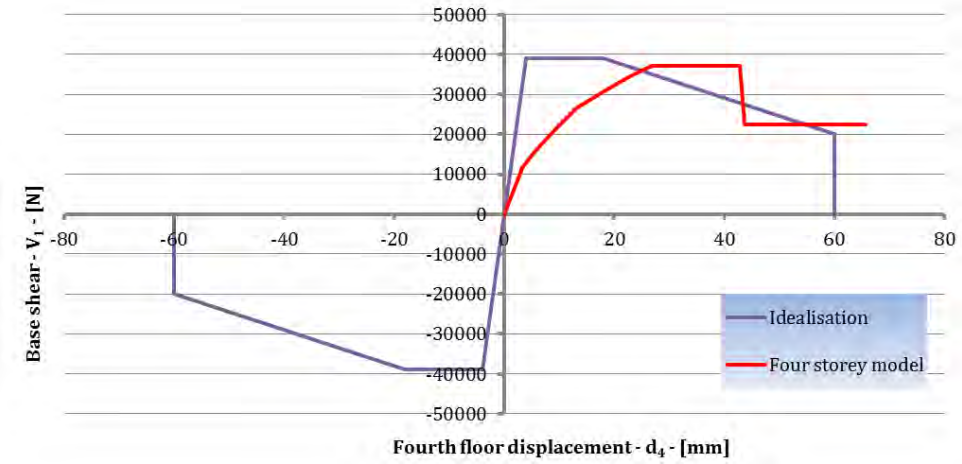

Figure 6.81: Comparison between experimental curve and four storey model with control displacement at the top.

The previous Figure 6.80 and Figure 6.81 show that the structure's modelling with rigid floors, compared to that with deformable floors, enables a more accurate modelling. In particular, the stiffness of the system in the initial stages of elastic loading is very similar to the modelling that adopting rigid floors.

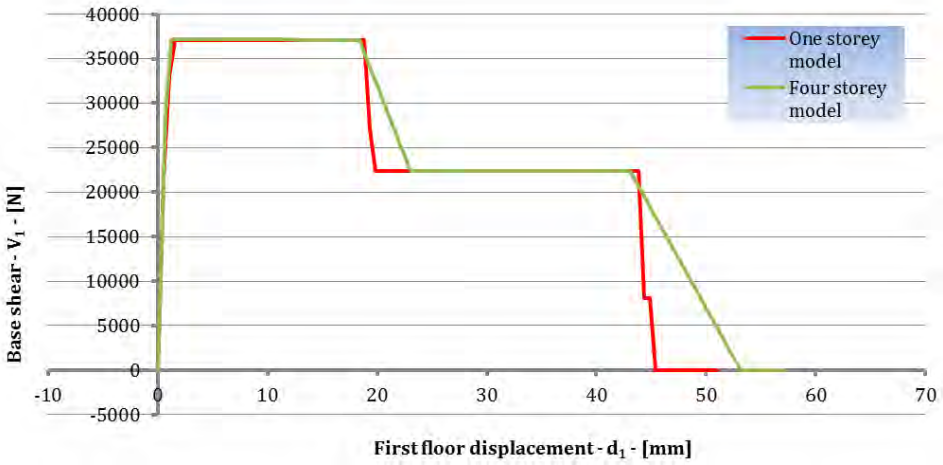

Figure 6.82: Comparison between one storey model and four storey model with control displacement at first storey.

7. Conclusions

This work addressed the issue of modelling masonry structures under seismic action. Although several contributions are currently available on this subject in the scientific literature, the present work is clearly intended at formulating and validating a design-oriented numerical procedure which actually implements the capacity models provided by the structural codes currently in force in Italy and Europe. Thus, a quick overview of the analysis methods which can be carried out by means of the FEM codes usually employed by practitioners is firstly presented.

Nevertheless, since those codes are not specifically thought for masonry structures, they often lack in simulating some specific effects, such as the interaction between axial force and shear strength. Consequently, a novel practice-oriented model is formulated by adopting the well-known "equivalent frame" approach and introducing nonlinear phenomena through a "lumped-plasticity" technique.

This model has been implemented in MatLab® (see chapter 5) and is able to simulate all failure modes of masonry walls and spandrels actually considered within the relevant structural codes.

The numerical results carried out by means of the various numerical models considered in the present study led to reasonably accurate simulations of the mechanical behaviour of masonry structures observed in some experimental tests available in the scientific literature.

However, the novel numerical procedure described in chapter 5 should be still considered as a preliminary proposal, as some of the algorithms implemented

therein should be further enhanced in terms of numerical stability and efficiency.

The possible extension of the present model to the case of fully 3D structures as well as the implementation of a numerical routine for performing nonlinear time-history analyses are among the next developments of this research.

References

[1] ISTAT, 14° Censimento Generale della Popolazione e delle Abitazioni, (2001);

[2] Tomazevic M., Gams M., Shear resistance of unreinforced masonry walls, ZAG, Slovenian National Building and Civil Engineering Institute;

[3] Ceroni F., Edifici in muratura e centri storici, Giornata di studio, Il terremoto dell'Aquila del 6 Aprile 2009, Università degli Studi del Sannio;

[4] O.P.C.M. 28 Aprile 2006 n. 3519, Criteri generali per l'individuazione delle zone sismiche e per la formazione e l'aggiornamento degli elenchi delle medesime zone, (Gazzetta Ufficiale n. 108 del 11 Maggio 2006);

[5] CSLLPP, Linee Guida per la valutazione e riduzione del rischio sismico del patrimonio culturale con riferimento alle norme tecniche per le costruzioni, Testo allegato al parere n. 66 dell'Assemblea Generale del Consiglio Superiore del LL.PP., reso nella seduta del 21 Luglio 2006;

[6] D.M. Infrastrutture 14/01/2008, Approvazione delle nuove norme tecniche per le costruzioni, (GU n. 29 del 4 Febbraio 2008, Supplemento Ordinario n. 30);

[7] Iacobelli F., Progetto e verifica delle costruzioni in muratura in zona sismica, EPC Libri;

[8] Bernardini, The vulnerability of buildings: a national scale evaluation of seismic vulnerability of ordinary buildings, CNR, National Group for Defence from earthquakes, Rome, (2000);

[9] Augenti N., Il calcolo sismico degli edifici in muratura, UTET Università;

[10] FEMA 273, NEHRP guidelines for the seismic rehabilitation of buildings, Federal Emergency Management Agency, (1997);

[11] FEMA 356, Prestandard and commentary for the seismic rehabilitation of buildings, Federal Emergency Management Agency, (2000);

[12] ATC 40, Seismic evaluation and retrofit of concrete buildings, Volume 1, Applied Technology Council, (1996);

[13] Regio Decreto 18 Aprile 1909 n. 193, Norme tecniche ed igieniche obbligatorie per le riparazioni, ricostruzioni e nuove costruzioni degli edifici pubblici elencati nel R.D. 15 Aprile 1909 e ne designa i comuni, (Pubblicato sulla Gazzetta Ufficiale n. 95 del 22 Aprile 1909);

[14] Regio Decreto 16 Novembre 1939, XVIII, n. 2229, Norme per la esecuzione delle opere in conglomerato cementizio semplice od armato, (pubblicato nel Suppl. Ord. alla Gazzetta Ufficiale, n. 92 del 18 Aprile 1940);

[15] Circ. M.LL.PP. 2 Novembre 1981, n. 895, L. 02/02/1974 n. 64 art. 30, Interpretazione della normativa transitoria in materia di edilizia antisismica;

[16] D.M. n. 39 del 03/03/1975, Disposizioni concernenti l'applicazione delle norme tecniche per le costruzioni in zona sismica, G.U. 08/04/1975 n. 93;

[17] Circolare Ministero del LL.PP. del 30 Luglio 1981 n. 21745, Istruzioni per l'applicazione della normativa per la riparazione ed il rafforzamento degli edifici danneggiati dal sisma;

[18] Tomazevic M., The computer program POR, Report ZRMK, Institute for Testing and Research in Material and Structures, Ljubljana;

[19] D.M. LL.PP. del 16/01/1996, Norme tecniche per le costruzioni in zona sismica, Ministero dei Lavori Pubblici e Ministero dell'Interno;

[20] D.M. LL.PP. del 20/11/1987, Norme tecniche per la progettazione, esecuzione e collaudo degli edifici in muratura e per il loro consolidamento;

[21] Circ. M.LL.PP. 10/04/1997 n. 65, Istruzioni per l'applicazione delle Norme tecniche per le costruzioni in zone sismiche di cui al Decreto Ministeriale 16/01/1996;

[22] O.P.C.M. 3431, Ordinanza n. 3431, Ulteriori modifiche ed integrazioni all'ordinanza del Presidente del Consiglio dei Ministri n. 3274 del 20 Marzo 2003, recante Primi elementi in materia di criteri generali per la classificazione sismica del territorio nazionale e di normative tecniche per le costruzioni in zona simica, Presidenza del Consiglio dei Ministri, (2005);

[23] Circolare 2 Febbraio 2009 n. 617 C.S.LL.PP., Istruzioni per l'applicazione delle Nuove norme tecniche per le costruzioni di cui al DM 14/01/2008, Ministero delle Infrastrutture e dei Trasporti, (GU n. 47 del 26/02/2009, Supplemento Ordinario n. 27);

[24] Legge N. 1086 del 1971, Norme per la disciplina delle opere di conglomerato cementizio armato, normale e precompresso ed a struttura metallica, (G.U. 21-12-1971, n. 321);

[25] Legge 2 Febbraio 1974, n. 64, Provvedimenti per le costruzioni con particolari prescrizioni per le zone sismiche;

[26] CNR – DT 200/2004, Istruzioni per la Progettazione, l'Esecuzione ed il Controllo di Interventi di Consolidamento Statico mediante l'utilizzo di Compositi Fibrorinforzati, Materiali, strutture di c.a. e di c.a.p. e strutture murarie, Consiglio Nazionale delle Ricerche, 13 Luglio 2004, Rev. 7 Ottobre 2008, Roma;

[27] Consiglio Superiore LL.PP., Linee guida per la Progettazione, l'Esecuzione ed il Collaudo di Interventi di Rinforzo di strutture in c.a., c.a.p. e murarie mediante FRP, (2009);

[28] Eurocode 6-1-1, Design of masonry structures – Part 1-1: General rules for reinforced and unreinforced masonry structures, (2005), CEN, European Committee for standardization;

[29] Eurocode 6-2, Design of masonry structures – Part 2: Design consideration, selection of materials and execution of masonry, (2006), CEN, European Committee for standardization;

[30] Eurocode 6-3, Design of masonry structures – Part 3: Simplified analysis methods for unreinforced masonry structures, (2006), CEN, European Committee for standardization;

[31] Eurocode 8-1, Design of structures for earthquake resistance – Part 1: General rules, seismic actions and rules for buildings, (2004), CEN, European Committee for standardization;

[32] Eurocode 8-3, Design of structures for earthquake resistance – Part 3: Assessment and retrofitting of buildings, (2005), CEN, European Committee for standardization;

[33] Tomazevic M., Shear resistance of masonry walls and Eurocode 6: shear versus tensile strength of masonry, ZAG, Slovenian National Building and Civil Engineering Institute;

[34] Rizzano G., Riabilitazione Strutturale, Parte 1: Analisi e verifica degli edifici in muratura ordinaria, Università degli Studi di Salerno, (2010);

[35] Turnsek V., Cacovic F., Some experimental results on the strength of brick masonry walls, Proc. Of the 2nd Intern. Brick Masonry Conference, Stoke-on-Trent, pp. 149-156, (1971);

[36] Benedetti D., Tomazevic M., Sulla verifica sismica di costruzioni in muratura, Ingegneria Sismica, vol. 1, n. 0,(1984);

[37] Muller H., Mann W., Failure of shear-stressed masonry, An enlarged theory, tests and application to shear, in Proc. of the British Ceramic Society, London, p. 30, (1982);

[38] Faella C., Consalvo V., Nigro E., Influenza della snellezza geometrica e delle fasce di piano sulla valutazione della resistenza ultima di pareti murario multipiano, Atti dell'8° Convegno Nazionale ANIDIS L'Ingegneria sismica in Italia, Taormina, 21 – 24 Settembre 1997, Dipartimento di Ingegneria Civile, Università degli Studi di Salerno;

[39] Magenes G., Bolognini D., Braggio C., Metodi semplificati per l'analisi sismica non lineare di edifici in muratura, Gruppo Nazionale per la Difesa dai Terremoti;

[40] Braga F., Liberatore D., A finite element for the analysis of the response of masonry buildings, Proc. Of the 5th North American Masonry Conference, Urbana, pp. 201-212, (1990);

[41] Calderoni B., Lenza P., Rossi P. P., Sperimentazione in laboratorio e modellazione numerica di edifici in muratura soggetti a carichi orizzontali, Atti del Convegno Nazionale La Meccanica delle Murature tra Teoria e Progetto, Messina, (1996);

[42] Aktinson A., Amadei P. B., Saeb S., Sture S., Response of masonry bed joints in direct shear, Journal structural engineering div. ASCE 115, (1989);

[43] Chiostrini S., Vignoli A., Modellazione numerica di prove distruttive di pareti in muratura sottoposte ad azioni orizzontali, Atti del VII Convegno L'Ingegneria Sismica in Italia, Siena, (1995);

[44] Zienkiewicz O.C., CBE, FRS, FREng, R.L. Taylor, The Finite Element Method, Volume 1, 2, 3;

[45] Bathe K.J., Finite Element Procedures, Massachusetts Institute of Technology;

[46] DT2, Raccomandazioni per la riparazione strutturale degli edifici in muratura, Regione Autonoma Friuli Venezia-Giulia, (1978);

[47] Dolce M., Schematizzazione e modellazione per azioni nel piano delle pareti, Corso sul consolidamento degli edifici in muratura in zona sismica, Ordine degli Ingegneri, Potenza, (1989);

[48] Fajfar P., M.EERI, A Nonlinear Analysis Method for Performance Based Seismic Design, Earthquake Spectra, vol. 16, No. 3, pp. 573 – 592, Faculty of Civil and Geodetic Engineering, University of Ljubljana, (2000);

[49] Albanesi T., Nuti C., Analisi Statica Non Lineare (Pushover), Dipartimento di Strutture, Università degli Studi di Roma Tre, (2007);

[50] Amadio C., Rinaldin G., Macorini L., An equivalent frame model for nonlinear analysis of unreinforced masonry buildings under in-plan cyclic loading, ANIDIS 2011, XIV Convegno;

[51] Faella C., Metodi di analisi delle strutture intelaiate, Argomenti di teoria e tecnica delle costruzioni, Volume 2, CUES;

[52] CSI, Computer & Structures Inc., CSI Analysis Reference Manual for SAP2000®, ETABS®, and SAFE®, Berkeley, California, USA;

[53] Langhaar H., Dimensional Analysis and Theory of Models, John Wiley and Sons, New York, (1951);

[54] Harris H. G., Sabnins G. M., Structural Modeling and Experimental techniques, CRC Press (Boca Raton), (1999);

[55] Tomazevic M., Gams M., Seismic behaviour of YTONG houses: model shaking table tests, ZAG, Slovenian National Building and Civil Engineering Institute, Ljubljana, (2010);

[56] Bonocore S., Tesi di Laurea, Comportamento sismico di strutture in muratura: esame comparato di metodi di analisi previsti dalle recenti normative, Relatore: Dott. Ing. Enzo Martinelli, Università degli Studi di Salerno;

[57] Bosco M., Ghersi A., Marino E.M., Una più semplice procedura per la valutazione della risposta sismica delle strutture attraverso analisi statica non lineare, Materiali ed approcci innovativi per il Progetto in Zona Sismica e la Mitigazione della Vulnerabilità delle Strutture, Università degli Studi di Salerno, Consorzio ReLUIS, 12–13 Febbraio 2007;

[58] Chen S. Y., Moon F.L., Yi T., A macroelement for the nonlinear analysis of in–plan unreinforced masonry piers, Department of Civil, Architectural and Environmental Engineering, Drexel University, Philadelphia, PA 19104, United States, (2008);

[59] Circ. M.LL.PP. 15/10/1996 n. 252, Istruzioni per l'applicazione delle Norme tecniche per il calcolo, l'esecuzione ed il collaudo delle opere in cemento armato normale e precompresso e per le strutture metalliche di cui al D.M. 9 Gennaio 1996;

[60] Circ. M.LL.PP. 4 Gennaio 1989, n. 30787, Legge 2 Febbraio 1974 n. 64 art. 1, Istruzioni in merito alle norme tecniche per la progettazione, esecuzione e collaudo degli edifici in muratura e per il loro consolidamento;

[61] Cudrig A., Tesi di Laurea, Prove cicliche di taglio su muratura non armata con sottile strato di malta nei giunti orizzontali e giunti verticali a secco, Relatore: Prof. Gubana Alessandra, Correlatori: Prof. Ing. Miha Tomazevic, Dott. Ing. Matija Gams, Università degli Studi di Udine;

[62] Decreto Ministeriale 3 Marzo 1975, Approvazione delle norme tecniche per le costruzioni in zone sismiche, (Supplemento Ordinario della Gazzetta Ufficiale 8 Aprile 1975, n. 93);

[63] D.M. LL.PP. del 09/01/1996, Norme tecniche per il calcolo, l'esecuzione ed il collaudo delle strutture in cemento armato, normale e precompresso e per le strutture metalliche;

[64] D.M. LL.PP. del 16/01/1996, Norme tecniche relative ai Criteri generali per la verifica di sicurezza delle costruzioni e dei carichi e sovraccarichi, Ministero dei LL.PP. e Ministero dell'Interno;

[65] Gams M., Nelinearna seizmicna analiza stiri etaznega armirano betonskega okvirja z N2 metodo, Dinamika gradbenih konstrukcij z uporabo v potreste inzenirstvu, Podiplomski studij 2003/2004.

Acknowledgements

A special thanks to Prof. Enzo Martinelli, for believing in my abilities, for his courtesy and availability during the period of this study.
It's a must also thank to the ZAG – Slovenian National Building and Civil Engineering Institute, particularly to Marjana Lutman, Matija Gams and Prof. Miha Tomazevic, for their patience and their valuable contribution to the writing of this thesis.
Finally, thanks to Dr. Antonella Iannaccone, for her useful work of translation and Fabrizio Carpentieri, for his help in the graphics.